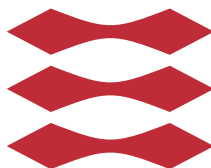# Modeling Pharmacokinetics and Pharmacodynamics of Glucagon for Simulation of the Glucoregulatory System in Patients with Type 1 Diabetes

Sabrina Lyngbye Wendt

Summary (English)

The goal of this thesis was to develop a pharmacokinetics/pharmacodynamics (PK/PD) model for glucagon. The proposed PD model included multiplication of the stimulating glucagon effect and inhibiting insulin effect on the endogenous glucose production (EGP). Moreover, the concentration-response relationship of glucagon and EGP was characterized by a non-linear function, where the response saturated for high concentrations of glucagon. The novel EGP model extended Hovorka's glucoregulatory model to include the effect of glucagon.

The PK/PD model described both regular glucagon and a novel glucagon analogue in healthy dogs. The extended glucoregulatory model translated to the human species and described glucose-insulin-glucagon dynamics in healthy subjects and patients with type 1 diabetes (T1D).

The extended glucoregulatory model was successfully validated by leave-one-out cross-validation in seven T1D patients which justified its use for simulations. The final model parameters were estimated from three to four datasets from each patient.

The validated extended glucoregulatory model was used for *in silico* studies. The model replicated a clinical study of the effect of glucagon at varying insulin levels. The simulations also suggested new glucagon doses to be tested in a similar *in vivo* study to provide new insight to the relationship between insulin, glucagon, and EGP. Finally, the model was used to conduct a large original simulation study investigating an insulin dependent glucagon dosing regimen for treatment of insulin-induced mild hypoglycemia.

Summary (Danish)

Målet med denne afhandling var at udvikle en farmakokinetik/farmakodynamik (PK/PD) model for glukagon. Den fremsatte PD model bestod af multiplikation mellem glukagons stimulerende effekt og insulins hæmmende effekt på den endogene glukose produktion (EGP). Derudover var dosis-respons forholdet mellem glukagon og EGP kendetegnet ved en ikke-lineær funktion, hvor responset opnåede mætning ved høje glukagon koncentrationer. Den nye EGP model udvidede Hovorkas model for blodsukkerregulering til også at inkludere effekten af glukagon.

PK/PD modellen beskrev både almindelig glukagon samt en ny glukagon analog i raske hunde. Den udvidede model for blodsukkerregulering kunne overføres til mennesker og beskrev glukose-insulin-glukagon dynamikken i raske frivillige og patienter med type 1 diabetes (T1D).

Den udvidede model for blodsukkerregulering blev succesfuldt valideret ved brug af leave-one-out krydsvalidering i syv T1D patienter, hvilket retfærdiggjorde dens brug til simuleringer. De endelige modelparametre for hver patient blev estimeret baseret på tre til fire datasæt.

Den validerede udvidede model for blodsukkerreguleringen blev anvendt til *in silico* studier. Modellen efterviste et klinisk studie, som undersøgte effekten af glukagon ved forskellige insulinniveauer. Simuleringsstudierne blev også brugt til at foreslå nye glukagon doser, som kunne testes i lignende *in vivo* forsøg og dermed bidrage med ny viden om forholdet mellem insulin, glukagon og EGP. Endelig blev modellen brugt til at gennemføre et omfattende originalt simuleringsstudie, som undersøgte insulinafhængige doseringsvejledninger for glukagon til behandling af insulininduceret mild hypoglykæmi.

Preface

This thesis was prepared in partial fulfilment of the requirements for acquiring an industrial PhD degree at the Technical University of Denmark (DTU). The project commenced mid March 2014 and the dissertation was handed in mid March 2017. The project was a collaboration between the department of Bioanalysis and Pharmacokinetics at Zealand Pharma A/S and the Scientific Computing section of the department of Applied Mathematics and Computer Science (DTU Compute). Carsten Boye Knudsen provided supervision from the company, and associate professor John Bagterp Jørgensen and professor Henrik Madsen provided supervision from the university.

During June 2015 to October 2015 the project was carried out at the division of Metabolic Diseases at Montreal Clinical Research Institute (IRCM). The external stay was hosted by associate professor Rémi Rabasa-Lhoret and assistant professor Ahmad Haidar.

The PhD project was funded by Zealand Pharma A/S and the Innovation Fund Denmark.

Kgs. Lyngby, 14-March-2017

Sabrina Lyngbye Wendt

Acknowledgements

Abbreviations

BG	blood glucose concentration
cAMP	cyclic AMP
CGM	continuous glucose monitor
CTSM	continuous time stochastic modeling
DM	diabetes mellitus
DMSO	dimethyl sulfoxide
EGP	endogenous glucose production
FDA	Food & Drug Administration
HbA1c	glycated hemoglobin A1c
IOB	insulin on board
IIR	insulin infusion rate
IM	intramuscular
IV	intravenous
MAP	maximum a posteriori
MAPE	mean absolute prediction error
MCMC	Markov Chain Monte Carlo
ML	maximum likelihood
MPE	mean prediction error
PD	pharmacodynamics
PID	partial integral derivative
PK	pharmacokinetics
SC	subcutaneous
T1D	type 1 diabetes
TDD	total daily dose
Tmax	time to maximum concentration
WHO	World Health Organisation

Contents

CHAPTER 1

Introduction

Diabetes mellitus (DM) or simply diabetes, is a chronic disorder where the body does not have the ability to control the blood glucose concentration (BG). Over time, untreated DM leads to irreversible damage to essential tissues of the body like nerves and blood vessels. The World Health Organisation (WHO) estimated that DM affected 422 million people world wide in 2014 [1]. The disease is either due to destruction (often autoimmune) or removal of insulin producing cells in the pancreas (type 1, 10%) or due to lifestyle related lowered insulin sensitivity by insulin consuming cells of the body (type 2, 90%).

For almost 100 years, diabetes patients have been treated with insulin which is a hormone that lowers the BG. Traditionally, type 1 diabetes (T1D) was controlled by measuring BG via multiple daily finger pricks and adjusting insulin dosage accordingly to maintain normoglycemic range (70-125 mg/dL or 4-7 mmol/L). The recent introduction of continuous glucose monitors (CGM) has significantly improved BG control in adults with T1D [2]. However, BG regulation using insulin only is a trade-off between achieving closer glycemic control, i.e. minimizing time in hyperglycemia (high BG), and increasing the risk of hypoglycemia (low BG) [3].

The biggest fear to parents of children with diabetes is an unnoticed hypo-glycemic event [4]. Hypoglycemic episodes occur when the ratio of glucose to insulin is out of balance: e.g. excessive insulin dosage, lack of glucose intake due to a missed meal or increased use of glucose because of aerobic exercise.
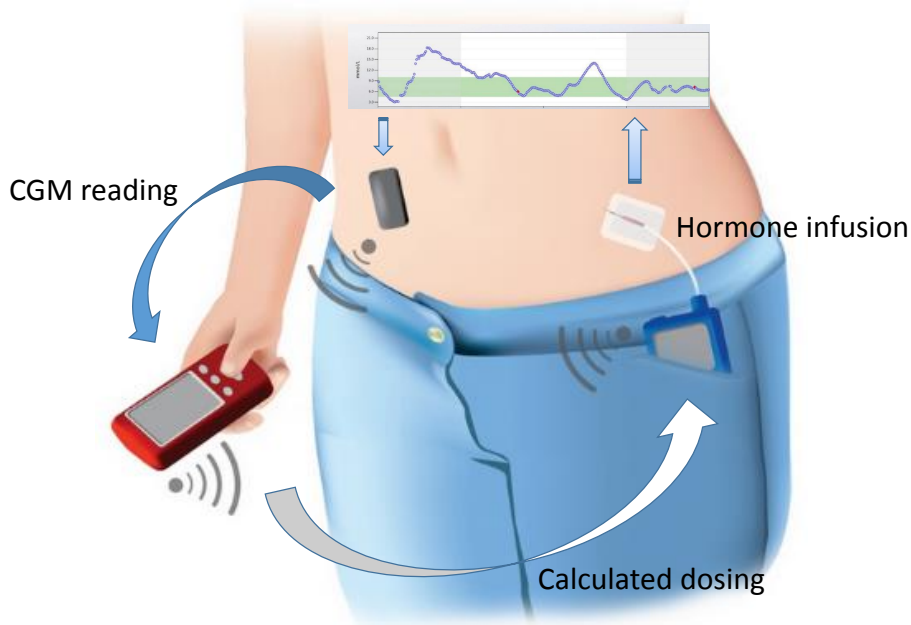
Figure 1.1: Concept of a closed loop artificial pancreas: The CGM measures
the glucose concentration, sends it to a control algorithm that de-
termines the hormone dosing, which is then delivered via a pump.

Depending on the severity of hypoglycemia it can lead to seizures, coma or even
death. Often, the dangerous events are not associated with warning symptoms
and they typically occur during sleep [3, 5]. Large population studies estimate
that 6% of deaths among young diabetes patients (< 40 years) can be attributed
to dead-in-bed syndrome most likely due to fatal hypoglycemia [6].
In the healthy body, BG is not regulated by insulin alone but by several hor-
mones serving to control BG e.g. glucagon that increases release of glucose from
storage as glycogen in the liver. To mimic non-diabetes function and improve
BG control, recent studies re-investigated the counterregulatory effect of using
glucagon together with insulin [7].

For more than forty years, scientists have worked on developing an artificial
pancreas to simplify the life of T1D patients by minimizing the daily treatment
decisions and thereby improve quality of life [8]. The artificial or bionic pan-
creas is an interconnected system of devices including a CGM, a subcutaneous
(SC) insulin (and glucagon) infusion pump and a control algorithm determining

the needed infusion(s) based on input from the CGM to maintain BG within normoglycemic range as illustrated in Figure 1.1. Glucagon in a dual hormone closed loop system may increase safety against hypoglycemia compared to a single hormone system.

The first modern *in vivo* study of closed-loop control by an algorithm using a dual hormone system was carried out in diabetic pigs in 2007 [9]. Since then, numerous bi-hormonal closed loop studies have been conducted under various conditions in direct comparison to single hormone closed-loop and/or conventional insulin therapy [10].

Published results using dual hormone therapy are encouraging as the future treatment of type 1 diabetes. The reason why glucagon is not yet part of pump treatment is due to its physical and chemical properties: the hormone rapidly forms amyloid fibrils turning the compound into insoluble gel that occludes the infusion tubes within hours [11]. Even though the antihypoglycemic effect of the hormone seems to be intact after storage at room temperature for seven days [9, 12], formation of fibrils may increase the immunogenic response towards glucagon leading to unfavorable side effects [13]. Therefore, to use glucagon in pump therapy, a stable version of the hormone is needed that can stay soluble without degrading at various temperatures and pH-values for an extended period of time. Currently, no such commercially available glucagon compound exists. However, Zealand Pharma A/S (Zealand) has developed a stable and soluble glucagon analogue which is currently in phase II development [14].

A more elaborate introduction of the hormone glucagon is written in Chapter 2. The chapter discusses the pharmacokinetics (PK), the pharmacodynamics (PD), and the different applications of glucagon. It also provides an overview of drugs being developed to replace the current unstable glucagon products.

1.1 Hypotheses and Aims

The main ambition in the project was to develop high quality PK/PD models of a novel glucagon analogue and regular glucagon. The models should be usable for simulations that could provide new insights into the glucoregulatory dynamics, optimizing study designs and ultimately accelerating the drug development of glucagon analogues. Furthermore, good models could be used for designing and testing dual hormone artificial pancreas control algorithms, which was however beyond the scope of this project.

The project was based on regular glucagon and when possible a novel glucagon analogue developed by Zealand. Previous research related to numerical modeling, simulation, optimization and control for an artificial pancreas provided a foundation for the project [15, 16, 17]. The project was structured in three

stages with distinct foci. The three stages represented natural progression and extension of previous research in the PhD project.

1. The first stage of the project focused on characterization of PK/PD properties of a novel soluble glucagon analogue and marketed glucagon in animals. Moreover, this stage aimed to develop a model of the glucose PD as a function of insulin and glucagon.

2. The second part of the project focused on applying the developed PK/PD model to human data. Moreover, this stage aimed to cross-validate the new PD model to be used for simulation studies.

3. The third stage of the project focused on using the human PK/PD model for clinical relevant simulation studies to aid in better understanding of the dynamics and design of experiments.

1.2 Contributions

This PhD project has contributed with five publications and five posters presented at conferences in Europe and the USA. A short resume of the publications are provided here in order of publication date.

Wendt *et al.* published a technical report with the title "PK/PD modelling of glucose-insulin-glucagon dynamics in healthy dogs after a subcutaneous bolus administration of native glucagon or a novel glucagon analogue" through the Technical University of Denmark in April 2016 [18]. The publication is included in Appendix A.
The report focused on developing a simulation model of the glucose-insulin-glucagon dynamics using data from healthy dogs. The Hovorka glucoregulatory model was expanded to include a model description of the stimulatory effect of glucagon on endogenous glucose production (EGP). The report explained the applied methods including maximum a posteriori (MAP) parameter estimation and profile likelihood analysis.
Moreover, the report compared PK/PD model parameters of regular reconstituted glucagon and a novel stable liquid glucagon analogue invented by Zealand. The PD model described data satisfactorily for both glucagon and the analogue, and the parameter estimates were not significantly different between the two compounds.
Some of the applied methods are thoroughly explained in Chapter 3.

To investigate if the glucose-insulin-glucagon model translated to the human species, Wendt *et al.* published a conference paper with the title "Modelling of

Glucose-Insulin-Glucagon Pharmacodynamics in Man" which was published at the 38th annual international conference of the IEEE Engineering in Medicine and Biology Society (EMBC'16) in Orlando, Florida during August 2016 [19]. The paper is included in Appendix B.

The paper focused on fitting the previously published glucose-insulin-glucagon model to data from healthy humans. Model parameters were estimated by MAP and parameter identifiability investigated with profile likelihood analysis. The model fitted data well and enabled simulations of the glucose-insulin-glucagon dynamics within physiologic concentration ranges: glucagon (180-8000 pg/mL), insulin (1.2-81.9 mU/L) and glucose (3.3-11.5 mmol/L).

The EGP model is compared to other glucose production models and discussed in Chapter 4.

A simulation model is rarely useful or trusted without validation, therefore Wendt *et al.* published a journal paper with the title "Cross-Validation of a Glucose-Insulin-Glucagon Pharmacodynamics Model for Simulation using Data from patients with Type 1 Diabetes" which was accepted for publishing in Journal of Diabetes Science and Technology in January 2017 and published online in February [20]. The published paper is included in Appendix C.

The paper focused on validating the proposed glucose-insulin-glucagon model in patients with T1D and providing the final model parameters of the virtual patients to be used for simulation studies. Maximum likelihood (ML) and MAP methods were used for parameter estimation. Validation was carried out as a four-fold leave-one-out cross-validation with data from eight patients and assessed using mean predictive error (MPE) and mean absolute predictive error (MAPE). The model was successfully validated in seven of the patients.

The complete glucoregulatory model with equations and parameters are presented in Chapter 5.

Wendt *et al.* then published a technical report with the title "Simulating Clinical Studies of the Glucoregulatory System: *in Vivo* Meets *in Silico*" through the Technical University of Denmark in February 2017 [21]. The report is included in Appendix D.

The report contains results of various simulation studies with the validated glucose-insulin-glucagon model including replication of an *in vivo* study. It also contains simulation studies to investigate the glucoregulatory dynamics of discontinuing insulin and glucose infusions prior to glucagon administration, the delayed effect of insulin, timing of data sampling, and carryover effects from multiple SC doses of glucagon. Based on simulations, the report discussed two hypotheses of how the interactions between insulin and glucagon impact the glucose response. Finally, a study design that could potentially explore if the hypotheses are true or false were proposed.

Chapter 5 presents highlights of the report.

The simulation model showed its clinical relevance in a paper with the title "Insulin Dependent Regimen of Mini-Dose Glucagon Treatment of Mild Hypoglycaemia in Patients with Type 1 Diabetes - A Simulation Study" which will be submitted to Diabetes Technology & Therapeutics in Spring 2017 [22]. A draft of the paper is included in Appendix E.

The paper presents an original simulation study with the seven validated virtual patients. After insulin-induced mild hypoglycemia the success of various sized glucagon boluses in restoring plasma glucose in the presence of varying insulin levels was evaluated. Insulin levels were interpreted as serum concentration or effect in the body either uncorrected or normalized to factors describing the individual insulin sensitivities. The success of glucagon in treating mild hypoglycemia was based on clinically relevant criteria.

Chapter 5 presents one of the study results.

1.2.1   Summary

In summary, the main contribution of this thesis is a mathematical model describing the effect of insulin and glucagon on the EGP in patients with T1D. The novel model is built into Hovorka's glucoregulatory model. The PD model is cross-validated using clinical data in seven T1D patients and the PK/PD model parameters are estimated using ML and MAP methods. The glucose-insulin-glucagon model can be used for simulations that can provide new insights to the glucose dynamics and be a supplement to clinical studies.

Glucagon

This chapter focuses on the hormone glucagon from a drug perspective. Effects of the body on the drug, PK, and effects of the drug on the body, PD, are explained. The PK for different possible administration routes of glucagon as well as the importance of assay choice for the PK/PD relationship are highlighted. Furthermore, this chapter provides a brief overview of the regulation of EGP. Current and future applications of glucagon include but are not limited to single-use rescue treatment from severe hypoglycemia, multi-use mini-dose for treatment of mild hypoglycemia, and safety feature in a dual hormone artificial pancreas. The chapter concludes with an overview of companies officially working on developing glucagon with increased physical and chemical stability and improved user-friendliness.

2.1 About the Peptide

Glucagon is a 29-amino acid polypeptide hormone secreted by the α cells of the islets of Langerhans in the pancreas. The portion of the pancreatic islets secreting glucagon is 20%. In the liver, glucagon acts by binding to membrane-bound receptors that activates G proteins and increases cyclic AMP (cAMP) synthesis, which ultimately lead to increased glucose output from the pancreas.

High glucagon concentrations cause breakdown of fats (lipolysis) in the adipose tissues whereas the hormone has little effect on skeletal muscle and the nervous system [23].

Natural glucagon is not physically nor chemically stable in an aqueous liquid solution at natural pH. Once dissolved, the peptide starts to aggregate and form fibrils which influences its reactivity. Degraded glucagon can also cause cytotoxic effects and should therefore be avoided [11].

2.2   Pharmacokinetics

Glucagon PK exert linear dose dependency after intravenous (IV) administration of 0.25-2.0 mg in healthy volunteers [24], and after SC administration of 0.11-0.44 mg in patients with T1D [25]. Although doses up to 1.0 mg was administered SC in the study by Blauw *et al.* [25], the two highest doses did not follow the same linear dose dependency as the smaller doses.

The less than expected concentrations of glucagon after high SC doses could be explained by differences in bioavailability. In general, the bioavailability of glucagon differs between administration routes as listed in Table 2.1. The low bioavailability of glucagon after SC administration was also observed in dogs [18]. Bioavailability following SC or intramuscular (IM) administration can only be determined if studies with IV PK data in same species are available since the PK after IV dosing is defined as reference. Following SC or IM administration, bioavailability can be modelled as elimination directly from the injection site, or by reducing the modelled administered dose with a fraction according to the bioavailability.

Table 2.1: Glucagon bioavailability by administration route calculated from Graf *et al.* using AUC_{0-inf} [24]. Bioavailability after IV administration is defined as 100%.

IV	SC	IM
100%	36%	26%

2.2.1   Intravascular PK

PK profiles of glucagon after IV administration are useful but rarely published. Mühlhauser *et al.* compared the PK profiles after IV, SC and IM administra-
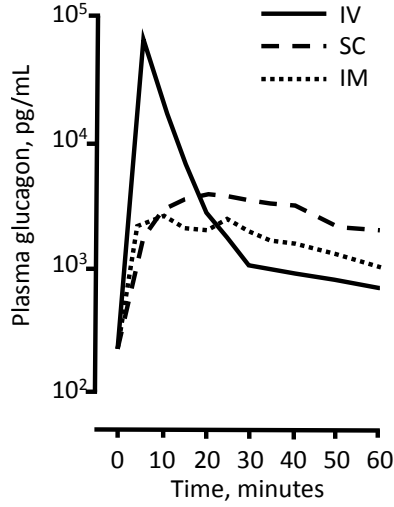
Figure 2.1: Plasma glucagon concentrations in healthy volunteers after injection of 1 mg glucagon at time 0, re-sketched from [26].

tion of glucagon in healthy volunteers as re-sketched in Figure 2.1 [26]. When viewed on a logarithmic scale, the PK profile after an IV glucagon bolus reveals to be biphasic. Normally for such an IV PK profile, the first phase represents distribution to peripheral tissues and the second phase represents elimination [27]. The biphasic PK profile and corresponding compartmental model are illustrated in Figure 2.2. The PK model for IV glucagon administration with a peripheral distribution compartment is mathematically described by:

$$\frac{\mathrm{d}Q_C(t)}{\mathrm{d}t} = u_{IV}(t) + k_r Q_P(t) - k_d Q_C(t) - k_e Q_C(t) \tag{2.1}$$

$$\frac{\mathrm{d}Q_P(t)}{\mathrm{d}t} = k_d Q_C(t) - k_r Q_P(t) \tag{2.2}$$

Q_C is the glucagon mass in the central measured compartment (plasma) and Q_P is the glucagon mass in the peripheral tissues. u_{IV} is the IV glucagon bolus. k_d is the transfer rate constant of distribution, k_r is the transfer rate constant of redistribution, and k_e is the elimination rate constant.

(a) Time-concentration profile, from [27].

(b) Compartmental model.
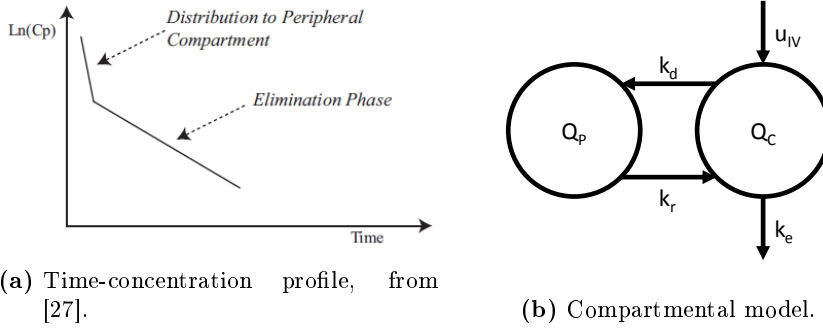
Figure 2.2: PK model for IV administration with a peripheral distribution compartment. The PK model is expressed mathematically by (2.1)-(2.2).

2.2.2 Extravascular PK

Building on the PK model for IV administration in (2.1)-(2.2), the PK model for SC or IM administration would add a compartment from which the dose is absorbed into the central compartment, see Figure 2.3. Mathematically this can be expressed as:

$$\frac{\mathrm{d}Q_I(t)}{\mathrm{d}t} = u_I(t) - k_a Q_I(t) \tag{2.3}$$

$$\frac{\mathrm{d}Q_C(t)}{\mathrm{d}t} = k_a Q_I(t) + k_r Q_P(t) - k_d Q_C(t) - k_e Q_C(t) \tag{2.4}$$

$$\frac{\mathrm{d}Q_P(t)}{\mathrm{d}t} = k_d Q_C(t) - k_r Q_P(t) \tag{2.5}$$

Q_I is the glucagon mass at the extravascular site. u_I is the glucagon bolus delivered either SC or IM. k_a is the absorption rate constant.

When the absorption phase is slower than the distribution phase it is not possible to separate the two from one another. Separate phases for absorption and distribution are not visible in glucagon PK data from humans and dogs after SC or IM bolus injection [18, 26], thus the model for extravascular administration of glucagon is for practical purposes reduced to:

$$\frac{\mathrm{d}Q_I(t)}{\mathrm{d}t} = u_I(t) - k_a Q_I(t) \tag{2.6}$$

$$\frac{\mathrm{d}Q_C(t)}{\mathrm{d}t} = k_a Q_I(t) - k_e Q_C(t) \tag{2.7}$$

Figure 2.4 visualizes a theoretical example of time-concentration profile and
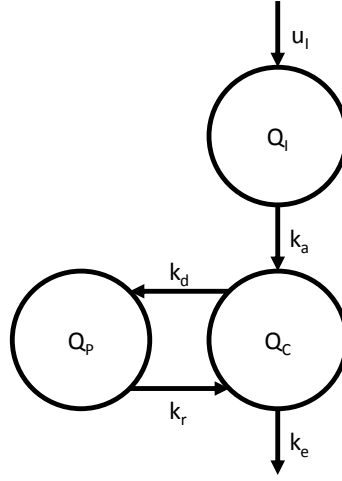
Figure 2.3: PK model for SC or IM administration with a peripheral distribution compartment. The PK model is expressed mathematically by (2.3)-(2.5).

compartmental model describing extravascular glucagon administration. The model was used by Wendt *et al.* to fit glucagon PK data after SC administration in dogs, healthy volunteers and T1D patients [18, 20]. A simpler version of the model to describe SC glucagon PK was used by Haidar *et al.* with k_a being equal to k_e [28].

Various other and more complex models describing exogenous glucagon administration have been proposed by Lv *et al.* [29]. The best model turned out to be the simplest depicted in Figure 2.5 and described mathematically by

$$\frac{\mathrm{d}Q_I(t)}{\mathrm{d}t} = u_I(t) - k_a Q_I(t) - k_{e,I} Q_I(t) \tag{2.8}$$

$$\frac{\mathrm{d}Q_T(t)}{\mathrm{d}t} = k_a Q_I(t) - k_t Q_T(t) \tag{2.9}$$

$$\frac{\mathrm{d}Q_C(t)}{\mathrm{d}t} = k_t Q_T(t) - k_e Q_C(t) + k_e Q_{basal} \tag{2.10}$$

$k_{e,I}$ is the elimination rate constant from the injection site, Q_T is a transit compartment, k_t is the transfer rate constant from the transit compartment to the central compartment, and Q_{basal} is the constant endogenous production. Comparing (2.8)-(2.10) to (2.6)-(2.7) the only differences are an extra transit compartment, bioavailability modelled by elimination directly from the injection site, and basal concentration modelled by a constant endogenous production countered by the elimination in steady state. However, adding an extra

(a) Time-concentration profile, from [27].

(b) Compartmental model.
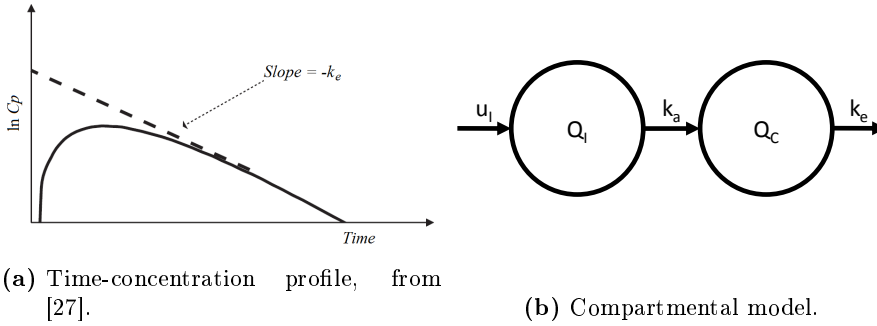
Figure 2.4: PK model for SC or IM administration. The PK model is expressed mathematically by (2.6)-(2.7).
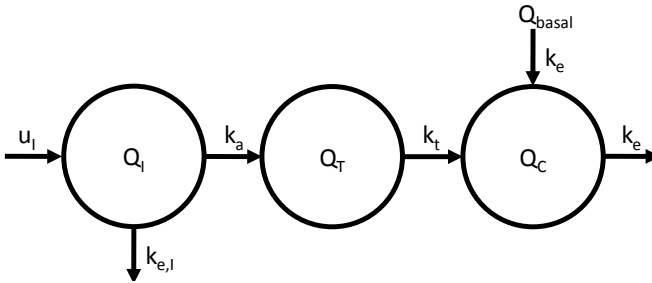
Figure 2.5: PK model for SC administration described by Lv *et al.* [29]. The PK model is expressed mathematically by (2.8)-(2.10).

transit compartment and modeling bioavailability as elimination from the injection site would require measurements of both compartments in order for all the parameters to be identifiable. With no figures showing actual data fitting of the complex models, the increased complexity and uncertainty seem unnecessary when simpler models are sufficient to describe glucagon PK after extravascular administration as published by Haidar *et al.* and Wendt *et al.* [18, 20, 28].

Usually, both healthy and T1D patients have a basal level of glucagon. The basal concentration can be modelled by adding a constant mass to (2.1) or (2.7) so that it equals 0 in steady state as demonstrated in (2.10). Another option is adding a constant concentration when calculating the glucagon concentration in the central compartment from the mass Q_C [18, 20, 28].
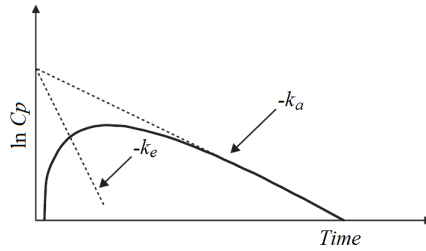
Figure 2.6: Time-concentration profile after extravascular administration with flip-flip kinetics, from [27].

2.2.3   Flip-flop kinetics

The PK exerts flip-flop kinetics when elimination rate is faster than absorption rate after extravascular administration [27, 30, 31]. Figure 2.6 illustrates how the interpretation of the time-concentration profile after SC administration changes compared to Figure 2.4a. Flip-flop kinetics can be identified when the half-life is longer following extravascular dose administration compared to intravascular [31]. Reading off the plot by Mühlhauser *et al.* [26], the half-life of glucagon is around 10 minutes after IV injection and close to 60 minutes after SC administration. Graf *et al.* found glucagon half-lives of 13, 27 and 23 minutes after IV, SC and IM injections, respectively [24]. Both studies confirm that glucagon exerts absorption limited elimination after extravascular dose administration which was also pointed out by Wendt *et al.* [18]. Knowledge of flip-flop behaviour is important in order to estimate the correct apparent clearance (Cl_F) and apparent volume of distribution ($V_{d,F}$) which are related as $k_e V_{d,F} = Cl_F$. Due to the flip-flop phenomenon, the values of k_a and k_e can swap without changing the fit. To avoid this pitfall, k_e can be parametrized so it is always greater than or equal to k_a by $k_a + \Delta k$ with Δk being positive or zero *et al.* [20, 31].

2.2.4   Assays for Sample Analysis

The absolute measured glucagon concentration in clinical samples should be compared between studies with caution since commercially available glucagon assays differ in their detection specificity, precision and accuracy [32]. Because of these differences, glucagon PK model parameters estimated from clinical data analysed by different methods, can not necessarily be compared. Changes in assay performance could influence all PK model parameters (absorption rate, elimination rate, clearance, baseline). Moreover, when glucagon PK is influ-
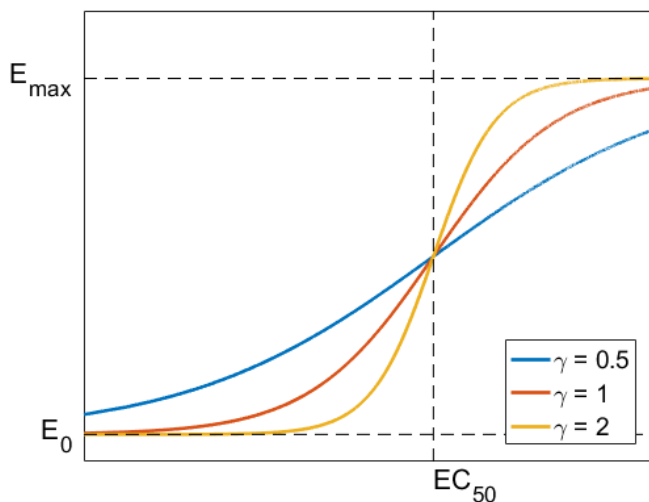
Figure 2.7: Illustration of the sigmoid E_{max} model for different values of γ with a logarithmic x-axis.

enced, parameters describing the response sensitivity to glucagon in the PD model will be influenced, too. Therefore, interpreting parameters of a PD model with glucagon as input can not be isolated from the method used for glucagon sample analysis [33]. This subject will be discussed further in Chapter 4.

2.3   Pharmacodynamics

Glucagon acts through binding to a receptor as mentioned in Section 2.1. Generally, receptor mediated responses can be modelled by the *full* Hill equation also called the sigmoid E_{max} model [34]

$$E = E_0 + \frac{(E_{max} - E_0)C^\gamma}{EC_{50}^\gamma + C^\gamma} \tag{2.11}$$

E is the effect, E_0 is the baseline effect, E_{max} is the maximal effect, EC_{50} is the concentration producing half maximal effect, C is drug concentration and γ translates to number of drug molecules per receptor. When γ is equal to 1, (2.11) reduces to the Hill equation. Figure 2.7 displays the graphical interpretation of γ in (2.11).
There is a limited number of receptors available for stimulation, thus the re-
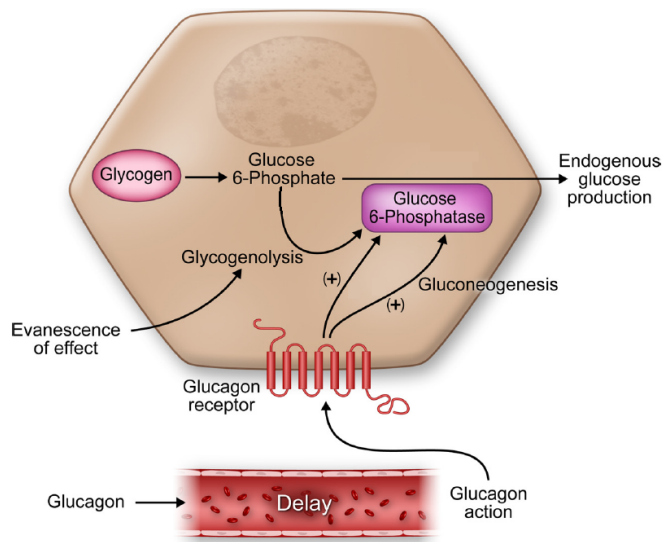
Figure 2.8: Glucagon action model, modified from [35]. Illustration of how glucagon acts via receptor mechanisms to stimulate EGP by glycogenolysis and gluconeogenesis, and the evanescence effect governing glycogenolysis only.

sponse to glucagon must saturate for high concentrations of the hormone. Saturation of dose-response was observed in two previously mentioned studies where healthy volunteers received 1 mg glucagon SC and IM which produced very similar glucose responses, even though the bioavailability between the two administration routes differ as outlined in Table 2.1 [24, 26].

Glucagon primarily affects the liver where it stimulates breakdown of glycogen to glucose through glycogenolysis [36]. The liver is highly sensitive to small changes in the glucagon concentration ($<$10 pg/mL) and responds immediately to the stimulus; thus the hormone acts as a "fine tuner" of the glucose output. Glucagon has no acute effect on formation of glucose from precursors such as lactate, pyruvate, amino acids, and glycerol known as gluconeogenesis [37]. However, during prolonged hypoglycemia exceeding three hours, glucagon stimulates gluconeogenesis rather than glycogenolysis [38]. The ambient glucose level itself does not influence the immediate response to exogenously dosed glucagon [25]. Figure 2.8 illustrates the glucagon action on the liver.

During continued exposure to glucagon, glycogenolysis wanes over time [36, 39, 40, 41]. This phenomenon has been named the evanescence effect. An explanation for the transitory response to glucagon might be desensitization of the cAMP receptor [42]. The reduced responsiveness to glucagon seem to be fully

expressed after two hours of continuous stimulation both *in vivo* and *in vitro* [36, 39, 40, 41, 42]. The refractory period needed to restore normal glucagon responsiveness remains unknown *in vivo* and little is known *in vitro* [43].

Glucagon is not the only hormone influencing the glucose homoeostasis; as opposed to glucagon, insulin inhibits glucose production [36]. However, insulin has little if any effect on gluconeogenesis in both healthy volunteers and T1D patients, whereas it efficiently inhibits glycogenolysis [36, 44, 45]. A study in healthy volunteers found that the glucose production was completely suppressed when insulin levels exceeded 60 mU/L [46]. Another study compared the glucose production during high glucagon and basal insulin, high insulin and basal glucagon, and high concentrations of both insulin and glucagon in dogs [47]. The response to glucagon during high insulin infusion was blunted. This indicates that insulin is more powerful at inhibiting glucose production than glucagon is at stimulating it. In line with these findings, a study in T1D patients by El Youssef *et al.* found that the response to micro-doses of glucagon depends on the ambient insulin level [48]. This inability of glucagon to stimulate glucose production sufficiently in the presence of high insulin levels was also observed in a closed-loop study by Russell *et al.* [49], where the average insulin level was highest among the group in which glucagon was ineffective in preventing hypoglycemia.

2.4 Modes of Use

As glucagon raises the blood glucose, the hormone could be used for treatment in all indications having difficulties keeping the blood glucose above hypoglycemia. The application is not limited to T1D, although that will be the prevailing disease to treat. Within diabetes management glucagon can be used in several different modes with increasing complexity: as a one-time rescue treatment, as multiple daily correcting bolus injections, and in a closed-loop dual hormone artificial pancreas. Glucagon also has the potential to be used in a glucagon-only pump for patients with no glucagon production or increased insulin production.

2.4.1 Rescue Treatment

Patients with T1D have a blunted endogenous glucagon response to hypoglycemia making it difficult to recover from low blood sugars [50]. If the patient experiences severe hypoglycemia and is unconscious there is two options to increase glucose levels: glucose IV, or glucagon SC or IM. A person without a

(a) GlucaGen HypoKit, Novo Nordisk **(b)** Glucagon Emergency Rescue Kit, Eli
[52]. Lilly and Company [53].

Figure 2.9: Currently marketed glucagon for treatment of severe hypo-
glycemia.

medical background or training is not able to insert an IV catheter, but most
people can give a SC or IM injection. The currently marketed rescue kits in
Figure 2.9 with 1 mg glucagon involve several difficult and crucial preparation
steps and the drug is therefore often not administered as intended by the manu-
facturer. In a study examining the usability of GlucaGen HypoKit, an average
of 20-30% of the intended dose was not administered and 69% of parents expe-
rienced handling difficulties [51].

2.4.2 Treatment of Mild Hypoglycemia

More often than severe hypoglycemia, patients with T1D experience mild hy-
poglycemia while still concious. To increase their blood glucose levels, patients
have to ingest carbohydrates like dextrose which are rapidly absorbed. This
snacking behaviour unintentionally but inevitably increases the total daily calo-
rie intake of the patient. Another means of increasing glucose levels slightly, is
through mini-doses of glucagon [54]. Administering glucagon rather than oral
carbohydrates when patients experience mild hypoglycemia will metabolize al-
ready ingested calories thereby increasing the energy expenditure of the patient
[55].
A study by Ranjan *et al.* in T1D patients showed that boluses of 100-300 μg
glucagon was sufficient to increase the blood glucose levels after insulin-induced
mild hypoglycemia [56]. Strategies for mini-doses of glucagon in combination
with a closed-loop single hormone artificial pancreas have only started to emerge
[57].
There are a few caveats to treating mild hypoglycemia with glucagon. As high-
lighted in Section 2.3, the ambient insulin level inhibits the glucose stimulating
effect of glucagon and must therefore be considered. Moreover, Ranjan *et al.*
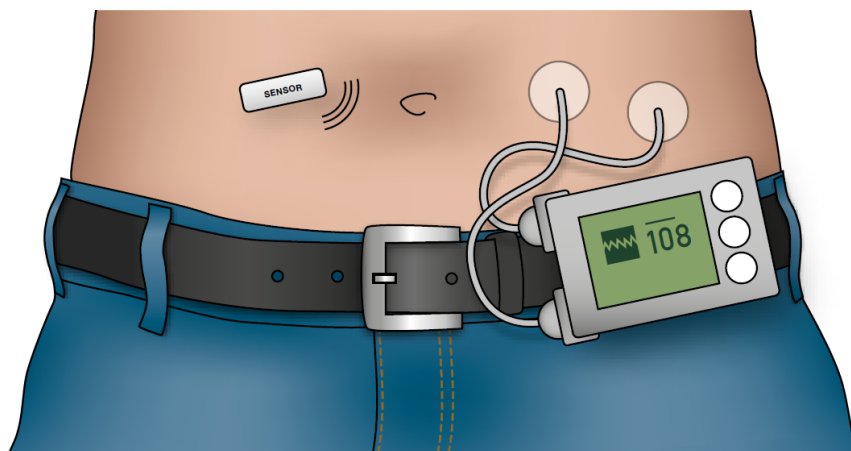
Figure 2.10: The concept of a dual hormone artificial pancreas: infusion sets for insulin and glucagon, sensor for continuous glucose monitoring, and dual chamber pump with insulin and glucagon wirelessly receiving glucose measurements and controlling hormone infusions.

found that a low carbohydrate diet impairs the effect of glucagon in treating mild insulin-induced hypoglycemia [58]. This impairment is speculated to be due to decreased storage of glycogen for glycogenolysis. On the contrary, Castle *et al.* found that eight mini-doses of glucagon within 18 hours did not deplete the glycogen stores in the liver nor did they influence the response of subsequent boluses [59].

2.4.3   The Dual Hormone Artificial Pancreas

Although substitution of oral carbohydrates with glucagon as a treatment option for mild hypoglycemia is sought, it will inevitably introduce another decision point for T1D patients. Instead, automating the decision making of both insulin and glucagon administration will alleviate the burden of diabetes care and is the ultimate treatment goal for T1D as illustrated in Figure 2.10. Less than a decade after the first feasibility trials of dual hormone closed-loop glucose control in pigs [9, 60], several closed-loop solutions both single and dual hormone are being developed worldwide [61]. The American Food & Drug Administration (FDA) has encouraged the development of artificial pancreas systems and approved the first single hormone closed-loop device in Autumn 2016, the Medtronic Minimed 670G [62, 63]. However, a community of patients and care-

givers called OpenAPS have long been desperately waiting for a commercial solution and in the meantime they built their own artificial pancreas devices, willing to put their glucose regulation in the "hands" of algorithms and devices not rigorously tested nor approved by the authorities [64]. These individuals are probably the ones having most experience with the use of closed-loop systems in real life without restrictions other than personal ones. They found that using a self-built system rather than controlling their glucose levels themselves, their HbA1c dropped, time in range increased and most subjects experienced increased sleep quality.

Undoubtedly, in T1D patients dual hormone closed loop systems increase time in target and reduce the risk of hypoglycemia compared to conventional therapy [65, 66, 67, 68, 69, 70]. Researchers argue whether a single hormone closed-loop system is sufficient for treatment of T1D or if a dual hormone artificial pancreas with glucagon adds benefits outweighing the increased complexity and costs associated with a second hormone [8, 7, 10, 71, 72, 73, 74]. With the ongoing debate, it is surprising that only few studies demonstrate head-to-head comparisons of single and dual hormone artificial pancreas systems [10]. The first study to make direct comparisons found that dual hormone closed-loop reduced hypoglycemia and the need for oral carbohydrates compared to single hormone closed-loop [75]. Subsequent studies from the group located in Montréal, Quebec have showed varying benefits of dual hormone versus single hormone, although the risk of hypoglycemia seems reduced in the dual hormone setting [76, 77, 78, 79].

Advocates of including glucagon in a dual hormone artificial pancreas argue that glucagon can prevent hypoglycemia induced from exercise. A study in T1D patients found that dual hormone closed-loop outperformed single hormone closed-loop during announced continuous and interval exercise [80], whereas another study did not find further benefits of glucagon compared to adjustment of insulin infusion before exercise onset [81]. In the latter study it should be noted that patients had glucose levels in the higher end of the normoglycemic range borderline hyperglycemia before exercise onset. Patients would instinctively refrain from exercise due to the fear of hypoglycemia when the blood glucose is in the lower normoglycemic range or borderline hypoglycemia [82]. In those situations, glucagon would add a major benefit to a closed-loop system. Moreover, a study in T1D patients found that including glucagon in an artificial pancreas can alleviate the cumbersome burden of counting carbohydrates before meal ingestion [83].

The dual hormone artificial pancreas might not only benefit T1D patients, but potentially also type 2 diabetes patients [84]. Patients becoming diabetic from one day to the other e.g. after removal of the pancreas due to cancer or chronic pancreatitis, will benefit from an automatic closed-loop device that safely and efficiently controls the blood glucose, too. Moreover, a dual hormone closed-loop system could be applied to critically ill patients not necessarily having diabetes but admitted to the intensive care unit. These patients are prone to experience

stress-induced hyperglycemia, and hypoglycemia following septic shock and thus a safe and automated device for blood glucose regulation would reduce costs and increase survival rate [85].

2.4.4   Glucagon-only Pump

Glucagon is not only relevant for treatment of hypoglycemia in T1D patients. An orphan disease named congenital hyperinsulinism belongs to the category of hyperinsulinemic hypoglycemia [86]. Patients simply produce too much insulin leading to frequent episodes of hypoglycemia. A glucagon-only closed-loop device could be used to continuously monitor the blood glucose and provide correcting boluses of glucagon throughout the day to prevent and treat hypoglycemia.

2.5   Drugs in Development

The development of new drugs takes several years, and the time from a drug is discovered till it reaches the consumer is increasing. The increasing time and cost associated with drug development is mainly due to regulatory authorities demanding larger and longer clinical trials. Traditionally, drug development can be divided in distinct phases:

- pre-clinical: Studies in animals
- clinical: Trials in humans
    - phase I: Trials in healthy volunteers - focus on safety
    - phase II: Trials in small number of patients - focus on efficacy
    - phase III: Trials in large number of patients - confirmation of safety and efficacy

Pre-clinical and clinical trials are conducted to evaluate drug safety, efficacy and dosing. Computer simulations with reliable population models can aid drug-development by allowing *in silico* trials exploring dosing size and regimen further, and investigate the effects of potential changes in clearance or metabolism [87].
The extent of clinical trials required to obtain approval from the authorities for a new drug depend on the novelty of the drug compared to previously approved

and marketed drugs. Thus getting approval of an analogue to a hormone, rather than an optimized pharmaceutical formulation of an already approved hormone, requires substantially more work and increased costs [88].

As described in Section 2.1, glucagon is not stable in an aqueous liquid solution and must be reconstituted immediately before use through numerous steps making it prone to errors. Various pharmaceutical companies across the globe are or were therefore focusing on creating a ready-to-use product. Some approaches have failed including immobilizing glucagon in a micelle [89, 90] and developing a glucagon analogue [91, 92]. Officially, there is currently four companies competing in accessing the market with an improved solution to treating hypoglycemia with glucagon. Eli Lilly and Company is altering the delivery route circumventing the need for stability in liquid solution [93]. The remaining three companies focus on developing liquid stable glucagon: Xeris Pharmaceuticals by optimizing the formulation [94], Adocia by adding excipients [95], and Zealand Pharma by altering the sequence of the original peptide thereby creating an analogue [14].

2.5.1   Nasal Glucagon by Eli Lilly and Company

In 2015 Eli Lilly and Company acquired a glucagon nasal powder from Locemia Solutions for intranasal administration [93]. The product consists of ten percent glucagon in dry powder and is intended for absorption through the nasal mucosa [96].

The absorption of nasal glucagon appear to be delayed compared to IM administration [97]. Moreover, the bioavailability after intranasal administration is lower than after IM injection, since a three times higher dose is required through the intranasal route to produce a similar response [96]. The intranasal administration of glucagon was associated with more adverse events related to head, nose, eyes, and throat than IM administration [97].

As of beginning 2017, the product is in phase III [93].

2.5.2   XeriSol™ Glucagon by Xeris Pharmaceuticals

The American based company Xeris Pharmaceuticals is developing an improved formulation for native human glucagon named XeriSol™ Glucagon (XeriSol) [94]. The native peptide is stabilized in a non-aqueous solution containing dimethyl sulfoxide (DMSO) [98]. The drug is stable for up to six days in a pump and intended for SC administration. Figure 2.11 visualizes product examples.

The PK/PD in pigs were similar to results obtained with GlucaGen (Novo Nordisk, Bagsværd, Denmark) [98, 99]. Similarity with GlucaGen was also

Figure 2.11: Example of product looks for XeriSol [94].

observed in diabetes patients [100]. However, with increasing doses, patients experienced more irritation at the injection site using XeriSol than Novo's product which could be related to the DMSO in the XeriSol formulation. Similarly to marketed glucagon, the response to mini-doses of XeriSol was dampened by the presence of insulin [101].

As of end 2016, the product for rescue treatment is in preparation for phase III [94]. The product for pen mini-dose treatment and a dual hormone artificial pancreas device is in phase II, whereas it is in preparation for phase I for treatment of congenital hyperinsulinism and for use in a glucagon-only pump.

2.5.3   BioChaperone® Glucagon by Adocia

The French company Adocia is developing a stable aqueous solution of recombinant human glucagon named BioChaperone (BC) Glucagon [95]. The native peptide is stabilized by forming a physical complex with an excipient. The drug is stable at neutral pH and intended for injection.

Based on the few preclinical results published online [95], the BC Glucagon appears to have similar effects on the glucose response as GlucaGen. The results are reported without standard errors and therefore it is not possible to conclude if the response to BC Glucagon wanes faster than the response to GlucaGen. The PK profile of BC glucagon is not published.

Currently, the product is in preclinical development. Adocia is planning to initiate a phase I trial before the end of 2017 [95].

2.5.4   Dasiglucagon by Zealand Pharma

The Danish company Zealand Pharma is developing a liquid stable glucagon analogue in aqueous solution named Dasiglucagon (proposed International Non-

Figure 2.12: Example of the look of a ready-to-use rescue pen for treatment of severe hypoglycemia with Dasiglucagon.

proprietary Name) or ZP4207 [14]. The drug is intended for SC administration. Figure 2.12 illustrates a product example.

Data from the clinical trials have not been published. However, the results confirm that Dasiglucagon is safe, well tolerated, and can raise the blood glucose level after insulin-induced hypoglycemia in T1D patients [14]. Results from another phase I trial confirm that Dasiglucagon can be used for multiple daily injections making it suitable for use in a pump or a dual hormone artificial pancreas device [102].

At the end of 2016, the product for rescue treatment and for use in a dual hormone artificial pancreas device is in phase II.

CHAPTER 3

Methods

This chapter focuses on describing the theory of the methods for model fitting applied in this thesis. Likelihood principles and their applications in parameter estimation are discussed along with parameter sensitivity analysis using profile likelihood. The chapter presents practical and advanced usage of the software package CTSM for R [103], but also illustrates workarounds to problems not yet handled directly by the package.

3.1 Model Basics

This section defines the model structure for representation of a physical system. It also provides the math associated with simulation and prediction of the future states of a system. Finally, a useful variable transformation is explained.

3.1.1   Ordinary Differential Equations

Deterministic ordinary differential equations (ODEs) can be used to model a physical system with known structure. Generally, an ODE with discrete-time observations corrupted by measurement noise is defined as

$$\mathrm{d}x_t = f(x_t, u_t, t, \theta) \cdot \mathrm{d}t \tag{3.1}$$

$$y_k = h(x_k, u_k, t_k, \theta) + e_k \quad e_k \sim N_{idd}(0, S_k) \tag{3.2}$$

x_t is the state of the system, $f(\cdot)$ is the model, u_t is the input, t is time, θ is the parameter set, y_k is the discrete observations, and e_k is the measured errors, i.e. observation noise, assumed to be independent and identically distributed (i.i.d.) following a Gaussian distribution with mean zero and variance S_k [104]. Equation (3.1) is the continuous ODE and (3.2) is the discrete observation equation.

3.1.2   Stochastic Differential Equations

One does not always know the true underlying system generating observations. This is particularly true for physiological systems. In such cases, the discrepancies between the deterministic model and data from the physical system is composed of noise from two sources: measurement noise and systemic noise. The system noise covers structural model deficiencies either from effects described incorrectly by the model or from effects not accounted for by the model. The magnitude of the systemic noise can be identified using stochastic differential equations (SDEs) with discrete-time noise corrupted measurements as

$$\mathrm{d}x_t = f(x_t, u_t, t, \theta) \cdot \mathrm{d}t + \sigma(x_t, u_t, t, \theta) \cdot \mathrm{d}w_t \quad \mathrm{d}w_t \sim N_{idd}(0, I \cdot \mathrm{d}t) \tag{3.3}$$

$$y_k = h(x_k, u_k, t_k, \theta) + e_k \qquad\qquad\qquad e_k \sim N_{idd}(0, S_k) \tag{3.4}$$

The only difference between the ODE formulation in (3.1) and the SDE formulation in (3.3) is the stochastic system noise $\sigma(x_t, u_t, t, \theta) \cdot \mathrm{d}w_t$. Thus, solving an SDE with a very small value of σ is approximating solving an ODE. The term $f(x_t, u_t, t, \theta) \cdot \mathrm{d}t$ is called the drift and is the main process driving the system when σ is smaller than one. The diffusion term is denoted by $\mathrm{d}w_t$. Together, the drift and the diffusion describes the physical state of the system.

3.1.3   Simulation

In a simulation, the system does not change over time. Moreover, the initial conditions are the only known measurements of the systems and therefore de-

termines the entire time course of the simulation. This can mathematically be expressed as

$$\hat{y}_{n|0} \quad \text{given} \quad x(t_0) = x_0 \tag{3.5}$$

An ODE as defined in (3.1) can be simulated through Euler's forward method

$$x_{n+1} = x_n + \Delta t \cdot f(x_n, u_n, \theta) \tag{3.6}$$

One realization of an SDE can be simulated in the same manor by drawing one value of Δw_n from the distribution and keeping it constant throughout the simulation using the Euler-Maruyama method:

$$x_{n+1} = x_n + \Delta t \cdot f(x_n, u_n, \theta) + \sigma(x_n, u_n, t_n, \theta) \cdot \Delta w_n \quad \Delta w_n \sim N_{iid}(0, I\Delta t) \tag{3.7}$$

The mean realization of an SDE, thus when Δw_n is zero, corresponds to the ODE solution.

3.1.4   Prediction

In the case of ODEs, prediction and simulation of a system are identical because the state is exact given the state at a previous time point. The mean prediction of a system of SDEs corresponds to simulation of an ODE. But as opposed to ODEs, prediction and simulation are not identical when considering SDEs because of the stochastic system noise which changes the system from each realization to the next.
The following illustrates prediction of the system defined in (3.3)-(3.4). The one-step prediction is defined as

$$\hat{y}_{n+1|n} \quad \text{given} \quad x(t_n) = x_n \tag{3.8}$$

More generally, the k-step prediction is defined as

$$\hat{y}_{n+k|n} \quad \text{given} \quad x(t_n) = x_n \tag{3.9}$$

Due to dw_t being a random process, the uncertainty of $\hat{x}_{n+k|n}$ and thereby $\hat{y}_{n+k|n}$ increases with increasing number of k.
Predictions are initialized with an estimate of the current state based on the previous state and the current covariance based on the previous covariance

$$\hat{x}_{k|k-1} \quad P_{k|k-1} \tag{3.10}$$

The observation equation is then linearised

$$\hat{y}_{k|k-1} = h(\hat{x}_{k|k-1}, u_k, t_k, \theta) \tag{3.11}$$

$$C_{k|k-1} = \frac{\partial h(\hat{x}_{k|k-1})}{\partial x} \tag{3.12}$$

$C_{k|k-1}$ is the derivative of the observation equation $h(\cdot)$ with respect to x evaluated at $\hat{x}_{k|k-1}$. The errors are then calculated using the extended Kalman filter as

$$\epsilon_k = y_k - \hat{y}_{k|k-1} \tag{3.13}$$

$$R_{k|k-1} = C_{k|k-1}P_{k|k-1}C_{k|k-1}^T + S_k \tag{3.14}$$

$$K_k = P_{k|k-1}C_{k|k-1}^T(R_{k|k-1})^{-1} \tag{3.15}$$

ϵ_k is the observation error vector, $R_{k|k-1}$ is the observation covariance matrix, S_k is the variance of the observation noise, and K_k is the Kalman gain. The filtered values of the state, $\hat{x}_{k|k}$, and covariance, $P_{k|k}$, are then calculated as

$$\hat{x}_{k|k} = \hat{x}_{k|k-1} + K_k\epsilon_k \tag{3.16}$$

$$P_{k|k} = P_{k|k-1} + K_kR_{k|k-1}K_k^T \tag{3.17}$$

The new 1-step predictions are found by solving the following system of differential equations

$$\frac{d\hat{x}_k(t)}{dt} = f(\hat{x}_k(t)) \qquad\qquad \hat{x}(t_k) = \hat{x}_{k|k} \tag{3.18}$$

$$\frac{dP_k(t)}{dt} = \frac{\partial f(x)}{\partial x}P_k(t) + P_k(t)\left(\frac{\partial f(x)}{\partial x}\right)^T + \sigma\sigma^T \quad P_k(t_k) = P_{k|k} \tag{3.19}$$

$$\hat{x}_{k+1|k} = \hat{x}_k(t_{k+1}) \tag{3.20}$$

$$P_{k+1|k} = P_k(t_{k+1}) \tag{3.21}$$

Table 3.1 shows a direct comparison of the steps involved in predictions of ODEs and SDEs using the same notation.

3.1.5 Lamperti Transformation

Some implementations for solving SDEs do not allow the system noise to depend directly on the state of the system as defined in (3.3) [104]. Thus, the system equations must be written in a form satisfying

$$dz_t = f(z_t, u_t, t, \theta) \cdot dt + \sigma(u_t, t, \theta) \cdot dw_t \tag{3.22}$$

Table 3.1: Direct comparison of 1-step prediction in ODEs and SDEs. A) model structure. B) initial condition(s). C) linearisation of the observations. D) filtering. E) filtered state. F) updated system. G) one step prediction.

	ODE	SDE
A	$dx_t = f(x_t, u_t, t, \theta) \cdot dt$ $y_k = h(x_k, u_k, t_k, \theta) + e_k \qquad e_k \sim N_{idd}(0, S_k)$	$dx_t = f(x_t, u_t, t, \theta) \cdot dt + \sigma(x_t, u_t, t, \theta) \cdot dw_t \qquad dw_t \sim N_{idd}(0, I \cdot dt)$ $y_k = h(x_k, u_k, t_k, \theta) + e_k \qquad e_k \sim N_{idd}(0, S_k)$
B	$\hat{x}_{k|k-1}$	$\hat{x}_{k|k-1}$ $P_{k|k-1}$
C	$\hat{y}_{k|k-1} = h(\hat{x}_{k|k-1}, u_k, t_k, \theta)$ $R_{k|k-1} = S_k$	$\hat{y}_{k|k-1} = h(\hat{x}_{k|k-1}, u_k, t_k, \theta)$ $C_{k|k-1} = \dfrac{\partial h(\hat{x}_{k|k-1})}{\partial x}$
D	$\epsilon_k = y_k - \hat{y}_{k|k-1}$	$\epsilon_k = y_k - \hat{y}_{k|k-1}$ $R_{k|k-1} = C_{k|k-1} P_{k|k-1} C^T_{k|k-1} + S_k$ $K_k = P_{k|k-1} C^T_{k|k-1} (R_{k|k-1})^{-1}$
E	$\hat{x}_{k|k} = \hat{x}_{k|k-1}$	$\hat{x}_{k|k} = \hat{x}_{k|k-1} + K_k \epsilon_k$ $P_{k|k} = P_{k|k-1} + K_k R_{k|k-1} K^T_k$
F	$\dfrac{d\hat{x}_k(t)}{dt} = f(\hat{x}_k(t)) \qquad \hat{x}(t_k) = \hat{x}_{k|k}$	$\dfrac{d\hat{x}_k(t)}{dt} = f(\hat{x}_k(t))$ $\dfrac{dP_k(t)}{dt} = \dfrac{\partial f(x)}{\partial x} P_k(t) + P_k(t) \left(\dfrac{\partial f(x)}{\partial x}\right)^T + \sigma\sigma^T \qquad \hat{x}(t_k) = \hat{x}_{k|k} \qquad P_k(t_k) = P_{k|k}$
G	$\hat{x}_{k+1|k} = \hat{x}_k(t_{k+1})$	$\hat{x}_{k+1|k} = \hat{x}_k(t_{k+1})$ $P_{k+1|k} = P_k(t_{k+1})$

To maintain the property of state dependent diffusion without explicitly writing it in the state equations, the SDE may be transformed using the Lamperti transformation [104, 105, 106]. Generally, the Lamperti transformation is expressed as

$$\Psi = \int \frac{1}{\sigma(\xi)} \mathrm{d}\xi|_{\xi=x_t} \tag{3.23}$$

In the special case were the system noise is directly proportional to the state, i.e $\sigma(x_t) = x_t$, the Lamperti transformation uses the following change of variables according to (3.23)

$$\Psi(x_t) = \log(x_t) = z_t \Leftrightarrow x_t = e^{z_t} \tag{3.24}$$

$$\Psi'(x_t) = \frac{1}{x_t} \tag{3.25}$$

$$\Psi''(x_t) = -\frac{1}{x_t^2} \tag{3.26}$$

(3.24)-(3.26) are inserted into Itô's lemma [107]

$$\mathrm{d}z_t = \Psi'(x_t) \cdot \mathrm{d}x_t + \frac{1}{2}\Psi''(x_t) \cdot \sigma^2(x_t) \cdot \mathrm{d}t \tag{3.27}$$

$$= \frac{1}{x_t}\mathrm{d}x_t - \frac{1}{2}\frac{1}{x_t^2}\sigma^2(x_t) \cdot \mathrm{d}t \tag{3.28}$$

The transformation is best illustrated with an example. Consider a simple two states model often used to describe PK of SC administered drugs distributing in one plasma compartment with state dependent diffusion

$$\mathrm{d}x_1(t) = (u(t) - k_1 x_1(t)) \cdot \mathrm{d}t + \sigma_1 x_1(t)\mathrm{d}w_1 \tag{3.29}$$

$$\mathrm{d}x_2(t) = (k_1 x_1(t) - k_2 x_2(t)) \cdot \mathrm{d}t + \sigma_2 x_2(t)\mathrm{d}w_2 \tag{3.30}$$

Using (3.28) the system in (3.29)-(3.30) is transformed to

$$\mathrm{d}z_1(t) = \frac{1}{x_1(t)}\left((u(t) - k_1 x_1(t)) \cdot \mathrm{d}t + \sigma_1 x_1(t)\mathrm{d}w_1\right) - \frac{1}{2}\frac{1}{x_1^2(t)}\sigma_1^2 x_1^2(t)\mathrm{d}t \quad (3.31)$$

$$= \left(\frac{u(t)}{x_1(t)} - k_1\right) \cdot \mathrm{d}t + \sigma_1 \mathrm{d}w_1 - \frac{1}{2}\sigma_1^2 \mathrm{d}t \quad (3.32)$$

$$= \left(u(t) \cdot e^{-z_1(t)} - k_1 - \frac{\sigma_1^2}{2}\right) \cdot \mathrm{d}t + \sigma_1 \mathrm{d}w_1 \quad (3.33)$$

$$\mathrm{d}z_2(t) = \frac{1}{x_2(t)}\left((k_1 x_1(t) - k_2 x_2(t)) \cdot \mathrm{d}t + \sigma_2 x_2(t)\mathrm{d}w_2\right) - \frac{1}{2}\frac{1}{x_2^2(t)}\sigma_2^2 x_2^2(t)\mathrm{d}t$$
$$(3.34)$$

$$= \left(k_1 \frac{x_1(t)}{x_2(t)} - k_2\right) \cdot \mathrm{d}t + \sigma_2 \mathrm{d}w_2 - \frac{1}{2}\sigma_2^2 \mathrm{d}t \quad (3.35)$$

$$= \left(k_1 \cdot e^{z_1(t)-z_2(t)} - k_2 - \frac{\sigma_2^2}{2}\right) \cdot \mathrm{d}t + \sigma_2 \mathrm{d}w_2 \quad (3.36)$$

Equation (3.24) is used to transform the solution back to the units of the original system.

3.2 Likelihood Principles

The likelihood measures how likely a set of parameters are given a model and data. Different parameters of the model will give different values of the likelihood function. Finding the parameter set that maximizes the likelihood function for given data and model gives the ML.

The likelihood is equal to the probability density considered as a function of the parameter set, θ, and a time series, Y_N, of N observations exemplified in Figure 3.1.

$$L(\theta, Y_N) = p(Y_N|\theta) = \left(\prod_{k=1}^{N} p(y_k|Y_{k-1}, \theta)\right) p(y_0|\theta) \quad (3.37)$$

where

$$Y_k = [y_k, y_{k-1}, ..., y_1, y_0] \quad (3.38)$$

Thus the likelihood is a product of the initial probability density, $p(y_0|\theta)$, and all subsequent conditional probability densities. Practically, this approach is computationally infeasible as it would involve solving the Fokker-Planck equation
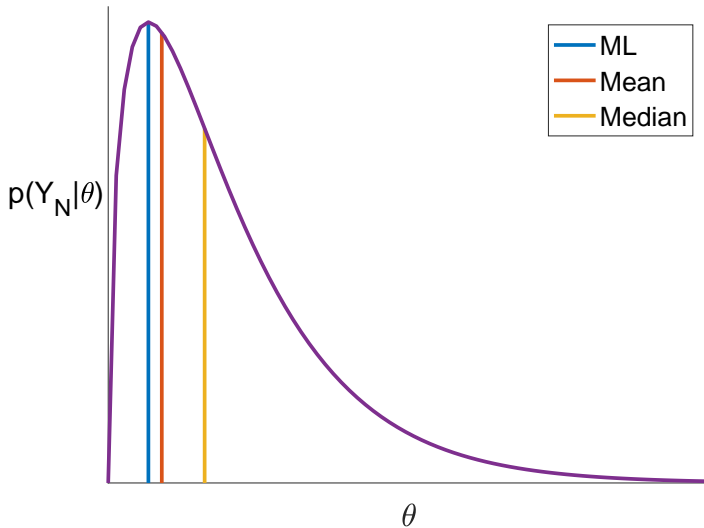
Figure 3.1: Qualitative example of a non-symmetrical one-dimensional likelihood function. The likelihood function could have multiple local maxima. The likelihood function has the same dimensionality as the number of parameters in θ. The ML estimate, mean estimate and median estimate are illustrated for comparison.

and instead Kalman filtering can be used. When the model structure is linear the Kalman filter is exact. However, when the model structure is nonlinear the extended Kalman filter must be used which only provides approximations of the observation error and covariance. By using (3.13)-(3.14) equation (3.37) becomes

$$p(Y_N|\theta) = \left(\prod_{k=1}^{N} \frac{\exp\left(-\frac{1}{2}\epsilon_k^T R_{k|k-1}^{-1}\epsilon_k\right)}{\sqrt{\det(R_{k|k-1})}\left(\sqrt{2\pi}\right)^l} \right) p(y_0|\theta) \tag{3.39}$$

In practice, one rarely maximizes the likelihood function, instead the negative log-likelihood is used for minimization. Conditioning the posterior probability on y_0 and taking the negative logarithm on both sides we obtain the negative log-likelihood function

$$-\log(p(Y_N|\theta, y_0)) = \frac{1}{2}\sum_{k=1}^{N} \left(\log(\det(R_{k|k-1})) + \epsilon_k^T R_{k|k-1}^{-1}\epsilon_k \right) \tag{3.40}$$

$$+\frac{1}{2}\log(2\pi)\sum_{k=1}^{N} l$$

Consequently, the ML-parameters are determined by computing

$$\hat{\theta}_{ML} = \arg\min_{\theta \in \Theta} \left\{ \sum_{k=1}^{N} \left(\log(\det(R_{k|k-1})) + \epsilon_k^T R_{k|k-1}^{-1} \epsilon_k \right) \right\} \tag{3.41}$$

ϵ_k is the one-step prediction error defined in (3.13) and $R_{k|k-1}$ is the covariance defined in (3.14) computed using the extended Kalman filter.

Kalman filter approximations can similarly be used during k-step predictions as during 1-step predictions. For the Kalman filter to be a good approximation it requires a sufficiently fast sampling frequency and accuracy of observations. Further details on Kalman filtering can be found in [108].

3.2.1 Profile Likelihood

Visualization of the likelihood function becomes difficult when a parameter set includes more than three parameters. Cross sections of the likelihood function are called likelihood profiles. The simplest likelihood profile of parameter θ_i is found by keeping all other parameters of θ constant and then plotting the likelihood as a function of θ_i. With this approach, the value of θ_i that maximizes the likelihood function depends on the choice of fixed parameters in θ. However, this approach largely underestimates the uncertainties of the profiled parameter. A better approach to likelihood profiling is for fixed values of the parameter θ_i to optimize the likelihood for all other parameters of θ, and then plot the optimal likelihood as a function of θ_i [109, 110]. Mathematically this is defined as

$$L_p(\theta_i, Y_N) = \max_{\theta \setminus \theta_i} L(\theta, Y_N) \tag{3.42}$$

The value of θ_i that maximizes $L_p(\theta_i, Y_N)$ is the global maximizer of the likelihood function.

The profile likelihood of a parameter can be used to evaluate whether the parameter in the model is identifiable. Identifiability of parameters are determined by model structure (structural identifiability) and the input dynamics (practical identifiability) [109].

Structural identifiability is related to having a unique representation of the model for each parameter set. Profile likelihood analysis provides a method for investigating the parameter identifiability even in large complex systems, where it can be difficult to evaluate the model uniqueness directly.

Practical identifiability is related to the dynamics of the input. Thus, a model can only identify parameters describing dynamics present in data used for model fitting. Also in this case, profile likelihood analysis is a powerful tool.

A parameter is identifiable only if the maximum of the profile likelihood is well defined [109]. Whether the maximum of the profile likelihood of θ_i is well defined
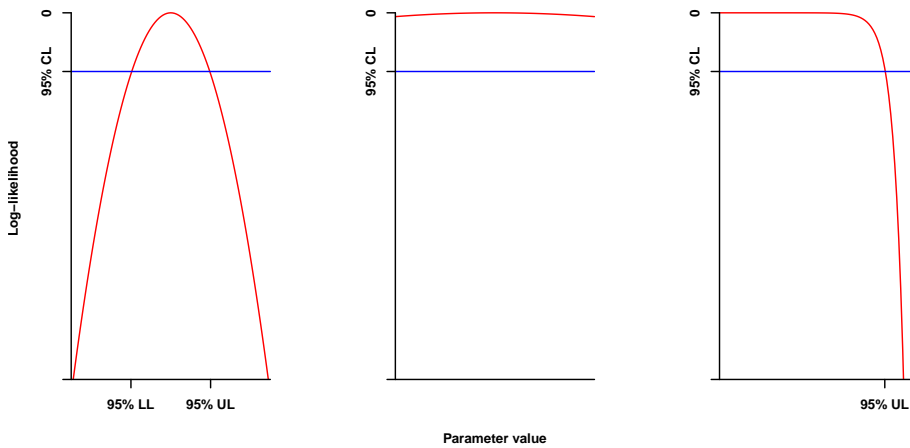
Figure 3.2: Theoretical examples of three types of profile likelihood plots; from left to right: highly peaked (identifiable), flat (structural non-identifiable), and asymmetric (practical non-identifiable). The 95% confidence limit (CL) is blue. The x-axis shows the 95% lower limit (LL) and upper limit (UL) of the parameter value. Graph from [18].

is evaluated using a 100(1-α)% confidence interval bound by when the natural logarithm of a likelihood ratio test exceeds a chi-squared distribution [110].

$$\log\left(\frac{L_p(\theta_i, Y_N)}{L(\hat{\theta}, Y_N)}\right) = \log(L_p(\theta_i, Y_N)) - \log(L(\hat{\theta}, Y_N)) > -\frac{1}{2}\chi_{1-\alpha}^2 \qquad (3.43)$$

In words, the profile likelihood is log-transformed yielding the profile log-likelihood. The maximum value of the profile log-likelihood is subtracted from the profile log-likelihood so that the maximum function value is zero. The limit of the confidence interval is determined by the 100(1-α) percentile of the chi-squared distribution with one degree of freedom. As an example, a 95% confidence interval of a model parameter is bound by the log-likelihood ratio exceeding approximately -1.92. A profile likelihood confidence interval could be asymmetric, whereas e.g. the Wald statistic applies a quadratic and thus symmetric approximation of the confidence interval [110]. Figure 3.2 provides examples of symmetric and asymmetric profile likelihoods that are either identifiable or non-identifiable.

3.2.2 Bayesian Inference

Bayesian estimates refer to parameters of a model being treated as random variables belonging to some distribution. To fit a parameter in a Bayesian framework, a prior distribution of the parameter is needed. The prior distribution of a parameter describes the population, whereas a single realization of the parameter from the distribution describes an individual.

The parameters of the prior distribution are called hyper-parameters i.e. if a prior follows a normal distribution, two hyper-parameters define it: mean (μ) and standard deviation (σ). A normally distributed prior for parameter θ_i is thus defined as

$$\theta_i \sim N(\mu_{\theta_i}, \sigma_{\theta_i}^2) \tag{3.44}$$

The estimated parameter will then be a summary of the posterior probability density function conditioned on the data and the prior. The posterior distribution of a parameter, θ, given the data, Y_N, is identified using Bayes' theorem.

$$p(\theta|Y_N) = \frac{p(Y_N|\theta)p(\theta)}{p(Y_N)} \tag{3.45}$$

$p(\theta)$ is the prior distribution of θ, $p(Y_N)$ is the marginal distribution, and $p(Y_N|\theta)$ is the likelihood of Y_N given θ as defined in (3.37).

Finding the set of parameters given data, a model and prior distributions of parameters yielding the maximum of the posterior distribution is called MAP.

3.2.3 Maximum a Posteriori Estimation

MAP estimation is an optimization approach seeking the parameter estimate that maximizes the posterior distribution [111]. Maximizing (3.45) then reduces to optimizing:

$$p(\theta|Y_N) \propto p(Y_N|\theta)p(\theta) \tag{3.46}$$

MAP estimation reduces to maximizing the likelihood function when the prior is a uniform distribution, i.e. $p(\theta)$ is constant, see (3.37) and (3.46). This indicates that ML is a special case of MAP. Also, the weaker a prior is, i.e. having a large standard deviation, the less difference there is between MAP estimation and ML. In general, one distinguishes between informative (highly peaked) and non-informative (not peaked) priors. Thus, the likelihood profile of a parameter estimated by MAP is composed of the likelihood of the parameter itself conditioned on the data and the prior parameter distribution.

Introducing the following notation where σ_θ is a matrix with the prior standard deviations in the diagonal and R_θ is the prior correlation matrix:

$$\mu_\theta = E\{\theta\} \tag{3.47}$$

$$\Sigma_\theta = \sigma_\theta R_\theta \sigma_\theta = V\{\theta\} \tag{3.48}$$

$$\epsilon_\theta = \theta - \mu_\theta \tag{3.49}$$

Assuming that the prior parameters follow Gaussian distributions as defined in (3.44) and using equation (3.39), the posterior distribution in (3.46) can be rewritten as

$$p(\theta|Y_N) \propto \left(\prod_{k=1}^{N} \frac{\exp\left(-\frac{1}{2}\epsilon_k^T R_{k|k-1}^{-1}\epsilon_k\right)}{\sqrt{\det(R_{k|k-1})}\left(\sqrt{2\pi}\right)^l} \right) p(y_0|\theta) \frac{\exp\left(-\frac{1}{2}\epsilon_\theta^T \Sigma_\theta^{-1}\epsilon_\theta\right)}{\sqrt{\det(\Sigma_\theta)}\left(\sqrt{2\pi}\right)^p} \tag{3.50}$$

Conditioning the posterior probability on y_0 and taking the negative logarithm gives:

$$-\log(p(\theta|Y_N, y_0)) \propto \frac{1}{2}\sum_{k=1}^{N}\left(\log(\det(R_{k|k-1})) + \epsilon_k^T R_{k|k-1}^{-1}\epsilon_k\right) + \tag{3.51}$$

$$\frac{1}{2}\left(\left(\sum_{k=1}^{N} l\right) + p\right)\log(2\pi) + \frac{1}{2}\log(\det(\Sigma_\theta)) + \frac{1}{2}\epsilon_\theta^T \Sigma_\theta^{-1}\epsilon_\theta$$

The MAP solution is found by solving the nonlinear optimization problem:

$$\hat{\theta}_{MAP} = \arg\min_{\theta \in \Theta}\{-\log(p(\theta|Y_N, y_0))\}$$

$$= \arg\min_{\theta \in \Theta}\left\{ \sum_{k=1}^{N}\left(\log(\det(R_{k|k-1})) + \right.\right. \tag{3.52}$$

$$\left.\left. \epsilon_k^T R_{k|k-1}^{-1}\epsilon_k\right) + \log(\det(\Sigma_\theta)) + \epsilon_\theta^T \Sigma_\theta^{-1}\epsilon_\theta \right\}$$

This nonlinear optimization can be non-trivial to solve analytically through gradient-methods, but can be approximated with a finite difference method [112]. Another method for finding the MAP solution is by using Markov Chain Monte Carlo (MCMC) simulations. MCMC is a brute force method that samples from the posterior distribution to create a rough shape of the posterior distribution and thereby estimates the MAP solution as implemented in Win-BUGS [113, 114]. It is computationally time consuming because it can require thousands of samples before reaching convergence. On the contrary, gradient methods converge faster, but suffer great difficulties if the objective function is noisy with local gradients not leading to a smaller value of the objective function.

3.3 Parameter Estimation in CTSM-R

Continuous time stochastic modeling (CTSM) is also known as grey-box modeling with one or more system equations being stochastic [111]. One tool to handle CTSM is the CTSM-R package for R [103]. The software package uses likelihood principles as described in Section 3.2 and a finite-difference approximation method to gradient-based optimization method to find the most likely set of model parameters for a series of observations.

The commands of the following sections will refer to R functions and the R environment thereby providing some practical information for use of the CTSM-R package, which might not be straightforward.

Algorithm 1 Defining CTSM-R model and estimating model parameters.

Require: ctsmr
    Define CTSM-R model object: model = ctsm$new()
    Define system equations:
    model$addSystem(dx1~(Dose-x1/tmax)*dt+sigma1*dw1)
    model$addSystem(dx2~(x1/tmax-x2/tmax)*dt+sigma2*dw2)
    Define observation equation:
    model$addObs(conclog~log(1/tmax*x2/(BW*ClF)*1e6+Ib))
    Define observation variance: model$setVariance(conclog~exp(ls))
    Define input: model$addInput(Dose)
    Set options e.g.: model$options$InitialVarianceScaledIdentity = TRUE and
    model$options$inputinterpolation = FALSE
    Build CTSM-R model: ctsmr:::Compile(model)
    Set initial values for states and parameters (only a subset shown):
    model$setParameter(x10=0, Ib=c(μ_{I_b},min$_{I_b}$,max$_{I_b}$)),
    tmax=c(μ_{tmax},min$_{tmax}$,max$_{tmax}$,psd=σ_{tmax})
    Fit ← model$estimate(data)

3.3.1 Fitting One Data Set

To fit a single data set using CTSM-R, one must first define the model, set the initial guesses for model states and parameters and then estimate the model parameters as in Algorithm 1. Various options can be set depending on the problem at hand. Model parameters and initial values of states can be estimated in the CTSM-R environment as indicated in Algorithm 1, where x10 is the initial value of state x1 which is fixed, I_b is a parameter estimated by ML, and tmax is a parameter estimated by MAP. Further practical information can be found in [103].

3.3.2   Fitting Multiple Data Sets

CTSM-R also allows parameter estimation in multiple independent data sets. However, the package requires that initial values are equal in all data sets. As this is rarely the case in biological data sets, the objective function must be defined manually and an appropriate optimizer chosen [103]. To implement MAP estimation for multiple data sets, first the negative log-likelihood as a function of a data set and a parameter set was defined as in Algorithm 2. The joint likelihood function for multiple data sets was calculated as in Algorithm 3. The optimal parameter set across multiple datasets was then found by optimizing Algorithm 3 using constrained optimization with `nlminb()`.

It should be noted, that Algorithm 3 has a minor error leading to the priors having unchanged influence despite multiple datasets. The MAP solution for J datasets should have been implemented as

$$
\hat{\theta}_{MAP,J} = \arg\min_{\theta \in \Theta} \left\{ \sum_{j=1}^{J} \left(\sum_{k=1}^{N} \left(\log(\det(R_{k|k-1})) + \right. \right. \right. \tag{3.53}
$$
$$
\left. \left. \left. \epsilon_k^T R_{k|k-1}^{-1} \epsilon_k \right) \right) + \log(\det(\Sigma_\theta)) + \epsilon_\theta^T \Sigma_\theta^{-1} \epsilon_\theta \right\}
$$

Thus, the more datasets available, the proportionally less impact of the priors on the MAP solution.

Algorithm 2 Manual implementation of the negative log-likelihood.

> **function** −Log-Likelihood(parameters, data)
>> $(\text{data}_{\text{predict}}, \text{SD}_{\text{predict}}) \leftarrow \text{predict}(\text{parameters, data}))$
>> $y \leftarrow \text{data}$
>> $\hat{y} \leftarrow \text{data}_{\text{predict}}$
>> $y_{SD} \leftarrow \text{SD}_{\text{predict}}$
>> log-likelihood $\leftarrow -\frac{1}{2} \sum_{n=1}^{N} \frac{(y-\hat{y})^2}{y_{SD}^2} - \sum_{n=1}^{N} \log y_{SD} - (N-1)\frac{1}{2} \log 2\pi$
>> **return** −log-likelihood
> **end function**

3.3.3   Calculating the Parameter Uncertainties

When CTSM-R is not used for optimization of the model parameters, the associated uncertainties are not estimated directly. The parameter uncertainties can

---

Algorithm 3 Manual implementation of MAP estimate of multiple data sets.

Require: Set prior distribution of parameter$_i \sim \mathrm{N}(\mu_i, \sigma_i)$
   function $-$MULTIDATA MAP(parameter$_{i=1..I}$, data$_{j=1..J}$)
      $V_{MAP} \leftarrow 0$
      for j=1..J **do**
         Set initial values for data$_j$
         $V_{MAP} \leftarrow V_{MAP} + -$Log-Likelihood(parameter$_{i=1..I}$, data$_j$) ...
         $-\sum\limits_{i=1}^{I}$ dnorm(parameter$_i$,mean=μ_i,sd=σ_i,log=TRUE)
      end for
      return $-V_{MAP}$
   end function

---

then be calculated using an approximation of the inverse Hessian, which provides the curvature of the log-likelihood function [110]. Calculations of parameter uncertainties using R are explained in Algorithm 4. We used the function `hessian` from the R package `numDeriv` to approximate the Hessian. The parameter "r" controls the precision of the numerically derived Hessian with a default value of 4. In some cases it was necessary to increase the precision at the cost of more evaluations in order to get non-negative diagonal elements of the inverse Hessian.

Algorithm 4 Estimation of model parameter uncertainties using the Hessian.

Require: numDeriv
   Calculate the Hessian as hessian(object function, optimized parameters, method="Richardson", method.args=list(r=6), extra parameters to object function)
   Calculate Hessian^{-1} by solve(Hessian)
   Calculate the SD of parameters by $\sqrt{\mathrm{diag}(\mathrm{Hessian}^{-1})}$

3.3.4   Optimization with Genetic Algorithms

Object functions defined outside the CTSM-R environment, but using optimizations from the package for parts of the calculations can sometimes be noisy. This noise can stem from numerical approximations. As an example, if one wishes to optimize the distribution of population parameters, i.e. the priors for MAP estimation, based on multiple individual datasets, the object function for the problem can be noisy. When the object function is non-smooth, gradient based optimizers have difficulties converging to the global maximum and are likely to
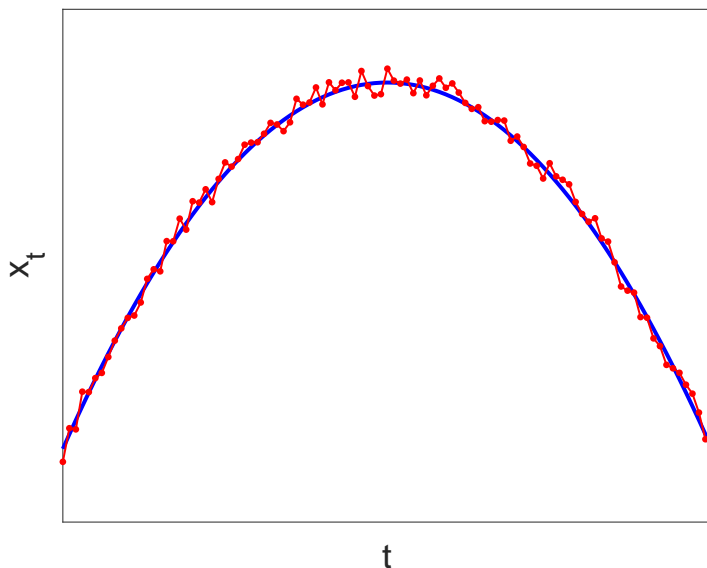
Figure 3.3: Example of the true object function (blue) and the noisy realization of the object function (red). Many local maxima are present in the noisy realization of the object function.

stop in a local maximum instead [115]. Although they are computationally fast, if one uses a gradient based optimizer on the noisy object function exemplified in Figure 3.3, the solution will highly depend on the starting guess. To avoid this, a non-gradient based optimizer like genetic algorithms (GA) could be used for optimizations of non-smooth object functions [116].

GA can be slow and computationally heavy. However, with some tuning of the optimizer settings, GA often reach fast convergence. Moreover, the optimization can be speeded up by allowing parallel computations. The tuning is a compromise between getting to the solution fast and not stopping the iterations sooner than the parameter space has been explored sufficiently. Although GA have global convergence one can not be completely certain that the optimizer finds the global maximum - there might still exist a solution with an even better fit that has yet to be discovered.

The principles of GA are inspired by biological evolution. A population of possible parameter sets are created at the beginning of each iteration. During an iteration the value of the object function is determined for each parameter set. To find the population of the next iteration the best parameter sets of the current iteration are used to build new parameter sets by combining different parts of the best parameter sets with each other (cross-over) and occasionally introduce ran-

dom parameter values (mutations). The optimization is stopped when the best solution does not improve after a certain number of consecutive populations. Tuning of GA involves setting the population size, cross-over rate, mutation rate, number of best solutions to keep for next iteration (elitism), maximum number of iterations, and maximum number of runs without improvement.

CHAPTER 4

Models of Endogenous Glucose Production

This chapter focuses on presenting and discussing models of a small part of the glucoregulatory system - the glucose production of the liver. Large glucoregulatory models including many different effects like meals and exercise are not described, but can be found in the literature [117, 118, 119]. The here presented models describe how the EGP is stimulated by glucagon and some models describe the inhibitory effects of insulin, too. Models of EGP without glucagon action are not considered [117, 120].

Simulations provide a direct comparison of the responses of the different models to a glucagon bolus and a glucagon infusion. Furthermore, models including the effect of insulin on EGP are compared using simulation of a glucagon bolus preceded by an insulin bolus. The models in sections 4.6-4.8 each contain one unique element: the evanescence effect of glycogenolysis, the glucagon rate of change, and saturation of glycogenolysis. All proposed models are discussed at the end of the chapter and related to the physiology described in Chapter 2.

4.1 Simulation Scenario

The EGP models in this chapter were implemented in MATLAB along with glucagon and insulin PK models. The glucagon PK model was described by (4.1)-(4.3). Similarly, the insulin PK model was described by (4.4)-(4.6).

$$\frac{\mathrm{d}Z_1(t)}{\mathrm{d}t} = u_C(t) - k_1 Z_1(t) \tag{4.1}$$

$$\frac{\mathrm{d}Z_2(t)}{\mathrm{d}t} = k_1 Z_1(t) - k_2 Z_2(t) \tag{4.2}$$

$$C(t) = \frac{k_2 Z_2(t)}{W \cdot Cl_{F,C}} + C_b \tag{4.3}$$

$$\frac{\mathrm{d}X_1(t)}{\mathrm{d}t} = u_I(t) - \frac{X_1(t)}{t_{max}} \tag{4.4}$$

$$\frac{\mathrm{d}X_2(t)}{\mathrm{d}t} = \frac{X_1(t)}{t_{max}} - \frac{X_2(t)}{t_{max}} \tag{4.5}$$

$$I(t) = \frac{1}{t_{max}} \frac{X_2(t)}{W \cdot Cl_{F,I}} 10^6 + I_b \tag{4.6}$$

The glucagon and insulin PK models are explained in details in Section 5.1. For the current purpose of comparable EGP simulations, the PK model parameters were based on a single virtual patient with parameters listed in Table 4.1. The EGP models were implemented in MATLAB according to the original scientific publications to the best of the author's knowledge.

Table 4.1: Specific model parameter values used for simulation of the glucagon and insulin PK models. Occasionally, some of these parameters are also included in the EGP models.

Parameter	Value	Unit
W	69	kg
k_1	0.058	min^{-1}
k_2	0.058	min^{-1}
$Cl_{F,C}$	159	mL/kg/min
C_b	10.9	pg/mL
t_{max}	67.9	min
$Cl_{F,I}$	17.4	mL/kg/min
I_b	8.7	mU/L
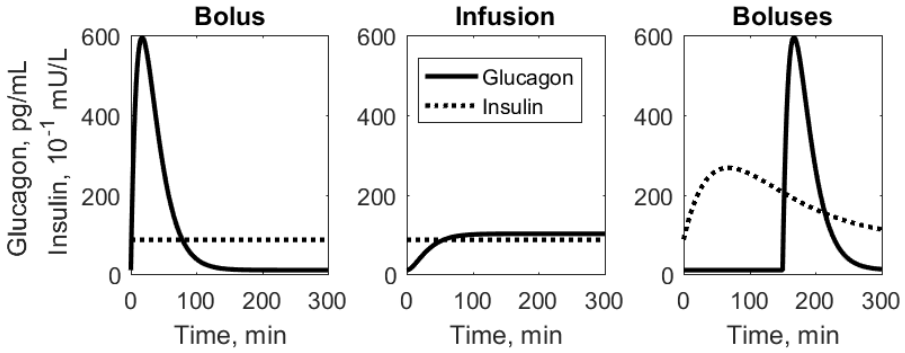
Figure 4.1: Simulated plasma glucagon and serum insulin concentrations after a SC glucagon bolus of 0.3 mg (left), SC continuous glucagon infusion of 1 μg/minute (middle), and SC insulin bolus of 4 U at t=0 and SC glucagon bolus of 0.3 mg at t=150 (right).

The PK models were used to perform three simulation scenarios:

- Euglycemic clamp (5 mmol/L), constant basal insulin (I_b), SC glucagon bolus of 0.3 mg at t=0

- Euglycemic clamp (5 mmol/L), constant basal insulin (I_b), SC glucagon infusion of 1 μg/minute starting at t=0

- Euglycemic clamp (5 mmol/L), SC insulin bolus of 4 U at t=0, SC glucagon bolus of 0.3 mg at t=150 minutes

The simulated glucagon and insulin concentrations of each of these scenarios are displayed graphically in Figure 4.1 and were used as inputs to the EGP models to compare their strengths and weaknesses, and to investigate how certain parameters influence the model responses to glucagon.

4.2   Extension of the Minimal Model

One of the oldest glucoregulatory models including the effects of insulin on glucose was published by Bergman in 1979 and is known as the minimal model [121]. In 2013, Herrero *et al.* suggested an extension to the model including the effects of glucagon on the net EGP [122]. Mathematically the glucagon-extended minimal model is:

$$EGP(t) = [C_E(t) - I_E(t)]G(t)V_{d,G} + S_G[G_b - G(t)] \tag{4.7}$$

$$\frac{\mathrm{d}C_E(t)}{\mathrm{d}t} = k_C S_C[C(t) - C_b] - k_C C_E(t) \tag{4.8}$$

$$\frac{\mathrm{d}I_E(t)}{\mathrm{d}t} = k_I S_I[I(t) - I_b] - k_I I_E(t) \tag{4.9}$$

G, C and I are the plasma glucose, glucagon, and insulin concentrations and G_b, C_b, and I_b denotes the basal values thereof. I_E and C_E are the actions of the effect compartments of insulin and glucagon on the net EGP. S_G is the glucose sensitivity on promoting or inhibiting the EGP. S_C is the glucagon sensitivity and k_C is the transfer rate constant of glucagon from plasma to the effect compartment. S_I is the insulin sensitivity and k_I is the transfer rate constant of insulin from plasma to the effect compartment. $V_{d,G}$ is the glucose volume of distribution per mass.

Compared to the publication, (4.7) is rewritten to emphasize that the effects of insulin and glucagon are additive and that the absolute difference in glucagon and insulin actions interact with the plasma glucose concentration to yield the EGP. Moreover, with this formulation the contribution to the EGP from the deviation in glucose concentration from basal becomes obvious.

Table 4.2: Specific model parameter values used for simulation of the Herrero *et al.* EGP model [122].

Parameter	Value	Unit
S_G	NA	μmol/kg/min per mmol/L
k_C	0.210	min^{-1}
S_C	$1.25{\cdot}10^{-4}$	min^{-1} per pg/mL
k_I	0.002	min^{-1}
S_I	$1.16{\cdot}10^{-3}$	min^{-1} per mU/L
$V_{d,G}$	160	mL/kg

Data used for the model building originated from a clinical study of eleven subjects with T1D undergoing a dual-hormone closed-loop study for 27 hours [67]. Thus neither glucose, glucagon or insulin were constant during the entire time of the study.

Figure 4.2: EGP simulations of the model proposed by Herrero *et al.* [122] after a SC glucagon bolus (left), SC glucagon infusion (middle), and SC insulin bolus followed 150 minutes after by a SC glucagon bolus (right), see Figure 4.1 for the corresponding PK profiles. The solid curves (left and middle) show the responses using a published parameter value of S_C [122], and the dashed curves show responses when S_C is three times as large. The solid curve (right) show the impact of insulin above basal. The dotted curve is equal to the solid curve of the left graph with 150 minutes delay.

Table 4.2 lists the model parameter values of (4.7)-(4.9) used for the simulations displayed in Figure 4.2. As the glucose level is clamped at basal, 5 mmol/L, the last part of (4.7) equals zero and thus the value of S_G is non-relevant for the present simulations and omitted from the table. The value of C_b was more than four times greater reported by Herrero *et al.* than the value of the glucagon PK simulation model, which could be attributed to assay differences [32]. The difference in basal glucagon levels could lead to a mismatch in glucagon sensitivity. Figure 4.2 displays the EGP responses using the published glucagon sensitivity compared to a sensitivity increased by a factor of three following a SC bolus injection and initiation of a SC glucagon infusion. As the glucagon sensitivity is increased, the EGP responses to both glucagon disturbances are also increased. Overall, the EGP responses to glucagon follow the dynamics of the plasma glucagon concentrations with a slight delay representing the transfer of glucagon to the effect compartment.

Figure 4.2 also compares the EGP response in the presence or absence of a preceding insulin bolus. The dotted line of the right graph equals the solid line of the left graph although with a 150 minutes delay. Increasing insulin above basal but maintaining basal glucagon, the EGP becomes negative. The response to the glucagon bolus measured by peak EGP is somewhat dampened in the presence of the insulin bolus, even when correcting for the negative EGP.

4.3   UVA/PADOVA Type 1 Diabetes Simulator

The only FDA approved simulator of the glucoregulatory system was built in a collaboration between University of Virginia and University of Padova [118]. The model was extended by Dalla Man *et al.* to include the effects of glucagon on EGP [123]. The EGP is described by the following equations:

$$EGP(t) = G_{GNG} - S_G G(t) - S_I I_E(t) + S_C C_E(t) \tag{4.10}$$

$$\frac{\mathrm{d}C_E(t)}{\mathrm{d}t} = k_C \cdot \max(C(t) - C_b, 0) - k_C C_E(t) \tag{4.11}$$

$$\frac{\mathrm{d}I_E(t)}{\mathrm{d}t} = -k_I[I_E(t) - I_{rem}(t)] \tag{4.12}$$

$$\frac{\mathrm{d}I_{rem}(t)}{\mathrm{d}t} = -k_I[I_{rem}(t) - I(t)] \tag{4.13}$$

G, C, and I are the plasma glucose, glucagon, and insulin concentrations. C_b is the basal glucagon concentration. G_{GNG} is a constant EGP contribution that could correspond to gluconeogenesis. S_G, S_C, and S_I are glucose, glucagon and insulin sensitivities on EGP. I_E and C_E are insulin and glucagon concentrations in the effect compartments. I_{rem} is a remote insulin compartment. k_C and k_I are transfer rate constants of glucagon and insulin.

Breaking (4.10) into its elements it consists of two stimulating EGP terms and two inhibiting EGP terms. One stimulating term depends on the delayed glucagon action while the other is completely independent of glucose, insulin or glucagon. The stimulating effect of glucagon is only present when the glucagon concentration is above basal. The EGP inhibiting terms depend on the plasma glucose and the delayed insulin action. The glucose level will always inhibit EGP, even at low blood glucose concentrations.

Table 4.3: Specific model parameter values used for simulation of the Dalla Man *et al.* EGP model [123].

Parameter	Value	Unit
G_{GNG}	6	μmol/kg/min
S_G	0.678	μmol/kg/min per mmol/L
S_I	0.3	μmol/kg/min per mU/L
S_C	0.25	μmol/kg/min per pg/mL
k_C	0.2	min^{-1}
k_I	0.033	min^{-1}

Table 4.3 lists the model parameter values of (4.10)-(4.13) used for the simulations displayed in Figure 4.3. The parameter values were guessed by the author since the model has undisclosed parameter values.
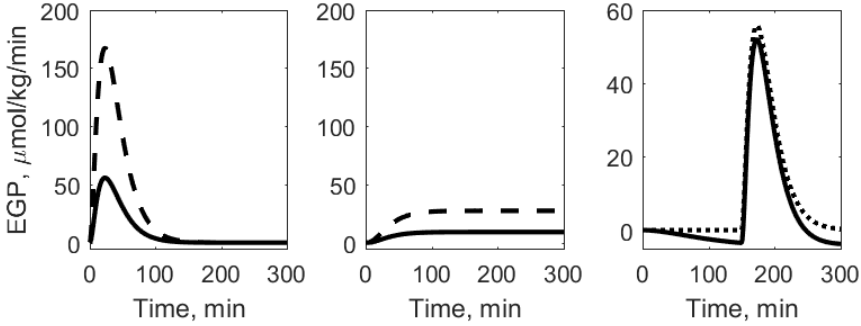
Figure 4.3: EGP simulations of the model proposed by Dalla Man *et al.* [123] after a SC glucagon bolus (left), SC glucagon infusion (middle), and SC insulin bolus followed 150 minutes after by a SC glucagon bolus (right), see Figure 4.1 for the corresponding PK profiles. The solid curves (left and middle) show the responses using a parameter value of 0.2 for k_C, and the dashed curves show responses when k_C is reduced by a factor of four. The solid curve (right) show the impact of insulin above basal. The dotted curve is equal to the solid curve of the left graph with 150 minutes delay.

Generally, the EGP responses to glucagon follow the dynamics of the plasma glucagon concentrations with a delay representing the transfer of glucagon to the effect compartment. The parameter k_C controls the delay of glucagon action on EGP as exemplified in the left and middle graphs of Figure 4.3. The more delayed glucagon action on EGP is, the later will EGP reach maximum concentration after a bolus and steady state after SC infusion start. Moreover, when the time to maximum EGP response increases, the peak response decreases.

In this model, insulin is delayed twice as described by (4.12)-(4.13). The delayed effect of insulin on EGP is visible in the right graph of Figure 4.3, where the solid line represents the impact of insulin on EGP compared to the dotted line with insulin remaining constant at the basal level. With insulin above basal and glucagon at basal, the EGP becomes negative after the insulin action delay. The insulin level has very little influence on the EGP response to glucagon as the peaks of the two curves are almost identical.

4.4 Multiplicative Model

A semi-mechanistic integrated glucose-insulin-glucagon model was proposed by Schneck *et al.* [124]. The model includes multiplicative effects of glucose, insulin and glucagon and is formulated as:

$$EGP(t) = EGP_b \cdot \left(\frac{G_E(t)}{G_b} \frac{I_E(t)}{I_b} \frac{C_b}{C_E(t)} \right)^{-E_{GIC}} \tag{4.14}$$

$$\frac{\mathrm{d}C_E(t)}{\mathrm{d}t} = k_C[C(t) - C_E(t)] \tag{4.15}$$

$$\frac{\mathrm{d}I_E(t)}{\mathrm{d}t} = k_I[I(t) - I_E(t)] \tag{4.16}$$

G_b, I_b, and C_b are the basal concentrations of glucose, insulin and glucagon, respectively. Similarly, G_E, I_E, and C_E are the effect compartment concentrations of glucose, insulin, and glucagon. EGP_b is the basal EGP. E_{GIC} determines the stimulatory effect of glucagon and inhibitory effects of glucose and insulin on EGP. C is the plasma glucagon concentration and k_C is the transfer rate constant of glucagon from plasma to the effect compartment. Likewise, I is the plasma insulin concentration and k_I is the transfer rate constant from plasma to the effect compartment.

Equation (4.14) describes how EGP above basal depends on a multiplicative form of glucose, insulin and glucagon. When glucose and insulin exceed their basal levels, EGP is inhibited, whereas EGP is stimulated when glucose and insulin are below basal levels. On the contrary, EGP is stimulated when glucagon exceeds the basal level, and inhibited when glucagon is lower than basal.

Table 4.4: Specific model parameter values used for simulation of the Schneck *et al.* EGP model [124].

Parameter	Value	Unit
EGP_b	10.2	μmol/kg/min
E_{GIC}	0.79	-
k_C	0.118	min^{-1}
k_I	0.005685	min^{-1}

Table 4.4 lists the model parameter values of (4.14)-(4.16) used for the simulations displayed in Figure 4.4. The parameter of EGP_b is calculated based on the weight of the virtual subject whereas the other parameters are from [124]. As the glucose level is clamped at basal, 5 mmol/L, the fraction of the glucose contribution to EGP equals 1.

Generally, the EGP responses to glucagon during a euglycemic clamp with constant basal insulin follow the dynamics of the plasma glucagon concentrations
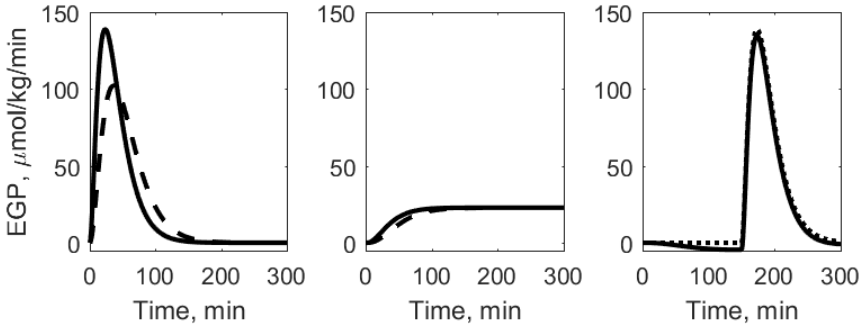
Figure 4.4: EGP simulations of the model proposed by Schneck *et al.* [124] after a SC glucagon bolus (left), SC glucagon infusion (middle), and SC insulin bolus followed 150 minutes after by a SC glucagon bolus (right), see Figure 4.1 for the corresponding PK profiles. The solid curves (left and middle) show the responses using a published parameter value of E_{GIC} [124], and the dashed curves show responses when E_{GIC} is half as large. The solid curve (right) show the impact of insulin above basal. The dotted curve is equal to the solid curve of the left graph with 150 minutes delay.

with a delay representing the transfer of glucagon to the effect compartment. The parameter E_{GIC} determines the size of the EGP response to the combined stimulatory and inhibitory effects of glucose, insulin and glucagon as exemplified in the left and middle graphs of Figure 4.4. When the parameter is reduced, the response is reduced as well.

The delayed effect of insulin on EGP is visible in the right graph of Figure 4.4, where the solid line represents the influence of insulin on EGP compared to the dotted line with insulin remaining constant at the basal level. With insulin above basal and glucagon at basal, the EGP decreases from its basal level of EGP_b. The insulin level has quite some influence on the EGP response to glucagon as the peak is noticeably lower in the presence of insulin.

4.5   Glucose-Glucagon Model

Inspired by the same model as in Section 4.4, Peng *et al.* proposed a different model [125]. The model includes additive effects of glucose and glucagon on EGP described by the following equation:

$$EGP(t) = EGP_b \cdot 0.5 \cdot \left[\left(\frac{G_E(t)}{G_b} \right)^{-E_G} + \left(\frac{C(t)}{C_b} \right)^{E_C} \right] \qquad (4.17)$$

EGP_b is the basal EGP. G_E is the glucose concentration in the effect compartment, G_b is the basal glucose concentration, and E_G is the inhibitory effect on EGP of glucose exceeding basal levels. C is the plasma glucagon concentration, C_b is the basal glucagon concentration, and E_C is the stimulatory effect on EGP of glucagon exceeding basal levels.

Equation (4.17) describes how the basal EGP is stimulated by glucagon concentrations exceeding basal and glucose concentrations below basal. Similarly, EGP is inhibited when glucagon is below basal and glucose is above basal. The effects of glucose and glucagon levels different from basal are determined independently and the overall contribution to EGP is found by addition.

Table 4.5: Specific model parameter values used for simulation of the Peng *et al.* EGP model [125]. *25% of the original value.

Parameter	Value	Unit
EGP_b	7.53	μmol/kg/min
E_C	1.013*	-

Table 4.5 lists the model parameter values of (4.17) used for the simulations displayed in Figure 4.5. As the glucose level is clamped at basal, 5 mmol/L, the fraction of the glucose contribution to EGP equals 1 and the value of E_G becomes irrelevant. Notice in this model, that the effect of glucagon is directly proportional to the concentration in the plasma compartment without delay. The parameter of E_C used for simulations is one-fourth of the published value in order to have a response in the same range as the other simulations. With an even lower value of E_C the response to glucagon is further reduced as exemplified in Figure 4.5.

The influence of insulin on EGP is not captured in the model equations, and thus the third scenario with an insulin bolus preceding a glucagon bolus is not simulated.
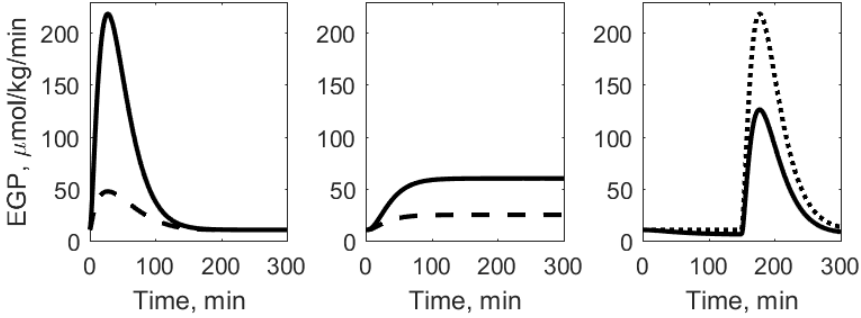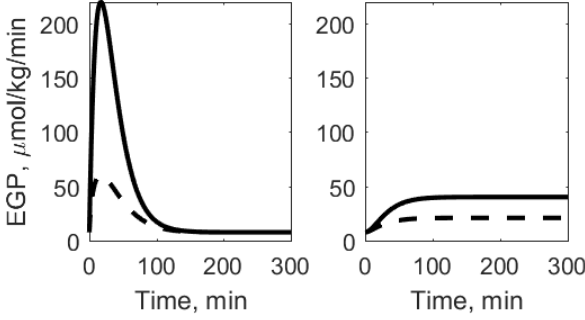
Figure 4.5: EGP simulations of the model proposed by Peng *et al.* [125] after a SC glucagon bolus (left), and SC glucagon infusion (right), see Figure 4.1 for the corresponding PK profiles. The solid curves show the responses using a value of 1.013 for E_C, and the dashed curves show responses when E_C is 0.675. The effect of insulin is omitted as it is not described by the model.

4.6   Glucagon Evanescence Effect

Based on data from a study with glucose clamp and constant insulin and IV glucagon infusions Hinshaw *et al.* proposed a new model of EGP [35]. The model is the first to describe the evanescence effect of glycogenolysis:

$$EGP(t) = k_{G6P}G_{6P}(t) \tag{4.18}$$

$$\frac{\mathrm{d}G_{6P}(t)}{\mathrm{d}t} = -k_{G6P}G_{6P}(t) + G_{GG}(t) + G_{GNG,b} \tag{4.19}$$

$$G_{GG}(t) = [G_{GG_b} + S_C \cdot \max(0, C(t) - C_{thres})] \cdot E(t) \tag{4.20}$$

$$E(t) = \frac{1}{2}\left[1 - \tanh\left(\frac{t - t_D}{\tau}\right)\right] \tag{4.21}$$

G_{6P} is glucose 6-phosphate and k_{G6P} is the rate of dephosphorylation. G_{GG} is the EGP contribution from glycogenolysis. G_{GG_b} and $G_{GNG,b}$ are the basal glycogenolysis and gluconeogenesis, respectively. S_C is the sensitivity of glycogenolysis to glucagon concentration, C, exceeding a threshold concentration, C_{thres}. E is the evanescence effect of glycogenolysis. t_D is the delay of the evanescence effect at which it reduces the glycogenolysis by 50% and τ is the time constant of the evanescence phenomenon.

Equations (4.18)-(4.21) describe how EGP depends on glucagon. EGP also depends on glucose indirectly as it affects gluconeogenesis with some delay. However, in this simulation with a euglycemic clamp the glucose dependency is neglected. The relationship between glucagon concentration and glycogenolysis
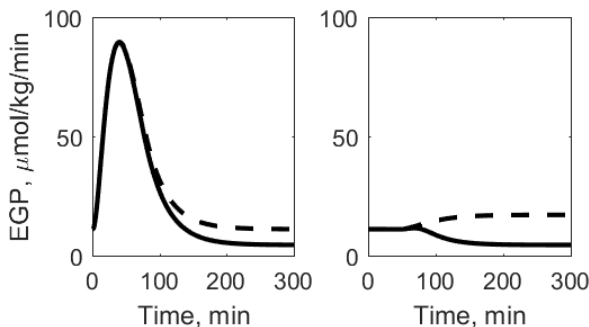
Figure 4.6: EGP simulations of the model proposed by Hinshaw *et al.* [35] after a SC glucagon bolus (left), and SC glucagon infusion (right), see Figure 4.1 for the corresponding PK profiles. The solid curves show the responses when including the evanescence effect as published [35], and the dashed curves show responses when neglecting the evanescence effect of the model. The effect of insulin is not shown as it is not included in the model.

is linear when glucagon exceeds a threshold, although it is dampened and made non-linear by the evanescence effect.

Table 4.6: Specific model parameter values used for simulation of the Hinshaw *et al.* EGP model [35].

Parameter	Value	Unit
k_{G6P}	0.032	min^{-1}
$G_{GNG,b}$	4.4	$\mu\text{mol/kg/min}$
$G_{GG,b}$	6.6	$\mu\text{mol/kg/min}$
S_C	0.272	$\mu\text{mol/kg/min per pg/mL}$
C_{thres}	80	pg/mL
t_D	74.77	min
τ	15.99	min

Table 4.6 lists the model parameter values of (4.18)-(4.21) used for the simulations displayed in Figure 4.6. The values of $G_{GG,b}$ and $G_{GNG,b}$ are guessed by the author based on Cherrington stating that basal EGP is approximately 11 μmol/kg/min with gluconeogenesis contributing 40% [36]. The value of S_C might be off by a factor of 10^3 because the unit is reported as per ng/mL in [35]. If assuming the unit is correct, the response to changes in glucagon from the threshold becomes very small and in fact the EGP response to a bolus and an infusion becomes practically identical. In this model, the effect of glucagon on EGP is not delayed but suppressed by the evanescence effect after t_D minutes.

The difference in the response with and without the evanescence effect is exemplified in Figure 4.6. Note, that the model was based on IV glucagon infusions which would reach steady state much faster than SC infusion of glucagon. Also, because neither the SC bolus or SC infusion yield a steep increase in glucagon concentration like an IV infusion would, the parameter accounting for a rapid increase in glucagon is ignored.
The influence of insulin on EGP is not captured in the model equations, and thus the third scenario with an insulin bolus preceding a glucagon bolus is omitted.

4.7   Glucagon Rate of Change

Based on a model comparison of nine published or new EGP models, Emami *et al.* found that a multiplicative relationship between insulin and glucagon was needed to describe the interaction between the two hormones [114]. Moreover, the glucagon rate of change was included in the final model description achieving the best fit:

$$EGP(t) = \max(1 - S_I I_E(t), 0) \cdot \max(G_{\Delta C}(t) + S_C C(t), 0) + G_{GNG} \quad (4.22)$$

$$\frac{\mathrm{d}G_{\Delta C}(t)}{\mathrm{d}t} = -k_{GdC} G_{\Delta C}(t) + S_{\Delta C} \Delta C(t) \quad (4.23)$$

$$\frac{\mathrm{d}I_E(t)}{\mathrm{d}t} = k_I [I(t) - I_E(t)] \quad (4.24)$$

I and C are the plasma insulin and glucagon concentrations. I_E is the insulin concentration in the effect compartment. $G_{\Delta C}$ is an effect compartment depending on the glucagon rate of change. S_I and S_C are insulin and glucagon sensitivities. $S_{\Delta C}$ is the sensitivity to glucagon rate of change. k_{GdC} and k_I are transfer rate constants. G_{GNG} is a constant EGP contribution independent of insulin and glucagon corresponding to gluconeogenesis.

Table 4.7: Specific model parameter values used for simulation of the Emami *et al.* EGP model [114].

Parameter	Value	Unit
G_{GNG}	5.54	μmol/kg/min
S_I	0.02	per mU/L
S_C	0.063	μmol/kg/min per pg/mL
$S_{\Delta C}$	0.0015	μmol/kg/min per pg/mL
k_{GdC}	0.022	min^{-1}
k_I	0.068	min^{-1}

Equations (4.22)-(4.24) describe how insulin and glucagon pull the EGP in op-
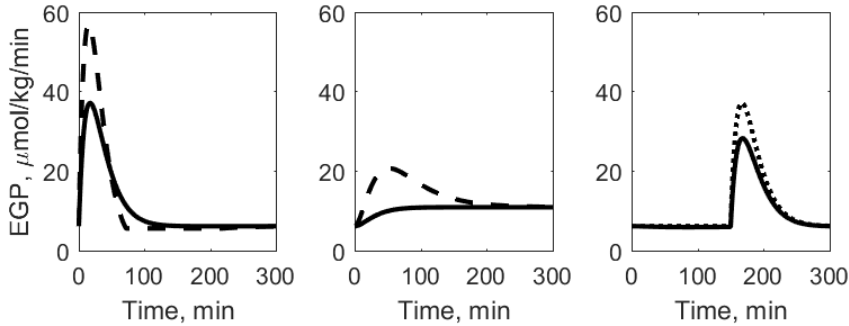
Figure 4.7: EGP simulations of the model proposed by Emami *et al.* [114] after a SC glucagon bolus (left), SC glucagon infusion (middle), and SC insulin bolus followed 150 minutes after by a SC glucagon bolus (right), see Figure 4.1 for the corresponding PK profiles. The solid curves (left and middle) show the responses using a published parameter value of $S_{\Delta C}$ [114], and the dashed curves show responses when $S_{\Delta C}$ is 35 (bolus) or 200 (infusion) times as large. The solid curve (right) show the impact of insulin above basal. The dotted curve is equal to the solid curve of the left graph with 150 minutes delay.

posite directions. The effect of glucagon vanishes when the remote insulin concentration exceeds S_I^{-1}. The model also includes an effect compartment related to the glucagon rate of change.

Data used for model building originated from a clinical study of 11 subjects with T1D undergoing a euglycemic glucose clamp with constant insulin infusions at various levels and multiple glucagon boluses [48]. Both glucose and insulin were constant throughout a study day.

Table 4.7 lists the model parameter values of (4.22)-(4.24) used for the simulations displayed in Figure 4.7. Overall, the EGP responses to glucagon follow the dynamics of the plasma glucagon concentrations. The rise and fall of EGP becomes steeper with an increased sensitivity to the glucagon rate of change as illustrated in the left and middle graphs of Figure 4.7. The increased steepness of EGP also shortens time to peak EGP with a few minutes. With a very high sensitivity to the glucagon rate of change, the EGP response to glucagon infusion start overshoots and returns to a baseline above basal.

The effect of insulin is visible in the right graph of Figure 4.7, where the solid line represents the influence of insulin on EGP compared to the dotted line with insulin remaining constant at the basal level. After the insulin bolus but with

glucagon remaining constant and basal, the EGP drops slightly from its basal level. The insulin level has an influence on the EGP response to glucagon as the peak is noticeably lower in the presence of insulin above basal.

4.8   Saturation of Glucose Production

Inspired by the model presented in section 4.7, Wendt *et al.* proposed yet another model of EGP [18]. The model was developed based on data from dogs who received very high glucagon boluses making it necessary to introduce a saturation effect of the response to glucagon. Furthermore, the model was tested in healthy volunteers [19], and validated using leave-one-out cross-validation in seven diabetes patients [20]. Using the same terminology as in the previous sections the model is described by the following equations:

$$EGP(t) = G_{GG}(t) + G_{GNG} \tag{4.25}$$

$$G_{GG}(t) = \frac{\max(1 - S_I I_E(t), 0)}{1 - S_I I_b}[E_{max} - G_{GNG}]\frac{C(t)}{C_{E50} + C(t)} \tag{4.26}$$

$$\frac{\mathrm{d}I_E(t)}{\mathrm{d}t} = k_I[I(t) - I_E(t)] \tag{4.27}$$

G_{GG} and G_{GNG} are the glycogenolysis and gluconeogenesis, respectively. S_I is the insulin sensitivity, I_E is the insulin concentration in the effect compartment, and I_b is the basal insulin concentration. C is the glucagon concentration, C_{E50} is the glucagon concentration at which the response is half maximum, and E_{max} is the maximum response at basal insulin. k_I is the transfer rate constant of insulin from plasma to the effect compartment.

Equations (4.25)-(4.27) describe how the EGP depends on insulin and glucagon. Insulin reduces the response to glucagon and completely suppresses the response when the remote insulin concentration exceeds S_I^{-1}. The glycogenolytic response to glucagon follows Michaelis-Menten kinetics and saturates for high concentrations of glucagon.

Table 4.8: Specific model parameter values used for simulation of the Wendt *et al.* EGP model [20].

| Parameter	Value	Unit
G_{GNG}	6	μmol/kg/min
S_I	0.0415	per mU/L
E_{max}	84.4	μmol/kg/min
C_{E50}	285	pg/mL
k_I	0.0068	min^{-1}
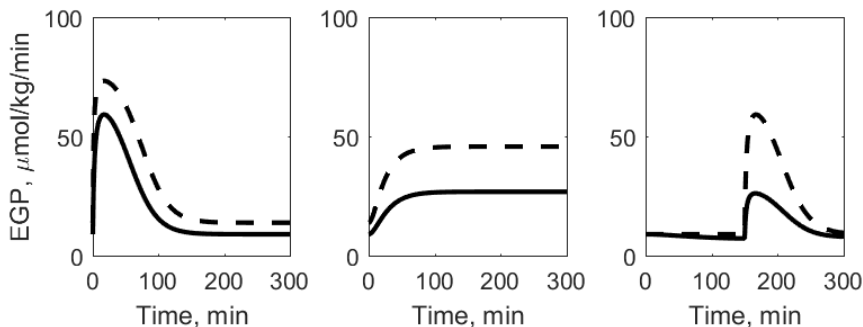
Figure 4.8: EGP simulations of the model proposed by Wendt *et al.* [20] after a SC glucagon bolus (left), SC glucagon infusion (middle), and SC insulin bolus followed 150 minutes after by a SC glucagon bolus (right), see Figure 4.1 for the corresponding PK profiles. The solid curves (left and middle) show the responses using a published parameter value of C_{E50} [20], and the dashed curves show responses when C_{E50} is reduced by a factor of 2.85. The solid curve (right) show the impact of insulin above basal. The dotted curve is equal to the solid curve of the left graph with 150 minutes delay.

Data used for model validation originated from a clinical study of 8 subjects with T1D undergoing four study days with an insulin bolus followed by a glucagon or saline bolus [56]. Neither glucose, insulin or glucagon were constant during an entire study day.

Table 4.8 lists the model parameter values of (4.25)-(4.27) used for the simulations displayed in Figure 4.8. The EGP responses to glucagon boluses are not as peaked as previous simulations which might be explained by the high glucagon concentrations leading to saturation of the EGP response during parts of the simulation. The value of C_{E50} influences the glucagon concentration at which the response saturates - the smaller the value, the lower glucagon concentration is required to reach maximum response. Changes in C_{E50} influences the overall magnitude and the peakedness of the EGP response as illustrated in the left and middle graphs of Figure 4.8.

The effect of insulin is visible in the right graph of Figure 4.8, where the solid line represents the influence of insulin on EGP compared to the dotted line with insulin remaining constant at the basal level. After the insulin bolus but with glucagon remaining constant and basal, the EGP drops slightly from its basal level. The insulin level has a pronounced influence on the EGP response to glucagon as the peak is noticeably lower in the presence of insulin above basal.

4.9 Model Comparison

The seven presented models of glucagon's effect on EGP have some similarities but also numerous differences. This section compares the models to each other, and discusses the models in relation to the known physiology explained in Section 2.3. Model comparison is based on the general structure, the dynamic responses to a glucagon bolus or infusion, the absolute responses to glucagon at basal insulin and following an insulin bolus, and the steady state glucagon concentration-response relationship.

4.9.1 Model Structure

The models in the previous sections seek to describe the EGP response to glucagon. Three of the models depend on glucagon delayed by an effect compartment [122, 123, 124], whereas the four other models depend directly on the plasma glucagon concentration [20, 35, 114, 125]. Four of the seven models depend on insulin delayed by a single effect compartment [20, 114, 122, 124], and one model delays insulin by two effect compartments [123]. Thus two of the models do not describe the effect of insulin on EGP [35, 125].
Table 4.9 provides an overview of some of the most important structural model features: glucose dependency, interaction (multiplicative) or independence (additive) relationship of glucagon and insulin effects, constant production from independent mechanism, evanescence effect of glycogenolysis, glucagon rate of change dependency, and saturation of glucose response to glucagon.

Table 4.9: Comparison of structural model elements in the seven presented EGP models: glucose level (G), insulin level (I), glucagon level (C), gluconeogenesis (G_{GNG}), evanescence effect (E), glucagon rate of change (ΔC), saturation of EGP response (EGP_{max}).

Model	G	$I + C$	$I \cdot C$	G_{GNG}	$E(t)$	ΔC	EGP_{max}
Herrero [122]	×	×					
Dalla Man [123]	×	×		×			
Schneck [124]	×		×				
Peng [125]	×						
Hinshaw [35]	×			×	×		
Emami [114]			×	×		×	
Wendt [20]			×	×			×

4.9.2   Impact of Glucose

Four of the presented models explicitly include the effects of glucose on EGP.
Two models describe an additive effect of glucose and glucagon [123, 125],
whereas two other models present a multiplicative relationship between glu-
cose and glucagon [122, 124]. The model by Hinshaw *et al.* includes the effect
of glucose indirectly by increasing gluconeogenesis after prolonged hypoglycemia
[35]. The remaining two models are not influenced by the glucose level [20, 114].
As outlined in Section 2.3, the ambient glucose level does not influence the im-
mediate effect of glucagon on EGP. Therefore, the models with multiplicative
relationships of glucagon and glucose seem least physiologic. Moreover, gluca-
gon stimulates gluconeogenesis rather than glycogenolysis after three hours of
hypoglycemia. Though the model by Hinshaw *et al.* describes this phenomenon,
it only describes this for a specific blood glucose level of 3.3 mmol/L and is thus
not generalizable to other hypoglycemic glucose levels. Furthermore, the number
of delay compartments determining the delay of the hypoglycemia stimulating
effect on gluconeogenesis are not public available.

4.9.3   Impact of Insulin

The EGP models behave very similar after a glucagon bolus during euglycemia
and constant basal insulin concentration. Though, in the models including
the effects of insulin, the EGP response to glucagon changes in the presence
of a preceding insulin bolus and the model differences become more obvious.
Due to the extra remote insulin compartment, the insulin action is delayed
the longest in the model by Dalla Man *et al.*, see Figure 4.9. Comparing the
EGP responses in Figures 4.2-4.4 and 4.7-4.8, we observe that insulin has little
influence on the EGP response to glucagon when the model structure has an
additive relationship of insulin and glucagon [122, 123]. On the contrary, when
the insulin-glucagon relationship is multiplicative, the response to a glucagon
bolus in the presence of insulin is noticeably reduced [20, 114, 124]. Figure 4.9
shows that the absolute EGP responses using the Emami and Wendt models
in the presence of insulin are very similar. As outlined in Section 2.3, high
insulin levels suppress the EGP response to glucagon, and thus the models with
multiplicative descriptions of insulin and glucagon seem most physiologic as they
can describe this phenomenon. Another issue with the additive insulin-glucagon
models is visible in Figure 4.9, where the EGP becomes negative when insulin is
above basal and glucagon remains basal because the basal EGP is zero [122, 123].
The EGP being zero at basal and becoming negative during the simulation reveal
that an additive insulin-glucagon relationship is non-physiologic.
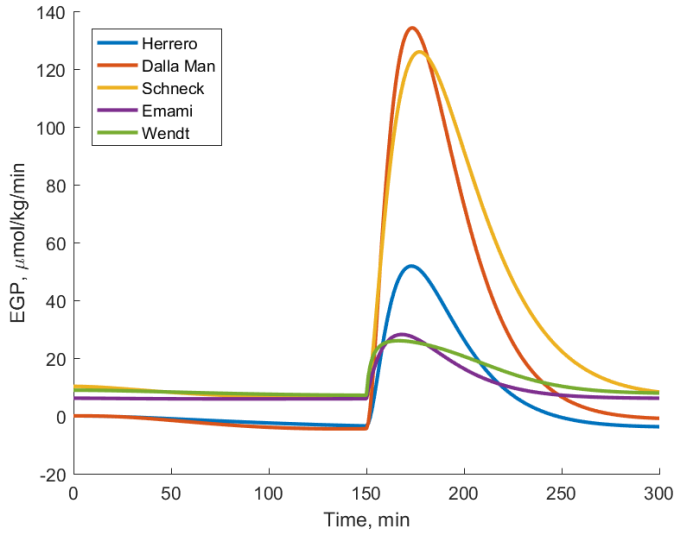
Figure 4.9: Direct comparison of EGP response to glucagon in the presence of insulin above basal. At time=0 a bolus of 4 U insulin was given followed by a glucagon bolus of 300 μg at time=150.

4.9.4 Glucagon time-response relationship

The EGP response generally follows the glucagon PK when insulin is basal, except when the evanescence effect is present [35], when the sensitivity to glucagon rate of change dominates [114], or when the glucagon response saturates for large parts of the simulated glucagon levels [20]. Figure 4.10 directly compares the seven EGP models at basal insulin using nominal parameter values. After an identical SC glucagon bolus, all models simulate a rise in EGP although with varying steepness and time of maximum response as seen in the left graph. After 100 to 150 minutes all models simulate that the EGP has returned to baseline which is zero in two models [122, 123] and around 10 μmol/kg/min according to the other models [20, 35, 114, 124, 125]. In Figure 4.11a, the EGP response to a glucagon bolus peaks after approximately 20 minutes and returns to baseline after 120 minutes. Comparing the left graph of Figure 4.10 to Figure 4.11a, the return to baseline is well captured by the EGP models, but several of them simulate a much slower time to maximum response.

Following initiation of an identical SC glucagon infusion, six of the models simulate with nominal parameter values that the EGP immediately increases and reach a steady state plateau within 100 minutes although at levels ranging from less than 10 to 60 μmol/kg/min as seen in Figure 4.10. The model by Hinshaw *et al.* stands out as the increase in EGP is delayed and the effect transient
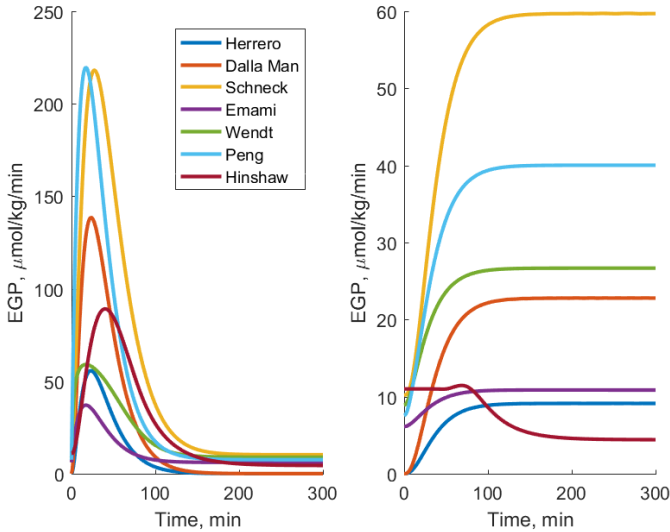
Figure 4.10: Direct comparison of simulated EGP responses to glucagon when
insulin is basal and parameter values are nominal. EGP re-
sponses after a 300 μg glucagon bolus (left) and initiation of
1 μg/min glucagon infusion (right).

which is due to the evanescence effect of glucagon included in the model. In
Figure 4.11b, the EGP response to initiation of a glucagon infusion rapidly in-
creases and then returns to a new elevated baseline after 120 minutes despite
the continued infusion of glucagon. Although the Hinshaw model includes the
evanescence effect, it still does not seem to capture the true time course of
EGP after glucagon infusion. However, remembering the middle graph of Fig-
ure 4.7, the response mimics the evanescence effect described in literature when
the sensitivity to glucagon rate of change is 200 times the nominal value.

The literature in Section 2.3 confirms that the EGP response to a continuous
glucagon stimulation wanes over time. Due to the mathematical formulation
in (4.21), the evanescence effect is irreversible due to the tangent hyperbolic
function. It is unclear what happens to the evanescence effect when multiple
doses are injected. Physiologically, when glucagon stimulation is discontinued
the EGP system might be desensitized for some time, but should then return to
normal. Having a refractory period where further stimulation does not produce
a response is well known from neurons essentially also acting through receptor
mechanisms although in such cases the refractory period only lasts for millisec-
onds. However, the reversal of the evanescence effect of glucagon is not studied
thoroughly and can therefore not be modelled until investigated in a clinical
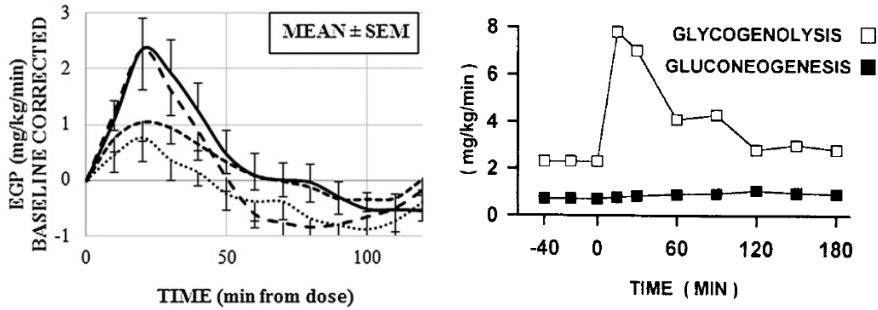
(a) EGP response to SC glucagon bo- **(b)** EGP response to an IV glucagon in-
luses, from [48].   fusion, from [36].

Figure 4.11: Time course of EGP response to glucagon.

setting. To have a reversible situation the evanescence effect could perhaps be modelled through a chain of compartments rather than a tangent hyperbolic function.

4.9.5   Absolute Glucagon Concentration

The left graph of Figure 4.1 displays the glucagon PK profile after a bolus of 300 μg based on the model and parameters summarized in Section 4.1. According to the model parameter, C_b, the baseline glucagon concentration for this virtual subject is 11 pg/mL. The glucagon PK model was based on data measured by a novel assay technique with high accuracy. Comparison of this assay to commercially available assays showed that they tend to overestimate the glucagon concentration by as much as 100% due to lack of specificity and precision [32]. This difference in assay performance could explain the variations in baseline glucagon concentration reported together with the models: ~48 pg/mL [122], ~130 pg/mL [124], ~60 pg/mL [125], ~35 pg/mL [35], and ~100 pg/mL [114]. Data used for model building by both Herrero *et al.* and Emami *et al.* were measured by an immunoassay from Millipore, and the data used by Hinshaw *et al.* was measured by a double antibody radio-immunoassay from Linco Research. Neither Schneck *et al.* nor Peng *et al.* provide information on which assay was used for sample analysis of glucagon. Thus, in all of these EGP models based on glucagon data with higher baseline than the virtual subject, the EGP responsiveness to glucagon i.e. the sensitivity, might be underestimated. Moreover, the model by Hinshaw *et al.* uses a specific threshold of 80 pg/mL to describe the concentration above which glucagon affects EGP. Applying this threshold to the virtual subject, the required glucagon concentration increase
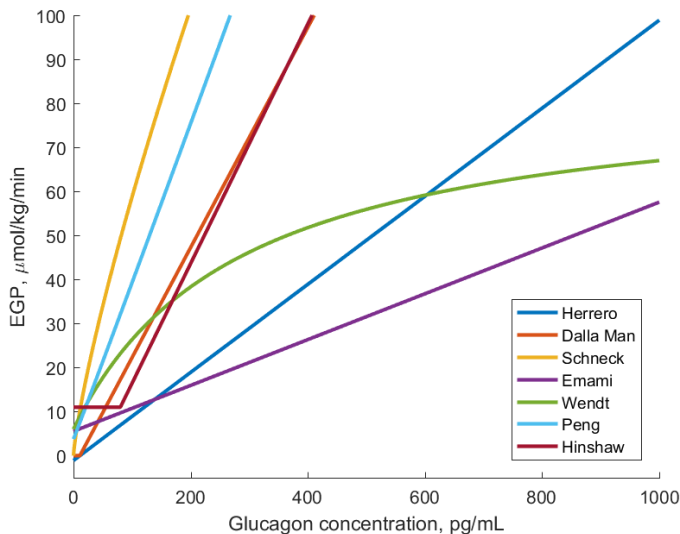
Figure 4.12: Comparison of the concentration-response relationship between glucagon and EGP for the presented EGP models assuming a steady state for discrete glucagon concentrations.

from baseline to yield an effect is close to 70 pg/mL, which conflicts with literature stating that even small glucagon increments of 10 pg/mL are effective in stimulating EGP [36].

These issues emphasize what was already pointed out in Section 2.2.4. Thus applying a PK model based on data from one method of sample analysis could lead to over or under estimation of the concentration-response sensitivity in the PD model if the PD parameters are based on glucagon data obtained by an assay with different accuracy.

4.9.6   Glucagon Concentration-Response Relationship

Although most of the EGP models are time-dependent, their behaviour in steady state for various levels of glucagon can be compared. Figure 4.12 presents the steady state EGP response to glucagon of the seven EGP models with nominal parameter values. Six of the models describe the glucagon-EGP relationship with a linear or piece-wise linear function. The model by Wendt *et al.* stands out as the only model describing a saturation of the EGP response to high concentrations of glucagon. As described in Section 2.3, glucagon stimulates EGP through a receptor mediated mechanism and therefore it makes physio-
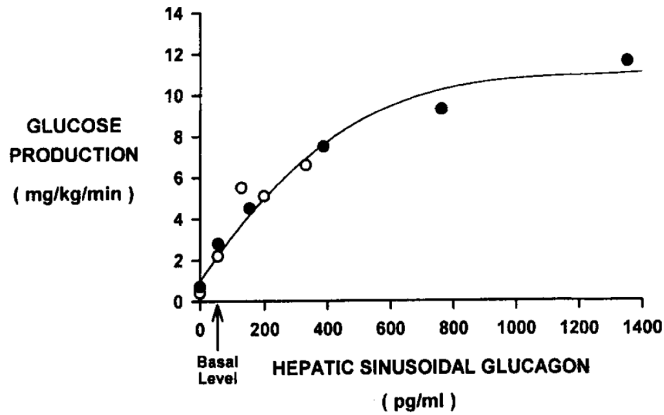
Figure 4.13: EGP as a function of glucagon concentration with data from dogs
(black dots) and humans (white dots), from [36]. To convert from
mg/kg/min to μmol/kg/min the value is multiplied by 5.55, thus
10 mg/kg/min = 55.5 μmol/kg/min.

logically sense to have a model with a maximum EGP response. Figure 4.13
provides another evidence that the EGP response to glucagon approaches sat-
uration for high glucagon concentrations. Comparing Figure 4.12 and 4.13, the
concentration-response relationship of the Wendt model compares well to the
clinical results in terms of maximum response and concentration yielding half
maximum effect. For low concentrations of glucagon not exceeding 400 pg/mL
a linear approximation of the glucagon-EGP relationship might be sufficient,
but for higher concentrations of glucagon, the discrepancies between the model
with saturation and the linear models become large. In the presented simula-
tion example with a bolus of 300 μg glucagon the plasma concentration reached
600 pg/mL and even at this concentration we observe large variations in the
size of the steady state EGP response. Notice, that the models by Herrero *et
al.* and Emami *et al.* having used the same assay for glucagon analysis, both
underestimate the EGP response to low concentrations of glucagon compared to
the Wendt model. The remaining four models seem to follow the Wendt model
for low concentrations of glucagon but greatly overestimates the EGP response
for glucagon concentrations exceeding $\sim$200 pg/mL.

It is interesting to observe how the models describe the EGP response to glu-
cagon for concentrations approaching zero. Figure 4.12 visualizes that both the
models by Dalla Man *et al.* and Hinshaw *et al.* require glucagon to exceed a
threshold before having a stimulatory effect on EGP. The model by Herrero *et
al.* reveals to be even more non-physiologic as the EGP becomes negative when
the glucagon concentration is zero.

4.9.7   Closing Remarks

Calculation of EGP from clinical data is not straightforward. A major limitation in development of EGP models is the data used for model building. The golden standard for measuring EGP is a triple tracer dilution technique followed by application of a two compartment model [126]. However, none of the above models have been developed based on data from a study using the triple tracer technique. Two studies used a single glucose tracer technique to estimate EGP [35, 114], and the remaining models were developed based on datasets with measurements of insulin, glucagon and glucose. Using a single tracer technique rather than a triple tracer technique, the calculations highly depend on the associated compartment model [127]. When EGP is not estimated, but included as part of a larger glucoregulatory model, the parameter values associated with the EGP model will depend even more on the encompassing model.

The present model comparison and discussion of seven published EGP models serves to highlight advantages and disadvantages of each model. Unfortunately, a single model does not seem to capture the full complexity of the EGP response to glucagon. This overview might inspire creation of more exhaustive glucagon-EGP models. Although, creating more complex models will also require more complex data preferably obtained using triple tracer technique and demonstrating the physiologic phenomenons sought to be described mathematically.

Simulating Glucoregulatory Dynamics

The first part of this chapter provides the model equations and parameters for a simulation model describing the glucoregulatory system in patients with T1D. The glucose PD model accounts for the effects of both insulin and glucagon on EGP. The equations and parameters of the associated insulin and glucagon PK models are provided for completeness. The model validation is briefly described. A discussion of the model strengths and weaknesses when applying it for simulations concludes the model presentation.

The second half of this chapter provides examples of what the glucose-insulin-glucagon simulation model have been used for. The selected *in silico* studies include replication of an *in vivo* study showing the effect of micro-boluses of glucagon at varying insulin levels. The *in vivo* study was also recreated by administering a wider range of glucagon boluses to further investigate the dose-response relationship of glucagon and EGP. Finally, the simulation model was used to propose glucagon dosing regimens for treatment of insulin-induced mild hypoglycemia depending on the ambient insulin level.

5.1 Simulation Model

The PK and PD simulation models in this section including equations and parameter values were published by Wendt *et al.* in Journal of Diabetes Science and Technology February 2017 [20]. This section serves as a summary of the glucoregulatory model providing the information necessary to discuss it and use it for simulations. For details on the model validation and parameter estimation not stated in this section, the reader is referred to [20], which is included in Appendix C.

5.1.1 Insulin Pharmacokinetics

The insulin PK model is adopted from Haidar *et al.* [28] and describes how insulin is transferred from the SC tissue to the central compartment using a simple two-state model with identical time constants for the absorption rate and the elimination rate.

$$\frac{\mathrm{d}X_1(t)}{\mathrm{d}t} = u_I(t) - \frac{X_1(t)}{t_{max}} \qquad X_{1,SS} = u_{I,SS} \cdot t_{max} \qquad (5.1)$$

$$\frac{\mathrm{d}X_2(t)}{\mathrm{d}t} = \frac{X_1(t)}{t_{max}} - \frac{X_2(t)}{t_{max}} \qquad X_{2,SS} = u_{I,SS} \cdot t_{max} \qquad (5.2)$$

$$I(t) = \frac{1}{t_{max}} \frac{X_2(t)}{W \cdot Cl_{F,I}} 10^6 + I_b \quad I_{SS} = \frac{u_{I,SS}}{W \cdot Cl_{F,I}} 10^6 + I_b \qquad (5.3)$$

Table 5.1: Interpretation of insulin PK model states, input, output and parameters.

Class	Variable	Unit	Interpretation
States	$X_1(t)$	U	mass due to SC dosing, in SC tissue
	$X_2(t)$	U	mass due to SC dosing, in serum
Input	$u_I(t)$	U/min	dose
Output	$I(t)$	mU/L	concentration in serum
Parameters	I_b	mU/L	basal concentration
	t_{max}	min	time to maximum serum concentration
	W	kg	body weight
	$Cl_{F,I}$	mL/kg/min	apparent clearance
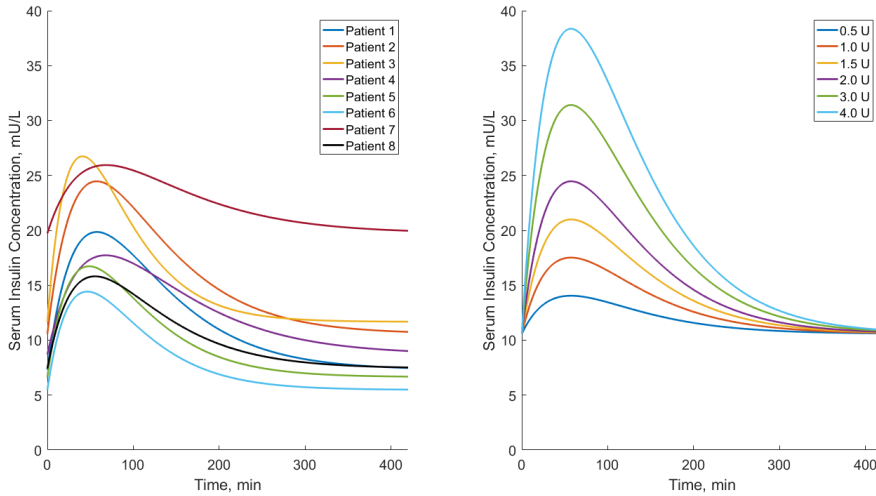
Figure 5.1: Examples of insulin PK profiles after one bolus administration of 2 U in eight virtual patients (left), and in one randomly selected virtual patient (no. 2) following various insulin boluses (right). The left orange curve is identical to the right purple curve.

Table 5.1 lists the interpretations of the insulin PK model variables. The steady state conditions are listed together with the model equations in (5.1)-(5.3). When the system is undisturbed, thus u_I being zero, both states are equal to zero and the serum concentration equals the basal concentration I_b, which is maintained by a constant basal insulin infusion. The basal concentration was modelled as a parameter due to the basal infusion rate being unknown in the data used for model fitting. However, rearranging the steady state equation in (5.3), the required insulin infusion rate to yield a specific basal steady state concentration can be obtained when the model parameters are known. The parameter, I_b, can then be omitted and replaced by an input describing the constant basal infusion accordingly.

The model could be expanded to handle IV insulin infusions by addition of an input variable to the second state equation in (5.2). Caution must be taken if the bioavailability after SC and IV administration are not identical as this will influence the model parameters. Moreover, as regular insulin exerts flip-flop kinetics [31], the elimination of drug estimated after SC administration will underestimate the true elimination of drug after IV administration due to the slow SC absorption. The slow SC absorption might also mask the existence of a distribution compartment that is clearly identified after IV administration and the model in (5.1)-(5.2) might therefore not be adequate to describe PK after IV administration after all. Chapter 2 explained the PK after intravascular and

extravascular administration in details and can be consulted for further clarification.

Section 5.1.5 presents individual insulin PK model parameter values and when they apply for eight virtual T1D patients. Figure 5.1 visualizes the differences in insulin PK after administration of an identical bolus to each patient of the virtual population, and the dose-concentration relationship in one of the patients.

5.1.2 Glucagon Pharmacokinetics

The glucagon PK model is adopted from Wendt *et al.* [18] and describes how glucagon is transferred from the SC tissue to the central compartment using a simple two-state model with different absorption rate and elimination rate constants, where the elimination rate is greater than or equal to the absorption rate.

$$\frac{\mathrm{d}Z_1(t)}{\mathrm{d}t} = u_C(t) - k_1 Z_1(t) \qquad Z_{1,SS} = \frac{u_{C,SS}}{k_1} \tag{5.4}$$

$$\frac{\mathrm{d}Z_2(t)}{\mathrm{d}t} = k_1 Z_1(t) - k_2 Z_2(t) \quad Z_{2,SS} = \frac{u_{C,SS}}{k_2} \tag{5.5}$$

$$C(t) = \frac{k_2 Z_2(t)}{W \cdot Cl_{F,C}} + C_b \qquad C_{SS} = \frac{u_{C,SS}}{W \cdot Cl_{F,C}} + C_b \tag{5.6}$$

The steady state conditions are listed together with the model equations in (5.4)-(5.6). When the system is undisturbed thus no SC glucagon bolus or infusion, both states are equal to zero and the plasma concentration equals the basal concentration maintained by a constant endogenous production.

Similar to the insulin PK model described in Section 5.1.1, the glucagon PK model can also be modified to include IV dosing of glucagon, although the same cautions apply regarding bioavailability, and underestimation of elimination of drug and applicability due to flip-flop kinetics. The PK of glucagon is explained in details in Section 2.2.

Table 5.2 lists the interpretations of glucagon PK model variables. Individual glucagon PK model parameter values of eight virtual patients with T1D are presented in Section 5.1.5. Figure 5.2 visualizes the differences in plasma glucagon concentration after an identical bolus administered to each patient of the virtual population, and the dose-concentration relationship in one of the patients.

Table 5.2: Interpretation of glucagon PK model states, input, output and parameters.

| Class	Variable	Unit	Interpretation
States	$Z_1(t)$	pg	mass due to SC dosing, in SC tissue
	$Z_2(t)$	pg	mass due to SC dosing, in plasma
Input	$u_C(t)$	pg/min	dose
Output	$C(t)$	pg/mL	concentration in plasma
Parameters	C_b	pg/mL	basal concentration
	k_1	min^{-1}	absorption rate constant
	k_2	min^{-1}	elimination rate constant
	W	kg	body weight
	$Cl_{F,C}$	mL/kg/min	apparent clearance
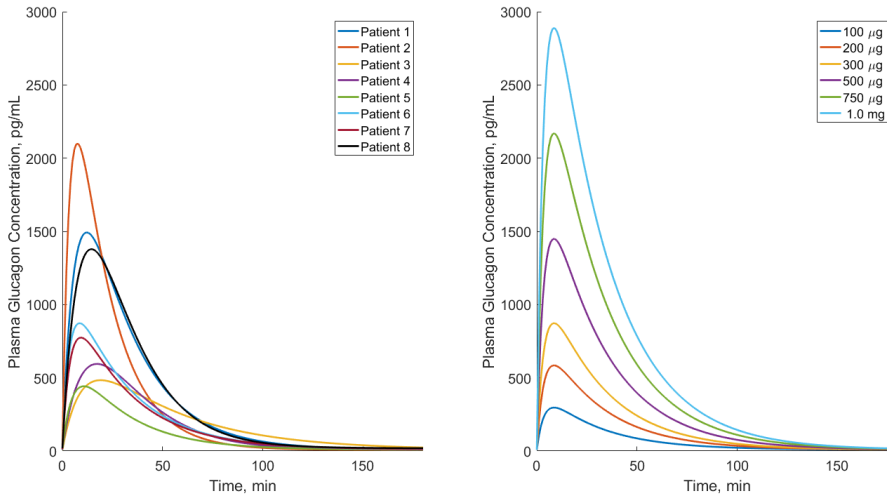
Figure 5.2: Examples of glucagon PK profiles after one bolus administration of 300 μg in eight virtual patients (left), and in one randomly selected virtual patient (no. 6) following various glucagon boluses (right). The left turquoise curve is identical to the right yellow curve.

5.1.3 Glucose Pharmacodynamics

The majority of the glucose PD model explained in the following was originally published by Hovorka *et al.* [117], and then extended with an EGP model including the effects of both insulin and glucagon by Wendt *et al.* [18]. The glucoregulatory model by Hovorka was chosen as the model foundation since it was validated using a multi tracer technique and the publication provided parameter values for six subjects, which served as prior information during parameter estimation.

The model extension was developed using preclinical data from healthy dogs [18], included in Appendix A. It was then tested with clinical data from healthy humans to confirm that the model extension translated to the human species [19], included in Appendix B. Finally, the PD model was cross-validated successfully in seven T1D patients [20], included in Appendix C. The complete model structure is described by (5.7)-(5.13).

$$\frac{\mathrm{d}Q_1(t)}{\mathrm{d}t} = -F_{01} - F_R - S_T x_1(t) Q_1(t) + k_{12} Q_2(t) + G_{GG}(t) + G_{GNG} \qquad (5.7)$$

$$\frac{\mathrm{d}Q_2(t)}{\mathrm{d}t} = S_T x_1(t) Q_1(t) - [k_{12} + S_D x_2(t)] Q_2(t) \qquad (5.8)$$

$$G_{GG}(t) = \frac{\max(1 - S_E x_3(t), 0)}{1 - S_E I_b} [E_{max} - G_{GNG}] \frac{C(t)}{C_{E50} + C(t)} \qquad (5.9)$$

$$G(t) = \frac{Q_1(t)}{V} \qquad (5.10)$$

$$\frac{\mathrm{d}x_1(t)}{\mathrm{d}t} = k_{a1}[I(t) - x_1(t)] \qquad (5.11)$$

$$\frac{\mathrm{d}x_2(t)}{\mathrm{d}t} = k_{a2}[I(t) - x_2(t)] \qquad (5.12)$$

$$\frac{\mathrm{d}x_3(t)}{\mathrm{d}t} = k_{a3}[I(t) - x_3(t)] \qquad (5.13)$$

Table 5.3 lists the interpretations of PD model states, inputs, outputs and parameters. In this model formulation, the EGP is the sum of G_{GG} and G_{GNG} as explained in detail in Section 4.8. Equations (5.14)-(5.18) list the steady state conditions of the model.
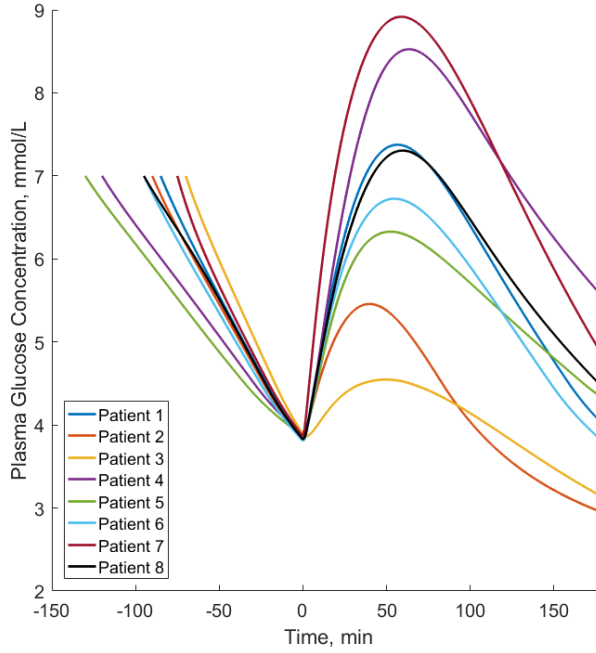
Figure 5.3: Examples of glucose PD profiles after an insulin bolus of 2 U followed by a glucagon bolus of 200 μg when the blood glucose decreased below 3.9 mmol/L in eight virtual patients.

$$Q_{1,SS} = G_{SS} \cdot V \tag{5.14}$$

$$Q_{2,SS} = Q_{1,SS} \frac{x_{1,SS}}{x_{2,SS} + k_{12}} \tag{5.15}$$

$$x_{1,SS} = I_b \tag{5.16}$$

$$x_{2,SS} = I_b \tag{5.17}$$

$$x_{3,SS} = I_b \tag{5.18}$$

Section 5.1.5 presents subject specific glucose PD model parameters. Figure 5.3 visualizes the differences in plasma glucose concentration after an identical SC insulin bolus followed by an identical SC glucagon bolus when plasma glucose decreased below 3.9 mmol/L in each patient of the virtual population.

Table 5.3: Interpretation of glucose PD model states, input, output and parameters.

Class	Variable	Unit	Interpretation
States	$Q_1(t)$	μmol/kg	glucose mass per W in the accessible compartment
	$Q_2(t)$	μmol/kg	glucose mass per W in the non-accessible compartment
	$x_1(t)$	mU/L	remote effects of insulin on glucose transport
	$x_2(t)$	mU/L	remote effects of insulin on glucose disposal
	$x_3(t)$	mU/L	remote effects of insulin on glycogenolysis
Inputs	$I(t)$	mU/L	insulin concentration in serum
	$C(t)$	pg/mL	glucagon concentration in plasma
Outputs	$G(t)$	nmol/L	glucose concentration in plasma
	$G_{GG}(t)$	μmol/kg/min	glucose production due to glycogenolysis
Parameters	G_{GNG}	μmol/kg/min	glucose production due to gluconeogenesis
	C_{E50}	pg/mL	glucagon concentration yielding half of maximum EGP
	E_{max}	μmol/kg/min	maximum EGP at basal insulin concentration
	F_{01}	μmol/kg/min	insulin independent glucose flux
	F_R	μmol/kg/min	renal glucose clearance
	$k_{12} \cdot 10^{-4}$	min^{-1}	transfer rate constant from Q_2 to Q_1
	$k_{a1} \cdot 10^{-4}$	min^{-1}	insulin deactivation rate constant
	$k_{a2} \cdot 10^{-4}$	min^{-1}	insulin deactivation rate constant
	$k_{a3} \cdot 10^{-4}$	min^{-1}	insulin deactivation rate constant
	$S_D \cdot 10^{-4}$	min^{-1}/(mU/L)	insulin sensitivity of glucose disposal
	$S_E \cdot 10^{-4}$	(mU/L)$^{-1}$	insulin sensitivity of glycogenolysis
	$S_T \cdot 10^{-4}$	min^{-1}/(mU/L)	insulin sensitivity of glucose transport
	V	mL/kg	glucose volume of distribution

5.1.4 Validation

The PD model validation used data from a glucagon dose-finding study in eight well-controlled patients with T1D [56]. The patients completed four similar study days in random order. On each study day, patients received a SC insulin bolus aiming to lower plasma glucose to 3 mmol/L. When plasma glucose decreased below 3.9 mmol/L, a single SC bolus of either 100 μg (visit B), 200 μg (visit C), 300 μg (visit D) glucagon, or saline (visit A) was administered. Serum insulin, plasma glucagon and plasma glucose was measured during the study. Model validation was carried out as a 4-fold leave-one-out cross-validation leaving all data from one visit out per fold. As each subject participated in four visits, each subject had four training datasets comprised of data from three visits and four corresponding test datasets with data from one visit:

- Training: B-C-D, Test: A

- Training: A-C-D, Test: B

- Training: A-B-D, Test: C

- Training: A-B-C, Test: D

Thus, all four visits were used for testing once without being used for optimization during that fold. To validate the PD model in a subject, at least one PD model test-fit of a dataset from a glucagon visit (B, C or D) should be accepted. The simulation accuracy of the model on datasets not used for parameter optimization was assessed by the bias calculated as the mean prediction error (MPE) and the precision calculated by the mean absolute prediction error (MAPE). A model test-fit was accepted if the MPE was less than $\pm 15\%$ and the MAPE was less than 20%. Datasets with MAPE of test-fits exceeding 50% was considered outliers and removed from further analysis. Therefore, the final individual model parameters were based on data from either three or four visits. Further details on study design, model validation and the results thereof can be found in [20].

5.1.5   Parameters

The majority of PK and PD model parameters are subject specific and listed in Table 5.4.

The insulin PK parameters describe insulin aspart (NovoRapid®, Novo Nordisk A/S, Bagsværd, Denmark) concentration in serum after SC bolus administration measured by a Mercodia assay (Mercodia AB, Uppsala, Sweden). The glucagon PK parameters describe glucagon (GlucaGen®, Novo Nordisk A/S, Bagsværd, Denmark) concentration in plasma after SC bolus administration measured by a novel assay technique with high accuracy [32]. Due to the flip-flop kinetics of both insulin and glucagon, where absorption rate is slower than elimination rate following SC administration, the elimination of drug will be underestimated compared to data following IV administration.

Other insulin and glucagon types might be described by the same PK models as defined in Sections 5.1.1 and 5.1.2, however their parameters will differ depending on assay accuracy and the formulation of drug-product - some agents will increase others decrease the absorption rate. Moreover, analogues of insulin and glucagon might have different potencies that would influence the sensitivities of the PD model.

It should be noted that both insulin and glucagon were sampled suboptimal in the clinical study. Insulin samples were missing around the time of expected maximum concentration (Tmax) and the exact dosing time of glucagon was uncertain. Due to the lack of dense sampling around Tmax, the insulin PK model could only be estimated by inferring prior knowledge on the parameters describing the kinetics, which could have introduced a bias. Given the short time to maximum concentration for glucagon, identification of the correct dosing time was critical. The most likely dosing time of glucagon was identified before estimation of the final glucagon PK parameters, which could have led to errors in Tmax of up to ±4 minutes.

The glucose PD model defined in Section 5.1.3 was validated using leave-one-out cross-validation in seven out of the eight T1D patients. The model parameters of patient 8 are reported although the model could not be validated in this subject. Therefore, simulations in the following sections include only subjects 1-7. The population of T1D patients were well-controlled and had no endogenous insulin production. The publication of the clinical study provides detailed patient characteristics [56].

A few parameters of the PD model were fixed for all subjects including the rate of gluconeogenesis, G_{GNG}, at 6 μmol/kg/min [37], and the glucose volume of distribution, V, at 160 mL/kg [117]. The renal clearance of glucose was zero unless the plasma glucose concentration exceeded 9 mmol/L in which case it was calculated as $0.003 \cdot (G-9) \cdot V$ [128]. Similarly, the insulin independent glucose flux was calculated as $F_{01} \cdot G/4.5$ when the plasma glucose concentration was

Table 5.4: Subject specific PK/PD model parameters used for simulations.

Parameter		Patient							
		1	2	3	4	5	6	7	8
W	[kg]	54	50	81	69	87	72	73	59
I_b	[mU/L]	7.3	10.6	11.7	8.7	6.6	5.5	19.7	7.4
t_{max}	[min]	57.6	57.3	40.8	67.9	48.5	46.5	68.5	55.4
$Cl_{F,I}$	[mL/kg/min]	18.9	18.5	14.8	17.4	17.3	24.6	23.7	26.8
C_b	[pg/mL]	10.7	7.6	7.6	10.9	8.7	8.9	11.6	19.0
k_1	[min^{-1}]	0.042	0.056	0.022	0.058	0.038	0.035	0.035	0.052
k_2	[min^{-1}]	0.14	0.26	0.10	0.058	0.19	0.28	0.25	0.090
$Cl_{F,C}$	[mL/kg/min]	94	106	114	159	200	125	136	91
C_{E50}	[pg/mL]	436	405	401	285	339	424	141	307
E_{max}	[μmol/kg/min]	56.4	67.4	57.4	84.4	65.4	60.1	78.0	75.3
F_{01}	[μmol/kg/min]	14.2	13.8	15.5	12.8	12.0	13.1	14.2	13.4
$k_{12} \cdot 10^{-4}$	[min^{-1}]	244	285	397	213	281	238	358	289
$k_{a1} \cdot 10^{-4}$	[min^{-1}]	16	15	18	18	15	10	49	37
$k_{a2} \cdot 10^{-4}$	[min^{-1}]	522	495	548	437	517	353	624	518
$k_{a3} \cdot 10^{-4}$	[min^{-1}]	215	231	327	68	235	74	178	154
$S_D \cdot 10^{-4}$	[min^{-1}/(mU/L)]	1.5	1.2	1.4	2.0	1.1	2.6	4.4	4.2
$S_E \cdot 10^{-4}$	[(mU/L)$^{-1}$]	155	334	237	415	229	404	140	463
$S_T \cdot 10^{-4}$	[min^{-1}/(mU/L)]	23	19	25	18	31	21	21	29

below 4.5 mmol/L [128].

5.1.6   Strengths and Limitations

Although the presented simulation model of the glucoregulatory system is detailed and accounts for many glucose-insulin-glucagon dynamics, it is still not perfect. This section serves to discuss pros and cons of the model. Moreover, it provides guidelines for when the model is appropriate to use and which dynamics it can not be expected to capture.

A model can only be expected to describe dynamics present in the data used for model development and parameter estimation, if data is sampled sufficiently often and at the right times. As an example, the PD model failed to identify the correct steady state glucose level [21]. This limitation arose because the data used for parameter estimation contained very little information about the insulin, glucagon and glucose levels before the system was disturbed with an insulin bolus. On the contrary, in the data used for parameter estimation, a steady state seemed to appear towards the end of the experiment when the glucose concentration was approaching hypoglycemia and both glucagon and insulin had returned to their baseline levels. This data sampling explains why the model assumes glucose steady state lower than one would expect at baseline levels of insulin and glucagon.

Unlike other datasets used for model development, this dataset was dynamic and included an insulin-only phase and an insulin-glucagon phase. Thus, the model is best used to describe glucose dynamics when insulin and glucagon levels are changing. As the effect of glucagon is governed by the evanescence effect during continuous exposure, the simulation model can not be used to simulate the glucose response to continued glucagon infusion. Datasets with constant glucose, insulin and/or glucagon levels should be used for investigating isolated dynamics like the evanescence effect.

During the experiment, the patients received relatively small correcting insulin boluses aiming to lower the blood glucose to 3 mmol/L. The dataset did not contain information about how the glucose dynamics i.e. the fall rate might change in the case of an over-bolus and can therefore not be expected to simulate this reliably.

Factors influencing the model parameters can not be included in the description of the parameters if the factors do not vary in the training dataset. As an example, exercise and stress are long known to alter the insulin sensitivity [82], and recently Ranjan *et al.* found that diet might influence the response to glucagon [58]. None of these factors are accounted for in the glucose PD model used for simulations in the following sections.

The model does not include a feedback mechanism of the glucose levels to the endogenous production of insulin and glucagon. Typically, patients with T1D do not have endogenous insulin production and therefore it is fair not to include this mechanism in a model describing the glucoregulatory system of this population. Although blunted, the glucagon production is existing in patients with T1D. However, the endogenous glucagon response to hypoglycemia corresponds to plasma increases observed after SC boluses of 1-10 μg [20]. With SC glucagon doses significantly larger than 10 μg, it is fair to neglect the possible endogenous glucagon response to hypoglycemia as the endogenous contribution will be minor.

Despite all the limitations, the model definitely also has some advantages. The model equations together with parameters describing seven T1D patients are public accessible [20]. The model describes the glucose dynamics of patients rather than healthy subjects and features both insulin and glucagon. The model describes a population for which it is relevant to have a simulation model so that researchers can develop improved treatment regimens for patients with T1D. Although the population is limited to seven patients, the model is validated using leave-one-out cross-validation, which is rarely executed when new models are proposed.

5.2   *In Silico* Studies

Having a reliable simulation model of the glucoregulatory system can aid in the planning of clinical trials and investigation of dose selection. *In silico* studies benefit over *in vivo* trials in not being restricted by the number of studies per subject or in total, the number of samples during same day experiments, and the amount of drug administrated. Moreover, nuisance factors disturbing clinical study outcomes are not present in simulation studies. The following sections present examples of applications for the simulation model just presented in Section 5.1.

5.2.1   Replication of an *in Vivo* Study

The simulation model was used to replicate a clinical study by El Youssef *et al.* with the title "Quantification of the Glycemic Response to Microdoses of Subcutaneous Glucagon at Varying Insulin Levels" [48]. The simulation study was published as a technical report with *in silico* replications of all *in vivo* results [21], which is included in Appendix D. This section presents highlights of

the technical report focusing on comparison of three *in silico* to *in vivo* results: time course of EGP after four different glucagon boluses, the EGP over 60 minutes separated by insulin infusion rate (IIR) and glucagon bolus size, and finally dose-response curves of glucagon and EGP separated by IIR.

The study was a cross-over where each patient participated in three study days of ten hours duration. Patients received IV IIRs of either low, medium or high. Glucose infusion rates were controlled using a proportional integral derivative (PID) controller aiming at a blood glucose concentration of 85 mg/dL. When blood glucose read below 60 mg/dL the controller regulated the glucose infusion rate every five minutes, otherwise every ten minutes. After an initial two hours run-in period the subjects received the first glucagon bolus. They received the second glucagon bolus after another two hours until a total of four glucagon boluses were delivered and observed for the following two hours. The glucagon boluses were delivered in a pseudo-random order by varying the initial dose, but keeping the order: 25 μg, 75 μg, 125 μg, and 175 μg (e.g. 125-175-25-75). Each subject received the same pseudo-random order of glucagon boluses during each study day. The *in vivo* study included 11 patients while the *in silico* study was based on the seven virtual patients. However, one virtual subject (no. 7) was excluded due to almost similar IIRs thereby almost no difference in EGP response at various insulin levels. The T1D patients in the *in vivo* study had slightly higher body mass indexes and were less well-controlled with higher HbA1c values than the virtual patients. However, we consider these population differences of minor importance. The *in vivo* study used regular human insulin (Humulin R, Eli Lilly and Company) and glucagon (GlucaGen, Novo Nordisk). The simulation model is based on GlucaGen too, but insulin is described by insulin aspart (NovoRapid, Novo Nordisk). Since the insulin infusion was constant during a study day the potential PK differences are negligible, but the PD effect of the two insulins could be different. The EGP was calculated using a single tracer technique *in vivo*, and obtained directly from the model *in silico*.

Figure 5.4b replicates Figure 5.4a with many similarities but also some differences showing the time course of EGP after four different glucagon boluses. Most importantly, the magnitudes of average peak EGP to the four glucagon doses were similar. The EGP increase appeared to be more rapid *in silico* than *in vivo* yielding a faster Tmax, which could be partly explained by a faster glucagon Tmax observed *in silico* than *in vivo*. However, with sampling of only every ten minutes the observed Tmax could be anywhere between 10-30 minutes and the simulated Tmax could be between 0-20 minutes (the average is in fact 12 minutes). If the true Tmax of EGP in response to glucagon was between 10-20 minutes, this agreed with both the observed and simulated results.

The *in vivo* estimated EGP returned fast to baseline and after 60 minutes it was below the production before injection of the preceding glucagon bolus. The simulated EGP had slower return to baseline and only slightly negative values after the lowest glucagon dose.

Figure 5.5a presents one of the most interesting results which is replicated by simulation in Figure 5.5b showing the EGP over 60 minutes separated by IIR and glucagon bolus size. The averages of the simulated data were different from the observed averages. However, considering the standard error of measurement of both datasets, the simulated data was not different from the observed data. The EGP responses to doses of glucagon during medium IIR were very similar to the EGP responses during low IIR in the measured data, whereas they were different between the responses during the two IIRs when simulating the experiments. The simulated data showed small increases in response to increasing glucagon boluses even at high IIR, which was not pronounced in the original observed data. In general, the standard error of measurements were smaller *in silico* than *in vivo*.

Figure 5.6b replicates Figure 5.6a, but without extrapolation of the dose-response curves of glucagon and EGP separated by IIR. The original graph shows the actual data in the dose-range of 25-175 μg glucagon and extrapolates the presumed trends down to 1 μg and up to 10 mg. Note, this is a wild extrapolation with no data to support it. Within the data-range the simulated results matched the observed results although the simulated EGP at low IIR tended to be higher than the observed. Having only four points very closely spaced on a log-scale, a single point can largely influence the overall interpretation of the curves.

In conclusion, the simulated results are similar to the results obtained *in vivo*. The simulation also emphasized some limitations of the clinical study which then inspired the simulation study in the following section.
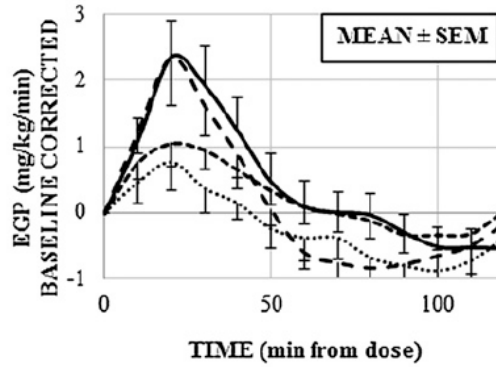
(a) *In vivo* from [48].
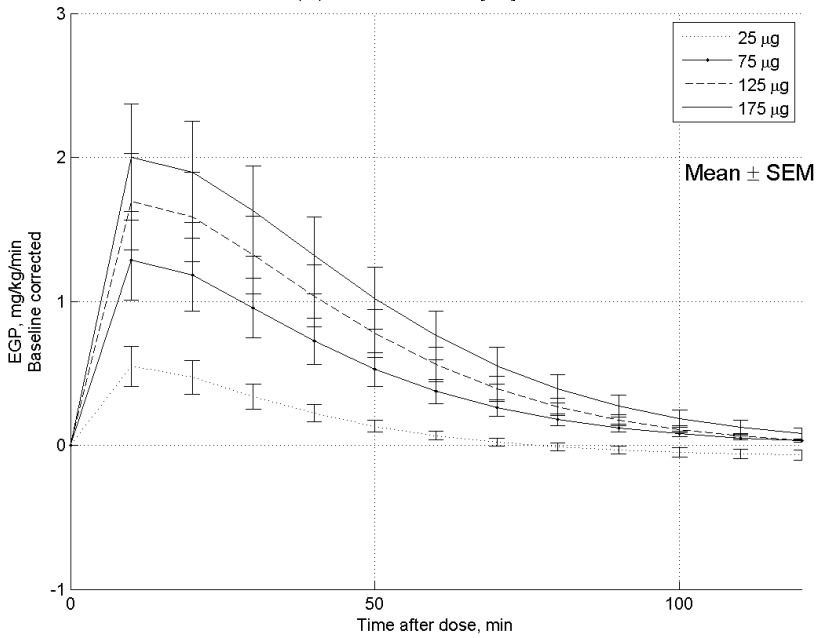
(b) *In silico* (n=6) from [21].

Figure 5.4: Time profiles of calculated EGP by glucagon dose, baseline corrected for EGP at the time of dose.

(a) *In vivo* from [48].

(b) *In silico* (n=6) from [21].
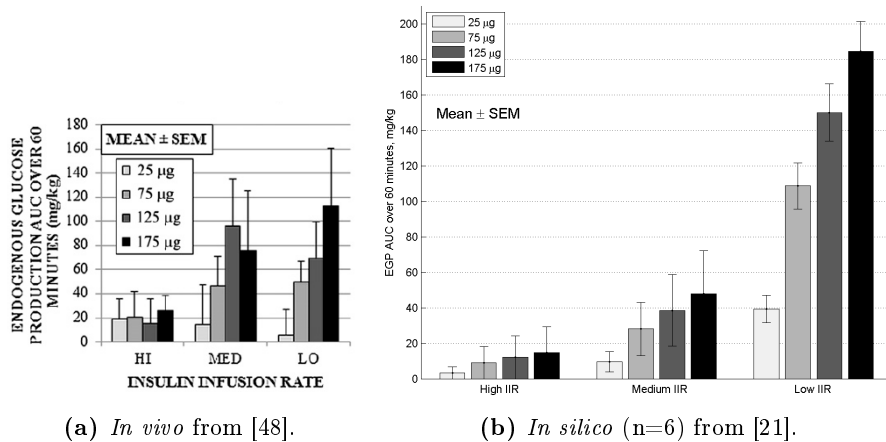
Figure 5.5: Mean EGP AUC separated by glucagon dose and insulin infusion rate.

(a) *In vivo* from [48].

(b) *In silico* (n=6 or 18) from [21].
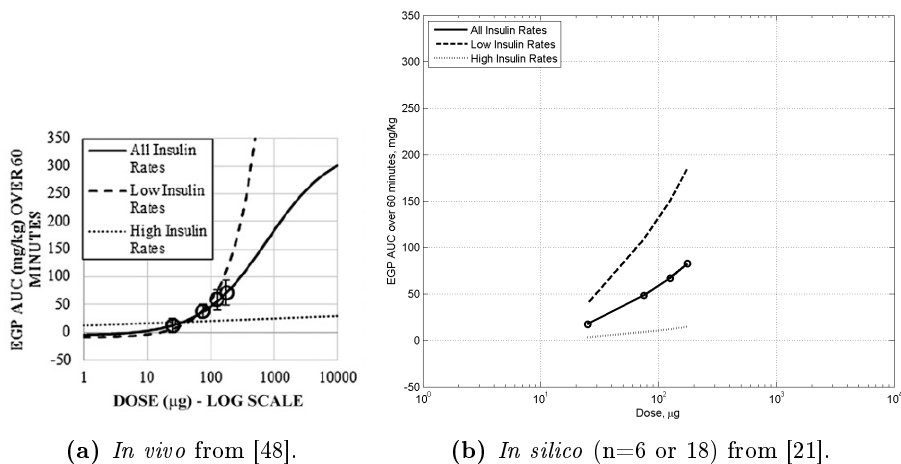
Figure 5.6: Dose-response curve across all doses, and for low and high insulin infusion rate experiments, estimated from simulated data.
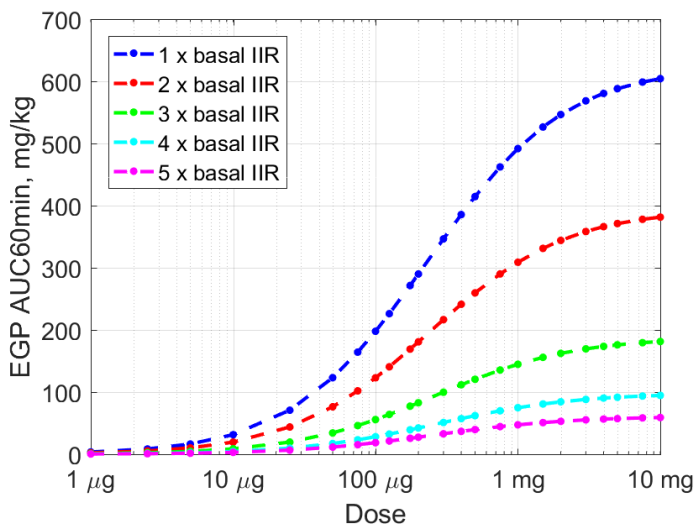
Figure 5.7: Simulated averages of seven T1D patients' dose-response curves of
glucagon boluses ranging from 1 μg to 10 mg at various insulin
levels expressed as multiples of the basal IIR, modified from [21].

5.2.2   Dose-Response Study

Inspired by the replicated *in vivo* study in Section 5.2.1, the simulation model
in Section 5.1 was used to further investigate the dose-response relationship of
glucagon and EGP at various constant insulin levels normalized to the basal
insulin level. This section presents the most important results and learnings
from the simulation study reported in [21]. The technical report is provided in
Appendix D.

The seven virtual patients were included in an *in silico* cross-over study that
comprised 115 study days per subject. At each study day, the IIR was constant
at one to five times the basal rate and the glucose infusion rate was controlled
every five minutes by a PID controller to maintain a glucose clamp of 5 mmol/L.
A glucagon bolus was administered at steady state and followed up till five hours
after the bolus. The effect of glucagon boluses in the range from 1 μg to 10 mg
was assessed by calculating the area under the EGP curve for the first 60 min-
utes following the bolus.

Figure 5.7 plots the results of the simulation study for each glucagon dose strati-
fied by IIR. The response to glucagon doses below approximately 25 μg are very
similar independent of IIR. However, with increasing glucagon doses the curves
for each IIR separate. The higher the IIR, the lower response to a glucagon

(a) ED_{50} independence of IIR.   **(b)** R_{max} independence of IIR.
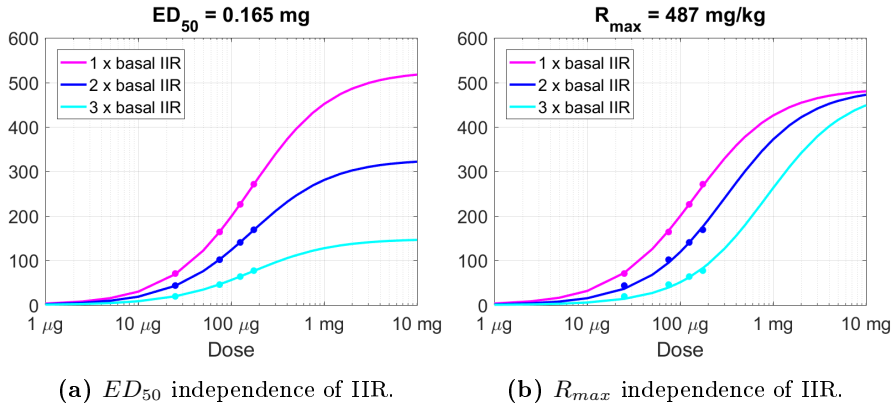
Figure 5.8: Fitted dose response curves when using doses of 25, 75, 125, and 175 μg as in the study by El Youssef *et al.* [48] assuming independence of insulin for either ED_{50} or R_{max}, from [21].

bolus. Small increases in glucagon dose during low IIR increase the response significantly although it seems to saturate for some glucagon dose. The individual curves could be described by classic Michaelis-Menten kinetics as defined in (2.11) in Chapter 2, with similar values for the concentration yielding half maximum response and distinct values for maximum response depending on the insulin level. This observation was expected, as the model used for simulations describes how insulin modulates the maximum achievable EGP response to glucagon, but does not influence the concentration yielding half-maximum response.

Whether the simulated dose-response curves in Figure 5.7 reflect the reality is currently unknown. Discussion with peers have led to two hypotheses of how the ambient insulin level might affect the EGP response to glucagon:

- insulin level influences the maximum response to glucagon (R_{max})

- insulin level influences the glucagon dose at which half-maximum response is achieved (ED_{50})

The hypotheses could be examined by carrying out a smaller *in vivo* study. However, the glucagon doses must be carefully chosen to make sure to capture the essential parts of the dose response curve. If all tested doses are below the true ED_{50} both hypotheses would describe the data equally well.
According to a small simulation study, the validity of the above hypotheses can not be investigated using the glucagon doses from the *in vivo* study in Section

(a) ED_{50} independence of IIR. (b) R_{max} independence of IIR.
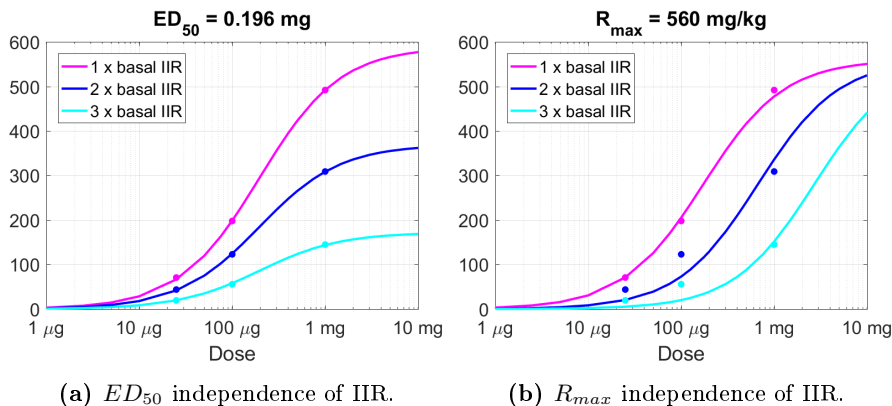
Figure 5.9: Fitted dose response curves when using SC glucagon doses of 25, 100, and 1000 µg assuming independence of insulin for either ED_{50} or R_{max}, from [21].

5.2.1, thus 25, 75, 125, and 175 µg as displayed with simulations in Figure 5.8. In the left graph, the ED_{50} is constant across all insulin levels and in the right graph the R_{max} is constant across all insulin levels. Because the four doses are within a narrow dose range and all doses are below the simulated ED_{50}, both hypotheses fit the simulated data equally well.

If the glucagon doses had been distributed across a larger dose range encompassing the ED_{50}, the difference between the hypotheses would be clearer according to a simulation study similar to the one just described. Figure 5.9 shows the results when using realistic glucagon doses spanning a larger dose range, thus 25 µg, 100 µg, and 1 mg. The graphs visualize a clear difference in the fitness of the two hypotheses making one more plausible than the other; that ED_{50} does not depend on ambient insulin levels, but that R_{max} does.

This simulation study has helped to identify which glucagon doses could be relevant to test in an *in vivo* study to investigate how the ambient insulin level influences dose-response of glucagon and EGP, and specifically test the hypotheses that insulin impacts maximum EGP response or the glucaogn dose at which half maximum EGP response occurs.

5.2.3 Dose Selection Study

Both of the previous simulation studies were designed to investigate the EGP response to glucagon at various insulin levels and how this interaction can be explored further. The simulation model can also be used for more practical purposes with direct relevance for clinicians and patients. We used the model in Section 5.1 to conduct *in silico* studies exploring insulin-dependent optimal glucagon dosing regimens for treatment of insulin-induced mild hypoglycemia based on clinically relevant criteria [22]. A draft of the paper is included in Appendix E.

As explained in Section 2.3, the EGP responsiveness to glucagon depends on the insulin level. Thus, the insulin level must influence the glucagon dose needed to recover from hypoglycemia. Currently, it is not possible to measure serum insulin concentration in real time, but research is being done to develop a continuous insulin monitor [129]. However, pumps with bolus calculators offer as standard calculation of insulin on board (IOB), which is provided as information to the user to avoid insulin stacking due to the slow insulin absorption and onset of action. The IOB approximates the remaining effect of insulin in the body after an insulin bolus.

The *in silico* study evaluated the effect of glucagon at various insulin levels interpreted as: serum insulin concentration uncorrected or normalized to basal insulin concentration, and IOB uncorrected or normalized to individual total daily dose (TDD) of insulin. The serum insulin concentration was directly obtained from the PK model and the IOB was calculated as a linear decay based on individual insulin action times. The insulin level interpreted as normalized serum concentration to basal was not included in the paper, but the results of the experiments are presented in this section.

At the beginning of each experiment in a study the patients' blood glucose were normoglycemic. The patients then received an individualized insulin bolus that would yield a predefined insulin level when the plasma glucose concentration decreased beyond the hypoglycemia threshold. At hypoglycemia, a glucagon bolus in the range of 25 μg to 2.5 mg was administered. The glucose response after the glucagon bolus was evaluated in terms of average success among the virtual patient population in raising the glucose concentration above 5 mmol/L, keeping glucose concentration less than 10 mmol/L and maintaining the glucose concentration above the threshold of hypoglycemia for at least two hours. The individual success criteria of recovering from hypoglycemia was summarized in a single variable describing the overall success of hypoglycemia treatment calculated as a weighted harmonic mean. The optimal glucagon bolus was chosen as the lowest dose yielding maximum overall success.

Figure 5.10 presents the optimal glucagon dose as a function of the insulin level
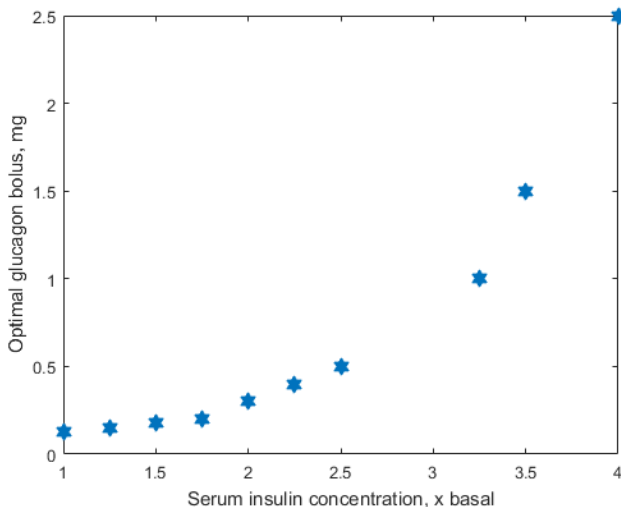
Figure 5.10: Optimal glucagon bolus for a population of T1D patients to re-
cover from insulin-induced mild hypoglycemia as a function of the
ambient insulin concentration normalized to basal insulin concen-
tration.

interpreted as serum insulin concentration normalized to basal insulin concentra-
tion. The graph showed that the higher ambient insulin concentration compared
to basal, the larger glucagon bolus was required to best treat the population for
hypoglycemia. At concentrations of insulin less than two and a half times the
basal value, glucagon boluses from 125 to 500 μg were ideal to treat the majority
of the virtual population for hypoglycemia. Notice, that an optimal glucagon
bolus might be suboptimal for an individual, but viewing the seven virtual pa-
tients as a population, the optimal doses could be given to any subject in the
population and still yield satisfying recovery from hypoglycemia in most cases.
With serum insulin concentrations exceeding two and a half times the basal level
it would be more desirable for the patient to consume a carbohydrate snack since
the optimal glucagon bolus to recover from mild hypoglycemia would be close
to the bolus of 1 mg used to rescue patients from severe hypoglycemia.
The normalized concentration was chosen over the absolute concentration, be-
cause one patient had very high basal concentration making the obtainable range
of absolute concentrations for all virtual patients very narrow and less meaning-
ful than the range obtained by normalising the concentration.
The studies interpreting insulin level by IOB had similar relationships between
insulin level and optimal glucagon dose. Mild hypoglycemia was treatable with
less than 0.5 mg glucagon when IOB was less than 2 U or IOB corresponded to
less than 6% of TDD.

This simulation study showed that unlike the fixed rescue bolus of 1 mg glucagon for treatment of severe hypoglycemia, there might not be a one-size-fits-all-solution to treatment of mild hypoglycemia because of the impeding insulin level highly influencing the effect of glucagon. The treatment success of mild hypoglycemia greatly depended on the ambient insulin level independent of if the level was assessed as a normalized concentration to basal, IOB or IOB normalized to TDD.

5.2.4 *In Silico* as Supplement to *in Vivo*

This section presented examples of application of a glucose-insulin-glucagon simulation model spanning replication of an independent clinical study, dose optimization for a clinical study, and a large original simulation study. The model was used to show the effect of glucagon on EGP at various insulin levels and also suggested new glucagon doses that should be applied clinically in a similar study design to further investigate the dose-response relationship of glucagon and EGP. Finally, the model was used to generate glucagon mini-bolus dosing regimens for patients with T1D to recover from insulin-induced mild hypoglycemia depending on the ambient insulin level.
The simulation model could be expanded to include models of e.g. meal absorption, exercise, and other hormones. Such a simulation model could be used in optimization of diabetes treatment and specifically in developing and testing control strategies for a dual hormone closed-loop device (artificial pancreas).
The simulation model can however not replace clinical studies. It should be regarded as a supplement that can aid in study design to maximize the yield of clinical studies and investigate glucoregulatory dynamics qualitatively.

CHAPTER 6

Conclusions

This thesis demonstrated methods for PK/PD modeling of glucagon, insulin, and glucose in biological data. It showed how likelihood principles and Bayesian methods can be used for parameter estimation in datasets not initially intended for modeling and thus not optimally sampled. The CTSM package for R proved to be useful for ML and MAP parameter estimation.

The project succeed in developing a SC PK model of glucagon and the glucagon analogue ZP-GA-1 in healthy dogs as documented in Appendix A. The same dataset was used to design a model describing the EGP as a function of both glucagon or ZP-GA-1 and insulin. A sigmoid E_{max} model described the effect of glucagon and ZP-GA-1 on EGP. A multiplicative relationship between the effects of insulin and glucagon or ZP-GA-1 on EGP was needed to capture that EGP is suppressed at high insulin concentrations. The EGP model was embedded in Hovorka's glucoregulatory model and fitted 20 datasets from five dogs well.
The novel EGP model of glucagon translated from healthy dogs to healthy humans. Only the PK/PD models of marketed glucagon was fitted to human data due to unavailability of data describing ZP-GA-1 in humans. The glucoregulatory model fitted ten datasets from ten healthy subjects well as documented in Appendix B.

In a model comparison, the novel EGP model showed both strengths and weak-

nesses compared to other published models. Among the strengths, it was not possible for the model to yield non-physiologic negative glucose production as the lowest output corresponded to the constant gluconeogenesis. The model included the effect of insulin and glucagon and could describe insulin's suppressing effect even at high glucagon concentrations. The immediate effect of glucose on EGP was not included in the model. The PK/PD model parameter values were published for seven validated T1D patients. Moreover, the novel model was the only model among the reviewed ones, that included physiologic saturation of response at high glucagon concentrations and matched the concentration-response relationship reported in literature.

However, the model failed to identify the correct glucose steady state and it did not account for the evanescence effect of glucagon.

Model parameters of insulin and glucagon PK models were estimated in a population of eight diabetes patients. The glucoregulatory model including the novel description of EGP was successfully validated by leave-one-out cross-validation in seven of the eight T1D patients. The model thus proved its validity for simulations of seven virtual subjects with T1D using the parameter sets of the seven validated patients. The final patient specific model parameter sets described three to four study days in each patient with SC glucagon boluses ranging 0 to 300 μg.

The simulation model replicated a clinical study within the uncertainty limits. Simulations were also used to recommend glucagon doses for a theoretical repetition of the *in vivo* study to further investigate the relationship between EGP and glucagon at various insulin levels. Finally, the simulation model was used to conduct a large original *in silico* study to determine the optimal glucagon mini-bolus to treat mild insulin-induced hypoglycemia at various insulin levels assessed as concentration or IOB based on clinically relevant criteria.

Although validated, the simulation model can not replace clinical studies, but it has proved to be a useful supplement and tool in the planning of studies.

6.1   Future Work

The novel EGP model has some limitations that could be subject for future studies and would justify collection of new physiologic data. More data describing the glucose concentration during steady state should be collected to identify the correct level thereof. The evanescence effect of glucagon also needs to be studied further in order to include it in an EGP model. Especially the refractory period indicating when normal glucagon responsiveness is restored after desensitization, should be investigated.

The simulation model could be used to conduct other *in silico* studies than the ones here presented. The simulation environment can also aid in the design of clinical studies to avoid common pitfalls and in the planning of relevant nominal sampling times.

It would be interesting to carry out the proposed dose-response study with a wide range of glucagon boluses to investigate how the effects of insulin and glucagon interact and influence the EGP. Furthermore, the proposed insulin-dependent glucagon dosing regimens would be highly relevant to study further *in vivo*.

Technical Report 1
PK/PD in Healthy Dogs

This appendix presents the technical report with the title "PK/PD modelling of glucose-insulin-glucagon dynamics in healthy dogs after a subcutaneous bolus administration of native glucagon or a novel glucagon analogue" published by the Technical University of Denmark in April 2016 [18].

PK/PD modelling of glucose-insulin-glucagon dynamics in healthy dogs after a subcutaneous bolus administration of native glucagon or a novel glucagon analogue

Sabrina Lyngbye Wendt[*,1,2,3], Jan Kloppenborg Møller[2], Carsten Boye Knudsen[1], Henrik Madsen[2], Ahmad Haidar[3,4], and John Bagterp Jørgensen[2]

[1]Department of Bioanalysis and Pharmacokinetics, Zealand Pharma A/S, Glostrup, Denmark
[2]Department of applied mathematics and computer science, Technical University of Denmark, Kongens Lyngby, Denmark
[3]Institut de Recherces Cliniques de Montréal, Montreal, Quebec, Canada
[4]Division of Experimental Medicine, McGill University, Montreal, Quebec, Canada

Version 1
April, 2016

Objective We aim to develop a simulation model of the complex glucose-insulin-glucagon dynamics based on physiology and data. Furthermore, we compare pharmacokinetic (PK) and pharmacodynamic (PD) characteristics of marketed reconstituted glucagon with a stable liquid glucagon analogue invented by Zealand Pharma A/S.

Research Design and Methods We expanded a physiological model of endogenous glucose production with multiplicative effects of insulin and glucagon and combined it with the Hovorka glucoregulatory model. We used a Bayesian framework to perform multidimensional MAP estimation of model parameters given priors reported in the literature. We used profile likelihood analysis to investigate parameter identifiability and reduce the number of model variables. We estimated model parameters in pre-clinical data from one cross-over study with a total of 20 experiments in five dogs. The dogs received two subcutaneous (SC) bolus injections of low and high doses of glucagon and ZP-GA-1 (20 and 120 nmol/kg).

Results We report posterior probability distributions and correlations for all identifiable model parameters. Based on visual inspection and residual analysis, the PD model described data satisfactorily for both glucagon and the analogue. Parameter estimates of the PD model were not significantly different between the two compounds.

Conclusions The new PK/PD model enables simulations of the glucose-insulin-glucagon dynamics after a SC bolus of glucagon or glucagon analogue. The novel glucagon analogue by Zealand Pharma A/S shows PK and PD characteristics similar to marketed glucagon.

Keywords: Pharmacokinetics, PK, Pharmacodynamics, PD, modeling, modelling, glucagon, glucagon analogue, glucose, insulin, glucoregulatory, ODE, SDE, MAP, simulation, profile likelihood

Contents

1 Introduction

Conventionally, diabetes type 1 is treated with multiple daily injections of insulin or continuous infusion of insulin using a pump. The stress of calculating the needed amount of insulin based on food intake, exercise and insulin sensitivity has led to research in creating an artificial pancreas (AP). A basic AP is a closed-loop (CL) system consisting of an insulin pump, a continuous glucose monitor (CGM) and a control algorithm to adjust insulin dosage through the pump based on CGM sensor readings.

Until recently, researchers and developers of the AP have mainly focused on a single hormone approach [1]. However, research in the field of dual hormone AP systems is growing substantially and clinical studies are being conducted by research groups in Boston [2–4], Montreal [5–8], Portland [9,10], and Amsterdam [11–14]. In multiple studies of single hormone open-loop (OL) versus single hormone CL and/or dual hormone CL systems these groups have demonstrated that time in range increases when using a CL system compared to an OL system. Moreover, comparative studies show significant reduction of time spent in hypoglycaemia and number of hypoglycaemic events using a dual hormone CL system versus a single hormone CL system [6,7,9].

The unstable nature of native glucagon in liquid formulation challenges the development of a dual hormone AP. The hormone is currently marketed in dry form and needs reconstitution daily [16, 17]. Immediately after reconstitution glucagon starts degrading and forming fibrils. The fibrillation can cause the pump tubing to occlude and the degradation reduces the efficacy of the compound. Currently, only reconstituted glucagon is available for dual hormone AP studies which frequently experience glucagon pump occlusions [3, 13, 14].

At least two pharmaceutical companies are developing glucagon stable in liquid solution suitable for pump use. Xeris Pharmaceuticals Inc. is developing native glucagon stabilized in dimethyl sulfoxide (DMSO) [18], whereas Zealand Pharma A/S is developing a glucagon analogue in aqueous solution [19]. With this ongoing development of liquid stable glucagon suitable for pump use, the realization of a dual hormone AP is becoming practically possible.

In silico experiments are useful during the development of a control algorithm for a dual hormone AP
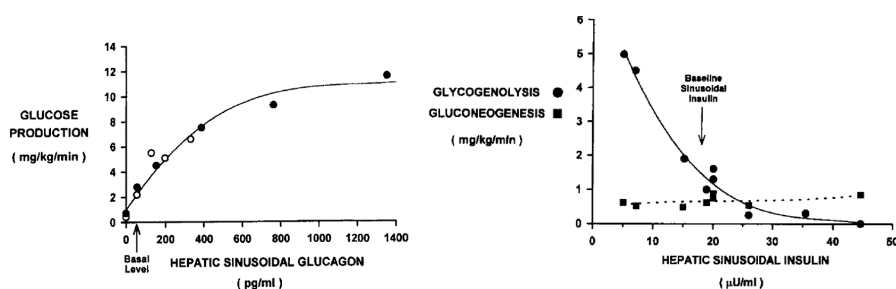
Figure 1: Endogenous glucose production due to glucagon and insulin. Left) The relationship between liver glucagon concentration and glucose production. Solid circles represent data from dogs, and open circles represent data from humans. Right) The relationship between liver insulin concentration and glucose production in dogs by gluconeogenesis and glycogenolysis. Data were acquired during basal arterial and portal glucagon concentrations, basal arterial insulin concentrations and mostly during euglycemia. Both graphs are from Cherrington [15].
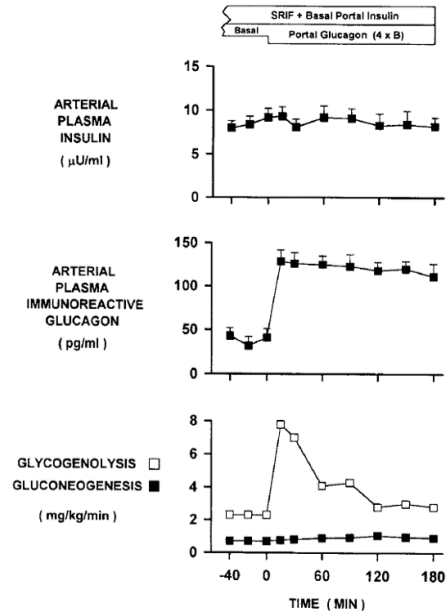
Figure 2: The effect of increased glucagon on glycogenolysis and gluconeogenesis in the dog. Somatostatin (SRIF) was given along with basal (B) replacement amounts of insulin and glucagon intraportally. At time zero the glucagon infusion rate was increased. The data is from Wada et al. [27].

before applying the algorithm in a clinical trial. Simulations *in silico* can also provide new insights in physiological system. A model describing the dynamics between glucose and insulin is validated by tracer data [20], and widely used in the literature for simulations of the endocrine regulatory system [21–23]. Recent proposed extensions include the effect of glucagon on endogenous glucose production (EGP) [24–26]. It is important to understand the glucose dynamics of the body to evaluate if these glucagon-glucose models are capturing the complexity of the reality.

The quantitative dynamics of insulin and glucagon on EGP are complex and not completely understood [15]. Two processes contribute to EGP: gluconeogenesis (GN) and glycogenolysis (GG). GN is the formation of glucose from non-carbohydrate substrates like glucogenic amino acids, glycerol, pyruvate and lactate. GG is the breakdown of stored glycogen in the liver to glucose. Studies show that glucagon and insulin have very little effect on GN as opposed to GG [15, 29, 30], see Figures 1 and 2. Thus the hormones influence mainly the EGP by regulating GG; glucagon stimulates it whereas insulin inhibits it. Increasing the glucagon concentration stimulates GG until a certain point where-after the response saturates. Saturation of response is typical for receptor mediated processes due to the limited number of receptors in a physiological system [31]. As opposed to glucagon, insulin inhibits GG and completely suppresses the breakdown of glycogen at insulin concentrations exceeding approximately 45 mIU/L [15]. A recent study by El Youssef et al. showed that at high insulin concentrations (46.0±12.5 mIU/L) the EGP is greatly reduced independent of the glucagon dose [28], see Figure 3. Moreover, the rates of EGP
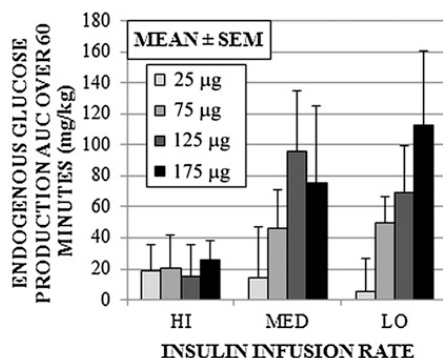
Figure 3: Endogenous glucose production with increasing glucagon doses (25, 75, 125, 175 μg) at high, medium and low insulin infusion rates (0.016±0.006 IU/kg/h, 0.032±0.003 IU/kg/h, 0.05±0.0 IU/kg/h) giving plasma insulin concentrations of 17.6±13.0 mIU/L, 29.1±8.9 mIU/L, and 46.0±12.5 mIU/L, respectively. The graph is from El Youssef et al. [28].

at high insulin concentrations match the rates of GN. The results are in agreement with previous studies showing that insulin suppresses GG but does not affect GN. These results suggest that the effect of insulin prevails over glucagon at high insulin concentrations. Some studies indicate that not only does the absolute glucagon concentration affect EGP but also the glucagon rate of change [15, 27].

The glucose kinetics model by Herrero et al. is based on the minimal model and describes the glucose changes with additive effects of insulin and of glucagon [25, 32]. The EGP model by Dalla Man et al. also describes the effects of insulin and of glucagon additively [24]. The glucose kinetics model of Hovorka includes the interaction of insulin and EGP, but does not describe the effect of glucagon on EGP [20]. The only model including the interaction and effect of both glucagon and insulin on EGP is proposed by Emami et al. [26]. This model approximates the EGP response to either glucagon or insulin with linear effects and includes the effect of glucagon rate of change on the EGP. The linear assumption of the EGP response to glucagon is fair as long as the glucagon concentration does not exceed approximately 400 pg/mL. Based on deviance information criterion the novel model outperformed several other models including the one proposed by Herrero et al. The model by Emami et al. assumes that the glycogen stores are never depleted. This is a valid assumption at normal conditions since a recent study showed that small repeated glucagon doses over a short time span did not significantly alter the glycogen stores even after an overnight fast [22].

This technical report presents a novel model of the glucose-insulin-glucagon dynamics by combining the validated insulin-glucose model and the physiological EGP model for the purpose of simulation. The insulin-glucose model by Hovorka et al. forms the basis of the dynamical system [20]. The model by Emami et al. extends the EGP part of the Hovorka model to include glucagon [26]. The EGP model is modified further to ensure saturation of the EGP at high glucagon concentrations in accordance with literature and physiological receptor activation concepts.

Furthermore, this report aims to thoroughly illustrate and explain the mathematical methods applied during the model fitting procedure of the pharmacodynamics model. The final model is fitted to individual

datasets using a multidimensional Bayesian framework. Parameter identifiability is investigated using profile likelihood analysis. Model validity is confirmed by estimating the noise contribution of the system using the grey-box modelling approach with stochastic differential equations (SDEs) [33]. After validation, final parameter estimation is conducted using the white-box modelling approach with ordinary differential equations (ODEs) making the model suitable for simulations. We use a programming environment in R created for continuous time stochastic modelling (CTSM) for the entire model fitting procedure [34].

Previously, PK data of this report were used for model fitting by a different technique and presented as a poster at the 8th International Conference on Advanced Technologies & Treatments for Diabetes (ATTD) in February 2015 [19]. PD results of this report were presented as a poster at the 9th ATTD in February 2016 [35].

Table 1: Data summary.

Study	Drug	Dose, nmol/kg	Dogs	Nominal Sample Times, minutes post dose
1	Glucagon	20	5	0, 5, 10, 15, 20, 30, 40, 50, 60, 75, 110, 140, 180
		120		
	ZP-GA-1	20		
		120		

2   Data

Zealand Pharma A/S is developing a new glucagon analogue with increased stability in liquid solution for treatment and better control of hypoglycemia in diabetes patients. The novel compound, ZP-GA-1, was tested against marketed glucagon (GlucaGen®, Novo Nordisk A/S) in pre-clinic. Both compounds are peptides and act as glucagon receptor agonists.

2.1   Data collection

Data originates from a pre-clinical study in dogs designed by Zealand Pharma A/S and conducted at Covance Laboratories Ltd (Covance site, Harrogate UK). The Institutional Animal Care and Use Committee approved the study and all procedures carried out on the dogs were in accordance with the Animals (Scientific Procedures) Act 1986. The study is summarized in Table 1 and described in Section 2.1.1.
Data was originally collected for the purpose of showing a PD effect of the glucagon analogue *in vivo* and to compare it with the PD effect of marketed glucagon.

2.1.1   Study 1

Five healthy Beagle dogs (bodyweight 13.6 ± 1.3 kg; mean $\pm$ SD) were included in this randomized cross-over study and named dog 1-5. At four dosing occasions each dog received a subcutaneous (SC) bolus injection of 20 or 120 nmol/kg glucagon or ZP-GA-1. Blood samples were collected at 0, 5, 10, 15, 20, 30, 40, 50, 60, 75, 110, 140, and 180 minutes after dose administration. Sample concentrations of glucagon and of ZP-GA-1 were analyzed using an in-house developed LC-MS/MS method. Plasma concentration of insulin was analyzed using a commercially available immunoassay from Meso Scale Discovery (MSD) (catalog no. K152BZC). Although the MSD assay was designed for mouse/rat plasma, an in-house validation showed that it was also valid for analysis of insulin in dog plasma. Plasma concentration of glucose was analyzed using Roche glucose method (UV test) [36]. Figure 4 presents an example of raw data from one dog in study 1.

2.2   Bioavailability

The bioavailability is obtained from the ratio between the dose-normalized area under the curve (AUC) after SC administration compared to IV. The AUC's were calculated using non-compartmental analysis (reported at Zealand Pharma A/S). The bioavailability varies between the drugs. Thus, for each drug the bioavailability is used in the input to the PK model, see summary in Table 2.

2.3   Unit conversion

In the study, glucagon and analogue concentrations were measured in nmol/L, insulin concentration was measured in pg/mL and glucose concentration was measured in mmol/L. Model parameters concerning glucagon and of insulin are often reported so that concentrations thereof should be in pg/mL and mIU/L,
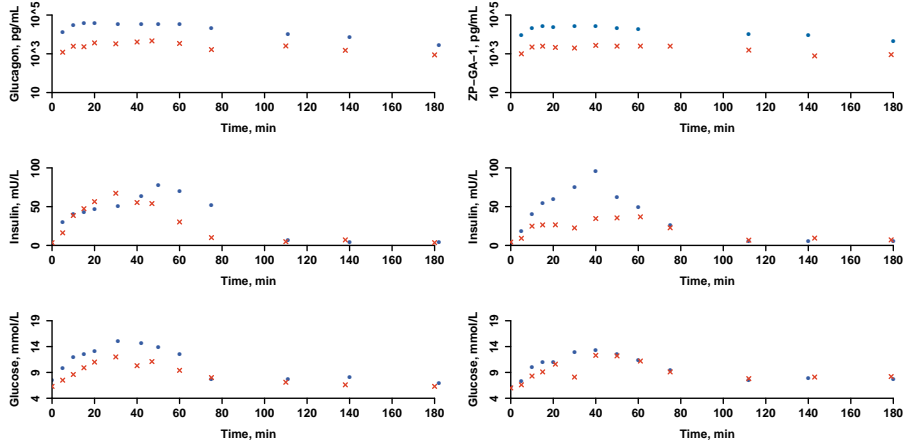
Figure 4: Raw data from dog 2 in study 1. Plasma concentrations after low or high doses of glucagon and ZP-GA-1 are red crosses or blue dots, respectively.

Table 2: Bioavailability and molar mass of glucagon and glucagon analogue in study 1.

Study	Drug	Bioavailability	Molar mass, g/mol
1	Glucagon	37.5%	3482.75
	ZP-GA-1	50%	3339.7

respectively [20, 21, 25]. The units of the PK and the PD data were converted to these generally used units before modelling.

2.3.1 Glucagon

To convert the plasma concentration of the administered compound from nmol/L to pg/mL, PK data is multiplied by the molar mass of the compound since the following yields units of pg/mL.

$$\frac{[\text{nmol}]}{[\text{L}]}\frac{[\text{L}]}{10^3\,[\text{mL}]}\frac{10^3\,[\text{pmol}]}{[\text{nmol}]}\frac{\text{MolarMass}\,[\text{pg}]}{[\text{pmol}]} \tag{1}$$

The molar masses of glucagon and the analogue are listed in table 2.

2.3.2 Insulin

To convert the insulin concentration from pg/mL to mIU/L, insulin PD data is multiplied by 0.023 since the following yields units of (mIU/L).

$$\frac{[\text{pg}]}{[\text{mL}]}\frac{10^3\,[\text{mL}]}{[\text{L}]}\frac{0.023\,[\text{IU}]}{[\mu g]}\frac{10^3\,[\text{mIU}]}{[\text{IU}]}\frac{[\mu g]}{10^6\,[\text{pg}]} \tag{2}$$

The assay used for analysis uses the WHO standard of 0.023 (IU/μg).

Table 3: List of removed outliers in the datasets substituted with linear interpolation of neighbouring observations. *Outlier not substituted by interpolation but removed.

Study	Dog	Drug	Dose, nmol/kg	Analyte	Time, min
1	1M	Glucagon	20	Glucagon	*6
1	1M	ZP-GA-1	20	Glucose	6
1	1M	ZP-GA-1	20	Glucose	16
1	2M	ZP-GA-1	20	Glucose	30
1	3M	Glucagon	20	Glucose	15
1	3M	Glucagon	20	Glucose	40

2.4   Basal concentrations

After an overnight fast in healthy human adults, the glucagon concentration is around 91 pg/mL (range 40-400 pg/mL) and the fasting insulin concentration is approximately 10-15 mIU/L [37]. Based on the two present studies, the basal insulin concentration in dogs are considerably lower with an average around 3 mIU/L and range 1.6-5.7 mIU/L, thus less than one third of the human basal insulin concentration. As there is a negative relationship between basal insulin concentration and insulin sensitivity in humans [38], this lower basal insulin concentration in dogs indicate a higher insulin sensitivity.

Basal glucagon concentration in dogs is around 41-54 pg/mL [27]. The lower level of quantification (LLOQ) for glucagon measured in study 1 was 0.2 nmol/L corresponding to nearly 700 pg/mL. All measurements at time zero were below LLOQ. The basal concentration of glucagon can thus not be determined in this study.

2.5   Data cleaning

No formal tests of the significance of an outlier were used but rather visual inspection. Table 3 lists all data points that the modeller considered to be outliers. The glucagon outlier appeared to have too high concentration after just 6 minutes, whereas the removed glucose observations showed sudden drops in glucose concentration that did not seem physiological. Figure 4 shows an example of such a data point with a drop at 30 minutes after the low dose of glucagon analogue ZP-GA-1. Figures 16-20 in Appendix A present raw data from all datasets including outliers.

3   Models

3.1   PK model

The glucagon pharmacokinetics (PK) are investigated using a simple model as formulated by Haidar et al. [39,40], defined in (3)-(5) and visualized in Figure 5. The PK model is a one-compartment model of the disturbance in plasma concentration from baseline after extravascular drug administration with first order absorption kinetics from the SC tissue to the plasma. The model has two states; the first corresponding to the SC tissue and the the second corresponding to the central compartment (plasma and instantaneous equilibrating tissues). The model includes two rate constants; one describing absorption from the SC tissue to the central compartment and another describing elimination from the central compartment. To minimize confusion, the parameter naming is kept as closely to the formulation by Haidar et al. as possible.

$$\frac{\mathrm{d}q_1(t)}{\mathrm{d}t} = u(t) - k_1 q_1(t) \qquad q_1(0) = 0 \tag{3}$$

$$\frac{\mathrm{d}q_2(t)}{\mathrm{d}t} = k_1 q_1(t) - k_2 q_2(t) \qquad q_2(0) = 0 \tag{4}$$

$$C(t) = \frac{k_2 q_2(t)}{\mathrm{w} Cl} \cdot 10^3 + C_b \tag{5}$$

Model input: $u(t) = \delta(t) \cdot \mathrm{Dose} \cdot \mathrm{bioavailability}$
Model observation: $C(t_n)$
Model output: $C(t)$
Fixed parameter(s): w, (C_b)
Model parameters: k_1, k_2, Cl, C_b

$C(t_n)$ is the measured glucagon concentration in plasma (nmol/L) at discrete timepoints, $n = 1, ..., N$. $C(t)$ is the simulated glucagon concentration in plasma at continuous time. C_b is the basal glucagon concentration in plasma (nmol/L). In case of administration of the glucagon analogue, C_b is fixed to zero as no basal level exists in the body.
w is the measured bodyweight (kg). Cl is the clearance rate normalized by weight (mL/kg/min). k_1 is the absorption rate constant and k_2 is the elimination rate constant (min^{-1}).
The concentration of glucagon in the central compartment is obtained by multiplying the content with an expression similar to per volume of distribution in (5). In classical PK it is trivial that clearance is equal to the product of the elimination rate constant and volume of distribution [31]. Since clearance is normalized by weight the denominator is multiplied by the bodyweight.
The bioavailability does not influence the fit of the model to data, but is necessary to get physiological parameter estimates of clearance. The Dose (nmol) is multiplied by the Dirac delta function to model the bolus injection at time zero.

A surrogate marker for the onset of action, t_{max}, is obtained analytically from the absorption and elimination rate constants.

$$t_{max} = \frac{\log(k_1/k_2)}{k_1 - k_2} \tag{6}$$

In (6) log is the natural logarithm.

3.2 PD model

3.2.1 Version 1.0 - Integrating Emami in Hovorka

The pharmacodynamics (PD) of glucagon and insulin on glucose are described by combining two published models. The glucose-insulin part of the model was published by Hovorka et al. [20] and listed in equations (7)-(12). A few changes to this model include removal of glucose input, removal of the labelled glucose kinetics, and parameter substitution of insulin sensitivities instead of ratios between activation and deactivation rate constants. To minimize confusion, the parameter naming is kept as closely to the original publication as possible. The model is initially in steady state, but could be initialized in any state.

$$\frac{dQ_1(t)}{dt} = -F_{01} - S_T x_1(t) Q_1(t) + k_{12} Q_2(t) + GG(t) \quad Q_1(0) = Q_{10} \tag{7}$$

$$\frac{dQ_2(t)}{dt} = S_T x_1(t) Q_1(t) - [k_{12} + S_D x_2(t)] Q_2(t) \qquad Q_2(0) = Q_1(0)\frac{x_1(0)}{x_2(0) + k_{12}} \tag{8}$$

$$G(t) = \frac{Q_1(t)}{V} \tag{9}$$

$$\frac{dx_1(t)}{dt} = k_{a1}[I(t) - x_1(t)] \qquad\qquad x_1(0) = I_b \tag{10}$$

$$\frac{dx_2(t)}{dt} = k_{a2}[I(t) - x_2(t)] \qquad\qquad x_2(0) = I_b \tag{11}$$

$$\frac{dx_3(t)}{dt} = k_{a3}[I(t) - x_3(t)] \qquad\qquad x_3(0) = I_b \tag{12}$$

$$\tag{13}$$

The model is extended to include a GG model as proposed by Emami et al. [26], defined in equations (14)-(15). The combined PD model is visualized in figure 5.

$$GG(t) = (1 - S_E x_3(t)) \cdot (S_{gd} E_{gd}(t) + S_g C(t))$$
$$\text{where } 1 - S_E x_3(t) \geq 0 \text{ and } S_{gd} E_{gd}(t) + S_g C(t) \geq 0 \tag{14}$$

$$\frac{dE_{gd}(t)}{dt} = -k_{gd}\left(E_{gd}(t) - \frac{dC(t)}{dt}\right) \tag{15}$$

Since CTSM-R does not accept if statements to supplement the state equations, the conditional statements are implemented as $\frac{1}{2} + \frac{1}{2} \cdot \tanh(100 \cdot "conditional\, statement")$ multiplied by the conditional statement. Thus, when the statement is positive the expression equals one, and when the statement is negative the expression is zero.

The PD model not only includes a term for the absolute concentration of glucagon, but also a term describing the glucagon rate of change in (15). The analytical solution to the glucagon rate of change is derived from (4)-(5) yielding units of nmol/L/min.

$$\frac{dC(t)}{dt} = \frac{k_2}{wCl} \cdot 10^3 \cdot (k_1 q_1(t) - k_2 q_2(t)) \tag{16}$$

Model inputs: $C(t)$, $\frac{dC(t)}{dt}$, $I(t)$
Model observation: $G(t_n)$
Model output: $G(t)$
Fixed parameters: V, I_b
Model parameters: F_{01}, k_{12}, S_T, S_D, S_E, k_{a1}, k_{a2}, k_{a3}, S_g, S_{gd}, k_{gd}

109

Wendt et al. DTU Compute Technical Report-2016-2 *3 MODELS*
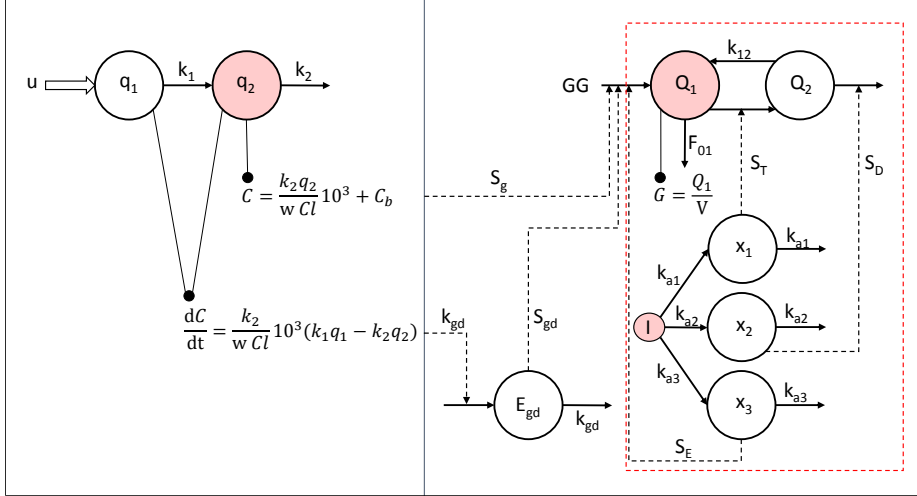
Figure 5: Schematic presentation of the full model including the PK part at the left and the PD part at the right. The open arrow symbolizes SC input of glucagon. Solid arrows indicate mass transfer to/from a compartment. Dashed arrows indicate effect without mass transfer. Solid lines ending with a dot indicate how an output is derived from the content of a compartment. Plasma compartments of glucagon, insulin and glucose are colored. A red dashed square surrounds the part of the model published by Hovorka et al. [20].

$C(t)$ and $\frac{dC(t)}{dt}$ are the simulated concentration (pg/mL) and rate of change (pg/mL/min) of glucagon in plasma at all times, respectively. $I(t_n)$ is the measured insulin concentration in plasma (mIU/L) at discrete timepoints, $n = 1, ..., N$. To match the time resolution of the glucagon input, the insulin observations are linearly interpolated to give the model input $I(t)$.

$G(t_n)$ is the measured glucose concentration in plasma (mmol/L) at discrete timepoints, $n = 1, ..., N$. $G(t)$ is the simulated glucose concentration in plasma at all times.

I_b is the basal insulin concentration for each dog averaged over a maximum of four occasions (mIU/L). V is the glucose volume of distribution and is fixed to 160 mL/kg based on literature [20].

F_{01} is the net total non-insulin-dependent glucose out-flux from the plasma compartment $\left(\frac{\mu\text{mol}}{\text{kg}\cdot\text{min}}\right)$. GN is included in F_{01} and assumed constant and independent of insulin and glucagon as this process is affected very little by the two hormones. k_{12} is the transfer rate constant from the non-accessible glucose compartment to the accessible plasma compartment (min^{-1}). S_T is the insulin sensitivity on glucose transport (min^{-1} per mIU/L). S_D is the insulin sensitivity on glucose disposal (min^{-1} per mIU/L). S_E is the insulin sensitivity on EGP (1/(mIU/L)). k_{a1}, k_{a2} and k_{a3} are insulin deactivation rate constants (min^{-1}).

S_g is the glucagon sensitivity on GG $\left(\frac{\mu\text{mol}}{\text{kg}\cdot\text{min}}\text{per pg/mL}\right)$. E_{gd} is a fictive rate of change compartment contributing to rate of change of GG due to glucagon rate of change (pg/mL/min). S_{gd} is the glucagon rate of change sensitivity on GG $\left(\frac{\mu\text{mol}}{\text{kg}}\text{per pg/mL}\right)$. k_{gd} is the delay of glucagon rate of change on EGP (min^{-1}).

The full PK-PD model is presented in figure 5.
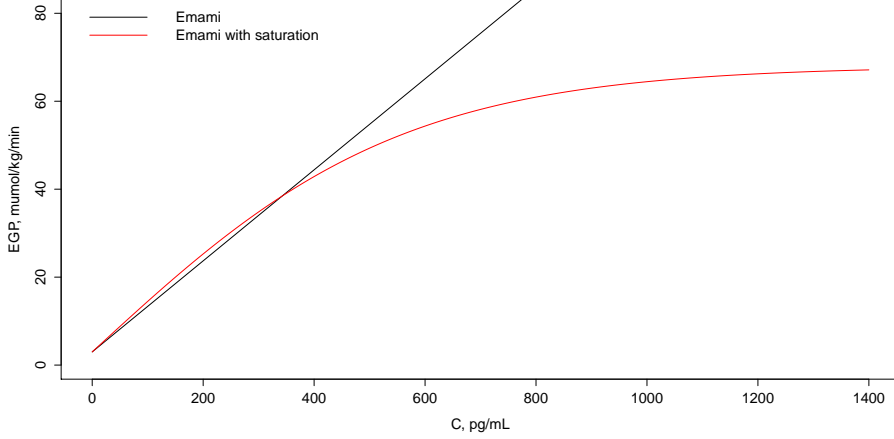
Figure 6: Comparison of GG model by Emami et al. [26] and modified model capturing the physiological saturation effect of glucagon on GG. The saturation part is proposed roughly to the data presented by Cherrington [15], compare with Figure 1. The graphed models assume basal insulin concentration and constant glucagon concentration. The curves do not start in (0,0) as GN is included.

3.2.2 Version 1.1 - Saturation of EGP

As reviewed in Section 1, GG saturates for some concentration of glucagon at basal insulin concentration, see Figure 1. The model stated in (14) is a linear approximation of the GG response to constant glucagon concentration and only covers the linear range of the dose response curve. No saturated data was available during the model development and therefore this dynamic was not captured in the model. However, the available data from Zealand Pharma A/S takes on very high concentrations of plasma glucagon and thus we assume that the GG response to glucagon is saturated for some parts of the studies if not the entire study duration. The GG model in (14) is modified to saturate GG at $65 \frac{\mu\text{mol}}{\text{kg}\cdot\text{min}}$ at basal insulin level. The saturation is approximated by a simple tangent hyperbolic function and figure 6 confirms that the linear part of the curve resembles the original linear formulation at basal insulin concentration. The GG model with saturation is

$$GG(t) = (1 - S_E x_3(t)) \cdot \frac{65}{0.69} \tanh\left(\frac{2.5}{1400} \cdot \frac{S_{gd} E_{gd}(t) + S_g C(t)}{S_g}\right)$$

where $(1 - S_E x_3(t)) \geq 0$ and $(S_{gd} E_{gd}(t) + S_g C(t)) \geq 0$ \hfill (17)

3.2.3 Version 1.2 - Basal insulin

Dogs have lower basal insulin concentrations than humans ($\sim$3 mIU/L versus $\sim$10 mIU/L), as described in section 2.4. Therefore, we can not assume that $(1 - S_E x_3(t))$ equals 0.69 at basal as in humans (calculated as $\text{EGP}_b/\text{EGP}_0$ from Hovorka et al. [20]). The model is thus changed to

$$GG(t) = \frac{(1 - S_E x_3(t))}{(1 - S_E I_b)} \cdot 65 \cdot \tanh\left(\frac{2.5}{1400} \cdot \frac{S_{gd} E_{gd}(t) + S_g C(t)}{S_g}\right)$$

where $(1 - S_E x_3(t)) \geq 0$ and $(S_{gd} E_{gd}(t) + S_g C(t)) \geq 0$ \hfill (18)
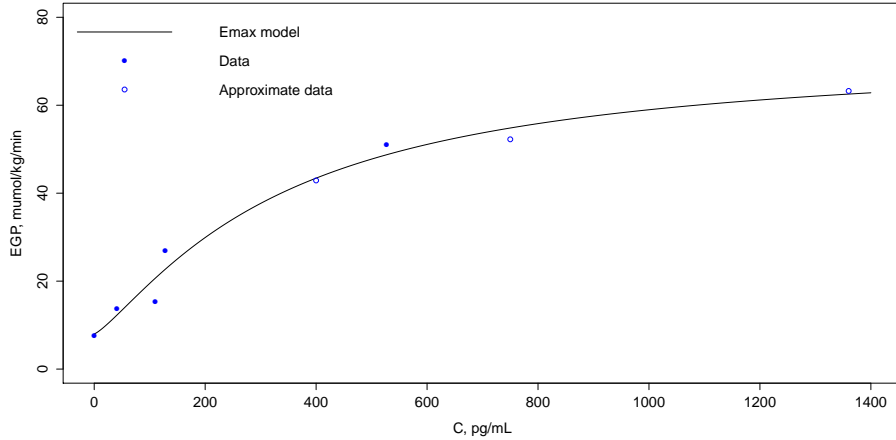
Figure 7: Relationship between plasma glucagon concentration and EGP. GN is constant and the GG is fitted with a sigmoid E$_{max}$ model. The graph assumes basal insulin concentration. The solid data points originate from [27, 41, 42] and the open dots are approximated from [15] since the original data could not be retrieved. Note that EGP is not zero at zero glucagon due to the glucagon independent GN.

The change ensures that GG saturates at 65 $\frac{\mu\text{mol}}{\text{kg}\cdot\text{min}}$ at basal insulin concentration. Moreover, this addition ensures that at higher insulin levels than basal, the saturation value of GG is lower than 65 $\frac{\mu\text{mol}}{\text{kg}\cdot\text{min}}$. Similarly, at lower insulin levels than basal the saturation value of GG is higher than 65 $\frac{\mu\text{mol}}{\text{kg}\cdot\text{min}}$. Qualitatively speaking, insulin "modulates" the maximum GG response to glucagon.

3.2.4   Version 2.0 - Sigmoid E$_{max}$ model

As discussed by Emami et al., the glucagon rate of change was added to the model to be able to capture the weakened response to a constant plasma glucagon concentration [26], also see Figure 2. Since we do not have data to describe this phenomenon and do not have a physiological explanation for how rate of change affects the GG response, we simplify the GG model to only depend on the absolute concentration of glucagon. We justify this with reference to Emami et al. who found that the GG model using both absolute glucagon concentration and glucagon rate of change was only slightly better than a similar model using only the absolute glucagon concentration [26].

To make the model parameters more physiological interpretable, we substitute the empirical tangent hyperbolic saturation model with the sigmoid E$_{max}$ model which is used to describe receptor mediated kinetics [43]. The sigmoid E$_{max}$ model is essentially a first order process at low concentrations, and a zero order process at high concentrations [31]. The model by Emami et al. in (14) describes the first order process and is approximated from data where first order kinetics apply [26]. The effect of plasma glucagon on the GG response is reformulated to comply with literature data [15, 27, 41, 42], and the mean prior parameter values of this model are identified by optimization. The data used to fit the parameters and the optimal solution is presented in Figure 7. The new GG model and the fitted parameters are listed
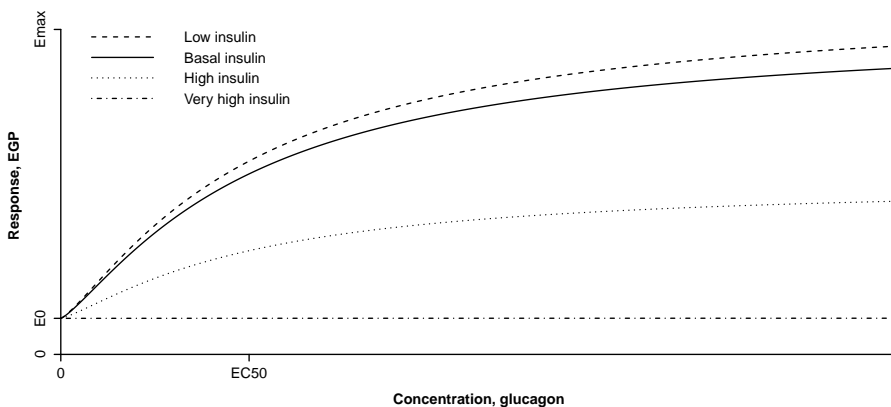
Figure 8: Qualitative visualization of the consequences of the multiplicative GG model showing how the total EGP response to glucagon changes at low, basal, high and very high insulin concentrations.

in (19).

$$GG(t) = \frac{(1 - S_E x_3(t))}{(1 - S_E I_b)} \cdot \left((E_{max} - E_0) \frac{C(t)^\gamma}{EC_{50}^\gamma + C(t)^\gamma} \right) \text{ where } (1 - S_E x_3(t)) \geq 0 \qquad (19)$$

$$E_{max} = 72.1 \frac{\mu\text{mol}}{\text{kg} \cdot \text{min}}, \quad E_0 = 8 \frac{\mu\text{mol}}{\text{kg} \cdot \text{min}}, \quad EC_{50} = 337.8 \frac{\text{pg}}{\text{mL}}, \quad \gamma = 1.25$$

The model describing the saturation of EGP due to glucagon consists of four parameters - two describing the minimum and maximum effect, E_0 and E_{max}, and two describing the curvature, EC_{50} and γ. E_0 is describing GN. EC_{50} is the concentration at the half maximum effect. The parameter γ reflects the number of molecules binding to one receptor and determines the steepness of the curve. We hypothesize that E_0 and E_{max} will be identical whether using marketed glucagon or the analogue. However, the parameters describing the curvature, i.e. the potency, might differ. Figure 8 visualizes the GG model with the multiplicative effect of glucagon and insulin qualitatively.

3.2.5 Final PD model

The equations describing the glucose-insulin-glucagon PD model are listed in (20)-(26) and the model visualized in Figure 9.

$$\frac{\mathrm{d}Q_1(t)}{\mathrm{d}t} = -F_{01} - S_T x_1(t)Q_1(t) + k_{12}Q_2(t) + GG(t) \qquad Q_1(0) = Q_{10} \tag{20}$$

$$\frac{\mathrm{d}Q_2(t)}{\mathrm{d}t} = S_T x_1(t)Q_1(t) - [k_{12} + S_D x_2(t)]\, Q_2(t) \qquad Q_2(0) = Q_1(0)\frac{x_1(0)}{x_2(0) + k_{12}} \tag{21}$$

$$GG(t) = \frac{(1 - S_E x_3(t))}{(1 - S_E \mathrm{I}_b)} \cdot \left((E_{max} - E_0)\frac{C(t)^\gamma}{EC_{50}^\gamma + C(t)^\gamma} \right) \text{ where } (1 - S_E x_3(t)) \geq 0 \tag{22}$$

$$G(t) = \frac{Q_1(t)}{\mathrm{V}} \tag{23}$$

$$\frac{\mathrm{d}x_1(t)}{\mathrm{d}t} = k_{a1}[I(t) - x_1(t)] \qquad\qquad x_1(0) = \mathrm{I}_b \tag{24}$$

$$\frac{\mathrm{d}x_2(t)}{\mathrm{d}t} = k_{a2}[I(t) - x_2(t)] \qquad\qquad x_2(0) = \mathrm{I}_b \tag{25}$$

$$\frac{\mathrm{d}x_3(t)}{\mathrm{d}t} = k_{a3}[I(t) - x_3(t)] \qquad\qquad x_3(0) = \mathrm{I}_b \tag{26}$$

Model inputs: $C(t)$, $I(t)$
Model observation: $G(t_n)$
Model output: $G(t)$
Fixed parameters: V, I_b
Model parameters: F_{01}, k_{12}, S_T, S_D, S_E, k_{a1}, k_{a2}, k_{a3}, E_0, E_{max}, EC_{50}, γ

The parameters and their units are described in previous sections 3.2.1-3.2.4.
We assume that F_{01} is constant at all times since we are not measuring any glucose concentrations below 4.5 mmol/L in the datasets to be fitted. However, for simulation purposes it is important to include the extended formulation of F_{01} taking the current glucose concentration into account [23].
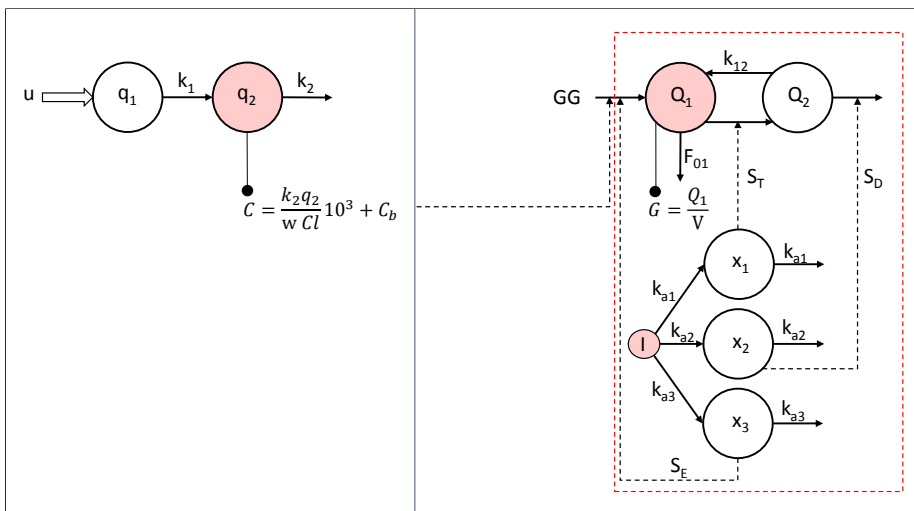
Figure 9: Schematic presentation of the final full model including the PK part at the left and the PD part at the right. The open arrow symbolizes SC input of glucagon. Solid arrows indicate mass transfer to/from a compartment. Dashed arrows indicate effect without mass transfer. Solid lines ending with a dot indicate how an output is derived from the content of a compartment. Plasma compartments of glucaogn, insulin, and glucose are colored. A red dashed square surrounds the part of the model published by Hovorka et al. [20].

4 Methods

4.1 Mathematical concepts

4.1.1 Maximum likelihood

The likelihood measures how likely a set of parameters are given data and a model. The likelihood is equal to the probability density considered as a function of the parameter set, θ, and a time series, Y_N, of N observations.

$$L(\theta, Y_N) = p(Y_N|\theta) \tag{27}$$

Different parameters of the model will give different values of the likelihood function. Finding the parameter set that maximizes the likelihood function for given data and a model gives the maximum likelihood (ML).

4.1.2 Profile likelihood

For a parameter, θ_i, and a time series, Y_N, of N observations, we can calculate the profile likelihood, which is defined as

$$L_p(\theta_i, Y_N) = \max_{\theta \backslash \theta_i} L(\theta, Y_N) \tag{28}$$

For a fixed value of θ_i the likelihood function is maximized across all other parameters of the parameter set θ which yields the profile likelihood of parameter θ_i [44, 45]. The profile likelihood of a parameter can be used to evaluate whether the parameter in the model is identifiable. Identifiability of parameters are determined by model structure (structural identifiability) and the input dynamics (practical identifiability) [44].

Structural identifiability is related to the transfer function from the input to the output. However, in large complex systems where the transfer function is non-trivial to derive, profile likelihood analysis provides a method for investigating the parameter identifiability.

Practical identifiability is related to the dynamics of the input. Thus, a model can only identify parameters describing dynamics present in data used for model fitting. Also in this case, profile likelihood analysis is a powerful tool.

A parameter is identifiable only if the maximum of the profile likelihood is well defined [44]. Whether the maximum of the profile likelihood of θ_i is well defined is evaluated using a $100(1-\alpha)\%$ confidence interval bound by when the natural logarithm of a likelihood ratio test exceeds a chi-squared distribution [45].

$$\log\left(\frac{L_p(\theta_i, Y_N)}{L(\hat{\theta}, Y_N)}\right) = \log(L_p(\theta_i, Y_N)) - \log(L(\hat{\theta}, Y_N)) > -\frac{1}{2}\chi^2_{1-\alpha} \tag{29}$$

In words, the profile likelihood is log-transformed yielding the profile log-likelihood. The maximum value of the profile log-likelihood is subtracted from the profile log-likelihood so that the maximum function value is zero. The limit of the confidence interval is determined by the $100(1-\alpha)$ percentile of the chi-squared distribution with one degree of freedom. As an example, a 95% confidence interval of a model parameter is bound by the log-likelihood ratio exceeding approximately -1.92. A profile likelihood confidence interval could be asymmetric, whereas e.g. the Wald statistic applies a quadratic and thus symmetric approximation of the confidence interval [45].

4.1.3 Bayesian inference

Bayesian estimates refer to parameters of a model being treated as random variables belonging to some distribution. To fit a parameter in a Bayesian framework a prior distribution of the parameter is needed. The parameters of the prior distribution are called hyper-parameters i.e. if a prior follows a normal distribution, two hyper-parameters define it: mean and standard deviation (SD). The estimated parameter will then be a summary of the posterior probability density function conditioned on the data.

The posterior distribution of a parameter, θ, given the data, Y_N, is identified using Bayes' theorem:

$$p(\theta, Y_N) = \frac{p(Y_N|\theta)p(\theta)}{p(Y_N)} \tag{30}$$

where $p(\theta)$ is the prior distribution of θ, $p(Y_N)$ is the marginal distribution and $p(Y_N|\theta)$ is the likelihood of Y_N given θ as defined in (27).

Finding the set of parameters given data, a model and prior distributions of parameters yielding the maximum of the posterior distribution is called maximum a posteriori (MAP).

4.1.4 Maximum a posteriori estimation

MAP estimation is an optimization approach seeking the parameter estimate that maximizes the posterior distribution [46]. Maximizing (30) then reduces to optimizing:

$$p(\theta, Y_N) \propto p(Y_N|\theta)p(\theta) \tag{31}$$

MAP estimation reduces to maximizing the likelihood function when the prior is a uniform distribution (i.e. $p(\theta)$ is constant), see (27) and (31). This indicates that ML is a special case of MAP. Also, the weaker a prior is (i.e. having a large standard deviation), the less difference there is between MAP estimation and ML. In general, one distinguishes between informative (highly peaked) and non-informative (not peaked) priors.

Introducing the following notation where σ_θ is a matrix with the prior standard deviations in the diagonal and R_θ is the prior correlation matrix:

$$\mu_\theta = E\{\theta\} \tag{32}$$
$$\Sigma_\theta = \sigma_\theta R_\theta \sigma_\theta = V\{\theta\} \tag{33}$$
$$\epsilon_\theta = \theta - \mu_\theta \tag{34}$$

Assuming that the priors all follow a Gaussian distribution, the posterior distribution can be rewritten as:

$$p(\theta|Y_N) \propto \left(\prod_{k=1}^{N} \frac{\exp\left(-\frac{1}{2}\epsilon_k^T R_{k|k-1}^{-1}\epsilon_k\right)}{\sqrt{\det(R_{k|k-1})}\left(\sqrt{2\pi}\right)^l} \right) p(y_0|\theta) \frac{\exp\left(-\frac{1}{2}\epsilon_\theta^T \Sigma_\theta^{-1}\epsilon_\theta\right)}{\sqrt{\det(\Sigma_\theta)}\left(\sqrt{2\pi}\right)^p} \tag{35}$$

Conditioning the posterior probability on y_0 and taking the negative logarithm gives:

$$-\log(p(\theta|Y_N, y_0)) \propto \frac{1}{2}\sum_{k=1}^{N}\left(\log(\det(R_{k|k-1})) + \epsilon_k^T R_{k|k-1}^{-1}\epsilon_k\right) + \frac{1}{2}\left(\left(\sum_{k=1}^{N} l\right) + p\right)\log(2\pi)$$
$$+ \frac{1}{2}\log(\det(\Sigma_\theta)) + \frac{1}{2}\epsilon_\theta^T \Sigma_\theta^{-1}\epsilon_\theta \tag{36}$$

The MAP solution is found by solving the nonlinear optimization problem:

$$\hat{\theta} = \arg\min_{\theta \in \Theta}\{-\log(p(\theta|Y_N, y_0))\} \tag{37}$$

This nonlinear optimization can be solved numerically through gradient-methods. Another method for finding the MAP solution is by using Markov Chain Monte Carlo (MCMC) simulations. MCMC is a brute force method that samples from the posterior distribution to create a rough shape of the posterior distribution and thereby estimates the MAP solution as implemented in WinBUGS [21, 26]. It is computationally time consuming because it can require thousands of samples before reaching convergence. On the contrary, gradient methods converge faster but suffer great difficulties if the objective function is noisy with local gradients not leading to a smaller value of the objective function.

4.1.5   Stochastic differential equations

Modelling a completely known physical system can be done using deterministic ordinary differential equations (ODEs) defined as

$$\frac{\mathrm{d}X}{\mathrm{d}t} = f(X(t), t) \tag{38}$$

$$y_k = X(t_k) + e_k \tag{39}$$

where $X(t)$ is the state of the system, $f()$ is the model, y_k is the discrete observations, and e_k is the measured errors, i.e. observation noise, assumed to be independent and identically distributed (i.i.d.) following a Gaussian distribution [47]. However, in biology one does not always know the true underlying system. In such cases, the discrepancies between the deterministic model and data from the physical system is composed of noise from two sources: measurement errors and systemic model errors. The magnitude of the systemic noise can be identified using stochastic differential equations (SDEs) defined as

$$\mathrm{d}x_t = f(x_t, u_t, t, \theta)\mathrm{d}t + \sigma(x_t, u_t, t, \theta)\mathrm{d}w_t \tag{40}$$

$$y_k = h(x_k, u_k, t_k, \theta) + e_k \tag{41}$$

The only difference between the ODE formulation in (38)-(39) and the SDE formulation in (40)-(41) is the diffusion term $\sigma(x_t, u_t, t, \theta)\mathrm{d}w_t$ corresponding to the system noise. Thus, solving an SDE with a very small value of σ is approximating solving an ODE. The term $f(x_t, u_t, t, \theta)\mathrm{d}t$ is called the drift and is the main process driving the system whereas the diffusion term is the system noise. Together, the drift and the diffusion describes the physical state of the system.

4.2   Application in CTSM-R

A team at the Technical University of Denmark (DTU) wrote a package for R allowing to do continuous time stochastic modelling (CTSM) [34, 46]. The package was used to obtain the results in this report. This subsection focuses on how the mathematical concepts in the previous subsection are applied in CTSM-R.

4.2.1   Model structure

CTSM-R accepts Itô SDEs in the state space form as presented in (40)-(41). However, CTSM-R does not allow the system noise to depend directly on the state of the system [47], and thus (40) changes to

$$\mathrm{d}x_t = f(x_t, u_t, t, \theta)\mathrm{d}t + \sigma(u_t, t, \theta)\mathrm{d}w_t \tag{42}$$

Letting the system noise depend on the state can be mitigated in CTSM-R using a transformation of variables called the Lamperti transform [47, 48].

Although the nonlinear equations describing the model in (20)-(26) are presented as ODEs, they are implemented in CTSM-R as SDEs. The ODE presentation is chosen for simplicity.

4.2.2   Initial values

The CTSM-R environment is sensitive to the initial values of the states and thus good initial values are needed to converge to a solution within a reasonable number of iterations. When fitting the PD model, the initial value of the observed state was automatically identified in most datasets as the plasma glucose concentration at time 0. If the initial plasma glucose was not available in one dataset, the initial concentration in the same dog at the other dosing occasions were averaged and used as the initial value of the dataset missing an initial observation. Using the measured or averaged initial glucose concentration the model parameters did not converge to a solution in al datasets. In those cases the initial value was adjusted manually until convergence was reached.

4.2.3   Prior information

In the following all hyper-parameters are fixed, thus all prior probability distributions of parameters are fixed. The values of the hyper-parameters are determined from literature [15, 20] and listed in Table 4. All parameters are assumed positive. All parameters of the Hovorka part of the model are assumed to follow a log-normal distribution, except F_{01} which is normally distributed [21]. We also assume that E_0, E_{max}, EC_{50}, and γ follow normal distributions.

The insulin sensitivities in [20] were overestimated compared to the results of [21]. As pointed out in Section 2.4, dogs appear to be more sensitive to insulin than humans and thus the estimates listed in [20] are kept as prior information. However, the standard deviation in the logarithmic domain is doubled to allow a different distribution than in humans. The standard deviations of the parameters describing the effect of glucagon on GG are unknown and thus arbitrarily defined as 25% of the mean value estimated from literature [15].

Overall, the prior correlation matrix has the structure presented in Table 5. The correlations of the parameters describing the glucagon part of the model are unknown and thus defined as zero. The values of the prior correlation matrix are calculated from individual parameter fits [20] and presented in Table 6. Fixing one or more of the parameters in the PD model leads to removal of the corresponding parameter rows and columns from the correlation matrix.

Table 4: Prior distributions of PD model parameters listed with source as (mean, SD) in the fitted domain and 95% confidence interval in non-transformed domain calculated as $\exp(\text{mean} \pm 2 \cdot \text{SD})$ if log-transformed and as $\text{mean} \pm 2 \cdot \text{SD}$ if non-transformed, respectively.

Parameter	Source	Transformation	Prior distribution	95% confidence interval
k_{12}	[20]	log	(-2.82, 0.46)	[0.02-0.1]
k_{a1}	[20]	log	(-5.69, 1.12)	[0.0004-0.03]
k_{a2}	[20]	log	(-2.89, 0.70)	[0.01-0.2]
k_{a3}	[20]	log	(-3.74, 0.77)	[0.005-0.1]
S_T	[20]	log	(-5.48, 1.46)	[0.0002-0.08]
S_D	[20]	log	(-7.58, 2.34)	[$5 \cdot 10^{-6}$-0.05]
S_E	[20]	log	(-3.19, 1.74)	[0.001-1.3]
F_{01}	[20]	-	(9.68, 2.14)	[5.4-14]
E_0	Section 3.2.4	-	(8, 2)	[4-12]
E_{max}	Section 3.2.4	-	(72.1, 18)	[36-108]
EC_{50}	Section 3.2.4	-	(337.8, 85)	[168-508]
γ	Section 3.2.4	-	(1.25, 0.3)	[0.65-1.85]

Table 5: Overall structure of the full prior correlation matrix.

	k_{12}	k_{a1}	k_{a2}	k_{a3}	S_T	S_D	S_E	F_{01}	E_0	E_{max}	EC_{50}	γ
k_{12}	1	$\rho_{k_{12},k_{a1}}$		$\cdots$		$\cdots$		$\rho_{k_{12},F_{01}}$	0	$\cdots$	$\cdots$	0
k_{a1}	$\rho_{k_{a1},k_{12}}$	$\ddots$	$\ddots$						$\vdots$			$\vdots$
k_{a2}			$\ddots$									
k_{a3}	$\vdots$			$\ddots$	$\ddots$				$\vdots$			$\vdots$
S_T				$\ddots$					$\vdots$			
S_D	$\vdots$				$\ddots$	$\ddots$			$\vdots$			$\vdots$
S_E						$\ddots$		$\rho_{S_E,F_{01}}$				
F_{01}	$\rho_{F_{01},k_{12}}$		$\cdots$		$\cdots$		ρ_{F_{01},S_E}	1	0			$\vdots$
E_0	0		$\cdots$		$\cdots$			$\cdots$	0	1	$\ddots$	
E_{max}	$\vdots$								$\ddots$	$\ddots$	$\ddots$	$\vdots$
EC_{50}	$\vdots$									$\ddots$	$\ddots$	0
γ	0	$\cdots$		$\cdots$		$\cdots$		$\cdots$		$\cdots$	0	1

Table 6: Values of the full prior correlation matrix.

	k_{12}	k_{a1}	k_{a2}	k_{a3}	S_T	S_D	S_E	F_{01}	E_0	E_{max}	EC_{50}	γ
k_{12}	1	0.73	-0.83	-0.14	0.27	0.46	0.22	0.07	0	0	0	0
k_{a1}		1	-0.97	-0.15	-0.23	-0.16	0.03	0.24	0	0	0	0
k_{a2}			1	0.08	0.20	0.05	0.08	-0.22	0	0	0	0
k_{a3}				1	-0.06	-0.16	-0.28	0.45	0	0	0	0
S_T					1	0.61	0.77	0.24	0	0	0	0
S_D						1	0.54	-0.51	0	0	0	0
S_E							1	0.02	0	0	0	0
F_{01}								1	0	0	0	0
E_0									1	0	0	0
E_{max}										1	0	0
EC_{50}											1	0
γ												1
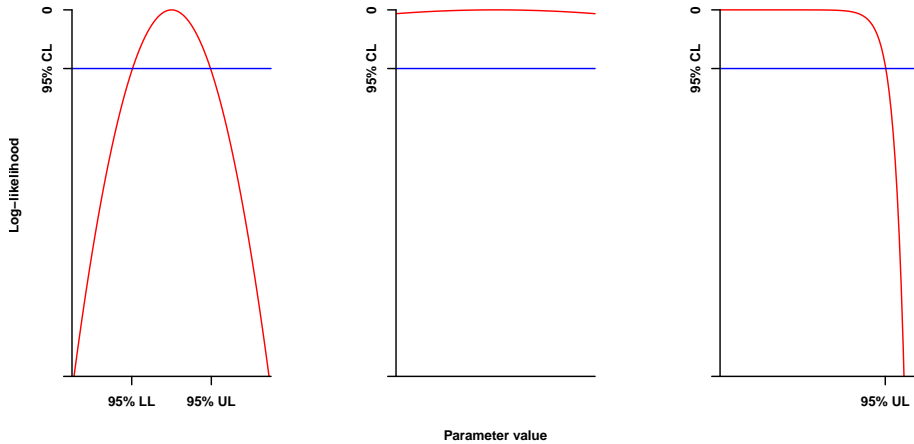
Figure 10: Theoretical examples of three types of profile likelihood plots; from left to right: highly peaked (identifiable), flat (structural non-identifiable), and asymmetric (practical non-identifiable). The 95% confidence limit (CL) is blue. The x-axis shows the 95% lower limit (LL) and upper limit (UL) of the parameter value.

4.2.4   Parameter identifiability

We have performed profile likelihood analysis of each model parameter using graphical presentation to investigate which model parameters are identifiable, see Figure 10 for examples of profile log-likelihood plots. A profile log-likelihood with values only exceeding the 95% confidence limit for the entire physiological range of a parameter indicates that the parameter is not structural identifiable, i.e. if the profile likelihood is flat, the parameter value does not influence the maximum achievable likelihood in fitting the dataset and might as well be fixed. To improve the parameter estimates of the remaining parameters, the unidentifiable parameters were fixed at their prior mean values. On the contrary, if a profile likelihood is highly peaked, the parameter is identifiable and should not be fixed. When a profile likelihood is asymmetric with either no upper or lower limit as seen in Figure 10 at the right, the parameter value is not practically identifiable and could also be fixed if the prior mean value is included in the 95% confidence interval. However, having a prior distribution it is not necessary to fix a parameter with an asymmetric profile log-likelihood but could increase the certainty of the remaining parameters.

As the calculation of a profile likelihood is very time consuming due to optimization of the remaining parameters for each fixed parameter value, the profile log-likelihood plots are initially very coarse with only few points. Profiles are refined as unidentifiable parameters are fixed and calculations are speeding up. Ideally, one should continue the cycle of fixing unidentifiable parameters until all remaining parameters are identifiable. In this study, we have only carried out five cycles of profile likelihood analysis. More parameters could possibly be fixed without changing the likelihood of the model fit significantly. Fitting a model containing unidentifiable parameters using MAP estimation is not wrong, but it comes at the expense of larger confidence intervals of the remaining parameters. The fitted values of parameters having flat or asymmetric profile likelihoods i.e. unidentifiable parameters will mainly be determined by the prior parameter distributions and less determined by data.

4.2.5   Model fitting and validation

Each PK dataset was fitted separately by ML using ODEs by fixing the system noise terms at small values. Since the PK model will be used for simulations we seek the ODE solution instead of the SDE solution. The basal concentration of glucagon was sought estimated. However, the basal level for the analogue was defined as zero and thus not estimated.

Each PD dataset was fitted separately by MAP with the priors listed in Table 4 and the correlation matrix displayed in Table 6. The parameters of each dataset were identified separately based on prior information rather than a population model. All parameters of the Hovorka model except F_{01} were fitted in the logarithmic domain as they are assumed to follow a log-normal distribution [21]. Moreover, all parameters were assumed to be positive. When dealing with small values like the transfer rate constants and sensitivities, log-transformation of the parameters ensure that they are always positive.

During the profile likelihood analysis the PD model was fitted as ODEs. After several model parameters were fixed we fitted the model using SDEs. However, since equations (21) and (24)-(26) were validated by tracer data in a previous publication [20], we fixed the diffusion terms of these states to small values and considered the equations as ODEs. The only modified and thus non-validated state was equation (20) and thus we estimated the diffusion term thereof. As described in Kristensen et al. [33], to validate the model structure, the model was first fitted using SDEs and if the diffusion term was insignificant, i.e. having a large p-value, the model was fitted again using ODEs to obtain the final parameter estimates for simulation purposes. However, if the diffusion term was not insignificant the model structure was incorrect [33]. The necessity of each of the varying model parameters was confirmed by significant p-values less than 0.05.

Furthermore, the model validity was investigated by residual analysis. Residuals should ideally be i.i.d. which was examined by plotting the residuals as a function of time and by plotting the autocorrelation function (ACF). The residuals plot can reveal if there is a drift or change in variance of the residuals over time i.e. if they are identically distributed. The ACF can reveal if there is a pattern in the residuals showing correlation between residuals at different lags i.e. if they are independent [49]. Moreover, very large values of the ACF exceeding the confidence limit imply that the model is not describing the data well.

Simulations of the mean prediction and standard deviations are carried out using extended Kalman filter without updating the states [34]. Predicting future values in a system with very little system noise and thus no updating corresponds to deterministic simulation.
It is however possible to perform stochastic simulations in CTSM-R by adding system noise to simulate real life experimental data [34]. Each realization of the stochastic process will be slightly different from another although determined by the size of the noise terms. We can interpret the actual data used for model fitting as one realization of the underlying stochastic process.

5   Results

Despite CTSM-R uses a robust estimation method [46], extreme outliers can largely impact the fit when the number of observations is small. Fitting of the PK data to the simple model was mostly robust to outliers. However, one PK datapoint as listed in Table 3 was so extreme that removing it greatly changed and improved the fit.
The PD model was more sensitive to outliers in both the input data and in the observations due to the large number of model parameters compared to number of observations. Six glucose observations appeared to be outliers as listed in Table 3. Due to the number of model parameters, the glucose observations had to

Table 7: Fitted or fixed PK model parameters (mean, SD). *Non significant. △Fixed.

Parameter	Unit	Glucagon	ZP-GA-1
k_1	min^{-1}	(0.134, 0.077)	(0.125, 0.072)
k_2	min^{-1}	(0.0159, 0.0048)	(0.0116, 0.0031)
Cl	mL/kg/min	(56.9, 13.2)	(88.5, 18.8)
C_b	pg/mL	0*	0△

Table 8: PK endpoints extracted from PK model fits (mean, SD).

PK endpoint	Unit	Dose level	Glucagon	ZP-GA-1
T_{max}	min	low	(23.9, 11.4)	(25.3, 9.4)
		high	(19.3, 5.4)	(22.4, 6.6)
C_{max}/Dose	nmol/L per nmol/kg	low	(0.059, 0.018)	(0.043, 0.010)
		high	(0.097, 0.017)	(0.059, 0.010)

be replaced by linear interpolation to maintain an identifiable model.

5.1   PK

5.1.1   Parameter estimates

Table 7 lists the average and standard deviation of the PK model parameters for each drug over the populations. As mentioned in section 2.4, it was not possible to measure low glucagon concentrations in any datasets. Due to this lack of data at low concentrations, it was not possible to estimate basal glucagon concentration in plasma.

The PK model fit is used as an input to the following PD model fitting and could also be used for simulation purposes.

5.1.2   PK Model fits

After fitting the PK model to data, relevant endpoints were extracted from the fits and presented in Table 8. Paired t-tests of the surrogate marker for onset of action, T_{max}, showed no difference between ZP-GA-1 and glucagon (p-value = 0.3).

C_{max} is significantly different for ZP-GA-1 compared to glucagon (p-value = 0.006).

Figure 11 displays examples of PK model fits with 95% confidence limits of the simulation both with regular and logarithmic base-10 y-axes (log_{10}). Figures 21-25 in Appendix B shows all PK fits.

5.2   PD

A few model building cycles have been carried out. The following sections only show results of the last and final model. However, the sections will refer qualitatively to observations made during the model building cycle to justify the decisions made by the model builder.

5.2.1   Reducing variables

Having a large model with twelve parameters and observation noise, some parameters had to be fixed to increase the certainty of other model parameters. To investigate which model parameters were unidentifi-
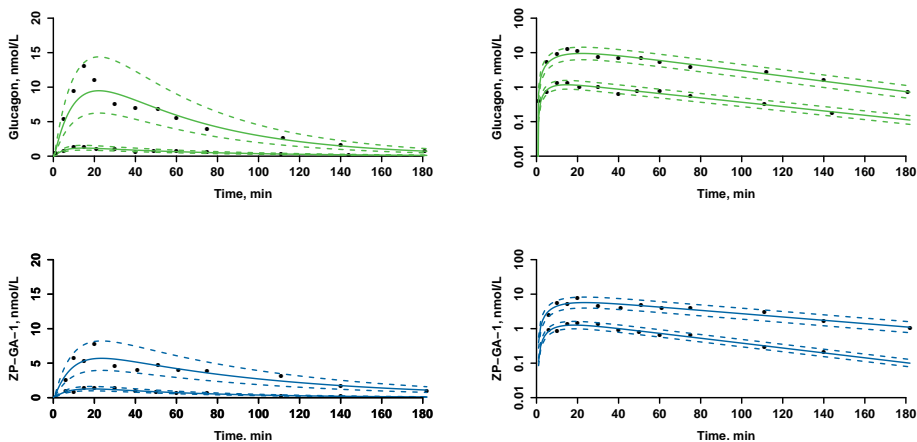
Figure 11: PK responses to low and high doses of glucagon and ZP-GA-1 in dog 3. Left graphs are with regular y-axes and right graphs are with logarithmic base-10 y-axes (log$_{10}$).

able, we plotted profile likelihoods of all parameters for each dataset. Figure 12a shows an example from the first cycle of profile likelihood analysis in one dataset. After the first cycle one parameter with a flat profile likelihood was fixed, and another cycle of profile likelihood analysis was carried out. These cycles continued until a total of four parameters were fixed at their prior mean values: k_{a2}, E_0, EC_{50}, and γ. However, γ was fixed at 1 since this reduced the model complexity and makes biologic sense. Figure 12b shows an example from the last cycle of profile likelihood analysis in the same dataset as above.

The reduction of variables is justified by reasoning regarding model structure and input dynamics. E_0 corresponding to GN can not be identified due to the model structure i.e. subtraction from E_{max}. The two parameters determining the curvature of the GG response to glucagon, EC_{50} and γ, can not be determined due to input dynamics. As previously mentioned, most dogs had very high plasma concentrations of glucagon or analogue during the entire study time and we therefore expect the GG response to be saturated at all times. Not having data with low glucagon concentrations makes it impossible to determine these parameters describing the response at low glucagon concentrations.

Unidentifiability of k_{a2} is likely due to the model structure since the parameter describes the insulin transfer that affects the glucose disposal of the non-accessible compartment. Determining the influence of insulin on glucose disposal requires tracer data which is not available.

(a) Initial profile likelihoods when no parameters are fixed.

(b) Fourth iteration of profile likelihood analysis when four parameters are fixed.

Figure 12: Profile likelihoods of all twelve model parameters in dog 3 after high dose of glucagon. Red points illustrate fixed parameter values. Red curves illustrate prior parameter distributions. Horizontal blue lines are 95% confidence limits of parameter values.

Wendt et al.   DTU Compute Technical Report-2016-2   *5   RESULTS*

Table 9: Ratio of datasets with significant p-values less than 0.05 corresponding to 95% confidence level when estimated in SE setting versus OE setting. P-values of fixed parameters do not exist but the parameters are included in the table for completeness.

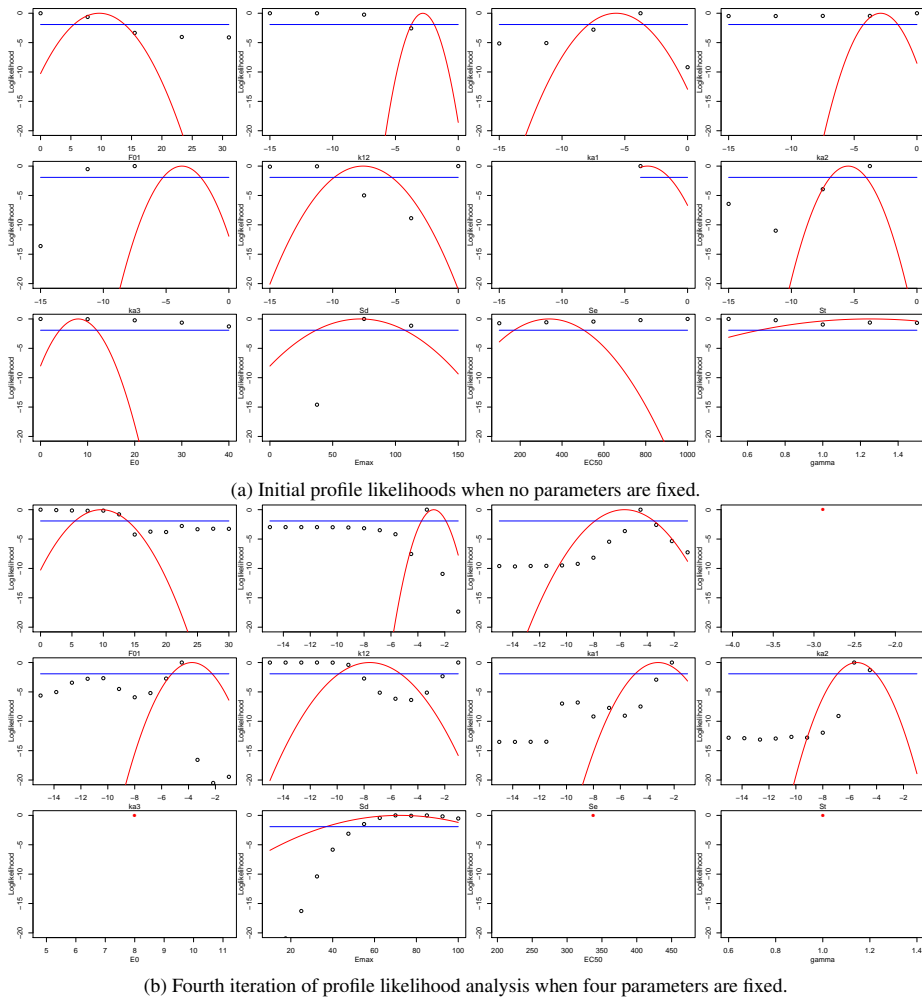| Parameter	Glucagon		ZP-GA-1	
	SE	OE	SE	OE
k_{12}	10/10	10/10	10/10	10/10
k_{a1}	10/10	10/10	10/10	10/10
k_{a2}	-			
k_{a3}	10/10	10/10	10/10	10/10
S_T	10/10	10/10	10/10	10/10
S_D	10/10	10/10	10/10	10/10
S_E	10/10	10/10	10/10	10/10
F_{01}	10/10	10/10	10/10	10/10
E_0	-			
E_{max}	7/10	10/10	9/10	10/10
EC_{50}	-			
γ	-			
σ_1	0/10	-	0/10	-

As an example, the increase in certainty of parameter value when reducing the number of variables is graphically evident for k_{a1} in Figure 12. At the initial cycle the 95% confidence interval of the logarithm of the parameter is approximately [-7 to -3], but reduces to [-5 to -3.5] when four parameters are fixed. Same tendency can be observed for other model parameters.

5.2.2   Model validity

After reduction of variables using profile likelihood analysis we investigate using SDEs if the model describes the physiological system adequately i.e. if the model has insignificant system noise. As previously argued, we only examine the noise of equation (20). Table 9 lists the proportion of datasets with significant p-values for each PD model parameter with and without the coefficient of the diffusion term, σ_1, for both of the compounds. Using SDEs we observe that the model parameters are significant at a 5% confidence level in the majority of datasets and that the diffusion coefficient is insignificant in all datasets. σ_1 is then fixed at a small value and the PD model parameters re-estimated using ODEs. After fixing σ_1, all model parameters are significant in all datasets. We can not reject that the model describes the underlying physiological system.

5.2.3   Residual Analysis

After the final estimation of PD model parameters using ODEs we analyse the standardized residuals to verify the quality of the model in describing data. Figure 13 shows an example of the standardized residuals plot and ACF showing i.i.d. residuals thus no trends in residuals and no significant correlation between residuals.

However, dealing with data having very few observations makes it challenging to be strict to the rules of i.i.d. residuals. Especially the residuals plot is difficult to interpret in most cases due to few observations. The ACF also has some limitations in that data was not equidistantly sampled. Most ACF are
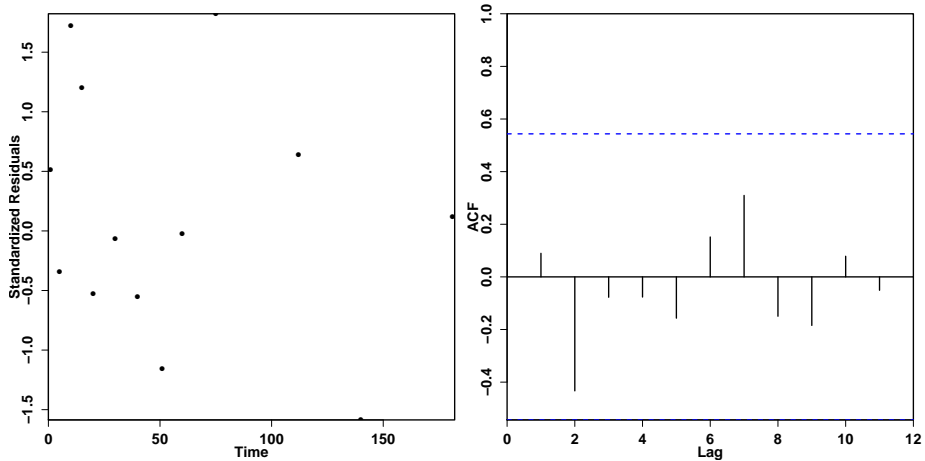
Figure 13: Example of standardized residuals plot and ACF of residuals of model fit to dataset from dog 3 after high dose of glucagon.

within the confidence limits.

Based on the residual analysis the model describes the dynamics in the data well.

5.2.4 PD Model fits

In Section 5.2.1 we reduced the number of PD model parameters by removing unidentifiable parameters. In Section 5.2.2 we described how the model structure is sufficient to capture the dynamics of the physical system. In Section 5.2.3 we confirmed that the fit did not give rise to trends in the residuals. Finally, we can verify that the model is satisfactory based on visual inspection of the PD model fit together with data. Figure 14 presents examples of PD model fits together with model inputs after administration of glucagon at low and high dose levels in one dog. In the two examples, the model is fitting data well with narrow confidence limits around the simulation. Within 100 minutes we observe a peak in glucose concentration and a return to baseline. At the end of the sampling period the glucose concentrations show a tendency to rise slowly.

Figure 15 presents examples of PD model fits together with model inputs after administration of ZP-GA-1 at low and high dose levels in one dog. The trends in data and the PD model fits are similar to the ones after administration of glucagon described above.

Figures 26-30 in Appendix C present all PD model fits.

(a) Dog 3, 20 nmol/kg.   (b) Dog 3, 120 nmol/kg.
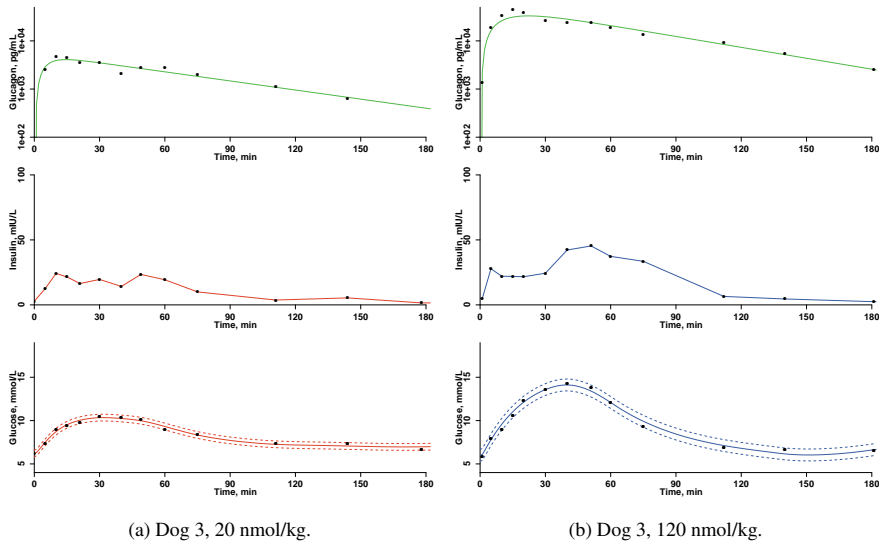
Figure 14: Plasma concentrations of PD model inputs glucagon and insulin together with PD model fit of glucose after administration of glucagon.

(a) Dog 3, 20 nmol/kg.   (b) Dog 3, 120 nmol/kg.
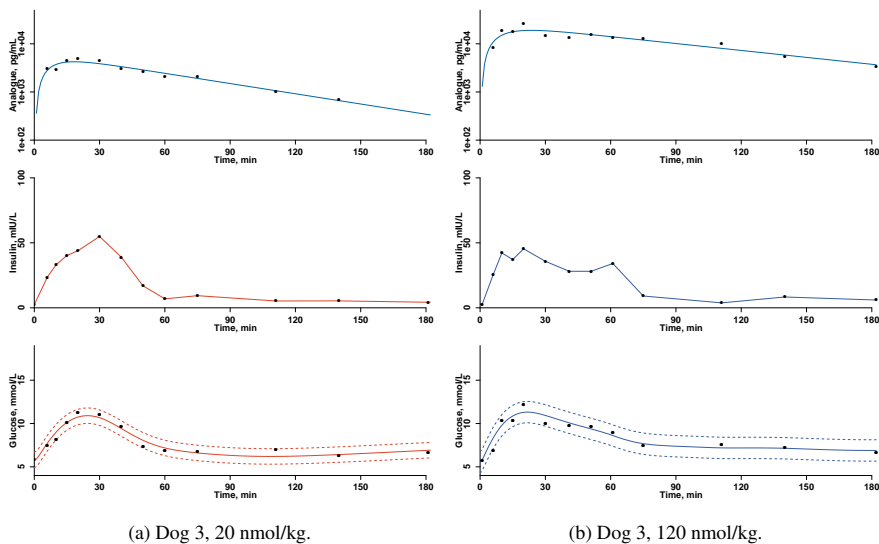
Figure 15: Plasma concentrations of PD model inputs ZP-GA-1 and insulin together with PD model fit of glucose after administration of ZP-GA-1.

Table 10: Posterior distributions of PD model parameters for the population in fitted domain reported as (mean, SD). Parameters not in parenthesis are fixed.

Parameter	Glucagon	ZP-GA-1
$\log(k_{12})$	(-2.87, 0.27)	(-3.02, 0.23)
$\log(k_{a1})$	(-5.19, 0.86)	(-5.90, 0.83)
$\log(k_{a2})$	-2.89	-2.89
$\log(k_{a3})$	(-4.88, 0.73)	(-4.70, 0.98)
$\log(S_T)$	(-5.65, 0.86)	(-5.35, 0.50)
$\log(S_D)$	(-9.11, 0.93)	(-8.72, 1.15)
$\log(S_E)$	(-2.71, 0.57)	(-2.95, 0.43)
F_{01}	(9.8, 1.5)	(9.6, 2.0)
E_0	8	8
E_{max}	(50.1, 13.7)	(53.8, 16.5)
EC_{50}	337.8	337.8
γ	1	1

5.2.5   Parameter estimates

We assume that the variations in parameters within dogs are negligible compared to the variations between dogs. As prior information we used Gaussian distributions and using the individually fitted parameters we can calculate similar posterior distributions of PD model parameters.

Table 10 lists the posterior distributions of each parameter separated by drug and study for the population of dogs. During the PK analysis we noticed that the onset of action and maximum concentration of glucagon were different between the studies. We therefore separate the parameters of the two studies in this analysis, too. During estimation, most parameters are log-transformed.

For ease of comparison to values reported in literature [20], the averages of the log-transformed parameters are transformed back and listed together with ranges in Table 11. Fixed parameters are listed for completeness in both tables.

Table 12 shows the posterior correlation matrix of both PK and PD model parameters.

The following Section describes observations related to these posterior distributions and correlations.

Table 11: Average of PD model parameters in normal domain together with range. Fixed parameters are listed for completeness.

Parameter	Glucagon	ZP-GA-1
k_{12}	0.057 (0.038-0.085)	0.049 (0.033-0.081)
k_{a1}	0.0056 (0.0019-0.0279)	0.0027 (0.0009-0.0192)
k_{a2}	0.055	0.055
k_{a3}	0.0076 (0.0038-0.0508)	0.0091 (0.0038-0.0657)
$S_T \cdot 10^{-4}$	35 (13-117)	48 (27-110)
$S_D \cdot 10^{-4}$	1.1 (0.2-3.8)	1.6 (0.6-35.8)
$S_E \cdot 10^{-4}$	666 (178-1323)	523 (281-892)
F_{01}	9.8 (8.0-13.1)	9.6 (5.3-12.3)
E_0	8	8
E_{max}	50.1 (26.6-73.2)	53.8 (24.1-71.8)
EC_{50}	337.8	337.8
γ	1	1

Table 12: Posterior correlation matrix of PK and PD model parameters and body weight.

	k_1	k_2	Cl	w	$\log(k_{12})$	$\log(k_{a1})$	$\log(k_{a3})$	$\log(S_T)$	$\log(S_D)$	$\log(S_E)$	F_{01}	E_{max}
k_1	1	0.26	0.33	-0.54	-0.08	-0.25	0.49	0.52	-0.01	-0.13	0.50	-0.55
k_2		1	-0.27	-0.24	0.34	0.17	0.12	0.16	-0.03	-0.11	0.27	0.04
Cl			1	-0.51	-0.37	-0.55	0.44	0.60	0.11	-0.22	0.35	-0.10
w				1	0.10	0.32	-0.46	-0.63	0.02	0.19	-0.55	0.25
$\log(k_{12})$					1	0.78	-0.13	-0.21	0.02	0.01	0.11	0.09
$\log(k_{a1})$						1	-0.45	-0.68	-0.44	0.31	-0.07	0.18
$\log(k_{a3})$							1	0.60	0.00	-0.80	0.78	-0.59
$\log(S_T)$								1	0.36	-0.32	0.53	-0.19
$\log(S_D)$									1	0.00	-0.45	0.04
$\log(S_E)$										1	-0.57	0.40
F_{01}											1	-0.40
E_{max}												1

Table 13: P-values of two-tailed paired t-tests comparing PD model parameter estimates of glucagon versus analogue within study.

Parameter	Glucagon vs. ZP-GA-1
k_{12}	0.29
k_{a1}	0.09
k_{a2}	-
k_{a3}	0.42
S_T	0.19
S_D	0.42
S_E	0.14
F_{01}	0.81
E_0	-
E_{max}	0.51
EC_{50}	-
γ	-

5.2.6   Native glucagon versus glucagon analogue

The reason for doing cross-over studies of glucagon and the glucagon analogue is to be able to compare the dynamics of the compounds without too many confounding factors like biological variations. Table 13 presents p-values of paired t-tests between glucagon and the glucagon analogue. No model parameters are significantly different on a 5% confidence level.

6   Discussion

In this report, we present a novel model describing how insulin and glucagon contribute to the EGP in dogs. The model is based on physiological knowledge and parameter estimates are based on data from pre-clinical studies in five dogs. The PD model description is contentious compared to most existing models in several ways: claiming that GG is completely suppressed when insulin concentration exceeds a threshold as in Hovorka et al. [20], claiming that GG saturates when glucagon concentration is high, and claiming a multiplicative effect of insulin and glucagon as in Emami et al. [26]. Moreover, we have used the model to compare PD characteristics of marketed glucagon and a novel glucagon analogue invented by Zealand Pharma A/S.

According to our PD model there exists a certain threshold of insulin concentration at which the GG is completely suppressed. From equation (22) the threshold can easily be identified using the insulin sensitivity on GG as S_E^{-1}. Using the average parameter estimate listed in Table 11 we find a threshold of less than 20 mIU/L. This threshold is considerably lower than the threshold identified by Cherrington as 45 mIU/L [15]. Also, El Youssef et al. found that insulin concentrations exceeding 40 mIU/L only results in EGP of roughly 20 mg/kg during 60 minutes [28]. This EGP production of ∼0.33 mg/kg/min is similar magnitude as GN of ∼0.5 mg/kg/min observed by Cherrington [15]. Thus, the results by El Youssef et al. at insulin concentrations exceeding 40 mIU/L could be explained by insulin's suppression of GG.
The human prior of S_E suggested an insulin threshold of 19 mIU/L [20], whereas a later publication suggested an average insulin threshold of 85 mIU/L based on the value of S_E [21]. However, both of these

estimates of S_E were based on human data. As discussed in Section 2.4 dogs have lower basal insulin levels than humans and are therefore more sensitive to insulin than humans. It is thus reasonable that the threshold at which the GG is completely suppressed is lower in dogs than in humans.

The graphs of raw data in Appendix A reveal that the dog's insulin concentrations exceed even the human threshold of GG suppression during at large parts of the study time. In some datasets we notice a slight increase in blood glucose concentrations during the last part of the study which could be explained by GG no longer being suppressed by insulin and a plasma glucagon concentration that is still much higher than basal levels. However, we only observe this slight increase in plasma glucose in some datasets. This could be explained by the delay in insulin action on plasma glucose described by the small rate constant with a half-life of approximately 90 minutes which corresponds to the remaining of the sampling period after plasma insulin concentrations have returned to baseline.

The diabetes community is speculating whether glucagon works when insulin inhibits GG. El Youssef et al. found in diabetes patients that increasing glucagon doses of 25-175 μg increases EGP at insulin concentrations less than 30 mIU/L [28], but increasing doses up to 175 μg have no effect on EGP at insulin concentrations exceeding 40 mIU/L as explained previously. Blauw et al. investigated the glucose response in patients with diabetes to various doses of glucagon from 0.1-1 mg at different blood glucose levels and concluded that blood glucose level was irrelevant to the glucose response to glucagon [50]. Unfortunately, the study does not report insulin concentrations. Ranjan et al. investigated the glucose response in diabetes patients to glucagon doses of 100-300 μg at insulin concentrations of 8-20 mIU/L and found no significant increase in glucose response after a glucagon dose of 300 μg compared to 200 μg [51]. A study by Graf et al. in healthy showed no further effect size of glucagon doses larger than 250 μg [52]. The studies by Ranjan et al. and Graf et al. suggest a saturation effect of glucagon in both healthy and patients with diabetes.

The glucagon doses used in the pre-clinical dog study ranged 20-120 nmol/kg (0.07-0.4 mg/kg) corresponding to human equivalent doses of 0.04-0.2 mg/kg using allometric scaling. Thus, the previous studies suggesting a saturation effect of glucagon doses exceeding 0.2 mg supports our observations that the glucose responses of the dogs were saturated at all dose levels.

According to Cherrington the GG response to glucagon is almost saturated for glucagon concentrations exceeding approximately 1000 pg/mL [15]. From the graphs of raw data in Figures 16-20 we observe that plasma glucagon concentrations are higher than 1000 pg/mL most of the study duration. We only have very limited data when glucagon concentrations are low. During the reduction of variables we recognized this fact since we were not able to identify the parameters describing GG response to glucagon at low concentrations, but only at saturated concentrations. We still believe that the sigmoid E_{max} model presented here is valid in describing the effect of glucagon on GG because it builds on knowledge from literature in particular Cherrington [15]. Moreover, we believe that this novel model is more physiologically correct than previous models based on the minimal model or a linear approximation since these models do not describe the saturation effect of glucagon on GG [24–26]. Future studies should be designed so that the plasma glucagon concentration does not yield saturated EGP response for the entire study duration.

The multiplicative effect of insulin and glucagon on GG was proposed by Emami et al. [26]. The idea was derived from Hovorka et al. who states that with increasing insulin concentration the total EGP decreases linearly [20]. The model by Emami et al. multiplies the effect of insulin as described by Hovorka et al. with an expression stating that GG increases linearly when glucagon increases.

In this report, we have extended the model by Emami et al. to include saturation of glucagon. As the glucose response to glucagon was saturated during the entire study time for most datasets, the sophisticated sigmoid E_{max} model practically reduces to a constant value and thus the expression for GG originally

36

proposed by Hovorka et al.

Despite the saturated GG response due to glucagon, the model assumes that the glucogen stores in the liver are never depleted. As the study was conducted over short time, this is a fair assumption. Moreover, the glucose response from breakdown of glycogen is suppressed by insulin most of the study time. Recent data shows that small frequent glucagon boluses do not deplete the glucogen stores [22]. The study by Castle et al. has a few limitations in that it was carried out over short time and all participant were well-fed and had good control of their diabetes. It is however especially the poorly controlled patients that would need the glucagon bolus regularly. The effects of repeated daily and long term use of glucagon remain unknown. Studies investigating the long term effects are needed to verify that the glucose response to glucagon does not change over time.

The used datasets posed other challenges than not covering low glucagon concentrations. The study was not optimal for the purpose of fitting models describing the glucose-insulin-glucagon dynamics nor designed for identifying how insulin and glucagon affect EGP. The datasets were sparsely sampled which made it necessary to fix some parameters in order to increase the certainty of the estimates of the remaining parameters. We used profile likelihood analysis to justify fixation of four PD model parameters. Residual analysis of time series with only 14 observations is challenging and should not be considered as strict as an analysis using ten times the number of observations. Not all residuals plot and ACFs showed i.i.d. but visual inspection of model fits confirmed that the model described data well for the purpose of simulation.
We chose not to do cross-validation of the model, as this would be a waste of our limited amount of data. Also, with inter and intra biological variation, we would not expect to get good PD model fits testing parameters estimated in one dataset in another. Only in cases with constant conditions can such cross validation methods lead to meaningful and fair results.

In this report we focused on fitting data from individual trials using prior information in order to obtain a model suitable for simulation of the glucose-insulin-glucagon dynamics. The posterior parameter distributions and correlation matrix form a population from which a parameter set can be sampled for simulation of a subject. The estimated model parameters depend on the prior parameter distributions to some extend. However, comparing the prior parameter distributions in Table 4 with the posterior parameter distributions in Table 10, we observe that most posterior distributions are much narrower than the initial prior distributions of parameters, i.e. the parameter distributions are more informative.
The parameter estimation could be re-done by performing population modelling thus determining, not only the individual model parameters, but the hyper-parameters, i.e. population parameters, too. We also expect this simulation model to be valid in describing human glucose-insulin-glucagon dynamics although possibly with different population parameter distributions and parameter correlations.

We used a simple PK model together with the novel PD model to compare glucagon with a novel glucagon analogue referred to as ZP-GA-1 invented by Zealand Pharma A/S. Comparing PK between compounds, we did not find any significant differences for ZP-GA-1 compared to glucagon. However, we did find a significantly higher peak concentration of the analogue compared to glucagon. This is in agreement with the higher bioavailability of the analogue compared to glucagon, see Table 2 in Section 2.2. Comparing PD model parameters between glucagon and the analogue we did not find any significant differences at a 95% confidence level. Therefore, we can not reject that the analogue has similar PD effect on the glucose response and has similar PK characteristics to marketed glucagon.

In conclusion, we developed a novel model of the complex glucose-insulin-glucagon dynamics based on physiology and data. We demonstrated that the model describes the glucoregulatory system well and enables simulations of glucose dynamics knowing insulin and glucagon plasma concentrations.

Comparisons of marketed glucagon with the novel glucagon analogue did not show any differences in PK or PD characteristics.

This report presents parameter estimates for simulations of the glucose-insulin-glucagon dynamics in dogs but could be extended to simulations of the human dynamics after obtaining parameter estimates based on similar studies in humans.

References

[1] R. Hovorka, "Closed-loop insulin delivery: from bench to clinical practice," *Nature Reviews Endocrinology*, vol. 7, no. 7, pp. 385–395, 2011.

[2] S. J. Russell, F. H. El-Khatib, D. M. Nathan, K. L. Magyar, J. Jiang, and E. R. Damiano, "Blood glucose control in type 1 diabetes with a bihormonal bionic endocrine pancreas," *Diabetes Care*, vol. 35, no. 11, pp. 2148–2155, 2012.

[3] S. J. Russell, F. H. El-Khatib, M. Sinha, K. L. Magyar, K. McKeon, L. G. Goergen, C. Balliro, M. A. Hillard, D. M. Nathan, and E. R. Damiano, "Outpatient glycemic control with a bionic pancreas in type 1 diabetes," *The New England Journal of Medicine*, vol. 371, no. 4, pp. 313–325, 2014.

[4] S. J. Russell, M. A. Hillard, C. Balliro, K. L. Magyar, R. Selagamsetty, M. Sinha, K. Grennan, D. Mondesir, L. Ehklaspour, H. Zheng, E. R. Damiano, and F. H. El-Khatib, "Day and night glycaemic control with a bionic pancreas versus conventional insulin pump therapy in preadolescent children with type 1 diabetes: a randomised crossover trial," *The Lancet Diabetes & Endocrinology*, vol. 4, pp. 233–243, 2016.

[5] A. Haidar, L. Legault, M. Dallaire, A. Alkhateeb, A. Coriati, V. Messier, P. Cheng, M. Millette, B. Boulet, and R. Rabasa-Lhoret, "Glucose-responsive insulin and glucagon delivery (dual-hormone artificial pancreas) in adults with type 1 diabetes: a randomized crossover controlled trial," *Canadian Medical Association Journal*, vol. 185, no. 4, pp. 297–305, 2013.

[6] A. Haidar, L. Legault, L. Matteau-Pelletier, V. Messier, M. Dallaire, M. Ladouceur, and R. Rabasa-Lhoret, "Outpatient overnight glucose control with dual-hormone artificial pancreas, single-hormone artificial pancreas, or conventional insulin pump therapy in children and adolescents with type 1 diabetes: an open-label, randomised controlled trial," *The Lancet Diabetes & Endocrinology*, vol. 3, no. 8, pp. 595–604, 2015.

[7] A. Haidar, L. Legault, V. Messier, T. M. Mitre, C. Leroux, and R. Rabasa-Lhoret, "Comparison of dual-hormone artificial pancreas, single-hormone artificial pancreas, and conventional insulin pump therapy for glycaemic control in patients with type 1 diabetes: an open-label randomised controlled crossover trial," *The Lancet Diabetes & Endocrinology*, vol. 3, no. 1, pp. 17–26, 2015.

[8] V. Gingras, R. Rabasa-Lhoret, V. Messier, M. Ladouceur, L. Legault, and A. Haidar, "Efficacy of dual-hormone artificial pancreas to alleviate the carbohydrate-counting burden of type 1 diabetes: A randomized crossover trial," *Diabetes & Metabolism*, vol. 42, pp. 47–54, 2015.

[9] J. R. Castle, J. M. Engle, J. El Youssef, R. G. Massoud, K. C. J. Yuen, R. Kagan, and W. K. Ward, "Novel use of glucagon in a closed-loop system for prevention of hypoglycemia in type 1 diabetes," *Diabetes Care*, vol. 33, no. 6, pp. 1282–1287, 2010.

[10] J. El Youssef, J. R. Castle, D. L. Branigan, R. G. Massoud, M. E. Breen, P. G. Jacobs, B. W. Bequette, and W. K. Ward, "A controlled study of the effectiveness of an adaptive closed-loop algorithm to minimize corticosteroid-induced stress hyperglycemia in type 1 diabetes," *Journal of diabetes science and technology*, vol. 5, no. 6, pp. 1312–1326, 2011.

[11] A. C. van Bon, J. Hermanides, R. Koops, J. B. L. Hoekstra, and J. H. DeVries, "Postprandial glycemic excursions with the use of a closed-loop platform in subjects with type 1 diabetes: a pilot study," *Journal of diabetes science and technology*, vol. 4, no. 4, pp. 923–928, 2010.

[12] A. C. van Bon, L. D. Jonker, R. Koebrugge, R. Koops, J. B. L. Hoekstra, and J. H. DeVries, "Feasibility of a bihormonal closed-loop system to control postexercise and postprandial glucose excursions," *Journal of diabetes science and technology*, vol. 6, no. 5, pp. 1114–1122, 2012.

[13] A. C. van Bon, Y. M. Luijf, R. Koebrugge, R. Koops, J. B. L. Hoekstra, and J. H. DeVries, "Feasibility of a portable bihormonal closed-loop system to control glucose excursions at home under free-living conditions for 48 hours," *Diabetes technology & therapeutics*, vol. 16, no. 3, pp. 131–136, 2014.

[14] H. Blauw, A. C. van Bon, R. Koops, and J. H. DeVries, "Performance and safety of an integrated bihormonal artificial pancreas for fully automated glucose control at home," *Diabetes, Obesity and Metabolism*, 2016.

[15] A. D. Cherrington, "Control of glucose production in vivo by insulin and glucagon," in *Comprehensive Physiology 2011, Supplement 21: Handbook of Physiology, The Endocrine System, The Endocrine Pancreas and Regulation of Metabolism*, First published in print 2001, pp. 759–785.

[16] Novo Nordisk A/S. (2015) GlucaGen (glucagon [rdna origin] for injection) patient information. [Online]. Available: http://www.novo-pi.com/glucagenhypokit.pdf

[17] Eli Lilly and Company. (2012) Information for the physician - glucagon for injection (rdna origin). [Online]. Available: http://pi.lilly.com/us/rglucagon-pi.pdf

[18] B. Newswanger, S. Ammons, N. Phadnis, W. K. Ward, J. Castle, R. W. Campbell, and S. J. Prestrelski, "Development of a highly stable, nonaqueous glucagon formulation for delivery via infusion pump systems," *Journal of diabetes science and technology*, vol. 9, no. 1, pp. 24–33, 2015.

[19] S. L. Wendt, A. Valeur, H. Madsen, J. B. Jørgensen, and C. B. Knudsen, "Pharmacokinetics modeling of glucagon and a novel glucagon analogue after subcutaneous administration in dogs," in *Diabetes technology & therapeutics*, vol. 17, no. S1, 2015, pp. A-109.

[20] R. Hovorka, F. Shojaee-Moradie, P. V. Carroll, L. J. Chassin, I. J. Gowrie, N. C. Jackson, R. S. Tudor, A. M. Umpleby, and R. H. Jones, "Partitioning glucose distribution/transport, disposal, and endogenous production during IVGTT," *American Journal of Physiology-Endocrinology and Metabolism*, vol. 282, no. 5, pp. E992–E1007, 2002.

[21] A. Haidar, M. E. Wilinska, J. A. Graveston, and R. Hovorka, "Stochastic virtual population of subjects with type 1 diabetes for the assessment of closed-loop glucose controllers," *IEEE Transactions on Biomedical Engineering*, vol. 60, no. 12, pp. 3524–3533, 2013.

[22] J. R. Castle, J. El Youssef, P. A. Bakhtiani, Y. Cai, J. M. Stobbe, D. Branigan, K. Ramsey, P. Jacobs, R. Reddy, M. Woods, and W. K. Ward, "Effect of repeated glucagon doses on hepatic glycogen in type 1 diabetes: Implications for a bihormonal closed-loop system," *Diabetes care*, vol. 38, no. 11, pp. 2115–2119, 2015.

[23] R. Hovorka, V. Canonico, L. J. Chassin, U. Haueter, M. Massi-Benedetti, M. O. Federici, T. R. Pieber, H. C. Schaller, L. Schaupp, T. Vering, and M. E. Wilinska, "Nonlinear model predictive control of glucose concentration in subjects with type 1 diabetes," *Physiological measurement*, vol. 25, no. 4, pp. 905–920, 2004.

[24] C. Dalla Man, F. Micheletto, D. Lv, M. Breton, B. Kovatchev, and C. Cobelli, "The UVA/PADOVA type 1 diabetes simulator: New features," *Journal of diabetes science and technology*, vol. 8, no. 1, pp. 26–34, 2014.

[25] P. Herrero, P. Georgiou, N. Oliver, M. Reddy, D. Johnston, and C. Toumazou, "A composite model of glucagon-glucose dynamics for *in silico* testing of bihormonal glucose controllers," *Journal of diabetes science and technology*, vol. 7, no. 4, pp. 941–951, 2013.

[26] A. Emami, J. El Youssef, R. Rabasa-Lhoret, J. Pineau, J. R. Castle, and A. Haidar, "Modelling glucagon action in patients with type 1 diabetes," 2016, submitted paper.

[27] M. Wada, C. C. Connolly, C. Tarumi, D. W. Neal, and A. D. Cherrington, "Hepatic denervation does not significantly change the response of the liver to glucagon in conscious dogs," *American Journal of Physiology - Endocrinology and Metabolism*, vol. 268, no. 2, pp. E194–E203, 1995.

[28] J. El Youssef, J. R. Castle, P. A. Bakhtiani, A. Haidar, D. L. Branigan, M. Breen, and W. K. Ward, "Quantification of the glycemic response to microdoses of subcutaneous glucagon at varying insulin levels," *Diabetes care*, vol. 37, no. 11, pp. 3054–3060, 2014.

[29] A. Adkins, R. Basu, M. Persson, B. Dicke, P. Shah, A. Vella, W. F. Schwenk, and R. Rizza, "Higher insulin concentrations are required to suppress gluconeogenesis than glycogenolysis in nondiabetic humans," *Diabetes*, vol. 52, no. 9, pp. 2213–2220, 2003.

[30] J. Girard, "The inhibitory effects of insulin on hepatic glucose production are both direct and indirect," *Diabetes*, vol. 55, no. Supplement 2, pp. S65–S69, 2006.

[31] S. Rosenbaum, *Basic pharmacokinetics and pharmacodynamics: An integrated textbook and computer simulations*, 1st ed.   John Wiley & Sons, Inc., 2011.

[32] R. N. Bergman, Y. Z. Ider, C. R. Bowden, and C. Cobelli, "Quantitative estimation of insulin sensitivity." *American Journal of Physiology-Endocrinology And Metabolism*, vol. 236, no. 6, pp. E667–E677, 1979.

[33] N. R. Kristensen, H. Madsen, and S. B. Jørgensen, "A method for systematic improvement of stochastic grey-box models," *Computers & chemical engineering*, vol. 28, no. 8, pp. 1431–1449, 2004.

[34] CTSM-R development team. (2015, April) Continuous time stochastic modeling in r: User's guide and reference manual. [Online]. Available: http://ctsm.info/pdfs/ctsmr-reference.pdf

[35] S. L. Wendt, C. B. Knudsen, J. B. Jørgensen, H. Madsen, and A. Haidar, "Modelling the glucose-insulin-glucagon dynamics after subcutaneous administration of native glucagon and a novel glucagon analogue in dogs," in *Diabetes technology & therapeutics*, vol. 18, no. S1, 2016, pp. A-134.

[36] Roche custom biotech. (2011) Glucose test principle. [Online]. Available: http://custombiotech.roche.com/content/dam/internet/dia/custombiotech/custombiotech_com/en_GB/pdf/Glucose_Test_Principle_05837804990_03.11.pdf

[37] D. C. Simonson and R. A. DeFronzo, "Glucagon physiology and aging: evidence for enhanced hepatic sensitivity," *Diabetologia*, vol. 25, no. 1, pp. 1–7, 1983.

[38] D. Matthews, J. Hosker, A. Rudenski, B. Naylor, D. Treacher, and R. Turner, "Homeostasis model assessment: insulin resistance and β-cell function from fasting plasma glucose and insulin concentrations in man," *Diabetologia*, vol. 28, no. 7, pp. 412–419, 1985.

Wendt et al.   DTU Compute Technical Report-2016-2   *REFERENCES*

[39] A. Haidar, D. Elleri, K. Kumareswaran, L. Leelarathna, J. M. Allen, K. Caldwell, H. R. Murphy, M. E. Wilinska, C. L. Acerini, M. L. Evans, D. B. Dunger, M. Nodale, and R. Hovorka, "Pharmacokinetics of insulin aspart in pump-treated subjects with type 1 diabetes: reproducibility and effect of age, weight, and duration of diabetes," *Diabetes Care*, vol. 36, no. 10, pp. e173–e174, 2013.

[40] A. Haidar, C. Duval, L. Legault, and R. Rabasa-Lhoret, "Pharmacokinetics of insulin aspart and glucagon in type 1 diabetes during closed-loop operation," *Journal of diabetes science and technology*, vol. 7, no. 6, pp. 1507–1512, 2013.

[41] A. D. Cherrington, J. E. Liljenquist, G. I. Shulman, P. E. Williams, and W. W. Lacy, "Importance of hypoglycemia-induced glucose production during isolated glucagon deficiency." *American Journal of Physiology - Endocrinology and Metabolism*, vol. 236, no. 3, pp. E263–E271, 1979.

[42] M. A. Davis, P. E. Williams, and A. D. Cherrington, "Effect of glucagon on hepatic lactate metabolism in the conscious dog," *American Journal of Physiology - Endocrinology and Metabolism*, vol. 248, no. 4, pp. E463–E470, 1985.

[43] M. A. Felmlee, M. E. Morris, and D. E. Mager, "Mechanism-based pharmacodynamic modeling," *Methods in Molecular Biology*, vol. 929, pp. 583–600, 2012.

[44] C. Kreutz, A. Raue, D. Kaschek, and J. Timmer, "Profile likelihood in systems biology," *The FEBS Journal*, vol. 208, pp. 2564–2571, 2013.

[45] H. Madsen and P. Thyregod, *Introduction to general and generalized linear models*.   CRC Press, 2011.

[46] N. R. Kristensen, H. Madsen, and S. B. Jørgensen, "Parameter estimation in stochastic grey-box models," *Automatica*, vol. 40, no. 2, pp. 225–237, 2004.

[47] R. Juhl, J. K. Møller, J. B. Jørgensen, and H. Madsen, *Prediction Methods for Blood Glucose Concentration*.   Springer, 2016, ch. Modeling and prediction using stochastic differential equations.

[48] J. K. Møller, J. Carstensen, and H. Madsen, "Structural identification and validation in stochastic differential equation based models - with application to a marine ecosystem NP-model," *Journal of the Royal Statistical Society, Series C*, 2011.

[49] H. Madsen, *Time series analysis*.   CRC Press, 2007.

[50] H. Blauw, I. Wendl, J. H. DeVries, T. Heise, and T. Jax, "Pharmacokinetics and pharmacodynamics of various glucagon dosages at different blood glucose levels," *Diabetes, Obesity and Metabolism*, vol. 18, no. 1, pp. 34–39, 2016.

[51] A. Ranjan, S. Schmidt, S. Madsbad, J. J. Holst, and K. Nørgaard, "Effects of subcutaneous, low-dose glucagon on insulin-induced mild hypoglycaemia in patients with insulin pump treated type 1 diabetes." *Diabetes, obesity & metabolism*, vol. Epub ahead of print, 2016.

[52] C. J. Graf, J. R. Woodworth, M. E. Seger, J. H. Holcombe, R. R. Bowsher, and R. Lynch, "Pharmacokinetic and glucodynamic comparisons of recombinant and animal-source glucagon after IV, IM, and SC injection in healthy volunteers," *Journal of pharmaceutical sciences*, vol. 88, no. 10, pp. 991–995, 1999.

Appendix

A   Raw data
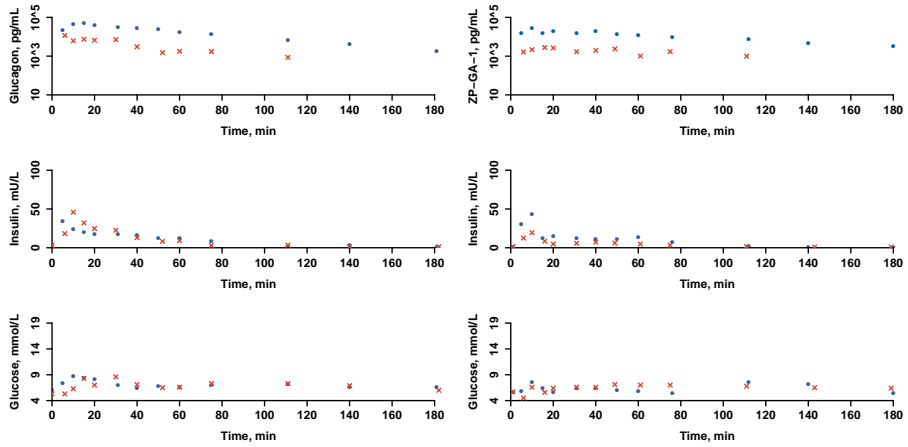
Figure 16: Raw PK and PD data with outliers measured in dog 1. Data from low or high doses of glucagon and ZP-GA-1 are red crosses or blue dots, respectively.
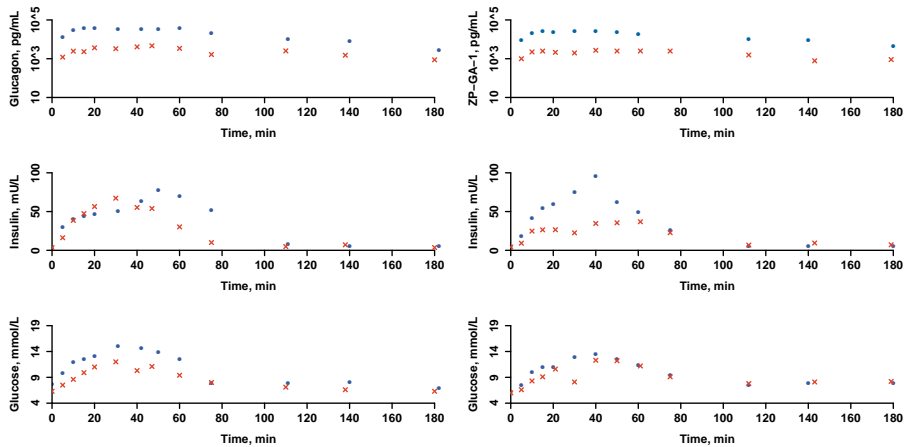
Figure 17: Raw PK and PD data with outliers measured in dog 2. Data from low or high doses of glucagon and ZP-GA-1 are red crosses or blue dots, respectively.
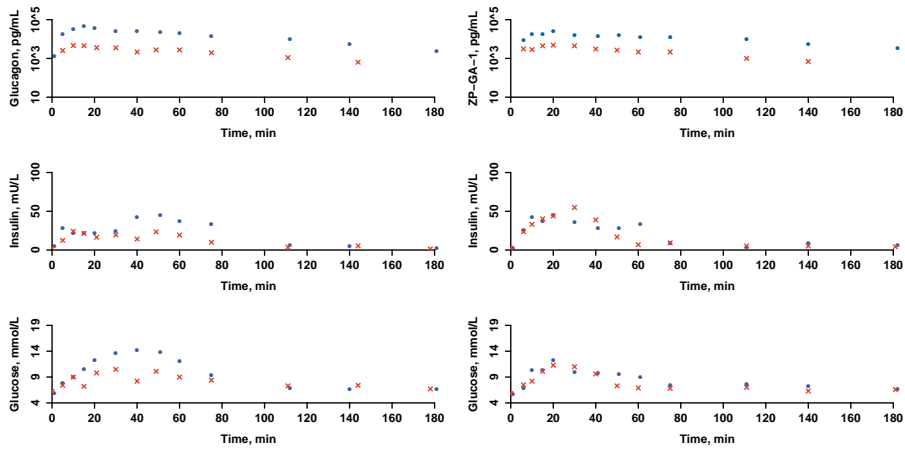
Figure 18: Raw PK and PD data with outliers measured in dog 3. Data from low or high doses of glucagon and ZP-GA-1 are red crosses or blue dots, respectively.
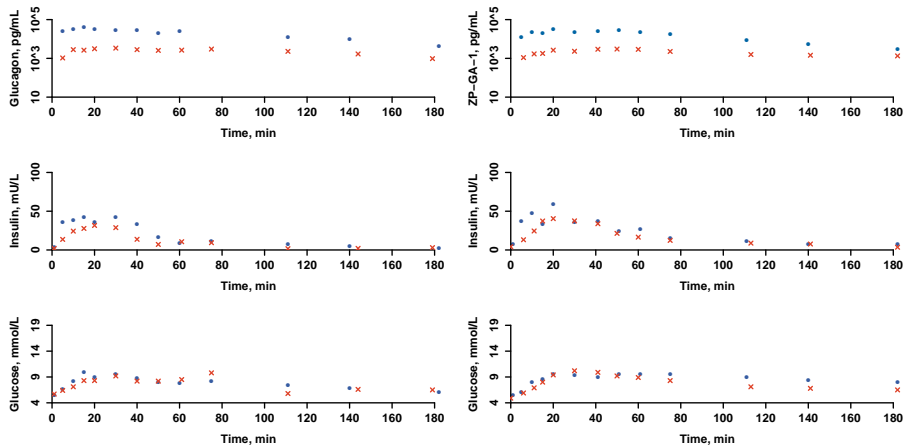
Figure 19: Raw PK and PD data with outliers measured in dog 4. Data from low or high doses of glucagon and ZP-GA-1 are red crosses or blue dots, respectively.
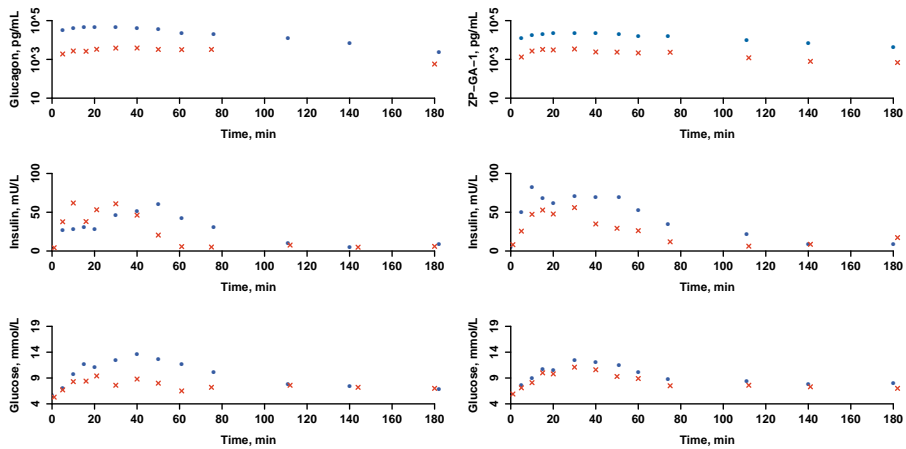
Figure 20: Raw PK and PD data with outliers measured in dog 5. Data from low or high doses of glucagon and ZP-GA-1 are red crosses or blue dots, respectively.

B   PK Model fits
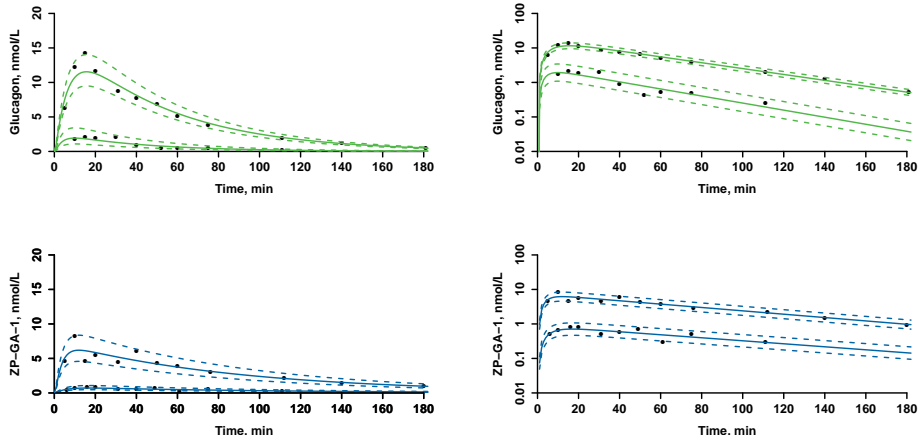
Figure 21: PK model fit after low and high doses of glucagon (green) and ZP-GA-1 (blue) in dog 1. Left graphs are with regular axes and right graphs are with $\log_{10}$ axes.
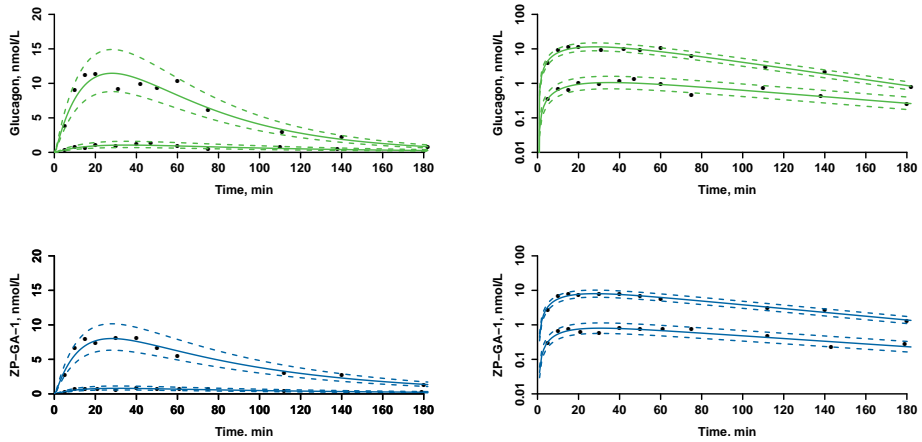
Figure 22: PK model fit after low and high doses of glucagon (green) and ZP-GA-1 (blue) in dog 2. Left graphs are with regular axes and right graphs are with $\log_{10}$ axes.
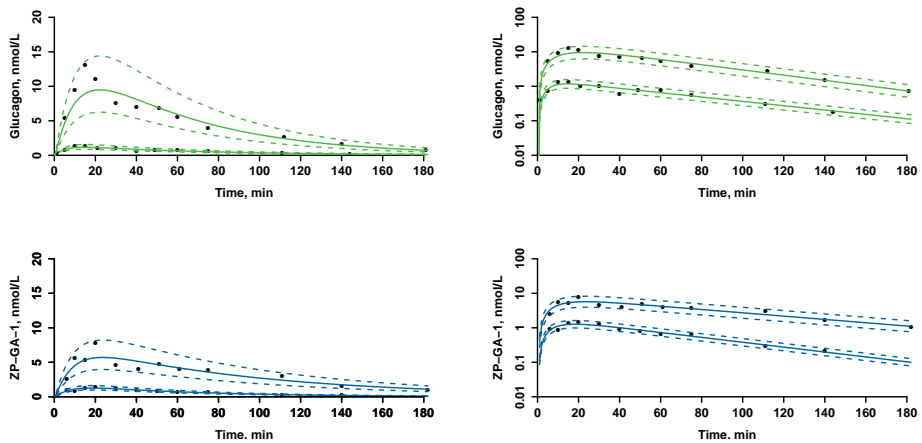
Figure 23: PK model fit after low and high doses of glucagon (green) and ZP-GA-1 (blue) in dog 3. Left graphs are with regular axes and right graphs are with $\log_{10}$ axes.
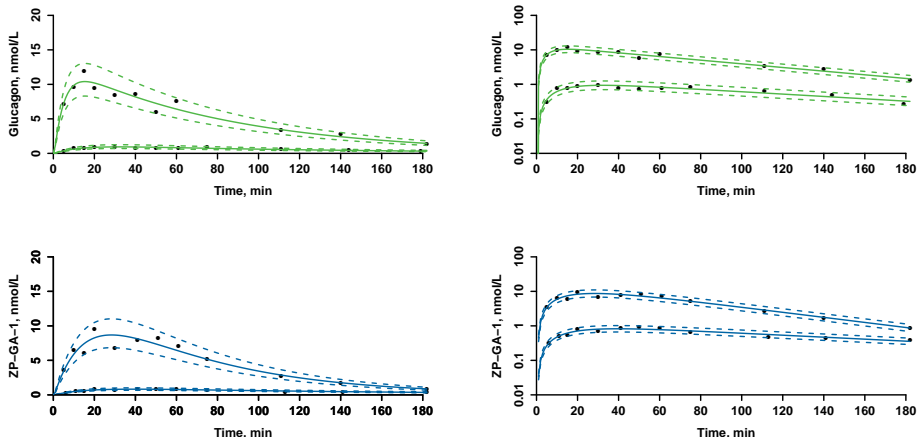
Figure 24: PK model fit after low and high doses of glucagon (green) and ZP-GA-1 (blue) in dog 4. Left graphs are with regular axes and right graphs are with $\log_{10}$ axes.
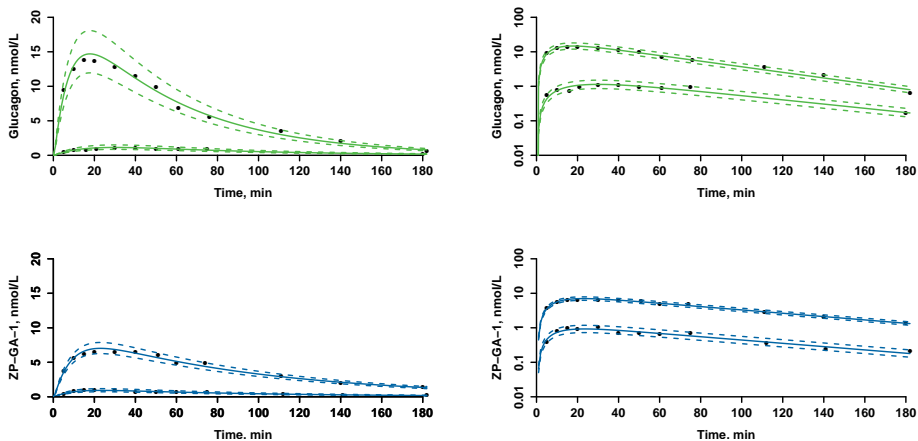
Figure 25: PK model fit after low and high doses of glucagon (green) and ZP-GA-1 (blue) in dog 5. Left graphs are with regular axes and right graphs are with $\log_{10}$ axes.

C   PD model fits

Wendt et al.   DTU Compute Technical Report-2016-2   *C   PD MODEL FITS*

(a) 20 nmol/kg of glucagon.

(b) 120 nmol/kg of glucagon.

(c) 20 nmol/kg of ZP-GA-1.

(d) 120 nmol/kg of ZP-GA-1.
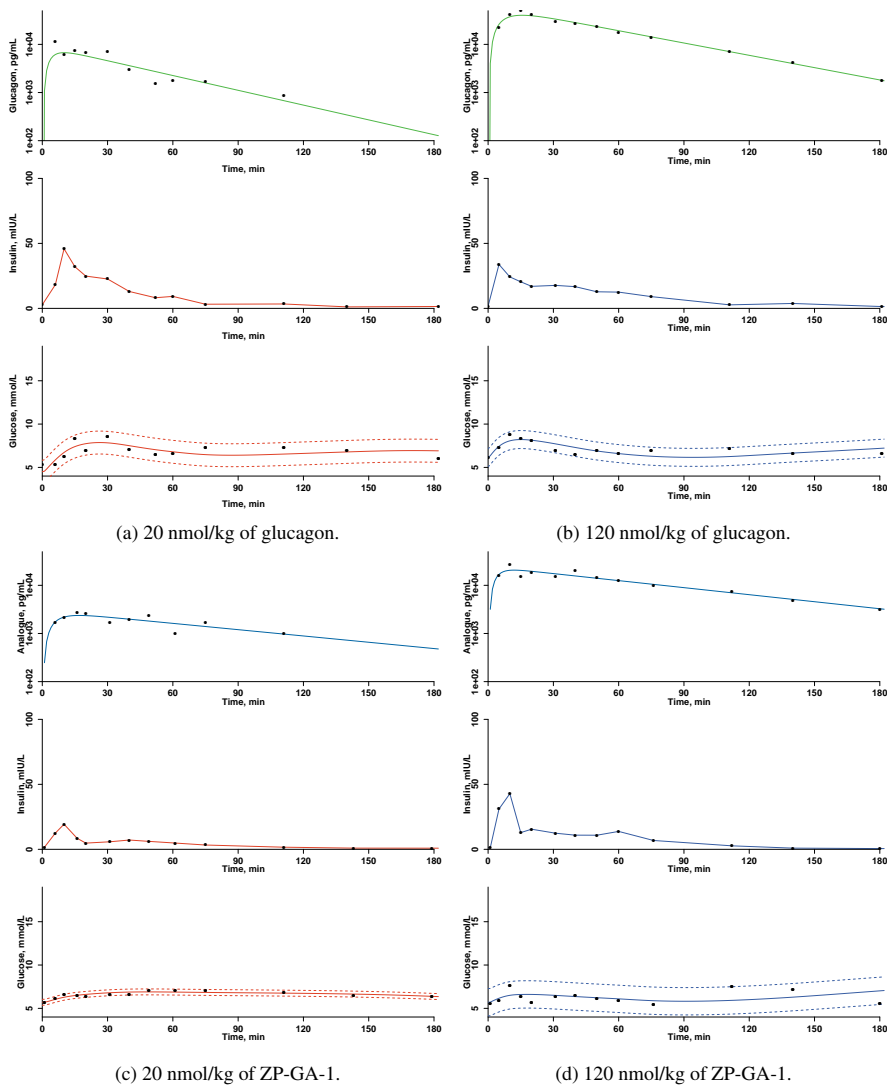
Figure 26: Plasma concentrations of PD model inputs glucagon and insulin together with PD model fit of glucose in dog 1. Administered doses and drugs are written in each subfigure.

(a) 20 nmol/kg of glucagon.

(b) 120 nmol/kg of glucagon.

(c) 20 nmol/kg of ZP-GA-1.

(d) 120 nmol/kg of ZP-GA-1.
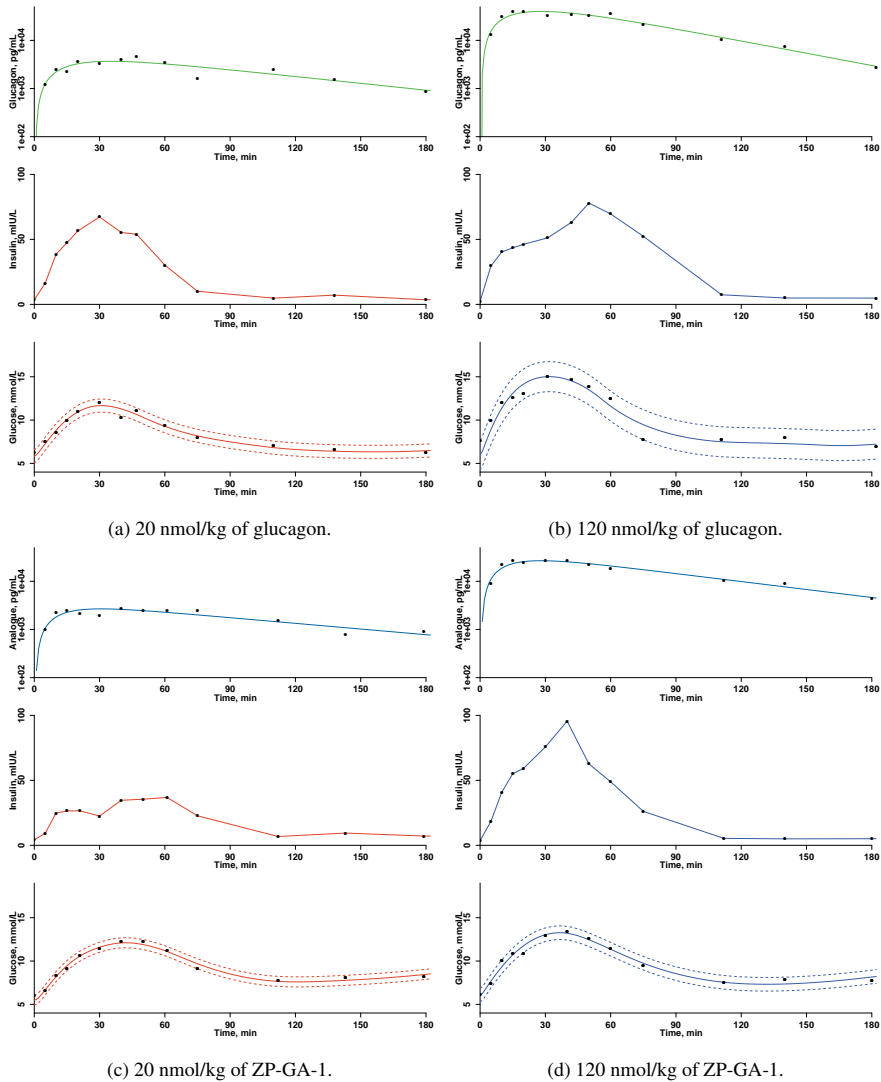
Figure 27: Plasma concentrations of PD model inputs glucagon and insulin together with PD model fit of glucose in dog 2. Administered doses and drugs are written in each subfigure.

Wendt et al.   DTU Compute Technical Report-2016-2   *C   PD MODEL FITS*

(a) 20 nmol/kg of glucagon.

(b) 120 nmol/kg of glucagon.

(c) 20 nmol/kg of ZP-GA-1.

(d) 120 nmol/kg of ZP-GA-1.
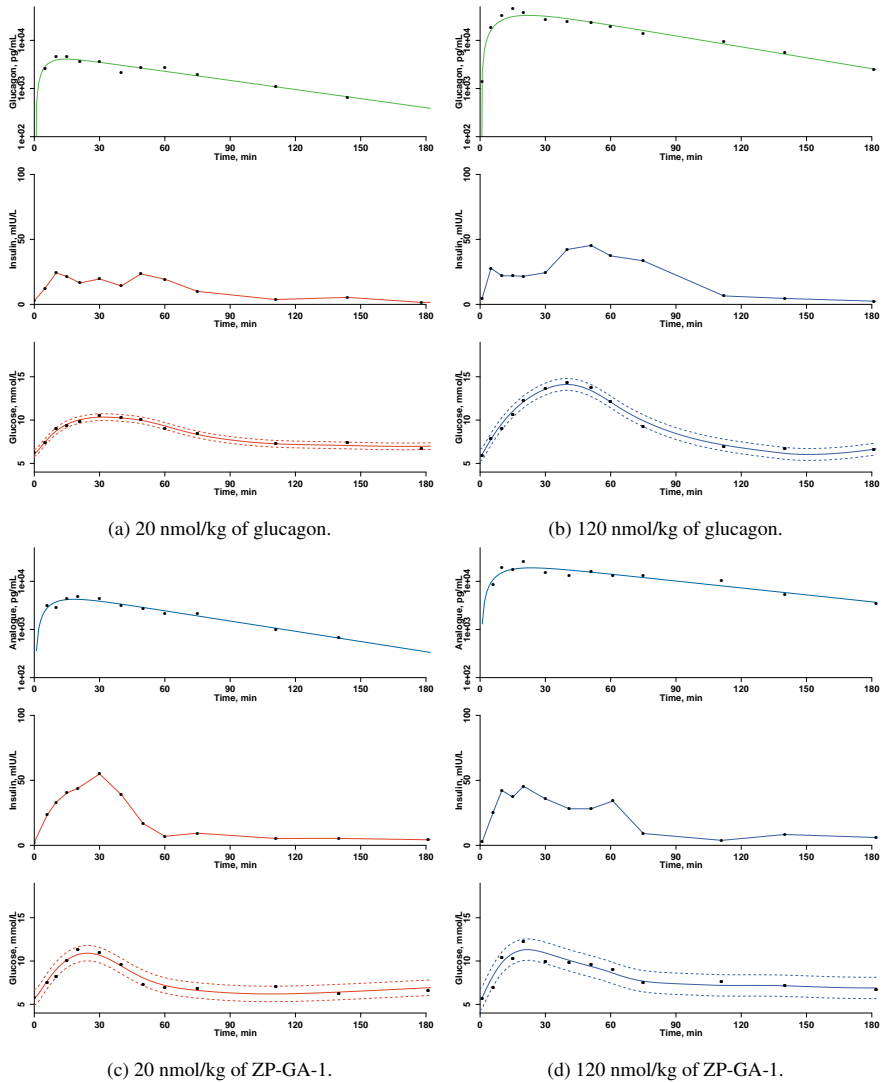
Figure 28: Plasma concentrations of PD model inputs glucagon and insulin together with PD model fit of glucose in dog 3. Administered doses and drugs are written in each subfigure.

(a) 20 nmol/kg of glucagon.

(b) 120 nmol/kg of glucagon.

(c) 20 nmol/kg of ZP-GA-1.

(d) 120 nmol/kg of ZP-GA-1.
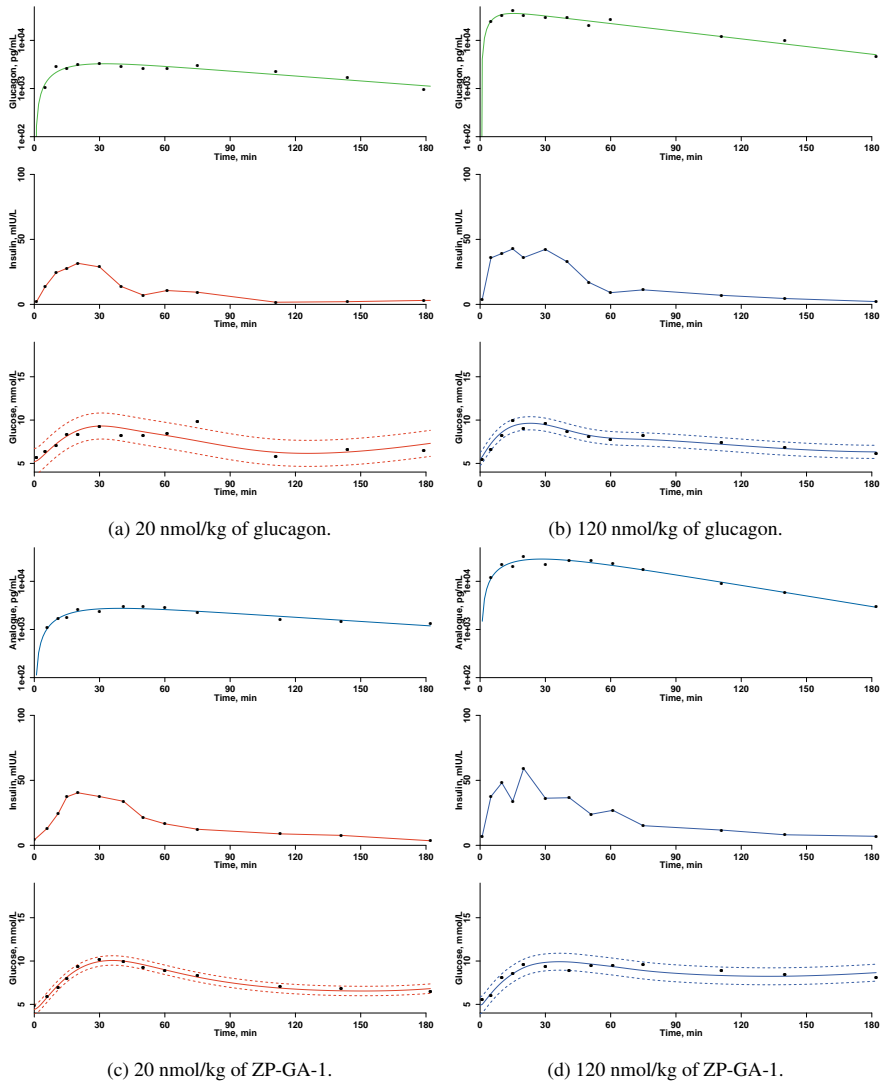
Figure 29: Plasma concentrations of PD model inputs glucagon and insulin together with PD model fit of glucose in dog 4. Administered doses and drugs are written in each subfigure.

(a) 20 nmol/kg of glucagon.

(b) 120 nmol/kg of glucagon.

(c) 20 nmol/kg of ZP-GA-1.

(d) 120 nmol/kg of ZP-GA-1.
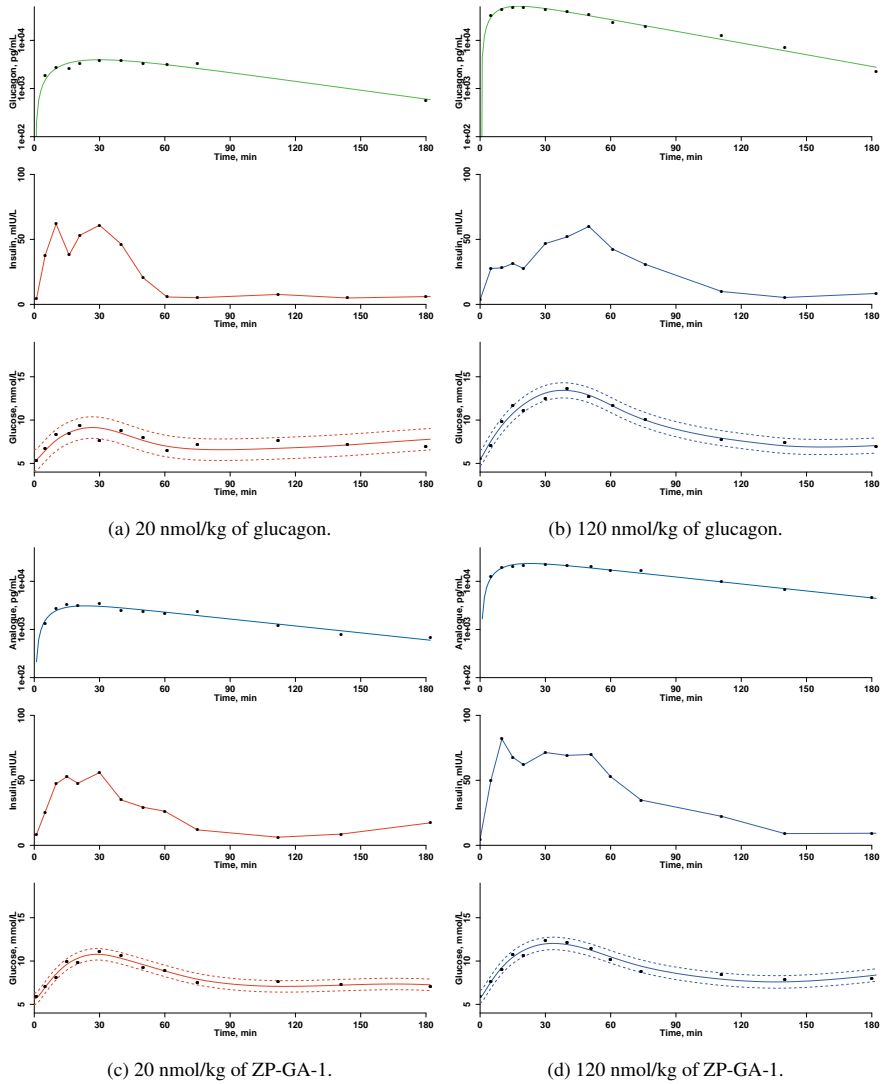
Figure 30: Plasma concentrations of PD model inputs glucagon and insulin together with PD model fit of glucose in dog 5. Administered doses and drugs are written in each subfigure.

APPENDIX B

Conference Paper
PD in Healthy Humans

This appendix presents the 1-page paper with the title "Modelling of Glucose-Insulin-Glucagon Pharmacodynamics in Man" accepted at the 38th annual international conference of the IEEE Engineering in Medicine and Biology Society (EMBC'16) in Orlando, Florida during August 2016 [19].

Modelling of Glucose-Insulin-Glucagon Pharmacodynamics in Man

S. L. Wendt[1,2], J. K. Møller[2], A. Haidar[3], C. B. Knudsen[1], H. Madsen[2], J. B. Jørgensen[2]

Abstract— **The purpose is to build a simulation model of the glucoregulatory system in man. We estimate individual human parameters of a physiological glucose-insulin-glucagon model. We report posterior probability distributions and correlations of model parameters.**

I. Introduction

In healthy individuals, insulin and glucagon work in a complex fashion to maintain blood glucose levels within a narrow range. Recent studies suggest a multiplicative effect of insulin and of glucagon on endogenous glucose production (EGP) [1].

II. Materials and Methods

A. PD Model

The pharmacodynamics (PD) model is mainly inspired by Hovorka et al. [2].

$$\dot{Q}_1(t) = -F_{01} - S_T x_1(t) Q_1(t) + k_{12} Q_2(t) + F_{IC}(t) \quad (1a)$$

$$\dot{Q}_2(t) = S_T x_1(t) Q_1(t) - (k_{12} + S_D x_2(t)) Q_2(t) \quad (1b)$$

$$\dot{x}_i(t) = k_i (I(t) - x_i(t)) \qquad i = 1, 2, 3 \quad (1c)$$

$Q_1(t)$ and $Q_2(t)$ are the masses of glucose per bodyweight (μmol/kg) in the accessible and non-accessible compartments. Glucose concentration (mmol/L) in the accessible compartment is $Q_1(t)/V$ with V fixed at 160 mL/kg. $I(t)$ is the insulin concentration (mIU/L) in the accessible compartment. $x_i(t)$ are the remote effects of insulin (mIU/L).

F_{01} is the non-insulin-dependent glucose flux. k_{12} and k_i are transfer rate constants. S_D, S_E, and S_T are insulin sensitivities.

The model in (1) is modified so $F_{IC}(t)$ is the insulin and glucagon dependent EGP [3].

$$F_{IC}(t) = \frac{(1 - S_E x_3(t))}{(1 - S_E I_{b,y})} \cdot \left((E_{max} - E_0) \frac{C(t)}{C_{E50} + C(t)} \right) \quad (2)$$

$C(t)$ is the glucagon concentration (pg/mL) in the accessible compartment. $I_{b,y}$ is the fixed basal insulin concentration (mIU/L) for subject y, and E_0 is the minimum EGP fixed at 8 μmol/(kg·min). E_{max} is the maximum EGP at $I_{b,y}$. C_{E50} is the glucagon concentration at half maximum EGP.

B. Parameter Estimation

We used maximum a posteriori to estimate PD model parameters and profile likelihood analysis to reduce unidentifiable parameters in data with measurements of glucose, insulin and glucagon from ten healthy male subjects who received a 1 mg subcutaneous bolus of marketed glucagon.

III. Results

TABLE I
POSTERIOR DISTRIBUTIONS OF PARAMETERS ACROSS POPULATION.

Parameter	Unit	Mean	SD
C_{E50}	pg/mL	407	39
E_{max}	μmol/(kg·min)	38.8	5.0
F_{01}	μmol/(kg·min)	10.5	0.95
$\ln(k_{12})$	min^{-1}	-3.48	0.26
$\ln(k_2)$	min^{-1}	-2.11	0.03
$\ln(k_3)$	min^{-1}	-4.20	0.74
$\ln(S_E)$	per mIU/L	-3.19	0.67
$\ln(S_T)$	min^{-1} per mIU/L	-5.73	0.54
$\ln(k_1)$	min^{-1}	-5.69	*
$\ln(S_D)$	min^{-1} per mIU/L	-7.58	*

* Fixed unidentifiable parameter.

TABLE II
POSTERIOR CORRELATION MATRIX OF IDENTIFIABLE PARAMETERS.

	C_{E50}	E_{max}	F_{01}	$k_{12}*$	k_2*	k_3*	S_E*	S_T*	BW
C_{E50}	1								
E_{max}	0.31	1							
F_{01}	0.32	-0.30	1						
$k_{12}*$	0.45	0.23	0.22	1					
k_2*	-0.63	0.06	-0.13	-0.30	1				
k_3*	0.13	-0.34	0.82	-0.02	-0.33	1			
S_E*	-0.82	-0.26	-0.40	-0.22	0.43	-0.35	1		
S_T*	-0.20	-0.22	-0.13	0.45	-0.28	-0.14	0.57	1	
BW	0.61	-0.43	0.39	0.24	-0.70	0.42	-0.60	0.00	1

* Correlation of ln-transformed parameter.

IV. Conclusions

The model enables simulations of the glucose-insulin-glucagon dynamics in man at the following concentrations: glucagon (180-8000 pg/mL), insulin (1.2-81.9 mIU/L) and glucose (3.3-11.5 mmol/L).

References

[1] A. Emami *et al.*, "Modelling glucagon action in patients with type 1 diabetes," *J-BHI*, 2016, submitted.

[2] R. Hovorka *et al.*, "Partitioning glucose distribution/transport, disposal, and endogenous production during IVGTT," *Am J Physiol Endocrinol Metab*, vol. 282, no. 5, pp. E992–E1007, 2002.

[3] S. L. Wendt *et al.*, "PK/PD modeling of glucose-insulin-glucagon dynamics in healthy dogs after a subcutaneous bolus administration of native glucagon or a novel glucagon analogue," DTU Compute, Tech. Rep. 2016-2, 2016.

[1] Department of Bioanalysis & Pharmacokinetics, Zealand Pharma A/S, DK-2600 Glostrup, Denmark slw@zealandpharma.com
[2] Department of Applied Mathematics and Computer Science, Technical University of Denmark, DK-2800 Kgs. Lyngby, Denmark jbjo@dtu.dk
[3] Department of Biomedical Engineering, McGill University, Montreal, Quebec, Canada

Journal Paper 1 PK/PD in Diabetes Patients

This appendix presents the journal paper by Wendt *et al.* with the title "Cross-Validation of a Glucose-Insulin-Glucagon Pharmacodynamics Model for Simulation using Data from patients with Type 1 Diabetes" published in Journal of Diabetes Science and Technology in February 2017 [20].

Original Article

Cross-Validation of a Glucose-Insulin-Glucagon Pharmacodynamics Model for Simulation Using Data From Patients With Type 1 Diabetes

Sabrina Lyngbye Wendt, MScBME[1,2], Ajenthen Ranjan, MD[3,4], Jan Kloppenborg Møller, MSc, PhD[2], Signe Schmidt, MD, PhD[3,4], Carsten Boye Knudsen, MSc, PhD[1], Jens Juul Holst, MD, DMSc[5], Sten Madsbad, MD, DMSc[3,5], Henrik Madsen, MSc, PhD[2], Kirsten Nørgaard, MD, DMSc[3], and John Bagterp Jørgensen, MSc, PhD[2]

Abstract

Background: Currently, no consensus exists on a model describing endogenous glucose production (EGP) as a function of glucagon concentrations. Reliable simulations to determine the glucagon dose preventing or treating hypoglycemia or to tune a dual-hormone artificial pancreas control algorithm need a validated glucoregulatory model including the effect of glucagon.

Methods: Eight type 1 diabetes (T1D) patients each received a subcutaneous (SC) bolus of insulin on four study days to induce mild hypoglycemia followed by a SC bolus of saline or 100, 200, or 300 μg of glucagon. Blood samples were analyzed for concentrations of glucagon, insulin, and glucose. We fitted pharmacokinetic (PK) models to insulin and glucagon data using maximum likelihood and maximum a posteriori estimation methods. Similarly, we fitted a pharmacodynamic (PD) model to glucose data. The PD model included multiplicative effects of insulin and glucagon on EGP. Bias and precision of PD model test fits were assessed by mean predictive error (MPE) and mean absolute predictive error (MAPE).

Results: Assuming constant variables in a subject across nonoutlier visits and using thresholds of ±15% MPE and 20% MAPE, we accepted at least one and at most three PD model test fits in each of the seven subjects. Thus, we successfully validated the PD model by leave-one-out cross-validation in seven out of eight T1D patients.

Conclusions: The PD model accurately simulates glucose excursions based on plasma insulin and glucagon concentrations. The reported PK/PD model including equations and fitted parameters allows for in silico experiments that may help improve diabetes treatment involving glucagon for prevention of hypoglycemia.

Keywords

cross-validation, glucagon, glucoregulatory model, parameter estimation, simulation model, type 1 diabetes

The treatment goal for patients with type 1 diabetes is near-normalization of plasma glucose levels. Few patients achieve this even with intensive insulin treatment.[1] New approaches with automatic glucose controlled insulin and glucagon delivery, known as a dual-hormone artificial pancreas (AP), may offer a solution to improve glycemic control.[2-6] To design and tune control algorithms for AP devices prior to in vivo tests, a validated simulation model capturing the dynamics between glucose, insulin and glucagon is needed to perform helpful in silico experiments.[7-9]

Glucagon primarily affects hepatic glucose production by increasing glycogenolysis, while the rate of gluconeogenesis seems less affected by changes in both insulin and glucagon concentrations.[10] Currently marketed glucagon is approved as a 1 mg rescue-treatment for severe hypoglycemia, although the interest in mini-dose glucagon is increasing.[11,12] Recent

[1]Zealand Pharma A/S, Glostrup, Denmark
[2]Department of Applied Mathematics and Computer Science, Technical University of Denmark, Kgs. Lyngby, Denmark
[3]Department of Endocrinology, Hvidovre University Hospital, Hvidovre, Denmark
[4]Danish Diabetes Academy, Odense, Denmark
[5]Faculty of Health and Medical Sciences, University of Copenhagen, Copenhagen, Denmark

Corresponding Author:
Sabrina Lyngbye Wendt, Zealand Pharma A/S, Smedeland 36, DK-2600 Glostrup, Denmark.
Email: slw@zealandpharma.com

studies proved that the glycemic response to low-dose gluca-gon is dependent on ambient insulin levels,[13] but neither on plasma glucose level[14,15] nor on prior glucagon dosing.[16] At high circulating insulin concentrations (50-60 mU/l), the endogenous glucose production (EGP) is completely inhib-ited,[17] and at insulin levels exceeding ~40 mU/l the EGP can-not be stimulated by glucagon.[13]

The ability of insulin to suppress the glycogenolytic response to glucagon at high insulin concentration is not reflected in previously published models of glucose-gluca-gon dynamics.[18-20] A comparative study found that a multi-plicative relationship was needed to describe insulin's inhibitory effect and glucagon's stimulating effect on glyco-genolysis with insulin overriding the effect of glucagon at high concentrations of both hormones.[21] Recently, we extended the multiplicative model by incorporating the interaction between insulin and glucagon on glycogenoly-sis.[13,22] The model extension was developed using preclini-cal data from dogs and was fitted to clinical human data in previous studies.[23,24] In this article, we aim to validate the multiplicative glucose-insulin-glucagon model for simula-tion studies in humans using data from eight patients with type 1 diabetes.

Methods

Data Collection

Clinical data originated from a glucagon dose-finding study in eight well-controlled patients with type 1 diabetes (5 females, age range: 19-64 years, BMI range: 20.0-25.4 kg/m^{2}, HbA1c range: 6.1-7.4%), who were insulin pump-treated and had no endogenous production of insulin.[25] Table S1 summarizes the patient characteristics. In brief, the patients completed four similar study days in random order. On each study day, patients arrived at the research facility in the morning in a fasting state. A subcutaneous (SC) insulin bolus (NovoRapid®, Novo Nordisk A/S, Bagsværd, Denmark) was administered via the patient's insulin pump, aiming to lower plasma glucose to 54 mg/dl if no interventions were made. The insulin bolus was cal-culated based on each patient's individual sensitivity fac-tor, which was determined prior to the first study visit using a standard procedure.[26] When plasma glucose reached ≤70 mg/dl, a single SC bolus of either 100 µg (visit B), 200 µg (visit C), 300 µg (visit D) glucagon (GlucaGen®, Novo Nordisk A/S, Bagsværd, Denmark), or saline (visit A) was administered (see Figure 1). Blood was sampled and analyzed for plasma glucose (YSI 2300 STAT Plus, Yellow Springs Instrument, Yellow Springs, OH), plasma glucagon[27] and serum insulin aspart (Mercodia AB, Uppsala, Sweden). The insulin pump continuously infused insulin as a basal rate during the study days. The insulin infusion rate was adjusted before the first study day, to keep near constant blood glucose values in the fasting and
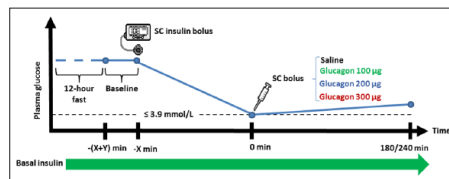
Figure 1. Schematic design of the study days. Baseline blood samples were taken at time –(X+Y). An insulin bolus was given after Y minutes. In a few cases, multiple insulin boluses had to be administered to lower the plasma glucose sufficiently. When the plasma glucose measured below 70 mg/dl, a saline or glucagon bolus was given depending on the study day. At 180 or 240 minutes after the saline/glucagon bolus the experiment was stopped. Basal insulin infusion continued throughout the experiment. From t = –x to t = 0, plasma glucose was measured every 15-30 minutes, while plasma glucagon and serum insulin were measured every 60 minutes. Plasma glucose was measured every 5 minutes from t = 0 to t = 60, every 10 minutes from t = 60 to t=120 and then every 15 minutes. Plasma glucagon and serum insulin were measured every 5 minutes from t = 0 to t = 15, every 15 minutes from t = 15 to t = 60, every 30 minutes from t = 60 to t = 120, and then every 60 minutes.

resting condition. The individual insulin infusion basal rates were similar between study visits.

Models

When applying a pharmacokinetic (PK) model, we assume that all increases in insulin and glucagon concentrations are due to exogenously dosed drugs so that endogenous produc-tion is constant or negligible.

Insulin Pharmacokinetic Model. Previous studies showed that a simple two-state model with identical time constants for absorption and elimination could be used to describe the PK of insulin aspart after SC dosing.[28]

$$\frac{dX_1(t)}{dt} = u_I(t) - \frac{X_1(t)}{t_{max}}$$

$$\frac{dX_2(t)}{dt} = \frac{X_1(t)}{t_{max}} - \frac{X_2(t)}{t_{max}}$$

$$I(t) = \frac{1}{t_{max}}\frac{X_2(t)}{W \cdot Cl_{F,I}}10^6 + I_b$$

Table 1 lists the interpretations of the insulin PK model parameters and their units. The insulin concentration in serum is the sum of external rapid acting insulin dosage and basal infusion. The model assumes steady state insulin

Table 1. Interpretation of Insulin PK (Top Rows), Glucagon PK (Middle Rows), and Glucose PD (Bottom Rows) Model Parameters and Their Units.

Parameter	Unit	Interpretation
$X_1(t)$	U	Insulin mass due to exogenous dosing, in SC tissue
$X_2(t)$	U	Insulin mass due to exogenous dosing, in serum
$u_I(t)$	U/minute	Insulin dose
t_{max}	minutes	Time from dose to maximum serum concentration
W	kg	Body weight
$Cl_{F,I}$	ml/kg/minute	Apparent insulin clearance
I_b	mU/l	Steady state insulin concentration
$I(t)$	mU/l	Insulin concentration in serum
$Z_1(t)$	pg	Glucagon mass due to exogenous dosing, in SC tissue
$Z_2(t)$	pg	Glucagon mass due to exogenous dosing, in plasma
$u_C(t)$	pg/minute	Glucagon dose
k_1	minute^{-1}	Absorption rate constant
k_2	minute^{-1}	Elimination rate constant
$Cl_{F,C}$	ml/kg/minute	Apparent glucagon clearance
C_b	pg/ml	Steady state glucagon concentration
$C(t)$	pg/ml	Glucagon concentration in plasma
$Q_1(t)$	μmol/kg	Glucose mass per W in the accessible compartment
$Q_2(t)$	μmol/kg	Glucose mass per W in the nonaccessible compartment
$x_1(t)$	mU/l	Remote effects of insulin on glucose transport
$x_2(t)$	mU/l	Remote effects of insulin on glucose disposal
$x_3(t)$	mU/l	Remote effects of insulin on glycogenolysis
$G(t)$	mmol/l	Glucose concentration in plasma
$G_{GG}(t)$	μmol/kg/minute	Glucose production due to glycogenolysis
G_{GNG}	μmol/kg/minute	Glucose production due to gluconeogenesis
F_{01}	μmol/kg/minute	Insulin independent glucose flux
F_R	μmol/kg/minute	Renal glucose clearance
S_T	minute^{-1}/(mU/l)	Insulin sensitivity of glucose transport
S_D	minute^{-1}/(mU/l)	Insulin sensitivity of glucose disposal
S_E	l/mU	Insulin sensitivity on glycogenolysis
k_{12}	minute^{-1}	Transfer rate constant from the nonaccessible to the accessible compartment
k_{a1}	minute^{-1}	Insulin deactivation rate constant
k_{a2}	minute^{-1}	Insulin deactivation rate constant
k_{a3}	minute^{-1}	Insulin deactivation rate constant
E_{max}	μmol/kg/minute	Maximum EGP at basal insulin concentration
C_{E50}	pg/ml	Glucagon concentration yielding half of maximum EGP
V	ml/kg	Glucose volume of distribution

concentration, I_b, maintained by the basal infusion when no exogenous rapid acting insulin is dosed.

Glucagon Pharmacokinetic Model. A two-state model with different absorption and elimination rate constants can describe glucagon PK after SC dosing.[23]

$$\frac{dZ_1(t)}{dt} = u_C(t) - k_1 Z_1(t)$$

$$\frac{dZ_2(t)}{dt} = k_1 Z_1(t) - k_2 Z_2(t)$$

$$C(t) = \frac{k_2 Z_2(t)}{W \cdot Cl_{F,C}} + C_b$$

Table 1 lists the interpretations of the glucagon PK model parameters and their units. The glucagon concentration in plasma is the sum of constant endogenous glucagon, C_b, and external glucagon dosage. The model does not include an endogenous response to hypoglycemia.

Glucose Pharmacodynamic Model. The glucose PD model was originally derived by Hovorka et al[29,30] and further extended by Wendt et al.[23]

$$\frac{dQ_1(t)}{dt} = -F_{01} - F_R - S_T x_1(t) Q_1(t)$$
$$+ k_{12} Q_2(t) + G_{GG}(t) + G_{GNG}$$

$$\frac{dQ_2(t)}{dt} = S_T x_1(t) Q_1(t) - \left[k_{12} + S_D x_2(t)\right] Q_2(t)$$

$$G_{GG}(t) = \frac{1 - S_E x_3(t)}{1 - S_E I_b}\left((E_{max} - G_{GNG}) \frac{C(t)}{C_{E50} + C(t)} \right)$$

$$G(t) = \frac{Q_1(t)}{V}$$

$$\frac{dx_1(t)}{dt} = k_{a1}\left[I(t) - x_1(t) \right]$$

$$\frac{dx_2(t)}{dt} = k_{a2}\left[I(t) - x_2(t) \right]$$

$$\frac{dx_3(t)}{dt} = k_{a3}\left[I(t) - x_3(t) \right]$$

Table 1 lists the interpretations of the glucose PD model parameters and their units. The endogenous glucose production is the sum of glycogenolysis, G_{GG}, and gluconeogenesis, G_{GNG}. The gluconeogenesis is fixed at 6 μmol/kg/minute.[10] F_{01} is constant when plasma glucose concentration exceeds 81 mg/dl.[30] The renal glucose clearance is zero when plasma glucose concentrations do not exceed 162 mg/dl.[30] The glucose volume of distribution is fixed at 160 ml/kg.[29]

Model Fitting

All model fitting was executed in R version 3.1.0 Spring Dance using the additional packages CTSM-R and num-Deriv.[31] Additional data handling was carried out using Microsoft Excel 2013. Unless stated otherwise, the results are reported as means with 95% Wald confidence intervals (CIs) derived from the inverse Hessian, which provides the curvature of the log-likelihood function.[32]

We fitted the insulin PK model using ordinary differential equations (ODEs) and estimated the log-normally distributed observation noise variance using maximum likelihood (ML).[33] Due to missing insulin data around the expected time of maximum insulin concentration both t_{max} and $Cl_{F,I}$ were estimated using maximum a posteriori (MAP) while I_b was estimated using ML. Prior distributions of t_{max} and $Cl_{F,I}$ were reported in Haidar et al[28] and further information regarding t_{max} was extracted from the product monograph on insulin aspart.[34] Table S2 lists the prior parameter distributions. No prior correlation between t_{max} and $Cl_{F,I}$ was assumed.

Insulin PK parameters were optimized on a subject basis to datasets from all four visits (8 parameter sets reported). Despite SC infusion rates of short acting insulin (ie, the basal rates) were similar per subject for all study visits, the baseline insulin concentration varied as evident from the raw data plotted in Figures S1-S7. Therefore, the parameter describing the steady

state insulin level was estimated separately for each visit. Using the subject specific optimized parameters, the insulin PK was simulated every minute and used as input to the PD model.

We fitted the glucagon PK model for visits B, C, and D using ODEs and estimated the log-normally distributed observation noise variance using ML. Plasma glucagon was sampled adequately to perform ML estimation of all parameters in the glucagon PK model. There was some uncertainty regarding the exact dosing time of the glucagon bolus, which was given after the blood sampling at time zero but before the next blood sampling five minutes after. Due to this uncertainty, we estimated the dosing time by choosing the discrete dosing time within the five-minute interval yielding the fit with the highest likelihood value and kept this updated dosing time throughout the data fitting and handling.

As the absolute elimination rate of glucagon is limited by the absorption rate, glucagon exerts flip-flop kinetics.[35] To avoid the flip-flop phenomenon and to reduce the population variation in the two time constants, k_2 was parameterized such that it was greater than k_1 in all datasets.

The glucagon PK parameters were estimated to the datasets from visits with glucagon dosing (24 parameter sets, data not shown) and the PK simulated every minute to be used as input when fitting the PD model. On a subject basis, the glucagon PK parameters were optimized to datasets from all three glucagon visits (8 parameter sets reported). Due to the limited amount of data, we assumed the parameters did not differ between the visits.

The data following administration of saline (visit A) were not fitted to the glucagon PK model but described using linear interpolation between measurements. These interpolated data were used as inputs to the PD model.

The PD model was fitted using ODEs and the log-normally distributed observation noise variance estimated using ML. The remaining parameters (E_{max}, C_{E50}, F_{01}, k_{12}, k_{a1}, k_{a2}, k_{a3}, S_D, S_E, S_T) were estimated using MAP with priors inspired by literature.[22,29] We used priors for the time constants rather than fixing the four parameters.[30] The time constants and the insulin sensitivities were log-transformed during the parameter estimation. Table S2 lists the prior PD model parameter distributions. The PD model parameters have units yielding a glucose output measured in mmol/l, but the output is converted and graphically displayed with units of mg/dl. We assumed no prior correlation between parameters. As previously mentioned, glucose volume of distribution and gluconeogenesis were both fixed based on literature.[10,29] I_b was fixed for each subject based on their average steady state insulin concentration. The final PD model parameters were obtained by optimizing the fit to all nonoutlier visits by each subject (8 parameter sets reported).

Pharmacodynamic Model Validation

To quantify the simulation accuracy of the model on datasets not used for parameter optimization, the bias was calculated

by the mean prediction error (MPE) and the precision calculated by the mean absolute prediction error (MAPE). MPE and MAPE were calculated as percentages.[36]

$$MPE = \frac{1}{N}\sum_{j=1}^{N}\left[\left(\frac{pred_j - obs_j}{obs_j}\right)\times 100\right]$$

$$MAPE = \frac{1}{N}\sum_{j=1}^{N}\left[\left(\frac{|pred_j - obs_j|}{obs_j}\right)\times 100\right]$$

The variables $pred_j$ and obs_j are the jth predicted and observed value, respectively of a total of N observations. If the MPE is less than ±15% and the MAPE is less than 20%, we regard the model fit as accurate, precise and suitable for simulations. Cut-off limits were based on categorizing some fits as "good," "medium," and "bad" prior to knowledge of those fits' MPE and MAPE values by two independent raters. The limits were chosen so that all fits categorized as "good" by both raters would be accepted and all fits categorized as "bad" by both raters would not meet the acceptance criteria.

The PD model validation was carried out as a fourfold leave-one-out cross-validation leaving all data from one visit out per fold. As each subject participated in four visits, each subject had four *training* datasets comprised of data from three visits and four corresponding *test* datasets with data from one visit:

- *Training*: B-C-D, *Test*: A
- *Training*: A-C-D, *Test*: B
- *Training*: A-B-D, *Test*: C
- *Training*: A-B-C, *Test*: D

Thus, all four visits were used for testing once without being used for optimization during that fold. If the MAPE of a test fit exceeded 50%, the test visit was considered an outlier and removed from further analysis. After removal of the outlier dataset another round of leave-one-out was performed on the remaining three datasets. To validate the PD model in a subject, we required that at least one PD model test fit of a dataset from a glucagon visit (B, C or D) was accepted.

Results

Table 2 lists the estimated insulin PK model parameters. The fasting steady state insulin concentration had day-to-day variation within patients of up to 6 mU/l and ranged from 3.0 mU/l to 22.6 mU/l between subjects. The mean of all steady state insulin concentrations was 9.7 mU/l. The time to maximum concentration ranged from 40.8 to 68.5 minutes and the apparent clearance ranged from 14.8 to 26.8 ml/kg/minute.

Table 3 lists the estimated glucagon PK model parameters and the calculated time to maximum concentration. The fasting steady state glucagon concentrations were similar in the range 7.6-11.6 pg/ml for all patients except patient 8 who had

Table 2. Summary of Insulin PK Model Parameters for Simulation With Range of Means and 95% CI or Mean and 95% CI.

Patient	I_b (mU/l)	t_{max} (min)	$Cl_{F,I}$ (ml/kg/min)
1	6.6-7.8 (6.0-8.3)	57.6 (50.9-64.3)	18.9 (17.3-20.6)
2	10.0-11.2 (9.1-12.0)	57.3 (48.8-65.9)	18.5 (16.1-21.2)
3	10.3-13.4 (9.7-14.0)	40.8 (37.6-44.0)	14.8 (13.6-16.1)
4	7.8-9.4 (7.4-9.9)	67.9 (63.5-72.2)	17.4 (16.6-18.3)
5	5.2-8.2 (4.8-8.8)	48.5 (44.7-52.4)	17.3 (15.7-19.0)
6	3.0-8.5 (2.3-9.4)	46.5 (41.7-51.3)	24.6 (22.9-26.3)
7	16.8-22.6 (15.6-23.6)	68.5 (60.6-76.4)	23.7 (21.3-26.4)
8	4.7-9.1 (4.4-9.6)	55.4 (49.6-61.2)	26.8 (24.8-29.0)

a concentration of 19.0 pg/ml. The absorption and elimination time constants ranged from 0.022 to 0.058 minute⁻¹ and 0.058 to 0.28 minute⁻¹, yielding a calculated time to maximum concentration of 7.5-19.1 minutes. The apparent clearance ranged from 91 to 200 ml/kg/minute.

Table 4 provides an overview of the leave-one-out cross-validation procedure of the PD model. The MPE and MAPE for the test fits are listed together with a dichotomous decision of acceptance or not using the criteria outlined in the "Pharmacodynamic Model Validation" section. Based on the MAPE during leave-one-out, we excluded four outlier datasets from further analysis and these four patients had a second round of leave-one-out including the remaining three datasets. Overall, the test fit was accepted two to three times out of three in three patients, and one to two times out of four in four patients. In patient 8 we did not accept any of the test fits even after removal of an outlier dataset. Figure 2 presents examples of PD model test fits and corresponding MPE and MAPE values of the test fits both passing and violating the acceptance criteria. In summary, the PD model successfully predicted unseen glucose data at least once in seven patients and therefore we regard the PD model as validated and suitable for simulation studies of these seven type 1 diabetes patients.

Table 5 lists the PD model parameters optimized to all nonoutlier visits in each patient with mean parameter values and 95% CI. The parameter describing the maximum EGP at steady state insulin concentration, E_{max}, ranged from 56 to 84 μmol/kg/minute. The glucagon concentration at which the effect is half maximum, C_{E50}, ranged from 141 to 436 pg/ml. Extrapolated to zero insulin and at basal glucagon concentration, the EGP ranged from 7 to 13.3 μmol/kg/minute. According to the inverse of the parameter describing the insulin sensitivity to EGP, S_E, the calculated insulin concentration at which the effect of glucagon shuts off ranged from 22 to 71 mU/l. Figures 3 and S1-S7 provide simulations of patient optimized PD model fits and data.

Discussion

We fitted simple PK models of serum insulin and plasma glucagon after SC bolus administrations of the hormones. The

Table 3. Summary of Glucagon PK Model Parameters for Simulation With Mean and 95% CI.

Patient	C_b (pg/ml)	k_1 (min^{-1})	k_2 (min^{-1})	$Cl_{F,C}$ (ml/kg/min)	t_{max} (min)
1	10.7 (9.4-12.0)	0.042 (0.036-0.048)	0.14 (0.10-0.22)	94 (83-105)	12.2
2	7.6 (6.9-8.3)	0.056 (0.052-0.062)	0.26 (0.18-0.38)	106 (96-116)	7.5
3	7.6 (5.9-9.3)	0.022 (0.018-0.028)	0.10 (0.06-0.17)	114 (96-132)	19.1
4	10.9 (9.2-12.6)	0.058 (0.011-0.313)	0.058 (NA)	159 (133-184)	17.3
5	8.7 (7.7-9.8)	0.038 (0.032-0.044)	0.19 (0.13-0.29)	200 (176-223)	10.7
6	8.9 (7.8-10.0)	0.035 (0.031-0.040)	0.28 (0.19-0.41)	125 (111-138)	8.6
7	11.6 (10.1-13.0)	0.035 (0.030-0.041)	0.25 (0.16-0.39)	136 (120-152)	9.2
8	19.0 (16.1-22.0)	0.052 (0.037-0.072)	0.090 (0.04-0.26)	91 (78-105)	14.5

simulated concentrations of insulin and glucagon were used as inputs to the PD model. We sought to validate the PD model for simulations in eight type 1 diabetes patients and succeeded in seven. Finally, we estimated the patient's individual PD model parameters.

The fitted insulin PK model assumes that all changes in serum insulin concentration are due to SC insulin dosing. This is a valid assumption as no patients had measureable endogenous insulin secretion after glucagon stimulation.[25] Patients' insulin levels are at steady state when no insulin bolus is administered.

The clinical study focused on generating data describing the effect of glucagon on glucose, and therefore only few data points describing the insulin PK were obtained. The insulin PK data were sampled very sparsely around the expected time of maximum concentration. The missing data did not allow for ML estimation of the insulin PK model. However, using literature informed prior distributions of both t_{max} and $Cl_{F,I}$ and optimizing for all four visits simultaneously we obtained reasonable fits by MAP estimation.[28,34]

As the insulin PK model was fitted to in-hospital sedentary patients, its application in patients with type 1 diabetes outside the hospital setting may be limited due to numerous factors affecting insulin absorption rate, sensitivity and bioavailability. Such factors could be accounted for by introducing time-variant model parameters, which was beyond the scope of this work.[9,37,38] Especially, differences in insulin absorption could explain the observed intrapatient variation in steady state insulin concentration despite equal basal rates at all four visits.

Patients with type 1 diabetes have a blunted glucagon response to hypoglycemia compared to healthy subjects.[39] The fitted glucagon PK model assumes that all changes in plasma glucagon concentration are due to SC dosing and that the endogenous production is constant or negligible. To verify this assumption, we determined the size of the endogenous glucagon response to hypoglycemia during the saline day and compared it to simulations of glucagon PK in each of the eight subjects (data not shown). We found that exogenous glucagon doses of 1-10 µg would equal the plasma glucagon increase to hypoglycemia. Since the endogenous glucagon response to hypoglycemia was at most one tenth of the administered dose during the glucagon days, this confirmed that the

endogenous response during these days was negligible compared to the exogenous dosed glucagon. However, the endogenous response was not negligible during the saline day and therefore the glucagon PK model was not applicable to those datasets.

The glucagon PK fit was challenged by the short time to maximum concentration combined with the uncertainty of the exact dosing time of glucagon. This could potentially result in an error in time to maximum concentration of up to ±4 minutes. However, this possible deviation has minor impact on the PD model fit when the glucagon PK fit is used as an input. Despite the dosing time uncertainty, the calculated times to maximum concentration are within reasonable range of population averages reported in the literature.[28,40] In the model by Haidar et al,[28] the glucagon absorption rate and elimination rate were identical which we only observed in patient 4. In the remaining seven patients, the elimination rate was significantly higher than the absorption rate. Moreover, having different absorption and elimination rate constants we observed a higher clearance rate. Compared to Haidar et al, we found lower basal concentration of glucagon, which could be attributed to differences in the assays for analysis of plasma glucagon concentration.[26]

Despite using informed priors for all PD model parameters, some optimized parameters are very different from the population mean and vary considerably more than originally listed in Hovorka et al.[29] However, the original reference is based on a population of only six subjects, which makes it unlikely that all true population variations were captured, and we believe, therefore, that our parameter estimates are still valid. Similarly, with a population of eight subjects, we did not fit a population model but focused on estimating parameters for each subject individually.

The limited human data on EGP response to glucagon are consistent with data from dogs.[22] As the human response to high glucagon concentrations has not been thoroughly investigated, the dog data provide best guesses of the human values. The maximum EGP due to glucagon and glucagon concentration at half-maximum effect at basal insulin average around 60 µmol/kg/minute and 300 pg/ml in dogs.[22] Our results match the reference values and therefore seem plausible.

We found that EGP at zero insulin and basal glucagon is somewhat lower than previous publications, which state

Table 4. PD Model Validation Using Leave-One-Out Cross-Validation.

Patient	Training visits	Test visit	MPE (%)	MAPE (%)	Accept? (Y/N)
1	BCD	A	−25.0	25.0	N
	ACD	B	−11.3	13.7	Y
	ABD	C	78.8	78.8	N[a]
	ABC	D	3.3	25.5	N
	BD	A	−10.3	11.1	Y
	AD	B	10.4	13.1	Y
	AB	D	4.0	21.3	N
2	BCD	A	29.1	29.8	N
	ACD	B	−18.2	18.7	N
	ABD	C	−6.3	7.5	Y
	ABC	D	6.3	10.0	Y
3	BCD	A	10.3	17.4	Y
	ACD	B	−2.3	8.6	Y
	ABD	C	23.4	24.6	N
	ABC	D	−20.1	20.1	N
4	BCD	A	−17.3	18.9	N
	ACD	B	−9.4	11.1	Y
	ABD	C	−23.6	23.7	N
	ABC	D	38.2	38.4	N
5	BCD	A	−13.4	13.4	Y
	ACD	B	−30.0	30.4	N
	ABD	C	−16.3	21.3	N
	ABC	D	74.6	74.6	N[a]
	BC	A	−1.7	4.5	Y
	AC	B	−9.8	14.1	Y
	AB	C	−7.5	17.4	Y
6	BCD	A	−23.5	24.2	N
	ACD	B	−4.5	12.0	Y
	ABD	C	59.0	59.0	N[a]
	ABC	D	−8.6	16.3	Y
	BD	A	−13.7	16.9	Y
	AD	B	16.7	17.5	N
	AB	D	4.7	15.8	Y
7	BCD	A	43.0	43.3	N
	ACD	B	−19.0	19.0	N
	ABD	C	−2.9	19.0	Y
	ABC	D	6.0	8.0	Y
8	BCD	A	−8.0	12.4	Y
	ACD	B	−32.9	33.0	N
	ABD	C	−14.5	24.2	N
	ABC	D	174.1	174.1	N[a]
	BC	A	−26.2	26.2	N
	AC	B	−24.6	24.6	N
	AB	C	42.5	42.5	N

Initially, data from three visits are used for training the model, ie, optimizing model parameters, and data from the fourth visit are used for testing the model with the optimized parameters.
[a]A test fit with MPE or MAPE exceeding 50% is considered an outlier. The outlier dataset is removed and another round of leave-one-out cross-validation is performed on the remaining three visits.

10-20 μmol/kg/minute[29] and ~30 μmol/kg/minute.[22] This might be due to the fixation of gluconeogenesis at 6 μmol/kg/
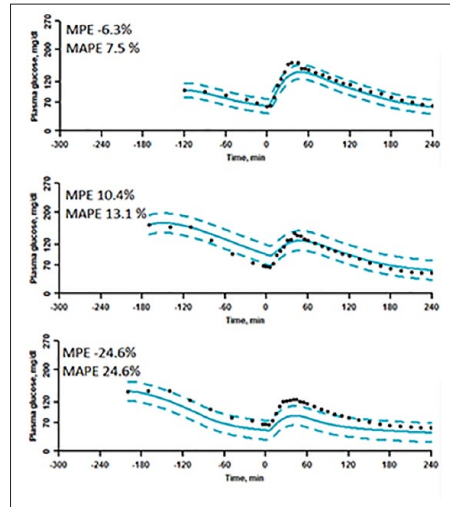

Figure 2. Examples of validation PD model fits with "good," "medium," and "bad" MPE and MAPE. Top graph is test of patient 2's visit C (accepted). Middle graph is test of patient 1's visit B (accepted). Bottom graph is test of patient 8's visit B (not accepted).

minute,[10] which is increased in subjects with poorly controlled type 1 diabetes compared to the present well-controlled patients or healthy subjects.[25,41] Assuming the proposed model of EGP is correct, the insulin concentration at which the glycogenolysis, hence the effect of glucagon, shuts off is reasonable compared to the limited publications showing glycogenolysis at various insulin concentrations.[22,42] Rizza et al found that the glucose production was suppressed by insulin beyond approximately 60 mU/l.[17] El Youssef et al found that at serum insulin concentrations beyond 40 mU/l glucagon concentrations below 450 pg/ml did not stimulate EGP.[13] Further clinical studies are needed to investigate whether high insulin concentrations completely suppress the effect of glucagon or whether the maximum EGP is still attainable though at higher glucagon concentrations.

A major limitation to some of the previously published models describing the effect of glucagon on glucose production is lack of validation.[18,21] We were able to mimic never-before-seen glucose data at least once and at most three times in seven of the eight subjects using the presented glucose PD model. We did not expect to accept the test fit of all nonoutlier datasets in each subject as the visits often described complimentary dynamics of the glucose-insulin-glucagon relationship; for instance the placebo day had very limited information on how different glucagon concentrations affects EGP as glucagon levels were

Table 5. Summary of PD Model Parameters for Simulation With Mean and 95% CI.

| ID	Data	C_{E50} (pg/ml)	E_{max} (μmol/kg/min)	F_{01} (μmol/kg/min)	$k_{12}*10^{-4}$ (min⁻¹)	$k_{a1}*10^{-4}$ (min⁻¹)	$k_{a2}*10^{-4}$ (min⁻¹)	$k_{a3}*10^{-4}$ (min⁻¹)	S_D*10^{-4} (min⁻¹/(mU/l))	S_E*10^{-4} ((mU/l)⁻¹)	S_I*10^{-4} (min⁻¹/(mU/l))
1	ABD	436 (355-517)	56.4 (51.1-61.8)	14.2 (12.9-15.5)	244 (181-330)	16 (7-35)	522 (221-1233)	215 (59-778)	1.5 (0.6-3.3)	155 (83-289)	23 (16-31)
2	ABCD	405 (339-471)	67.4 (59.3-75.5)	13.8 (12.8-14.7)	285 (223-363)	15 (7-35)	495 (236-1039)	231 (137-389)	1.2 (0.6-2.3)	334 (232-481)	19 (15-25)
3	ABCD	401 (327-475)	57.4 (49.8-65.0)	15.5 (14.2-16.8)	397 (277-568)	18 (8-42)	548 (268-1121)	327 (168-638)	1.4 (0.7-2.5)	237 (183-308)	25 (17-36)
4	ABCD	285 (226-344)	84.4 (73.9-94.8)	12.8 (11.3-14.4)	213 (157-289)	18 (9-36)	437 (183-1044)	68 (42-113)	2.0 (1.0-3.8)	415 (347-496)	18 (13-25)
5	ABC	339 (251-427)	65.4 (53.8-77.1)	12.0 (10.6-13.5)	281 (194-406)	15 (7-32)	517 (223-1201)	235 (95-586)	1.1 (0.4-2.6)	229 (127-415)	31 (20-47)
6	ABD	424 (333-515)	60.1 (46.3-74.0)	13.1 (11.7-14.5)	238 (172-330)	10 (4-22)	353 (102-1221)	74 (23-232)	2.6 (1.1-6.2)	404 (185-882)	21 (14-32)
7	ABCD	141 (96-187)	78.0 (68.9-87.1)	14.2 (12.2-16.1)	358 (252-509)	49 (23-105)	624 (319-1221)	178 (69-459)	4.4 (3.2-6.0)	140 (99-199)	21 (16-29)
8	ABC	307 (228-386)	75.3 (61.5-89.1)	13.4 (11.4-15.4)	289 (197-424)	37 (18-75)	518 (203-1324)	154 (68-348)	4.2 (2.8-6.5)	463 (377-569)	29 (20-42)
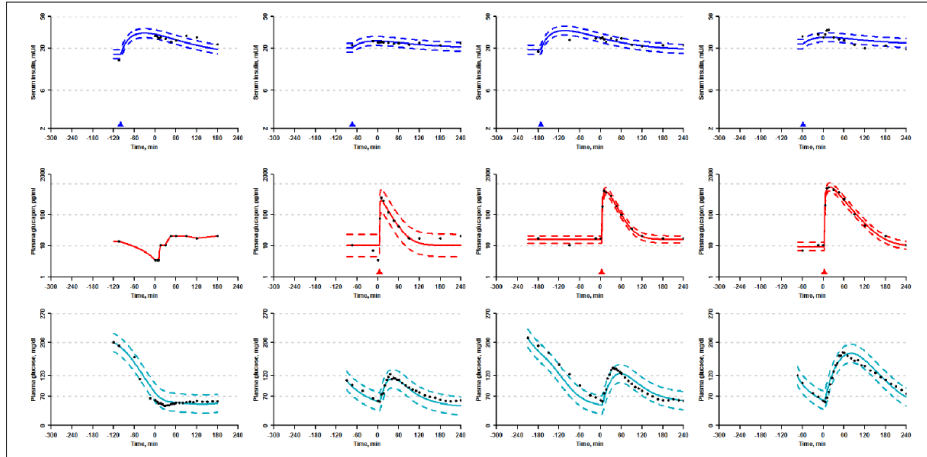
Figure 3. Data from all of patient 7's visits (left to right: visit A to D) with insulin PK model fits (top row, logarithmic y-axes) and glucagon linear interpolation or PK model fits (middle row, logarithmic y-axes) both used as inputs to the glucose PD model for simulation built with data from all four visits (bottom row). The triangles indicate dose time of the insulin and glucagon boluses, respectively.

changing very little. On the contrary, the placebo datasets were rich in information about the effects of insulin on plasma glucose. Some glucagon datasets had few observations of the effects of insulin on EGP as the plasma glucose some days reached the bolus threshold of 70 mg/dl quickly, for example, in subjects 2 and 7 shown in Figure S2 and Figure 3, respectively. As an example, this difference in data sampling can explain why it was not possible to validate the model using subject 2's visit B as the test dataset. For this particular patient, the placebo visit was stopped early and therefore does not contain much information about the insulin dynamics. Moreover, the insulin only phase of visit B lasted nearly five hours and only two hours during visits C and D. Leaving visit B out of the training dataset does not provide the model with enough information to predict the insulin dynamics present in visit B. We noted that in most cases when the test fit was not accepted there was a monotone bias in the residuals yielding almost equal values of absolute MPE and MAPE (see Table 4). This bias indicates that the test fit would either over- or undershoot compared to data and thus both insulin and glucagon dynamics of the test dataset were not well described by the training datasets. Analyzing the PD model parameters during leave-one-out in Tables S3-S10, we observed that when a test fit could not be accepted, usually one or more parameters were outside the CI obtained when fitting to all nonoutlier data. Therefore, failing to accept the test fit during a fold is not necessarily a sign of an incorrect

model structure. Rather it could emphasize that the test dataset contains unique information about the dynamics, which are not present in any of the training datasets.[43] However, in four patients one dataset was so different from the other three datasets that it had to be excluded from the final PD model estimation as it would otherwise affect the parameters and yield bad fits for all four study days.

Simulation models are rarely validated on unseen data. The only glucose model including glucagon that is currently validated and FDA approved has undisclosed parameter values and can only be accessed by payment.[19,44] We believe that this article is a step toward more openly sharing simulation models that will allow more research groups to test dual-hormone dosing strategies and control algorithms for managing diabetes before carrying out expensive simulations or clinical trials.

Conclusion

We have successfully validated a model describing the glucose-insulin-glucagon dynamics in seven type 1 diabetes subjects using leave-one-out cross-validation. We have reported model parameter sets with uncertainties for each subject, which could be used for in silico experiments. Simulations could also aid in optimizing treatment for type 1 diabetes patients such as glucagon dosing strategies for preventing hypoglycemia and tuning control strategies for an AP.

Abbreviations

AP, artificial pancreas; BMI, body mass index; BW, body weight; CI, confidence interval; EGP, endogenous glucose production; FDA, Food and Drug Administration; HbA1c, glycated hemoglobin A1c; MAP, maximum a posteriori; MAPE, mean absolute prediction error; ML, maximum likelihood; MPE, mean prediction error; ODE, ordinary differential equation; PD, pharmacodynamics; PK, pharmacokinetics; SC, subcutaneous; SD, standard deviation.

Declaration of Conflicting Interests

The author(s) declared the following potential conflicts of interest with respect to the research, authorship, and/or publication of this article: SLW is a full-time employee of Zealand Pharma. SS serves on the continuous glucose monitoring advisory board of Roche Diabetes Care and as a consultant to Unomedical. CBK is a full-time employee of Zealand Pharma and owns shares in Zealand Pharma. JJH has consulted for Merck Sharp & Dome, Novo Nordisk, and Roche. SM has served as a consultant or adviser to Amgen, Astra-Zeneca, Boehringer-Ingelheim, Bristol-Myers Squibb, Eli Lilly, Intarcia Therapeutics, Johnson & Johnson, Merck Sharp & Dohme, Novo Nordisk, Novartis Pharma, and Sanofi, has received a research grant from Novo Nordisk, and has received fees for speaking from Astra-Zeneca, Bristol-Myers Squibb, Eli Lilly, Merck, Sharp & Dohme, Novo Nordisk, Novartis Pharma, and Sanofi. KN serves as adviser to Medtronic, Abbott, and Novo Nordisk, owns shares in Novo Nordisk, has received research grants from Novo Nordisk, and has received fees for speaking from Medtronic, Roche, Rubin Medical, Sanofi, Novo Nordisk, Bayer, and Zealand Pharma. JBJ has served as a consultant for Novo Nordisk.

Funding

Supplemental Material

The supplemental materials are available at http://journals.sagepub.com/doi/suppl/10.1177/1932296817693254

References

1. Diabetes Control and Complications Trial Research Group. The effect of intensive treatment of diabetes on the development and progression of long-term complications in insulin-dependent diabetes mellitus. *N Engl J Med*. 1993;329:977-986.
2. Bátora V, Tárník M, Murgaš J, et al. The contribution of glucagon in an artificial pancreas for people with type 1 diabetes. In: *Proceedings of the 2015 American Control Conference*. Chicago, IL: IEEE; 2015:5097-5102.
3. Blauw H, van Bon AC, Koops R, DeVries JH. Performance and safety of an integrated bihormonal artificial pancreas for fully automated glucose control at home. *Diabetes Obes Metab*. 2016;18(7):671-677.
4. Haidar A, Rabasa-Lhoret R, Legault L, et al. Single- and dual-hormone artificial pancreas for overnight glucose control in type 1 diabetes. *J Clin Endocrinol Metab*. 2016;101(1):214-223.
5. Jacobs PG, El Youssef J, Reddy R, et al. Randomized trial of a dual-hormone artificial pancreas with dosing adjustment during exercise compared with no adjustment and sensor-augmented pump therapy. *Diabetes Obes Metab*. 2016;18(11):1110-1119.
6. Russell SJ, Hillard MA, Balliro C, et al. Day and night glycaemic control with a bionic pancreas versus conventional insulin pump therapy in preadolescent children with type 1 diabetes: a randomised crossover trial. *Lancet Diabetes Endocrinol*. 2016;4:233-243.
7. Haidar A. The artificial pancreas: how closed-loop control is revolutionizing diabetes. *IEEE Control Syst Mag*. 2016;36(5):28-47.
8. Kirchsteiger H, Jørgensen JB, Renard E, del Re L, eds. *Prediction Methods for Blood Glucose Concentration: Design, Use and Evaluation*. Cham, Switzerland: Springer; 2016.
9. Mansell EJ, Docherty PD, Chase JG. Shedding light on grey noise in diabetes modelling. *Biomed Signal Process Control*. 2017;31:16-30.
10. Nuttall FQ, Ngo A, Gannon MC. Regulation of hepatic glucose production and the role of gluconeogenesis in humans: is the rate of gluconeogenesis constant? *Diabetes Metab Res Rev*. 2008;24:438-458.
11. Chung ST, Haymond MW. Minimizing morbidity of hypoglycemia in diabetes: a review of mini-dose glucagon. *J Diabetes Sci Technol*. 2015;9(1):44-51.
12. Taleb N, Haidar A, Messier V, Gingras V, Legault L, Rabasa-Lhoret R. Glucagon in the artificial pancreas systems: potential benefits and safety profile of future chronic use. *Diabetes Obes Metab*. 2017;19(1):13-23.
13. El Youssef J, Castle JR, Bakhtiani PA, et al. Quantification of the glycemic response to microdoses of subcutaneous glucagon at varying insulin levels. *Diabetes Care*. 2014;37(11):3054-3060.
14. Blauw H, Wendl I, DeVries JH, Heise T, Jax T. Pharmacokinetics and pharmacodynamics of various glucagon dosages at different blood glucose levels. *Diabetes Obes Metab*. 2016;18(1):34-39.
15. Hinshaw L, Mallad A, Dalla Man C, et al. Glucagon sensitivity and clearance in type 1 diabetes: insights from in vivo and in silico experiments. *Am J Physiol Endocrinol Metab*. 2015;309(5):E474-E486.
16. Castle JR, Youssef JE, Bakhtiani PA, et al. Effect of repeated glucagon doses on hepatic glycogen in type 1 diabetes: implications for a bihormonal closed-loop system. *Diabetes Care*. 2015;38(11):2115-2119.
17. Rizza RA, Mandarino LJ, Gerich JE. Dose-response characteristics for effects of insulin on production and utilization of glucose in man. *Am J Physiol Endocrinol Metab*. 1981;240:E630-E639.
18. Herrero P, Georgiou P, Oliver N, Reddy M, Johnston D, Toumazou C. A composite model of glucagon-glucose dynamics for *in silico* testing of bihormonal glucose controllers. *J Diabetes Sci Technol*. 2013;7(4):941-951.
19. Dalla Man C, Micheletto F, Lv D, Breton M, Kovatchev B, Cobelli C. The UVA/PADOVA type 1 diabetes simulator: new features. *J Diabetes Sci Technol*. 2014;8(1):26-34.
20. Peng JZ, Denney WS, Musser BJ, et al. A semi-mechanistic model for the effects of a novel glucagon receptor antagonist on glucagon and the interaction between glucose, glucagon, and insulin applied to adaptive phase II design. *AAPS J*. 2014;16(6):1259-1270.

21. Emami A, El Youssef J, Rabasa-Lhoret R, Pineau J, Castle JR, Haidar A. Modelling glucagon action in patients with type 1 diabetes [published online ahead of print July 20, 2016]. *IEEE J Biomed Health Inform*.

22. Cherrington AD. Control of glucose production in vivo by insulin and glucagon. In: *Handbook of Physiology, the Endocrine System, the Endocrine Pancreas and Regulation of Metabolism*. New York, NY: John Wiley; 2001:759-785.

23. Wendt SL, Møller JK, Knudsen CB, Madsen H, Haidar A, Jørgensen JB. PK/PD modelling of glucose-insulin-glucagon dynamics in healthy dogs after a subcutaneous bolus administration of native glucagon or a novel glucagon analogue. *Final report* 2016-2. Kgs. Lyngby, Denmark: Technical University of Denmark, DTU Compute; 2016.

24. Wendt SL, Møller JK, Haidar A, Knudsen CB, Madsen H, Jørgensen JB. Modelling of glucose-insulin-glucagon pharmacodynamics in man. Paper presented at: IEEE EMBC 2016; August 16-20, 2016; Orlando, FL.

25. Ranjan A, Schmidt S, Madsbad S, Holst JJ, Nørgaard K. Effects of subcutaneous, low-dose glucagon on insulin-induced mild hypoglycaemia in patients with insulin pump treated type 1 diabetes. *Diabetes Obes Metab*. 2016;18(4):410-418.

26. Walsh J, Roberts R. *Pumping Insulin: Everything You Need for Success on a Smart Insulin Pump*. 4th ed. San Diego, CA: Torrey Pines; 2006.

27. Albrechtsen NJW, Hartmann B, Veedfald S, et al. Hyperglucagonaemia analysed by glucagon sandwich ELISA: nonspecific interference or truly elevated levels? *Diabetologia*. 2014;57(9):1919-1926.

28. Haidar A, Duval C, Legault L, Rabasa-Lhoret R. Pharmacokinetics of insulin aspart and glucagon in type 1 diabetes during closed-loop operation. *J Diabetes Sci Technol*. 2013;7(6):1507-1512.

29. Hovorka R, Shojaee-Moradie F, Carroll PV, et al. Partitioning glucose distribution/transport, disposal, and endogenous production during IVGTT. *Am J Physiol Endocrinol Metab*. 2002;282:E992-E1007.

30. Hovorka R, Canonico V, Chassin LJ, et al. Nonlinear model predictive control of glucose concentration in subjects with type 1 diabetes. *Physiol Meas*. 2004;25:905-920.

31. Juhl R, Møller JK, Jørgensen JB, Madsen H. Modeling and prediction using stochastic differential equations. In: Kirchsteiger H, Jørgensen JB, Renard E, del Re L, eds. *Prediction Methods for Blood Glucose Concentration: Design, Use and Evaluation*. Cham, Switzerland: Springer; 2016:183-209.

32. Madsen H, Thyregod P. *Introduction to General and Generalized Linear Models*. New York, NY: CRC Press; 2011.

33. Kristensen NR, Madsen H, Jørgensen SB. Parameter estimation in stochastic grey-box models. *Automatica*. 2004;40(2):225-237.

34. Novo Nordisk A/S. Product monograph, schedule D, NovoRapid®, insulin aspart. Updated March 11, 2016. Available at: http://www.novonordisk.ca/content/dam/Canada/ AFFILIATE/www-novonordisk-ca/OurProducts/PDF/novorapid-product-monograph.pdf. Accessed August 24, 2016.

35. Gabrielsson J, Weiner D. *Pharmacokinetic & Pharmacodynamic Data Analysis: Concepts and Applications*. 4th ed. Stockholm, Sweden: Apotekarsocieteten; 2006.

36. Owen JS, Fiedler-Kelly J. *Introduction to Population Pharmacokinetic/Pharmacodynamic Analysis With Nonlinear Mixed Effects Models*. New York, NY: John Wiley; 2014.

37. Hildebrandt P. Subcutaneous absorption of insulin in insulin-dependent diabetic patients. Influence of species, physicochemical properties of insulin and physiological factors. *Danish Med Bull*. 1991;38(4):337-346.

38. DeFronzo R, Simonson D, Ferrannini E. Hepatic and peripheral insulin resistance: a common feature of type 2 (non-insulin-dependent) and type 1 (insulin-dependent) diabetes mellitus. *Diabetologia*. 1982;23(4):313-319.

39. Arbelaez AM, Xing D, Cryer PE, et al. Blunted glucagon but not epinephrine responses to hypoglycemia occurs in youth with less than 1 yr duration of type 1 diabetes mellitus. *Pediatr Diabetes*. 2014;15(2):127-134.

40. Novo Nordisk A/S. Product monograph, GlucaGen®, glucagon. Updated June 1, 2016. Available at: http://www.paladinlabs.com/our_products/PM_GlucaGen_EN.pdf. Accessed October 6, 2016.

41. Kacerovsky M, Jones J, Schmid AI, et al. Postprandial and fasting hepatic glucose fluxes in long-standing type 1 diabetes. *Diabetes*. 2011;60:1752-1758.

42. Adkins A, Basu R, Persson M, et al. Higher insulin concentrations are required to suppress gluconeogenesis than glycogenolysis in nondiabetic humans. *Diabetes*. 2003;52:2213-2220.

43. Kreutz C, Raue A, Kaschek D, Timmer J. Profile likelihood in systems biology. *FEBS J*. 2013;208:2564-2571.

44. Kovatchev BP, Breton M, Dalla Man C, Cobelli C. *In silico* preclinical trials: a proof of concept in closed-loop control of type 1 diabetes. *J Diabetes Sci Technol*. 2009;3(1):44-55.

Technical Report 2
Simulation Studies

This appendix presents the technical report with the title "Simulating Clinical Studies of the Glucoregulatory System: *in Vivo* Meets *in Silico*" published by the Technical University of Denmark in February 2017 [21].

Simulating clinical studies of the glucoregulatory system: *in vivo* meets *in silico*

Sabrina Lyngbye Wendt[*,1,2], Ajenthen Ranjan[3,4],
Jan Kloppenborg Møller[2], Carsten Boye Knudsen[1], Jens Juul Holst[5],
Sten Madsbad[3,5], Henrik Madsen[2], Kirsten Nørgaard[3], and
John Bagterp Jørgensen[2]

[1]Department of Bioanalysis and Pharmacokinetics, Zealand Pharma,
Glostrup, Denmark
[2]Department of Applied Mathematics and Computer Science,
Technical University of Denmark, Kongens Lyngby, Denmark
[3]Department of Endocrinology, Hvidovre University Hospital,
Hvidovre, Denmark
[4]Danish Diabetes Academy, Odense, Denmark
[5]Faculty of Health and Medical Sciences, University of Copenhagen,
Copenhagen, Denmark

Version 1
January, 2017

Abstract: In this report we use a validated model of the glucoregulatory system including effects of insulin and glucagon for simulation studies in seven type 1 diabetes patients. Using simulations, we replicate the results from a clinical study investigating the effect of micro-doses of glucagon on glucose metabolism at varying ambient insulin levels. The report compares *in vivo* and *in silico* results head-to-head, and discusses similarities and differences. We design and simulate simple studies to emphasize the implications of some glucoregulatory dynamics which are ignored in most previous clinical studies: the effect of discontinuing insulin and glucose infusions prior to glucagon administration, the delayed effect of insulin, timing of data sampling, and carry-over effects from multiple subcutaneous doses of glucagon. We also use simulations to discuss two hypotheses of how insulin and glucagon might interact in influencing the glucose response. Following the simulations we propose a study design that potentially could explore if the hypotheses are true or false.
Keywords: Glucagon, Glucoregulatory system, Glucose, Insulin, Simulation

1

Preface

This technical report aims to discuss how to conduct clinical studies seeking to elucidate the dynamics in the glucoregulatory system with focus on glucagon. The discussion is based on published clinical data and simulation experiments using a newly validated glucose-insulin-glucagon model [1].

Simulation models describing insulin and glucagon pharmacokinetics and glucose pharmacodynamics are presented in the first section along with subject specific model parameters and their interpretations.

Second section presents an *in silico* replication of the highly cited study by El Youssef *et al.* from 2014 with the title "Quantification of the Glycemic Response to Microdoses of Subcutaneous Glucagon at Varying Insulin Levels" [2]. All results and graphs of the original paper are replicated using simulations. We present a comparison between the *in silico* and the *in vivo* results.

Third section describes a simulation study exploiting the ability of computer simulations to conduct infinite number of trials thereby creating smooth dose-response curves for glucagon at varying insulin levels with glucagon doses ranging from 1 μg to 10 mg. This section also discusses two possible hypotheses describing the interaction between insulin and glucagon, and suggests a study design that could evaluate the hypotheses.

Based on simulation studies and published clinical studies, fourth section discusses pearls and pitfalls for conducting clinical studies of the glucoregulatory system with focus on trials including glucagon. This last section contains a thorough discussion of the importance of clamp study designs and limitations to identify dynamics in data.

2

Abbreviations

AUC	area under the curve
AUC_{60}	AUC over 60 minutes
EGP	endogenous glucose production
HbA_{1c}	glycated hemoglobin A1c
IIR	insulin infusion rate
IQR	inter quartile range
MPC	model predictive control
PD	pharmacodynamic
PID	proportional integral derivative
PK	pharmacokinetic
SD	standard deviation
SS	steady state
SC	subcutaneous
Tmax	time to maximum concentration
T1D	type 1 diabetes

Contents

1 Simulation Model

The simulation models in this section including equations and parameter values were published by Wendt *et al.* [1]. For details on the model validation and parameter estimation the reader is kindly referred to the original publication. This section serves as a summary of the model providing the information necessary to use the model for simulations.

1.1 Insulin Pharmacokinetics Model

The insulin pharmacokinetics (PK) model is adopted from Haidar *et al.* [3] and described by equations (1)-(3).

$$\frac{\mathrm{d}X_1(t)}{\mathrm{d}t} = u_I(t) - \frac{X_1(t)}{t_{max}} \tag{1}$$

$$\frac{\mathrm{d}X_2(t)}{\mathrm{d}t} = \frac{X_1(t)}{t_{max}} - \frac{X_2(t)}{t_{max}} \tag{2}$$

$$I(t) = \frac{1}{t_{max}} \frac{X_2(t)}{W \cdot Cl_{F,I}} 10^6 + I_b \tag{3}$$

The steady state conditions of the system are both states, X_1 and X_2, equal to zero. The interpretations of the insulin PK model variables are listed in Table 1. Individual model parameter values are presented in Section 1.4.

Table 1: Interpretation of insulin PK model states, input, output and parameters.

Class	Variable	Unit	Interpretation
States	$X_1(t)$	U	insulin mass due to SC doing, in SC tissue
	$X_2(t)$	U	insulin mass due to SC dosing, in serum
Input	$u_I(t)$	U/min	insulin dose
Output	$I(t)$	mU/L	insulin concentration in serum
Parameters	I_b	mU/L	steady state insulin concentration
	t_{max}	min	time to maximum serum concentration
	W	kg	body weight
	$Cl_{F,I}$	mL/kg/min	apparent insulin clearance

5

1.2   Glucagon Pharmacokinetics Model

The glucagon PK model is adopted from Wendt *et al.* [4] and described by equations (4)-(6).

$$\frac{\mathrm{d}Z_1(t)}{\mathrm{d}t} = u_C(t) - k_1 Z_1(t) \tag{4}$$

$$\frac{\mathrm{d}Z_2(t)}{\mathrm{d}t} = k_1 Z_1(t) - k_2 Z_2(t) \tag{5}$$

$$C(t) = \frac{k_2 Z_2(t)}{W \cdot Cl_{F,C}} + C_b \tag{6}$$

The steady state conditions of the system are both states, Z_1 and Z_2, equal to zero. Table 2 lists the interpretations of glucagon PK model variables. Individual model parameter values are presented in Section 1.4.

Table 2: Interpretation of glucagon PK model states, input, output and parameters.

Class	Variable	Unit	Interpretation
States	$Z_1(t)$	pg	glucagon mass due to SC dosing, in SC tissue
	$Z_2(t)$	pg	glucagon mass due to SC dosing, in plasma
Input	$u_C(t)$	pg/min	glucagon dose
Output	$C(t)$	pg/mL	glucagon concentration in plasma
Parameters	C_b	pg/mL	steady state glucagon concentration
	k_1	min^{-1}	absorption rate constant
	k_2	min^{-1}	elimination rate constant
	W	kg	body weight
	$Cl_{F,C}$	mL/kg/min	apparent glucagon clearance

1.3   Glucose Pharmacodynamics Model

The glucose pharmacodynamics (PD) model was first developed using preclinical data from healthy dogs [4] and then tested with data from healthy humans [5]. Finally, the PD model was validated for simulations in seven type 1 diabetes patients [1]. The model structure is described by equations (7)-(13).

6

$$\frac{\mathrm{d}Q_1(t)}{\mathrm{d}t} = -F_{01} - F_R - S_T x_1(t)Q_1(t) + k_{12}Q_2(t) + G_{GG}(t) + G_{GNG} \quad (7)$$

$$\frac{\mathrm{d}Q_2(t)}{\mathrm{d}t} = S_T x_1(t)Q_1(t) - [k_{12} + S_D x_2(t)]Q_2(t) \quad (8)$$

$$G_{GG}(t) = \frac{1 - S_E x_3(t)}{1 - S_E I_b} \cdot \left((E_{max} - G_{GNG}) \frac{C(t)}{C_{E50} + C(t)} \right) \quad (9)$$

$$G(t) = \frac{Q_1(t)}{V} \quad (10)$$

$$\frac{\mathrm{d}x_1(t)}{\mathrm{d}t} = k_{a1}[I(t) - x_1(t)] \quad (11)$$

$$\frac{\mathrm{d}x_2(t)}{\mathrm{d}t} = k_{a2}[I(t) - x_2(t)] \quad (12)$$

$$\frac{\mathrm{d}x_3(t)}{\mathrm{d}t} = k_{a3}[I(t) - x_3(t)] \quad (13)$$

In equation (9), $1 - S_E x_3(t)$ is always greater than or equal to zero. Interpretations of PD model states, inputs, outputs and parameters are listed in Table 3. Subject specific model parameters are presented in Section 1.4. The steady state conditions of the model are listed in equations (14)-(18).

$$Q_{1,SS} = G_{SS} \cdot V \quad (14)$$

$$Q_{2,SS} = Q_{1,SS} \frac{x_{1,SS}}{x_{2,SS} + k_{12}} \quad (15)$$

$$x_{1,SS} = I_b \quad (16)$$

$$x_{2,SS} = I_b \quad (17)$$

$$x_{3,SS} = I_b \quad (18)$$

1.4   Model Parameters

The majority of PK and PD model parameters are subject specific and listed in Table 4. A few parameters are fixed for all subjects including the rate of gluconeogenesis, G_{GNG}, at 6 μmol/kg/min [6], and the glucose volume of distribution, V, at 160 mL/kg [7]. The renal clearance of glucose is zero unless the plasma glucose concentration exceeds 9 mmol/L in which case it is calculated as $0.003 \cdot (G - 9) \cdot V$ [8]. Similarly, the insulin independent glucose flux is calculated as $F_{01} \cdot G/4.5$ when the plasma glucose concentration falls below 4.5 mmol/L [8].

The glucose PD model was validated using leave-one-out cross-validation in seven out of eight type 1 diabetes patients. The model parameters of patient 8 are reported although the model could not be validated in this subject. Therefore, simulations in the following chapters are carried out using only subjects 1-7.

1.4   Model Parameters | *1   SIMULATION MODEL*

Table 3: Interpretation of glucose PD model states, input, output and parameters.

Class	Variable	Unit	Interpretation
States	$Q_1(t)$	μmol/kg	glucose mass per W in the accessible compartment
	$Q_2(t)$	μmol/kg	glucose mass per W in the non-accessible compartment
	$x_1(t)$	mU/L	remote effects of insulin on glucose transport
	$x_2(t)$	mU/L	remote effects of insulin on glucose disposal
	$x_3(t)$	mU/L	remote effects of insulin on glycogenolysis
Inputs	$I(t)$	mU/L	insulin concentration in serum
	$C(t)$	pg/mL	glucagon concentration in plasma
Outputs	$G(t)$	mmol/L	glucose concentration in plasma
	$G_{GG}(t)$	μmol/kg/min	glucose production due to glycogenolysis
Parameters	G_{GNG}	μmol/kg/min	glucose production due to gluconeogenesis
	C_{E50}	pg/mL	glucagon concentration yielding half of maximum EGP
	E_{max}	μmol/kg/min	maximum EGP at basal insulin concentration
	F_{01}	μmol/kg/min	insulin independent glucose flux
	F_R	μmol/kg/min	renal glucose clearance
	$k_{12} \cdot 10^{-4}$	min^{-1}	transfer rate constant from Q_2 to Q_1
	$k_{a1} \cdot 10^{-4}$	min^{-1}	insulin deactivation rate constant
	$k_{a2} \cdot 10^{-4}$	min^{-1}	insulin deactivation rate constant
	$k_{a3} \cdot 10^{-4}$	min^{-1}	insulin deactivation rate constant
	$S_D \cdot 10^{-4}$	min^{-1}/(mU/L)	insulin sensitivity of glucose disposal
	$S_E \cdot 10^{-4}$	(mU/L)$^{-1}$	insulin sensitivity of glycogenolysis
	$S_T \cdot 10^{-4}$	min^{-1}/(mU/L)	insulin sensitivity of glucose transport
	V	mL/kg	glucose volume of distribution

Table 4: Subject specific PK/PD model parameters used for simulations.

Parameter					Patient				
		1	2	3	4	5	6	7	8
W	[kg]	54	50	81	69	87	72	73	59
I_b	[mU/L]	7.3	10.6	11.7	8.7	6.6	5.5	19.7	7.4
t_{max}	[min]	57.6	57.3	40.8	67.9	48.5	46.5	68.5	55.4
$Cl_{F,I}$	[mL/kg/min]	18.9	18.5	14.8	17.4	17.3	24.6	23.7	26.8
C_b	[pg/mL]	10.7	7.6	7.6	10.9	8.7	8.9	11.6	19.0
k_1	[min^{-1}]	0.042	0.056	0.022	0.058	0.038	0.035	0.035	0.052
k_2	[min^{-1}]	0.14	0.26	0.10	0.058	0.19	0.28	0.25	0.090
$Cl_{F,C}$	[mL/kg/min]	94	106	114	159	200	125	136	91
C_{E50}	[pg/mL]	436	405	401	285	339	424	141	307
E_{max}	[μmol/kg/min]	56.4	67.4	57.4	84.4	65.4	60.1	78.0	75.3
F_{01}	[μmol/kg/min]	14.2	13.8	15.5	12.8	12.0	13.1	14.2	13.4
$k_{12} \cdot 10^{-4}$	[min^{-1}]	244	285	397	213	281	238	358	289
$k_{a1} \cdot 10^{-4}$	[min^{-1}]	16	15	18	18	15	10	49	37
$k_{a2} \cdot 10^{-4}$	[min^{-1}]	522	495	548	437	517	353	624	518
$k_{a3} \cdot 10^{-4}$	[min^{-1}]	215	231	327	68	235	74	178	154
$S_D \cdot 10^{-4}$	[min^{-1}/(mU/L)]	1.5	1.2	1.4	2.0	1.1	2.6	4.4	4.2
$S_E \cdot 10^{-4}$	[(mU/L)$^{-1}$]	155	334	237	415	229	404	140	463
$S_T \cdot 10^{-4}$	[min^{-1}/(mU/L)]	23	19	25	18	31	21	21	29

2   The Study by El Youssef *et al.*

In this section, using simulations we aim to replicate the clinical study by El Youssef *et al.* published in Diabetes Care November 2014 with the title "Quantification of the Glycemic Response to Microdoses of Subcutaneous Glucagon at Varying Insulin Levels" [2].

2.1   Study Design

The study by El Youssef *et al.* [2] included 11 type 1 diabetes (T1D) patients (5 females, age IQR: 36.5-46.0 years, BMI IQR: 23.0-31.1 kg/m^2, HbA$_{1c}$ IQR: 7.0-8.2%). The patients participated in three study days of each 10 hours duration with constant intravenous insulin infusion rate (IIR) of either low, medium or high. Average results during low, medium and high IIR are based on 10, 9, and 10 subjects, respectively. Glucose infusion rates were controlled using a proportional integral derivative (PID) controller aiming at a blood glucose concentration of 85 $\pm$ 20 mg/dL. When blood glucose read below 60 mg/dL the controller regulated the glucose infusion rate every five minutes, otherwise every ten minutes. After an initial two hours run-in period the subjects received the first glucagon bolus. They received the second glucagon bolus after another two hours until a total of four glucagon boluses were delivered and observed for the following two hours. The glucagon boluses were delivered in a pseudo-random order by varying the initial dose, but keeping the order: 25 μg, 75 μg, 125 μg, and 175 μg (25-75-125-175, 75-125-175-25, 125-175-25-75, 175-25-75-125). Each subject received the same pseudo-random order of glucagon boluses during each study day.
The study used regular human insulin (Humulin R, Eli Lilly and Company) and glucagon (GlucaGen, Novo Nordisk).

2.2   Simulation Study Details

In the *in silico* study we used the validated patient specific PK/PD models describing seven T1D patients (4 females, age range: 19-64 years, BMI range: 20.0-25.4 kg/m^2, HbA$_{1c}$ range: 6.1-7.4 %) presented in Section 1 [1]. All virtual subjects participated in experiments with low, medium and high IIRs. We followed the study design of the clinical study described in Section 2.1. We allowed initialization of patients at steady state (SS) at the beginning of the two hours run-in period by solving the patient specific equations for SS.
The insulin and glucagon PK/PD model parameters were based on a study using insulin aspart (NovoRapid, Novo Nordisk) and glucagon (GlucaGen, Novo Nordisk). As the IIRs are constant during the experiment the possible differences in insulin PK between Humulin R and NovoRapid are not confounding the study. Differences in insulin PD effects are relevant, however, we assume that the insulins have identical PD effects.

2.2.1   Determining Infusion Rates

The low and medium IIR were chosen based on individual basal infusion rates and the high IIR was fixed at 0.05 U/kg/h for all subjects. In the clinical study they used either

0.01 U/kg/h or the patient's average daytime basal rate as the lowest IIR, but the latter information was not available in the simulation study. Therefore, the individual low IIR was maximized to either 0.01 U/kg/h or the infusion rate yielding an insulin level equal to one and a half times the fasting serum insulin concentration. The medium IIR was chosen halfway between the low and high IIR.

The SS glucose infusion rate was calculated by solving individual glucoregulatory models at SS given the pre-specified insulin infusion rate.

2.2.2   Proportional Integral Derivative Controller

We implemented a simple proportional integral derivative (PID) controller with clipping to control the blood glucose concentration by adjusting the glucose infusion rate, as listed in equations (19)-(22).

$$e_k = G_{SS} - G_k \tag{19}$$

$$I_k = I_{k-1} + k_i \cdot \Delta t \cdot e_k \tag{20}$$

$$\mathrm{d}e_k = \frac{e_k - e_{k-1}}{\Delta t} \tag{21}$$

$$U_k = \max(0, U_{SS} + k_p \cdot e_k + I_k + k_d \cdot \mathrm{d}e_k) \tag{22}$$

G_{SS} is the glucose concentration at SS (set point of 85 mg/dL), G_k is the kth glucose observation, and e_k is the deviation from set point of the kth observation. I_k is the discretization of the integral of errors until k, calculated as the sum of the previous integral of errors, I_{k-1}, and the current integral of error weighted by k_i. $\mathrm{d}e_k$ is the discretization of the error derivative at k calculated by the backward difference. The updated glucose infusion rate, U_k, is the sum of the SS glucose infusion rate, U_{SS}, the error weighted by k_p, the integral of errors, and the error derivative weighted by k_d, unless the sum is negative, in which case the glucose infusion rate is set to zero. We used $k_p = 4$, $k_i = 1$, and $k_d = $ -2.

2.2.3   Calculation of Endogenous Glucose Production

The endogenous glucose production (EGP) due to glucagon was directly calculated using the PD model. EGP was baseline-corrected by subtracting the EGP level at the time of the most recent glucagon dose to avoid carry-over effects from previous glucagon doses or from baseline production maintained by the constant insulin infusion and SS glucagon concentration.

$$EGP_{Corrected}(t) = EGP(t) - EGP(t_{Dose,n}) \quad n = 1,...,4 \tag{23}$$

The baseline-corrected EGP can thus become negative when current EGP is less than at the time of the most recent glucagon dose. However, it can not be more negative than the difference between EGP at SS and EGP at the time of the most recent glucagon dose.

2.3 Results and Discussion

2.3.1 Insulin and Glucose Infusion Rates

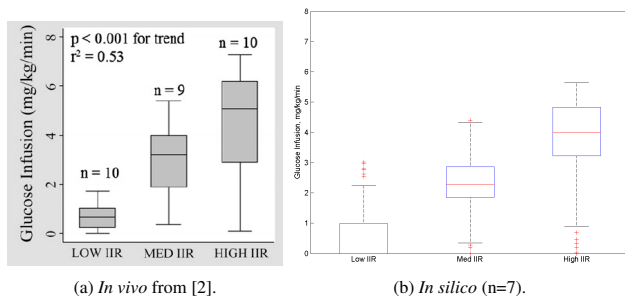(a) *In vivo* from [2].   (b) *In silico* (n=7).

Figure 1: Box plot of glucose infusion rate (mg/kg/min) across all studies, by insulin infusion group.

Table 5 compares the reported *in vivo* and simulated *in silico* average insulin and glucose infusion rates at low, medium and high IIRs. At a first glance, insulin infusion rates are very similar in the two studies based on averages and medians. However, the virtual study contained one patient (no. 7) having a very high basal IIR yielding a low IIR of 0.042 U/kg/h and a medium IIR of 0.046 U/kg/h. Ultimately, there was little differences between the three IIRs in this subject and therefore only minor differences in responses during the various insulin infusion rates. The high basal IIR indicates that the subject is not very sensitive to insulin and therefore the response to glucagon during the high IIR was little attenuated by the insulin level. No formal test was performed to exclude this subject. However, the low IIR and medium IIR are more than two standard deviations from the mean infusion rates reported *in vivo* which justifies the exclusion of the subject from the analysis of EGP response to glucagon at various insulin levels.

Table 5: Summary of insulin and glucose infusion rates *in vivo* and *in silico*. Infusion rates are reported as mean $\pm$ SD and median [IQR]. L = low, M = medium, H = high.

	IIR	*In Vivo*		*In Silico*	
Insulin	L	0.016 ± 0.006	0.014	0.018 ± 0.011	0.014
rate	M	0.032 ± 0.003	0.03	0.034 ± 0.006	0.032
U/kg/h	H	0.05 ± 0.00	0.05	0.05 ± 0.00	0.05
Glucose	L	0.7 ± 0.5	0.6 [0.2-1]	0.5 ± 0.8	0.0 [0.0-1.0]
rate	M	2.9 ± 1.3	3.2 [1.9-4]	2.1 ± 0.9	2.3 [1.9-2.9]
mg/kg/min	H	4.5 ± 2	5.1 [2.9-6.2]	3.8 ± 1.2	4.0 [3.2-4.8]

Summary statistics of glucose infusion rates are similar although the interquartile range

is narrower *in silico* than *in vivo*. This difference is also evident in Figure 1 showing smaller boxes but several outliers *in silico* compared to *in vivo*. Looking at the glucose infusion rates over time in Figure 2b, we observe a difference in the response to glucagon, thus the amount of decrease in glucose infusion rate compared to Figure 2a. Moreover, the glucose infusion rate at SS is slightly lower during medium and high IIRs. To the authors it is not clear how the large decrease in glucose infusion rate during high IIR displayed in Figure 2a relates to the small EGP area under the curve (AUC) displayed in Figure 8a.
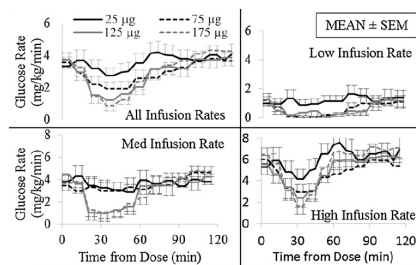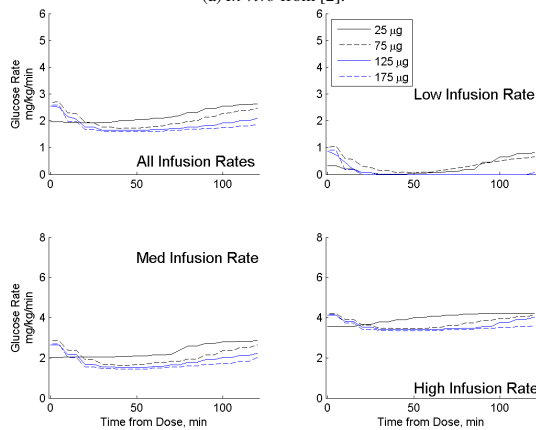

(a) *In vivo* from [2].

(b) *In silico* (n=7).

Figure 2: Mean glucose infusion (mg/kg/min) over time by insulin infusion rate group and glucagon dose: top left, all insulin infusion rates together; top right, bottom left, and bottom right, low, medium, and high insulin infusion rates, respectively.

2.3.2   Insulin and Glucose Concentrations

Table 6 compares reported and simulated serum insulin concentrations and plasma glucose concentrations after the two hours run-in period. The distribution of serum insulin levels are very similar in the clinical and virtual studies as seen in Figure 3. This confirms that the insulin PK model is applicable despite not being estimated from optimally sampled data as described in [1]. On the contrary, the plasma glucose concentrations differ. The glucose concentration is lower with less variation during the *in silico* experiment especially during low and medium IIR. This is probably due to differences in the PID controller settings achieving better control in the virtual population than in real subjects. Moreover, using the SS equations of the individual subjects we calculated the exact needed glucose infusion rate to counter the IIR. This is unfortunately not possible in real life. The plasma glucose concentration is equally well controlled during the high IIR which is probably due to the attenuated EGP response to glucagon.

Table 6: Serum insulin and plasma glucose concentrations *in vivo* and *in silico*. Concentrations are reported as mean $\pm$ SD and median [IQR]. L = low, M = medium, H = high.

	IIR	*In Vivo*		*In Silico*	
Serum	L	17.6 ± 13.0	11.0 [9.7-24.6]	15.0 ± 7.2	13.1 [10.2-17.1]
insulin	M	29.1 ± 8.9	28.1 [25.5-31.5]	29.7 ± 4.8	30.5 [28.0-31.9]
mU/L	H	46.0 ± 12.5	41.7 [37.5-46.8]	44.4 ± 7.8	45.1 [37.4-48.1]
Plasma	L	150.8 ± 68.3		100.5 ± 28.0	
glucose	M	92.9 ± 21.3		83.6 ± 14.6	
mg/dL	H	88.0 ± 16.0		83.4 ± 13.4	

(a) *In vivo* from [2].   (b) *In silico* (n=7).
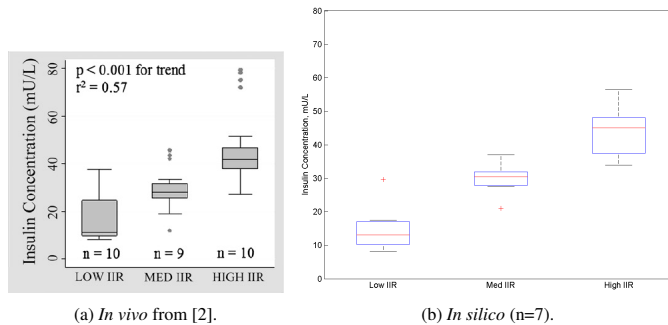
Figure 3: Box plot of serum insulin levels (mU/L) at low, medium, and high insulin infusion rates.

2.3.3   Glucagon

Table 7 compares time to maximum concentration (Tmax) of glucagon between the clinical and virtual studies stratified by glucagon dose. In both studies, Tmax did not dependent on glucagon dose. We found smaller Tmax with smaller variation *in silico* than *in vivo*. One should keep in mind that blood was only sampled every 10 minutes in the clinical study whereas data used for estimating glucagon PK model parameters for simulations were sampled every 5 minutes. Blood sampling every 10 minutes does not allow for accurate determination of glucagon's Tmax.

Comparisons of glucagon AUCs in Figure 4 and concentration time profiles in Figure 5 to the *in vivo* findings should be made with caution as absolute glucagon concentration highly depends on the assay [9]. Moreover, the *in vivo* study measured glucagon in serum whereas the *in silico* study simulated glucagon in plasma. Overall, *in silico* glucagon levels seem more variable, although with clearly separated average PK profiles for each dose.

Figure 5a and 5b show that the plasma glucagon concentration is still above SS two hours after most glucagon doses. Therefore, repeating glucagon dosing after only two hours will likely introduce some carry-over effects from the previous dose, even when baseline-corrected at the time of dose.

Table 7: Glucagon Tmax.

	Dose	*In Vivo*	*In Silico*
	25 μg	23.2 ± 13.5	11.1 ± 3.5
Glucagon Tmax	75 μg	17.1 ± 8.1	12.1 ± 4.3
min	125 μg	19.6 ± 6.1	12.1 ± 4.3
	175 μg	20 ± 9.6	12.1 ± 4.3

(a) *In vivo* from [2].   (b) *In silico* (n=21).
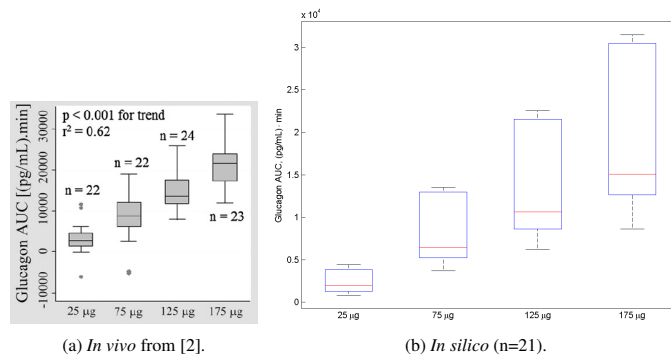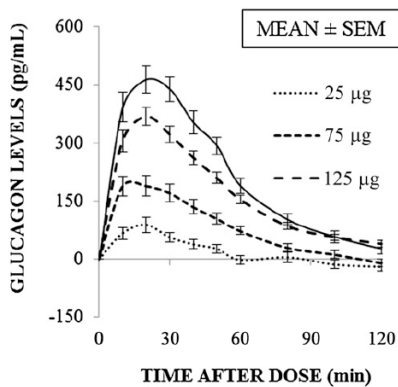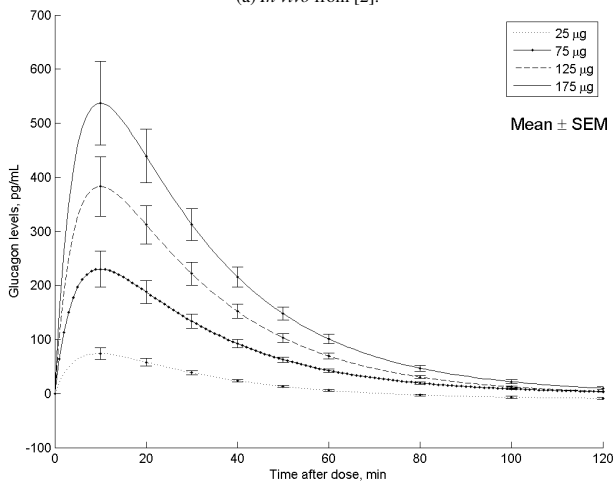
Figure 4: Box plot of glucagon plasma level AUC over 60 min, stratified by dose.

15

(a) *In vivo* from [2].

(b) *In silico* (n=21).

Figure 5: Mean incremental change in glucagon plasma levels (baseline corrected at time = 0).

2.3.4 Endogenous Glucose Production

The results in the following section highly depends on the method used for calculating EGP. In the *in vivo* study they derived the EGP from tracer data by fitting a two-compartment model. In the *in silico* study we calculated the EGP directly from the model description.

As mentioned in Section 2.3.1, one patient was considered an outlier because of nearly no difference in IIRs and was excluded from the following analysis of EGP due to glucagon at various insulin levels.

Figure 6b replicates Figure 6a with many similarities but also some differences. Most importantly, the magnitudes of average peak EGP to the four glucagon doses are similar. The EGP increase appears to be more rapid *in silico* than *in vivo* yielding a faster Tmax, which can be partly explained by the faster glucagon Tmax. However, with the sampling of every ten minutes the observed Tmax could be anywhere between 10-30 minutes and the simulated Tmax could be between 0-20 minutes (the average is in fact 12 minutes). If the true Tmax of EGP in response to glucagon is between 10-20 minutes, this fits with both the observed and simulated results.

The *in vivo* estimated EGP returned fast to baseline and after 60 minutes it was below the production before injection of the preceding glucagon bolus. The simulated EGP has slower return to baseline and we only observe slightly negative values after the lowest glucagon dose.

The average EGP over the first 60 minutes is somewhat higher *in silico* than *in vivo* as visualized in Figure 7b compared to Figure 7a. This difference is expected based on the simulated slower return to baseline just described. The simulated averages are however within the standard error of measurement of the observed data.

Perhaps the most interesting graph is Figure 8a which is replicated by simulation in Figure 8b. The averages of the simulated data are different from the observed averages. However, considering the standard error of measurement of both datasets the simulated data is not different from the observed data. The EGP responses to doses of glucagon during medium IIR were very similar to the EGP responses during low IIR in the measured data, whereas we observe a difference between the responses during the two IIRs when simulating the experiments. We also find a small increase in response to increasing glucagon boluses even at high IIR which is not pronounced in the original observed data. In general, the standard error of measurements are smaller *in silico* than *in vivo*.

Figure 9b is a replication of Figure 9a but without extrapolation. The original graph shows the actual data in the dose-range of 25-175 μg glucagon and extrapolates the presumed trends down to 1 μg and up to 10 mg. Note, this is a wild extrapolation with no data to support it. Within the data-range the simulated results match the observed results although the simulated EGP at low IIR tends to be higher than the observed. Having only four points very closely spaced on a log-scale, a single point can largely influence the overall interpretation of the curves.

2.3   Results and Discussion   2   THE STUDY BY EL YOUSSEF ET AL.
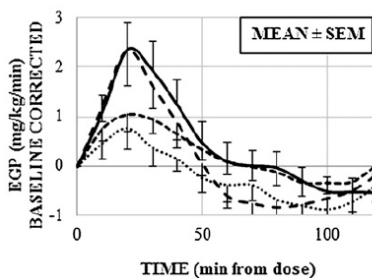
(a) *In vivo* from [2].
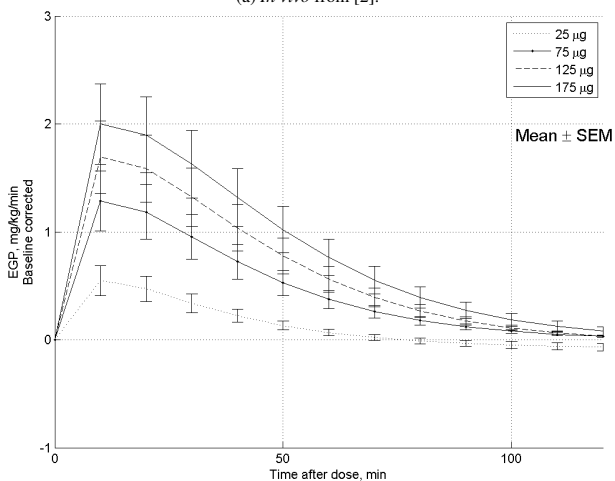
(b) *In silico* (n=6).

Figure 6: Time profiles of calculated EGP by glucagon dose, baseline corrected for EGP at the time of dose.

(a) *In vivo* from [2].   (b) *In silico* (n=18).
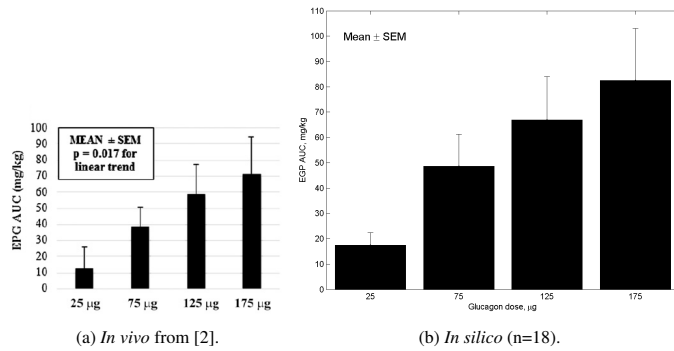
Figure 7: Mean EGP AUC over 60 min after the dose.

(a) *In vivo* from [2].   (b) *In silico* (n=6).
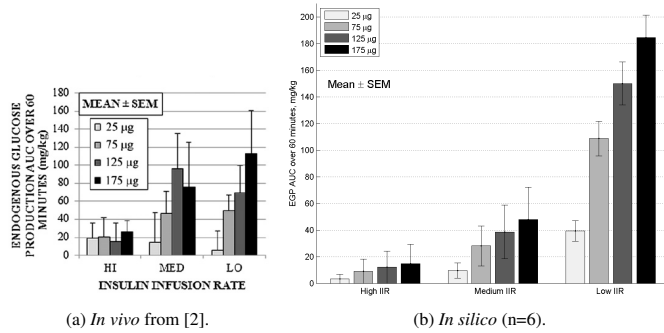
Figure 8: Mean EGP AUC separated by glucagon dose and insulin infusion rate.

19

2.3   Results and Discussion   *2   THE STUDY BY EL YOUSSEF ET AL.*

(a) *In vivo* from [2].

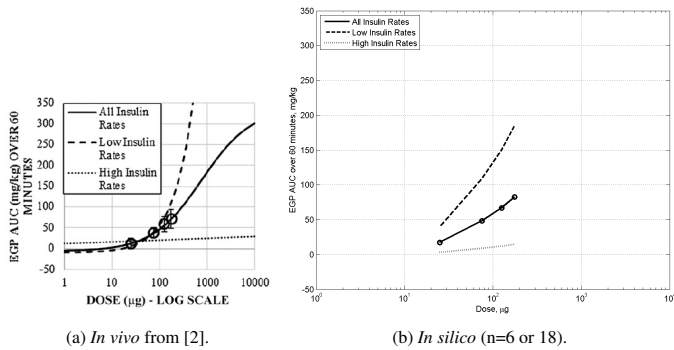(b) *In silico* (n=6 or 18).

Figure 9: Dose-response curve across all doses, and for low and high insulin infusion rate experiments, estimated from simulated data.
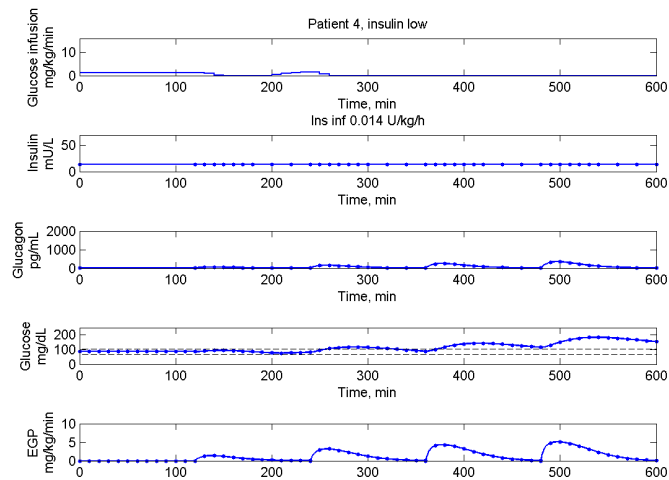
Figure 10: Example of simulated raw data from patient 4 during the low IIR with first bolus being 25 μg. Notice that the blood glucose concentration and glucose infusion rate do not return to SS before the next glucagon bolus is administered.

2.3.5   Examples of Simulated Raw Data

Figures 10 and 11 show examples of raw data from the simulation study. The points mark blood sampling times during the *in vivo* study.

The first figure presents data during low IIR and reveals that the blood glucose level cannot be kept within ± 20 mg/dL of the set point at all times. Especially after the higher doses of glucagon the blood glucose exceeds the upper limit. The graph also reveals that the glucose infusion rate is zero during most of the experiment. The explanation to this observation is that during low IIR the glucose infusion rate needed to maintain SS is equally low and cannot be lowered sufficiently after the glucagon boluses to maintain the blood glucose within the boundaries. Moreover, the plasma glucose concentration and glucose infusion rate do not return to SS before the next glucagon bolus administration.

The second figure shows data during medium IIR where the glucose infusion rate is never zero although decreased in response to glucagon boluses. The blood glucose is mostly kept within the boundaries.

The raw data from the study by El Youssef *et al.* [2] are not available, making it im-

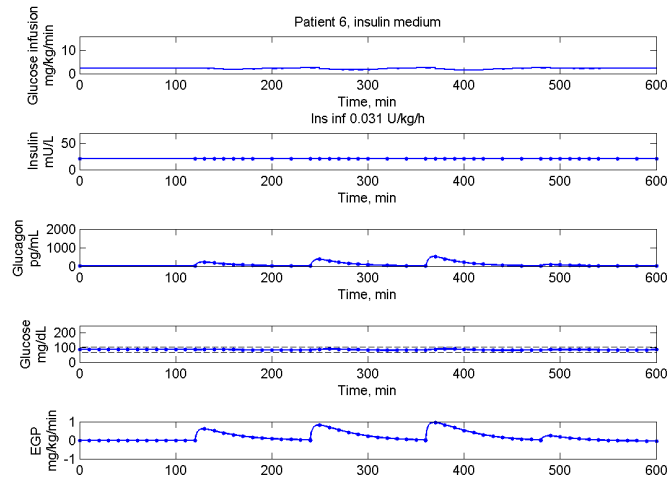*2.3   Results and Discussion*   *2   THE STUDY BY EL YOUSSEF ET AL.*

Figure 11: Example of simulated raw data from patient 6 during the medium IIR with first bolus being 75 μg. Notice how the glucose infusion is regulated to control the blood glucose close to the set point.

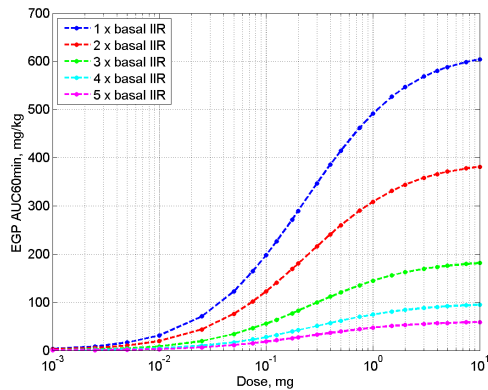possible to compare our examples to actual data.

22

Figure 12: Simulated average of seven T1D patients' dose-response curves of glucagon boluses ranging from 1 μg to 10 mg at various insulin levels expressed as multiples of the basal IIR.

3   Dose-Response Studies

In this section, we demonstrate the advantage of using simulations to conduct large cross-over studies that would not be feasible in real life. Moreover, we use simulations to design guidelines for realistically sized studies that, if the simulation model is correct, will provide the same information as the large *in silico* study, while exposing the patients to a limited number of experiments.

3.1   Study Design

The *in silico* study included seven T1D virtual patients [1], that each underwent 115 cross-over study days. Model equations and subject specific model parameters are listed in Section 1. At each study day, the IIR was constant at either 1, 2, 3, 4, or 5 times the basal IIR and the glucose infusion rate controlled every five minutes as described previously in Section 2.2.2 to maintain a glucose clamp of 5 mmol/L. After 60 minutes SS run-in period, a glucagon bolus was administered and simulation continued till 5 hours after the bolus. We simulated the effect of the following glucagon boluses: 1 μg, 2.5 μg, 5 μg, 10 μg, 25 μg, 50 μg, 75 μg, 100 μg, 125 μg, 175 μg, 200 μg, 300 μg, 400 μg, 500 μg, 750 μg, 1 mg, 1.5 mg, 2 mg, 3 mg, 4 mg, 5 mg, 7.5 mg, and 10 mg.

3.2   Results and Discussion

The EGP AUCs over 60 minutes (AUC_{60}) were calculated as described in Section 2.2.3. The average EGP AUC_{60} for each dose stratified by IIR were calculated and plotted in Figure 12. The response to glucagon doses below approximately 25 μg are very similar independent of IIR. However, with increasing glucagon doses the curves for each IIR separate. The higher the IIR, the less response to a glucagon bolus. Small increases in glucagon dose during low IIR increase the response significantly although it seems to saturate for some glucagon dose.

The results in Figure 12 represent classical dose-response curves and can be described mathematically by the Michaelis-Menten equation:

$$EGPAUC_{60min} = R_{max} \cdot \frac{Dose}{ED_{50} + Dose} \tag{24}$$

R_{max} is the maximum response and ED_{50} is the dose yielding the half-maximum response. The fitted R_{max} and ED_{50} for each IIR are summarized in Table 8. The ED_{50} does not seem to depend on the insulin level. On the contrary, R_{max} is highly dependent on the insulin level according to Table 8. This observation is expected, as the model used for simulations describes how insulin modulates the maximum achievable EGP response to glucagon, but does not influence the concentration yielding half-maximum response.

Table 8: Fitted parameters for dose-response relationship between glucagon and EGP at multiples of the average basal IIR.

IIR x basal	R_{max}, mg/kg	ED_{50}, mg
1	609	0.220
2	385	0.226
3	183	0.244
4	96	0.256
5	59	0.237

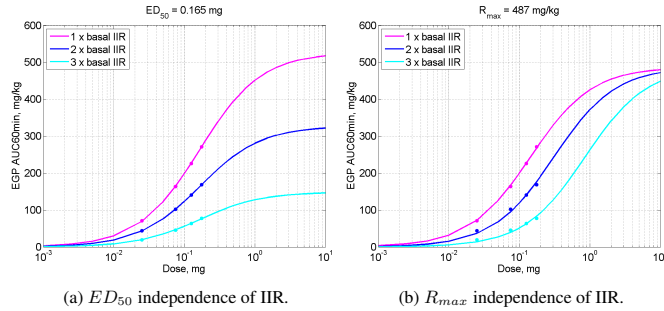(a) ED_{50} independence of IIR.   (b) R_{max} independence of IIR.

Figure 13: Fitted dose response curves when using doses of 25, 75, 125, and 175 μg as in the study by El Youssef *et al.* [2] assuming independence of insulin for either ED_{50} or R_{max}.

3.3   Dose Selection for an *in Vivo* Study

There is speculations to how the ambient insulin level affects the EGP response to glucagon. Two hypothesis are proposed:

- insulin level influences the maximum response to glucagon, R_{max}

- insulin level influences the glucagon dose at which half-maximum response is achieved, ED_{50}

The hypotheses could be examined by carrying out a smaller *in vivo* study. However, the glucagon doses must be carefully chosen to make sure to capture the essential parts of the dose response curve. If all tested doses are below the true ED_{50} both hypotheses would describe the data equally well. This pitfall is illustrated in the following example.

The *in silico* study just described in Section 3.1 was inspired by the results presented in Figure 9 in Section 2.3.4. Assuming the *in vivo* study was carried out again with the same glucagon doses of 25, 75, 125, and 175 μg at one to three times the basal IIR, would one be able to decide which parameter in equation (24) insulin affects?
To answer this question, we simulated the small study and fitted the parameters of (24) twice; first assuming ED_{50} was constant across insulin levels and then assuming R_{max} was constant across insulin levels. The results are presented in Figure 13. Because the four doses are within a narrow dose range and all doses are below the simulated "true" ED_{50}, both hypotheses fit the simulated data equally well. Although the case with equal ED_{50} represents the simulated "truth", the commonly identified ED_{50} is much lower than the parameter value presented in Table 8.
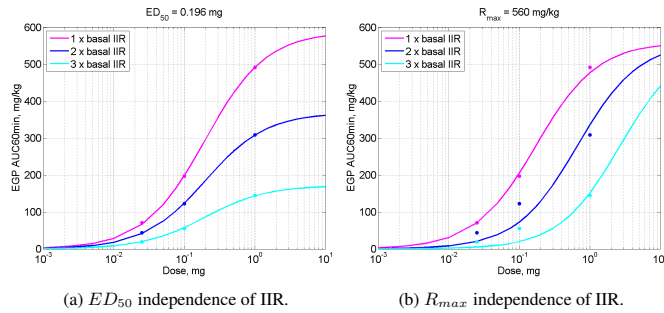
(a) ED_{50} independence of IIR.   (b) R_{max} independence of IIR.

Figure 14: Fitted dose response curves when using SC glucagon doses of 25, 100, and 1000 μg assuming independence of insulin for either ED_{50} or R_{max}.

If the glucagon doses had been distributed across a larger dose range encompassing the "true" ED_{50}, would it then be possible to determine how insulin affects EGP? Realistically, one can not administer more than 1 mg glucagon as a SC bolus injection which causes some limitations to the maximum possible dose range in an *in vivo* study. We simulated a small realistic study with three SC glucagon boluses of 25 μg, 100 μg, and 1 mg at one to three times the basal IIR. We then fitted (24) assuming either ED_{50} or R_{max} constant and independent of the ambient insulin level. Figure 14 presents the results using the model analyzed in Section 3.2 where ED_{50} is constant and independent of the ambient insulin level. The graphs visualize a clear difference in the fitness of the two hypotheses making one more plausible than the other; that ED_{50} does not depend on ambient insulin levels, but that R_{max} does. Moreover, the identified common ED_{50} is similar although a bit lower than the values listed in Table 8.

If this study was to be carried out in real life, biological variation between subjects might be dominating making it difficult to determine which hypothesis to accept and which to reject. Instead of relying on the inter-subject variation being low, one could fit (24) to data from individual subjects and hopefully reach the same conclusion in all subjects. The individually confirmed hypothesis could then be transferred to the population mean.

4   Pearls & Pitfalls

This section focuses on the *DOs* and *DON'Ts* when conducting clinical studies of the glucoregulatory system with focus on experiments involving glucagon. The points will be exemplified through simulations and references to literature. We hope that this section serves as an inspiration to researchers who are planning *in vivo* studies of the glucoregulatory system.

4.1   Glucose Clamps

The blood glucose clamp is a procedure used to maintain the same glucose level throughout an experiment either hypoglycaemic (below normal), euglycaemic (normal), or hyperglycaemic (above normal). The purpose of clamping the blood glucose is to eliminate the influence of varying glucose levels during an experiment where glucose is believed to affect the investigated mechanism. As an example, the glucose clamp procedure could be used during a gastric emptying study to eliminate the negative feedback mechanism between blood glucose concentration and gastric emptying rate [10].

The glucose clamp can be controlled using intravenous (IV) infusions of insulin and glucose. Somatostatin may be infused to inhibit endogenous production of hormones like insulin and glucagon in healthy subjects. The glucose regulating hormones are then clamped at continuous rates and as a minimum clamped at the basal rates to substitute for baseline concentrations. Somatostatin may not be necessary in clamp studies when investigating effects of exogenous supraphysiological glucagon doses in patients with type 1 diabetes having no endogenous insulin production.

4.1.1   Glucose Level and Glucose Infusion

An *in vivo* study by Hinshaw *et al.* points to that the glucose level does not influence the effect of glucagon [11]. However, Cherrington advocates there is an inhibitory effect of hyperglycemia on EGP [12]. Therefore, we recommend that the blood glucose concentration is kept close to a set point throughout a clamp experiment involving glucagon to minimize potential influence of the blood glucose concentration on EGP.

The simplest and fastest way to control the glucose level during a clamp is through IV glucose infusion. The glucose infusion can be controlled automatically using various controllers based on PID or Model Predictive Control (MPC). In Section 2.3.5 we demonstrated that a simple PID controller was sufficient to maintain the blood glucose close to a predefined set point while administering glucagon. Moreover, a simple PID controller is easy to implement and may assist investigators in keeping the blood glucose close to the predefined set point level. This is however only possible in cases when the insulin and glucose infusions are sufficiently high to allow for the glucose infusion to be reduced corresponding to the EGP contribution from the glucagon bolus.

4.1.2   Insulin Level and Insulin Infusion

Glucose clamps are not recommended to be controlled by IV insulin infusion although it occurs. Studies have showed that high insulin levels during euglycaemia suppress the

27

4.1   Glucose Clamps   *4   PEARLS & PITFALLS*
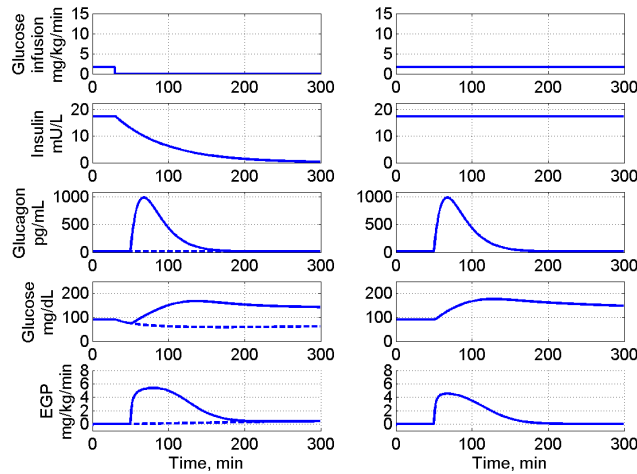

Figure 15: *In silico* demonstration of the dynamics when stopping or continuing IV insulin and glucose infusion during a clamp study in subject 4. Blood glucose was clamped at 5 mmol/L by twice the basal IIR and constant glucose infusion. After 30 minutes SS, glucose and insulin infusions were stopped (left column) and 20 minutes after either no bolus (dashed line) or a 0.5 mg SC glucagon bolus (solid line) was administered. In a different scenario, the insulin and glucose infusions continued throughout the study and a 0.5 mg SC glucagon bolus was administered (right column).

effect of glucagon on EGP [2, 13]. In Section 2 we verified that our simulation model achieved similar results as obtained *in vivo* by El Youssef *et al.* [2]. Should the insulin infusion then be kept constant throughout a clamp experiment? Yes. In the following we demonstrate *in silico* how much insulin levels influence the response to glucagon.

The first *in silico* study design is inspired by Blauw *et al.* [14] to demonstrate that it is difficult to interpret the glucose response to glucagon when too many dynamics influence the response. This situation is illustrated in Figure 15 by simulations and explained in the caption. When insulin and glucose infusions are stopped during a clamp procedure, the immediate response is a drop in glucose levels both due to the lack of glucose infusion and because the effect of insulin persists after the infusion is stopped. Although the glucose responses to glucagon in Figure 15 look fairly similar, more EGP is produced when the infusions are stopped as measured by the AUC. The increased EGP is hiding the drop in glucose that would have been seen if no glucagon bolus was

administered. Even when no glucagon bolus is administered the EGP increases slightly after infusion stop of insulin and glucose because of the fading insulin level.

It should be noted, that the insulin clearance parameters were estimated from data following SC insulin administration rather than IV administration, which could underestimate the actual clearance since it is limited by the slow and variable SC absorption.

The second *in silico* study design explores what happens if one uses insulin to control a glucose clamp rather than glucose. The blood glucose of a patient undergoing a glucose clamp responds immediately to the changes in the glucose infusion whereas the effect of insulin is delayed. An example to illustrate the delayed effect of insulin is demonstrated in Figure 16 by simulations and explained in the caption. Although the same glucagon bolus of 0.5 mg was given at the same insulin concentration, the responses were different - the larger the prior SC insulin bolus, the smaller response to glucagon. However, not all virtual patients seem to have as pronounced delayed response to insulin as in this example. The size of the delay highly depends on the parameter k_{a3} in the PD model which represents the rate constant of remote insulin action on EGP, see Table 4 in Section 1.4.

The simulated examples show that the insulin level highly influences the EGP response to glucagon and the effect of insulin can be delayed.

4.2 Dynamics in Data

A model can only be expected to describe dynamics present in the data used for model development and parameter estimation, if data is sampled sufficiently. To correctly estimate Tmax after a bolus administration in a PK model, data must be sampled densely around Tmax. If Tmax of a compound is expected to be 50 minutes, and no samples are collected the first two hours after dose administration, it is practically impossible to determine Tmax without inferring prior knowledge. More importantly, if Tmax is very short the exact notation of the dosing time is absolutely necessary in order to fit a meaningful PK model to data.

Furthermore, factors influencing the model parameters can not be included in the description of the parameters if the factors do not vary in the training dataset. As an example, exercise and stress are long known to alter the insulin sensitivity, and recently Ranjan *et al.* found that diet might influence the response to glucagon [15]. None of these factors are accounted for in the glucose PD model used for simulations throughout this report [1]. Moreover, the model does not include a feedback mechanism of the glucose levels to the endogenous production of insulin and glucagon.

4.2.1 Identifying Steady State

As described, the final fitted model is limited by the data used for estimating the model parameters. Thus identifying the correct steady state can be difficult if the data do not contain much information thereof. Figure 17 illustrates that the PD model described in [1] does not estimate the correct steady state. Initializing patient 7 at euglycaemia with
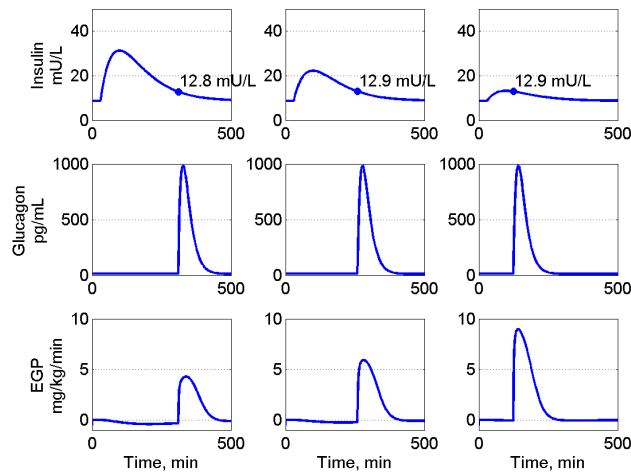
Figure 16: *In silico* demonstration of the delayed insulin effect on EGP. Blood glucose was clamped at 5 mmol/L by basal IIR and controlled via IV glucose infusion every 5 minutes using the PID controller explained in Section 2.2.2. After 30 minutes steady state, subject 4 received a SC insulin bolus of either 5 U (left), 3 U (middle) or 1 U (right). When the insulin concentration dropped below 13 mU/L a SC glucagon bolus of 0.5 mg was administered. The EGP responses are displayed in the bottom row; the 120 minutes AUCs are 323, 429, and 612 mg/kg, respectively.

baseline levels of insulin and glucagon as in Figure 17a, one would expect the glucose level to stay constant or at least approach a level similar to either of the observed initial values. However, the glucose concentration drops to a level below 50 mg/dL. The reason for this behaviour is explained in the data used for estimating the model parameters of patient 7 [1,16], see Figure 17b. The data contains very little information about the insulin, glucagon and glucose levels before the system is disturbed with an insulin bolus. On the contrary, it appears that a SS is achieved towards the end of the experiment when the glucose concentration is around 50 mg/dL and both glucagon and insulin have returned to their baseline levels. This phenomenon explains why the model assumes glucose SS lower than one would expect at baseline levels of insulin and glucagon.

4.2.2   Repeated Glucagon Boluses

When conducting experiments *in vivo* one naturally wishes to maximize the information from those experiments. Clinical studies are often set up to investigate multiple glucagon doses during each trial day [2, 14]. However, depending on the size of the glucagon bolus, it can take several hours before all administered drug is cleared from the system and plasma concentration has returned to baseline. As evident in Figure 17b, plasma glucagon has only just returned to baseline four hours after a SC bolus of 300 μg glucagon. Be reminded of Figure 10 in Section 2 where the continuous increase in glucose concentration is due to residual glucagon from the previous dose. One must allow sufficient time in-between experiments and perhaps lower ones expectations to what is practically possible to avoid carry-over effects from previous doses, rather than rushing too many experiments in short time.

4.2.3   The Glucagon Evanescence Effect

The glucagon evanescence effect is well known and documented since the early 1980s [11, 17, 18]. As implied in the name, the effect of glucagon tends to fade away over time. This trend is observed during clamp studies with constant insulin and glucagon levels where the EGP tends to return to baseline after approximately two hours although the glucagon level is still significantly elevated above the baseline level [11,18]. Mechanisms to explain this phenomenon could be degradation/aggregation of infused glucagon, hyperglycemia, intra-hepatic negative feedback mechanism or simply glycogen depletion.

As the evanescence effect is observed even during clamped euglycaemia, hyperglycemia can not solemnly explain the vanishing effect of glucagon [11].

Glycogen depletion seems like an easy explanation. However, the amount of infused glucagon during the study by Hinshaw *et al.* [11] was 0.54 μg/kg over three hours during the highest glucagon infusion rate. A study by Castle *et al.* [19] found that repeated boluses of 2 μg/kg did not deplete the liver even after an overnight fast. Therefore, it does not seem likely that the evanescence effect observed during clamp studies of glucagon is due to depletion of the glycogen stores in the liver.

In vitro data suggest that the glucagon evanescence effect is due to desensitization of the receptor regulated by cyclic AMP [20]. The reduced responsiveness to glucagon was fully expressed after 2 hours which fits well with *in vivo* data [11,18]. Hinshaw *et al.* [11] proposed a mathematical expression to capture the waning effect of glucagon. However, it is unclear for how long this evanescence effect persists and if a sudden increase in the glucagon infusion can overrule the evanescence phenomenon. More studies of the glucagon evanescence effect are needed to fully understand the underlying mechanisms and how the effect should be accounted for in a glucoregulatory model including glucagon.
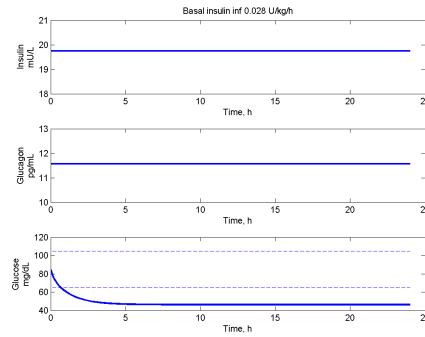
(a) Simulation of subject 7's modelled SS. Insulin and glucagon
are at baseline levels, and glucose concentration initiated at eugly-
caemia.
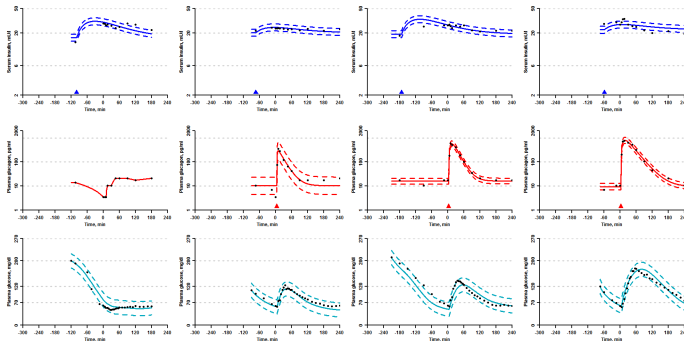
(b) Raw data and PK/PD model fits in subject 7: insulin PK (top), glucagon PK (middle), glucose
PD (bottom). Increasing glucagon boluses left to right: 0, 100, 200, 300 μg. Triangles indicate
time of insulin bolus (blue) and glucagon bolus (red). Please see [1] for further study details.

Figure 17: Comparison of modelled SS and data used for model building.

4.3 Summary

The learnings of the previous sections can be summed up in the following statements that should aid in the design of clinical studies:

- The glucose level during hypo- or euglycaemia does not influence the glucose response to glucagon.

- Theoretically, a simple PID controller can control the needed glucose infusion to maintain constant glucose levels when the insulin infusion is sufficiently high.

- The insulin infusion should be constant throughout the study duration.

- Nominal sampling times must be chosen carefully and actual sampling times noted meticulously.

- A model can only be expected to account for dynamics present in the dataset used for model building and parameter estimation.

- Less is more. Avoid multiple dynamics simultaneously by allowing enough time between disturbances of the glucoregulatory system.

- The effect of glucagon wanes over time despite constant infusion.

- Glucagon doses should be distributed across a wide range encompassing the true half maximum response in order to correctly identify the dose-response relationship.

REFERENCES   *REFERENCES*

References

[1] S. L. Wendt, A. Ranjan, J. K. Møller, S. Schmidt, C. B. Knudsen, J. J. Holst, S. Madsbad, H. Madsen, K. Nørgaard, and J. B. Jørgensen, "Cross-validation of a glucose-insulin-glucagon pharmacodynamics model for simulation using data from patients with type 1 diabetes," *Journal of Diabetes Science & Technology*, 2017.

[2] J. El Youssef, J. R. Castle, P. A. Bakhtiani, A. Haidar, D. L. Branigan, M. Breen, and W. K. Ward, "Quantification of the glycemic response to microdoses of subcutaneous glucagon at varying insulin levels," *Diabetes Care*, vol. 37, no. 11, pp. 3054–3060, 2014.

[3] A. Haidar, C. Duval, L. Legault, and R. Rabasa-Lhoret, "Pharmacokinetics of insulin aspart and glucagon in type 1 diabetes during closed-loop operation," *Journal of diabetes science and technology*, vol. 7, no. 6, pp. 1507–1512, 2013.

[4] S. L. Wendt, J. K. Møller, C. B. Knudsen, H. Madsen, A. Haidar, and J. B. Jørgensen, "Pk/pd modelling of glucose-insulin-glucagon dynamics in healthy dogs after a subcutaneous bolus administration of native glucagon or a novel glucagon analogue," Technical University of Denmark, Tech. Rep. 2, April 2016.

[5] S. L. Wendt, J. K. Møller, A. Haidar, C. B. Knudsen, H. Madsen, and J. B. Jørgensen, "Modelling of glucose-insulin-glucagon pharmacodynamics in man," in *Proceedings of the 38th Annual International Conference of the IEEE Engineering in Medicine and Biology Society*.   IEEE EMBS, 2016.

[6] F. Q. Nuttall, A. Ngo, and M. C. Gannon, "Regulation of hepatic glucose production and the role of gluconeogenesis in humans: is the rate of gluconeogenesis constant?" *Diabetes/Metabolism Research and Reviews*, vol. 24, no. 6, pp. 438–458, 2008.

[7] R. Hovorka, F. Shojaee-Moradie, P. V. Carroll, L. J. Chassin, I. J. Gowrie, N. C. Jackson, R. S. Tudor, A. M. Umpleby, and R. H. Jones, "Partitioning glucose distribution/transport, disposal, and endogenous production during IVGTT," *American Journal of Physiology-Endocrinology and Metabolism*, vol. 282, no. 5, pp. E992–E1007, 2002.

[8] R. Hovorka, V. Canonico, L. J. Chassin, U. Haueter, M. Massi-Benedetti, M. O. Federici, T. R. Pieber, H. C. Schaller, L. Schaupp, T. Vering, and M. E. Wilinska, "Nonlinear model predictive control of glucose concentration in subjects with type 1 diabetes," *Physiological measurement*, vol. 25, no. 4, pp. 905–920, 2004.

[9] N. J. W. Albrechtsen, B. Hartmann, S. Veedfald, J. A. Windeløv, A. Plamboeck, K. N. Bojsen-Møller, T. Idorn, B. Feldt-Rasmussen, F. K. Knop, T. Vilsbøll, S. Madsbad, C. F. Deacon, and J. J. Holst, "Hyperglucagonaemia analysed by glucagon sandwich elisa: nonspecific interference or truly elevated levels?" *Diabetologia*, vol. 57, no. 9, pp. 1919–1926, 2014.

[10] M. Horowitz, D. O'Donovan, K. L. Jones, C. Feinle, C. K. Rayner, and S. M., "Gastric emptying in diabetes: clinical significance and treatment," *Diabetic Medicine*, vol. 19, no. 3, pp. 177–194, 2002.

[11] L. Hinshaw, A. Mallad, C. D. Man, R. Basu, C. Cobelli, R. E. Carter, Y. C. Kudva, and A. Basu, "Glucagon sensitivity and clearance in type 1 diabetes: insights from in vivo and in silico experiments," *American Journal of Physiology, Endocrinology and Metabolism*, vol. 309, no. 5, pp. E474–E486, 2015.

[12] A. D. Cherrington, "Control of glucose production in vivo by insulin and glucagon," in *Comprehensive Physiology 2011, Supplement 21: Handbook of Physiology, The Endocrine System, The Endocrine Pancreas and Regulation of Metabolism*, First published in print 2001, pp. 759–785.

[13] K. E. Steiner, P. E. Williams, W. W. Lacy, and A. D. Cherrington, "Effects of insulin on glucagon-stimulated glucose production in the conscious dog," *Metabolism*, vol. 39, no. 12, pp. 1325–1333, 1990.

[14] H. Blauw, I. Wendl, J. H. DeVries, T. Heise, and T. Jax, "Pharmacokinetics and pharmacodynamics of various glucagon dosages at different blood glucose levels," *Diabetes, Obesity and Metabolism*, vol. 18, no. 1, pp. 34–39, 2016.

[15] A. Ranjan, S. Schmidt, C. Damm-Frydenberg, I. Steineck, T. R. Clausen, J. J. Holst, S. Madsbad, and K. Nørgaard, "Low carbohydrate diet impairs the effect of glucagon in the treatment of insulin-induced mild hypoglycemia: A randomized cross-over study," *Diabetes Care*, vol. Epub ahead of print, 2016.

[16] A. Ranjan, S. Schmidt, S. Madsbad, J. J. Holst, and K. Nørgaard, "Effects of subcutaneous, low-dose glucagon on insulin-induced mild hypoglycaemia in patients with insulin pump treated type 1 diabetes." *Diabetes, Obesity and Metabolism*, vol. 18, no. 4, pp. 410–418, 2016.

[17] A. Cherrington, P. Williams, G. Shulman, and W. Lacy, "Differential time course of glucagon's effect on glycogenolysis and gluconeogenesis in the conscious dog," *Diabetes*, vol. 30, no. 3, pp. 180–187, 1981.

[18] M. Wada, C. C. Connolly, C. Tarumi, D. W. Neal, and A. D. Cherrington, "Hepatic denervation does not significantly change the response of the liver to glucagon in conscious dogs," *American Journal of Physiology - Endocrinology and Metabolism*, vol. 268, no. 2, pp. E194–E203, 1995.

[19] J. R. Castle, J. El Youssef, P. A. Bakhtiani, Y. Cai, J. M. Stobbe, D. Branigan, K. Ramsey, P. Jacobs, R. Reddy, M. Woods, and W. K. Ward, "Effect of repeated glucagon doses on hepatic glycogen in type 1 diabetes: Implications for a bihormonal closed-loop system," *Diabetes care*, vol. 38, no. 11, pp. 2115–2119, 2015.

[20] F. R. DeRubertis and P. Craven, "Reduced sensitivity of the hepatic adenylate cyclase-cyclic amp system to glucagon during sustained hormonal stimulation," *Journal of Clinical Investigation*, vol. 57, no. 2, pp. 435–443, 1976.

Journal Paper 2
Simulations for Clinical
Recommendations

This appendix presents the draft journal paper by Ranjan *et al.* with the title "Insulin Dependent Regimen of Mini-Dose Glucagon Treatment of Mild Hypoglycaemia in Patients with Type 1 Diabetes - A Simulation Study" to be submitted to Diabetes Technology & Therapeutics in Spring 2017 [22].

Insulin Dependent Regimen of Mini-Dose Glucagon Treatment of Mild Hypoglycaemia in Patients with Type 1 Diabetes - A Simulation Study

Ranjan A[1,2], Wendt SL[3,4], Schmidt S[1,2], Madsbad S[1], Holst JJ[5], Madsen H[4], Knudsen CB[3], Jørgensen JB[4], Nørgaard K[1]

[1]Department of Endocrinology, Copenhagen University Hospital Hvidovre, Hvidovre, Denmark.
[2]Danish Diabetes Academy, Odense, Denmark.
[3]Department of Bioanalysis and Pharmacokinetics, Zealand Pharma, Glostrup, Denmark.
[4]Department of Applied Mathematics and Computer Science, Technical University of Denmark, Kgs. Lyngby, Denmark.
[5]Faculty of Health and Medical Sciences, University of Copenhagen, Copenhagen, Denmark.

Corresponding author:
Ajenthen Ranjan
Copenhagen University Hospital Hvidovre
Department of Endocrinology
Kettegaard Alle 30
2650 Hvidovre
Denmark
Email: Ajenthen.Ranjan.02@Regionh.dk
Phone: +45 38 62 63 78

Abstract: 271 / 250
Word Count: 2393/ 2000
Number of tables: 0 / 1
Number of figures: 5 / 1
Number of references: 20 / 15

Abstract

Objective: To propose an insulin-dependent glucagon dosing regimen for treatment of mild hypoglycaemia in patients with type 1 diabetes.

Methods: A validated insulin-glucagon pharmacodynamics model simulated three studies. The virtual patient population consisted of seven adults with insulin pump-treated type 1 diabetes. Each patient performed 170 experiments per study, in which 1 of 10 subcutaneous insulin boluses was administered to decrease plasma glucose (PG) from 7.0 mmol/l to below 3.9 mmol/l. For each experiment, the bolus size had to achieve similar target insulin levels in all patients. When PG reached 3.9 mmol/l, 1 of 17 subcutaneous glucagon boluses was administered. In each of the three studies, insulin levels were either estimated as serum insulin, insulin on board (IOB) or ratio of IOB to total daily insulin dose (IOB/TDD). Each study evaluated success of glucagon doses at varying insulin levels in recovering from mild hypoglycaemia. The optimal glucagon bolus was the lowest dose to cause a PG peak 5.0-10.0 mmol/l and sustain PG ≥3.9 mmol/l for 2 hours after the bolus.

Results: In all studies, PG response to glucagon declined with increasing insulin levels. The glucagon dose to optimally treat mild hypoglycaemia was exponentially related to insulin levels, regardless of how insulin was estimated. A 125 µg glucagon dose was needed to optimally treat mild hypoglycaemia when no bolus insulin were administered in all patients. In contrast, glucagon doses >500 µg were needed when serum insulin levels were >25 mU/l, IOB >2.0 U or IOB/TDD >6%.

Conclusion: Even though the proposed glucagon regimen needs confirmation in clinical trials, this is the first insulin-dependent glucagon dosing regimen for treatment of insulin-induced mild hypoglycaemia.

Introduction

Intensive insulin therapy is recommended for patients with type 1 diabetes due to improvements in glycaemic control and reduction of micro- and macrovascular complications. The risk of hypoglycaemia increases with intensified insulin therapy (1). The fear of hypoglycaemia holds patients from seeking optimal glycaemic control and affects quality of life negatively. Consequently, different adjunct therapies and advances in insulin therapy have been tested but none markedly improved glycaemic control, risk of hypoglycaemia and/or quality of life (2).

Some researchers suggest that low-dose glucagon as an add-on to insulin therapy may optimise glycaemic control and reduce hypoglycaemia risk (3). This dual-hormone approach has mainly been tested in settings with automatic delivery of the drugs (dual-hormone closed-loop system) (4,5). We believe that manual delivery of insulin and glucagon (open-loop dual-hormone therapy) may equally improve diabetes management. Haymond *et al.* showed the benefits of this concept in children with type 1 diabetes and gastroenteritis (6). To our knowledge, optimal glucagon doses to treat insulin induced mild hypoglycaemia have never been proposed for adults with type 1 diabetes. It is known that the anti-hypoglycaemic effect of glucagon highly depends on ambient insulin concentrations (7). Yet, no commercially available devices are able to measure insulin concentrations in real-time. Bolus calculators in insulin pumps have addressed this issue by using insulin on board (IOB) to reduce risk of insulin stacking and risk of hypoglycaemia (8,9). IOB is an approximated amount of active insulin, besides basal rate insulin, in the body and accounts for the pharmacodynamics of subcutaneously (SC) administered bolus insulin (10).

In view of that, our aim was to propose a glucagon-dosing regimen for treatment of mild hypoglycaemia depending on the ambient insulin level. We used a validated glucoregulatory model to simulate how different insulin levels would affect the glucose response to different glucagon doses. Subsequently, the optimal glucagon dose to treat mild hypoglycaemia was determined based on three clinically relevant criteria.

Methods

Data: In this study, we used insulin and glucagon pharmacokinetics (PK) models and a validated glucose-insulin-glucagon pharmacodynamics (PD) model to generate data from seven virtual type 1 diabetes patients (11). MATLAB 2016b (The MathWorks, Inc., Natick, MA) was used for model implementation and simulations. The population of virtual patients was based on seven adults (4 females, age range: 19-64 years, BMI range: 20.0-25.4 kg/m^2) with type 1 diabetes who were in good glycaemic control (HbA1c range: 6.1-7.4%), had no endogenous insulin production and had a reduced endogenous glucagon response to hypoglycaemia (12). The PD model is an extension of Hovorka's glucoregulatory model with effects of glucagon on endogenous glucose production (13). The expanded PD model was validated using leave-one-out cross-validation of three to four datasets in seven type 1 diabetes patients (11). The PK models assumed that changes in insulin and glucagon concentrations were only due to the administered drugs: insulin aspart (NovoRapid®, Novo Nordisk) and glucagon (GlucaGen®, Novo Nordisk). More details about the model have been published (11).

***In silico* experiments:** We executed three *in silico* studies to investigate the glucose response to different glucagon doses depending on the ambient insulin levels during insulin induced mild hypoglycaemia (Figure 1). In each experiment, a SC insulin bolus was administered at 7.0 mmol/l and a SC glucagon bolus

administered when plasma glucose (PG) concentration decreased below 3.9 mmol/l. Simulation of one experiment lasted for ten hours following the insulin bolus. Insulin bolus sizes were chosen so that patients had a predefined and similar insulin level at the time of glucagon bolus. Thus, patients received different insulin boluses to achieve same target of insulin levels. The three studies differed in the methods of estimating insulin levels. One study used serum insulin concentrations (se-insulin) obtained from the insulin PK model to describe the insulin level. The latter two studies used a linear decay function based on patient specific insulin action time to describe insulin on board (IOB) either unadjusted or as a ratio to the total daily dose of insulin (IOB/TDD). We investigated the glucagon efficacy at mild hypoglycaemia with following insulin levels:

1) *Serum insulin concentrations (se-insulin):* 19, 20, 21, 22, 23, 24, 25, 26, 27 or 28 mU/l

2a) *Unadjusted insulin on board (IOB):* 0.0, 0.25, 0.5, 0.75, 1, 1.5, 2, 2.5, 3, or 3.5 U

2b) *Ratio of IOB to total daily dose of insulin (IOB/TDD):* 0, 1, 2, 3, 4, 5, 6, 7, 8, or 10%

In all experiments, when PG reached 3.9 mmol/l, one of following 17 glucagon boluses was administered SC: 0.025, 0.05, 0.075, 0.1, 0.125, 0.15, 0.175, 0.2, 0.25, 0.3, 0.4, 0.5, 1.0, 1.5, 2.0, or 2.5 mg.

Treatment assessment: After each experiment, the success of a glucagon dose to treat mild hypoglycaemia but avoid hyperglycaemia was evaluated based on three dichotomous criteria: peak PG > 5.0 mmol/l (PG>5), peak PG ≤ 10.0 mmol/l (PG≤10) and PG > 3.9 mmol/l 120 min after the glucagon bolus (PG$_{120}$≥3.9) (figure 1). The success rate of a glucagon bolus in accomplishing each of these criteria was calculated at various insulin levels. For each combination of glucagon dose and insulin level, a weighted harmonic mean of the three success criteria was calculated as:

$$H = \frac{1}{\dfrac{0.4}{S_{PG>5}} + \dfrac{0.4}{S_{PG\leq10}} + \dfrac{0.2}{S_{PG_{120}\geq3.9}}}$$

, where S is the success rate, equal to the number of subjects fulfilling a criterion divided by the total number of subjects. For each insulin level, the lowest glucagon dose with the highest H-value was considered as the optimal bolus.

Results

Figures 2-4 show the percentage of patients achieving the predefined treatment criteria as function of the glucagon dose, stratified by se-insulin (Figure 2), IOB (Figure 3), and IOB/TDD (Figure 4). Here, the percentages of patients achieving the criterion of PG>5 (green line) and PG$_{120}$≥3.9 (red line) increased with increasing glucagon doses. The curves for PG>5 criterion were left-shifted compared to the curves for PG$_{120}$≥3.9 criterion, meaning that less glucagon was needed to fulfil the criterion of PG>5 compared with PG$_{120}$≥3.9. On the other hand, the percentage of patients fulfilling the criterion of avoiding hyperglycaemia, PG≤10, declined with increasing glucagon doses (blue line). For instance when patients had a PG of 3.9 mmol/l and IOB of 2U, a glucagon dose of 100 μg would increase PG>5.0mmol/l in 60% of patients, keep PG≥3.9 for two hours in 50% of patients, and keep PG < 10 mmol/l in all patients.

Figure 5 shows the optimal glucagon dosing regimen for treatment of mild hypoglycaemia as function of

insulin levels extracted from Figures 2-4. The relation between optimal glucagon dose and the insulin levels could be expressed as an exponential function, regardless of the method for estimating insulin levels.

Discussion

In this *in silico* study, we propose an insulin-based glucagon dosing regimen to treat mild hypoglycaemia in patients with type 1 diabetes. Three dosing regimens are proposed according to whether insulin levels were estimated as serum insulin concentration, IOB or ratio of IOB to TDD. As expected, the anti-hypoglycaemic effect of glucagon was highly dependent on insulin levels. If insulin levels were high, higher glucagon doses were needed to treat mild hypoglycaemia. This relation has previously been shown in another *in vivo* study by El Youssef *et al.*, who quantified the glycaemic effects of glucagon at various insulin levels (14). In previous *in silico* study, the presently used PK/PD model was able to simulate and replicate the data by El Youssef (15). Furthermore, the PD model was validated on data from another *in vivo* dynamic clinical dose finding study with three different SC injections of glucagon for treatment of insulin-induced mild hypoglycaemia (12). Therefore, we consider the model to be valid for estimating the optimal glucagon dose for treatment of mild hypoglycaemia at varying levels of insulin.

The strength of *in silico* studies is the ability to simulate large scale cross-over trials that are not feasible in real-life settings. In this study, we estimated the optimal glucagon dose at varying insulin levels based on virtual patients, each undergoing 170 cross-over visits per study. An optimal glucagon dose was achieved if PG increased from 3.9 mmol/l to a peak between 5.0-10.0 mmol/l, and was kept above 3.9 mmol/l for at least 120 minutes. The peak PG criterion was prioritised for the 2-hrs PG level. Consequently, we found an exponential relationship between the optimal glucagon doses to treat mild hypoglycaemia and the ambient insulin levels. However, the relationship tended to be linear in ranges of serum insulin from 19 to 25 mU/l, IOB from 0 to 2 U, and IOB/TDD from 0 to 5%. At very high insulin levels (se-insulin > 27 mU/l, IOB ≥3U, IOB/TDD>8%, the optimal glucagon dose exceeded the size used for severe hypoglycaemia. On the other hand, the lowest optimal glucagon dose was 0.125 mg when insulin levels were only maintained by basal insulin rate and bolus insulin was administered.

To our knowledge, this is the first study to propose a dosing regimen of glucagon in an open-loop setting. The focus has primarily been on the closed-loop dual-hormonal settings in which very low glucagon doses are frequently given to prevent hypoglycaemia. This frequent administration cannot be applied in the open-loop setting due to the inconvenience of multiple glucagon injections. Rather we consider low dose glucagon as an alternative to oral carbohydrate intake in treatment of mild hypoglycaemia. We can only speculate that low dose glucagon may provide more predictable glucose responses than oral carbohydrates in treatment of mild hypoglycaemia, especially concerning the risk of overeating and consequent post-rescue hyperglycaemia.

The glucagon dosing regimens were stratified by methods of estimating insulin levels. We included IOB because no real-time monitors of serum insulin concentrations are currently available (16). Furthermore, for many years insulin pumps with bolus calculators have used IOB feedback as standard to prevent insulin staking. IOB is a rough approximation of the active insulin in the body. The IOB is differently calculated depending on the bolus calculator manufacturer, i.e. linear or curvilinear (8). In the present study, we chose the linear approach as it is easier to understand than the curvilinear time profile. Each model of bolus calculators has distinct time profiles for IOB and most bolus calculators use a curvilinear time profile

because it better mimics the SC insulin PD profile (8). We consider the minor differences in IOB time profiles to be negligible for the success of glucagon treatment.

We applied the same criteria for optimal glucagon dose on a previous *in vivo* dose finding study (supplementary table 1). Here a glucagon dose of 0.200 mg was needed to restore mild hypoglycaemia with an average IOB of 0.9U or IOB/TDD of 2%. This dose was higher than proposed by the *in silico* study of 0.175 mg glucagon (figure 5). The success criteria used in this study are arbitrarily set and are no consensus exist on post rescue glucose excursion as well as for postprandial glucose excursions (17). We chose these targets from the American Diabetes Association recommendation (18). Treatment success would have been harder to succeed if peak PG had to be within 5-8 mmol/l as seen among healthy non diabetic individuals in a postprandial state. We consider the target levels to be clinically reasonable.

At some point the optimal glucagon doses were too high (>0.500 mg) as a treatment option for mild hypoglycaemia, primarily due to increased risk of side effects and unapproved total daily glucagon use. In a previous study, a single bolus of 0.500 mg glucagon tended to cause more nausea than 0.100 mg glucagon during mild hypoglycaemia (19). In the present study, we found that 500 µg glucagon was needed if serum insulin concentration was 25 mU/l, IOB was 2 U, or IOB was 6% of TDD. Therefore, if patients have mild hypoglycaemia with insulin levels above these critical limits, we suggest ingestion of carbohydrates rather than mini-dose glucagon to restore PG.

Since glucagon is currently only available in 1 mg vials and has to be reconstituted immediately before use, the therapy approach may not be feasible at the moment. However, stable soluble glucagon formulations may soon be on the market, and multi-dosing may be of interest for pharmaceutical companies developing such glucagon products. The proposed glucagon dosing regimen is based on reconstituted GlucaGen® from Novo Nordisk. The model parameters of the simulation model may need adjustments to describe other glucagon products.

Another approach recently suggested is the intranasal administration of glucagon (20). This approach may be easier to manage regarding the administration, but the intra-individual variation in glucose response may be higher compared with subcutaneous administrations. However, recent studies found similar PD profiles after intranasal administration of glucagon between left versus right nostrils and congestion versus non-congestion.

This study has limitations. First, the dose regimen was based on a simulation model which may not completely capture the real life events. The used samples size may not be transferable to a large scale population. Our virtual population consisted of only seven patients and thus the results of the optimal glucagon dose for other patients with type 1 diabetes may deviate. Further, the glucagon doses used were already predefined and categorically analysed, meaning the "actual" optimal glucagon dose may be between the doses used in this study. On the other hand, this is the first study to suggest an insulin-based dosing regimen for mini-doses of glucagon. We consider these findings as an initial step towards individual dose titration of glucagon for mild hypoglycaemia. Second, the validated model is based on human in-patient studies and do not take low carbohydrate diet (19), alcohol, exercise and stress into account. These factors may affect the glucose responses to insulin and glucagon. Finally, the model has only been validated on lean patients with type 1 diabetes. Since the optimal glucagon dose was not weight adjusted in this study, the responses may be different in an obese population. Still, the proposed dose regimen is an

approximation and should be further optimised by future trials with glucagon as treatment for mild hypoglycaemia in patients with type 1 diabetes.

In conclusion, we propose insulin-dependent glucagon dosing regimens for treatment of insulin induced hypoglycaemia. The regimens account for insulin levels evaluated as normalised serum insulin concentration, IOB and normalized IOB to TDD. The regimens were based on simulations of glucagon doses ranging from 25 μg to 2.5 mg and insulin doses yielding predefined insulin levels when blood glucose reached the hypoglycemia threshold. The proposed regimens therefore need to be adjusted or confirmed in a clinical trial in patients with type 1 diabetes.

Reference

1. Gubitosi-Klug RA, Lachin JM, Backlund JYC, Lorenzi GM, Brillon DJ, Orchard TJ. Intensive diabetes treatment and cardiovascular outcomes in type1 diabetes: The DCCT/EDIC study 30-year follow-up. Diabetes Care 2016;39:686–93

2. Frandsen CS, Dejgaard TF, Madsbad S. Non-insulin drugs to treat hyperglycaemia in type 1 diabetes mellitus. Lancet Diabetes Endocrinol 2016;8587:1–15

3. Reiband HK, Schmidt S, Ranjan A, Holst JJ, Madsbad S, Nørgaard K. Dual-hormone treatment with insulin and glucagon in patients with type 1 diabetes mellitus. Diabetes Metab Res Rev 2014;34:3–12

4. Russell SJ, Hillard MA, Balliro C, Magyar KL, Selagamsetty R, Sinha M, et al. Day and night glycaemic control with a bionic pancreas versus conventional insulin pump therapy in preadolescent children with type 1 diabetes: a randomised crossover trial. lancet Diabetes Endocrinol Elsevier Ltd; 2016;8587

5. Taleb N, Emami A, Suppere C, Messier V, Legault L, Ladouceur M, et al. Efficacy of single-hormone and dual-hormone artificial pancreas during continuous and interval exercise in adult patients with type 1 diabetes: randomised controlled crossover trial. Diabetologia Diabetologia; 2016;2561–71

6. Haymond MW, Schreiner B. Mini-dose glucagon rescue for hypoglycemia in children with type 1 diabetes. Diabetes Care 2001;24:643–5

7. El Youssef J, Castle JR, Bakhtiani PA, Haidar A, Branigan DL, Breen M, et al. Quantification of the glycemic response to microdoses of subcutaneous glucagon at varying insulin levels. Diabetes Care 2014;37:3054–60

8. Zisser H, Robinson L, Bevier W, Dassau E, Ellingsen C, Doyle FJ, et al. Bolus calculator: a review of four "smart" insulin pumps. Diabetes Technol Ther 2008;10:441–4

9. Bequette BW. Glucose Clamp Algorithms and Insulin Time-Action Profiles. J diabetes Sci Technol 2009;3:1005–13

10. Heise T, Meneghini L. Insulin Stacking Versus Therapeutic Accumulation: Understanding the Differences. Endocr Pract 2014;20:75–83

11. Wendt SL, Ranjan A, Møller JK, Schmidt S, Knudsen CB, Holst JJ, et al. Cross-Validation of a Glucose-Insulin-Glucagon Pharmacodynamics Model for Simulation Using Data From Patients With Type 1 Diabetes. J Diabetes Sci Technol 2017;

12. Ranjan A, Schmidt S, Madsbad S, Holst JJ, Nørgaard K. Effects of subcutaneous, low-dose glucagon on insulin-induced mild hypoglycaemia in patients with insulin pump treated type 1 diabetes. Diabetes Obes Metab 2016;18(4):410-8

13. Hovorka R, Canonico V, Chassin LJ, Haueter U, Massi-Benedetti M, Orsini Federici M, et al. Nonlinear model predictive control of glucose concentration in subjects with type 1 diabetes. Physiol Meas England; 2004;25:905–20

14. Castle JR, Youssef J El, Branigan D, Newswanger B, Strange P, Cummins M, et al. Comparative Pharmacokinetic/Pharmacodynamic Study of Liquid Stable Glucagon Versus Lyophilized Glucagon in Type 1 Diabetes Subjects. J Diabetes Sci Technol 2016;

15. Wendt, S. L., Ranjan, A., Møller, J. K., Boye Knudsen, C., Holst, J. J., Madsbad, S., Jørgensen, J. B.. Simulating

clinical studies of the glucoregulatory system: in vivo meets in silico. Technical University of Denmark, Tech. Rep. 1, February 2017.

16. Cohen N, Sabhachandani P, Sarkar S, Kahanovitz L, Lautsch N, Russell SJ, et al. Microsphere based continuous-flow immunoassay in a microfluidic device for determination of clinically relevant insulin levels. Microchim Acta Microchimica Acta; 2017;

17. Madsbad S. Impact of postprandial glucose control on diabetes-related complications: How is the evidence evolving? J Diabetes Complications 2016;30:374–85

18. ADA. Lifestyle Management - Standard of Medical Care. Diabetes Care 2017;40:S33–43

19. Ranjan A, Schmidt S, Damm-frydenberg C, Steineck I, Clausen TR, Holst JJ, et al. Low Carbohydrate Diet Impairs the Effect of Glucagon in the Treatment of Insulin-Induced Mild Hypoglycemia: A Randomized Cross-Over Study. Diabetes Care 2016;1–4

20. Rickels MR, Ruedy KJ, Foster NC, Piche CA, Dulude H, Sherr JL, et al. Intranasal Glucagon for Treatment of Insulin-Induced Hypoglycemia in Adults With Type 1 Diabetes: A Randomized Crossover Noninferiority Study. Diabetes Care 2015; 15–1498
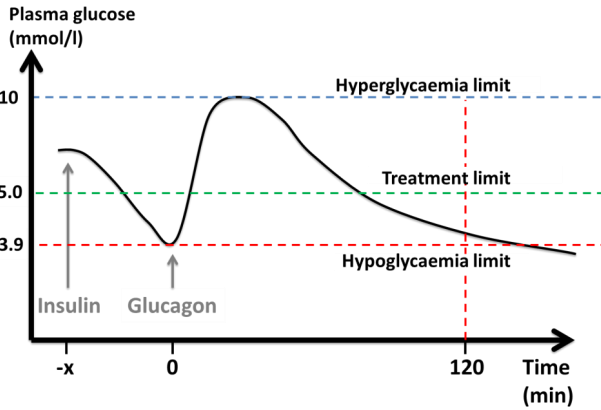
FIG. 1: Schematic description of study design and treatment assessment. In seven virtual patients, 1 of 10 boluses of subcutaneous insulin was administered (t=-x) to decrease PG from 7.0 mmol/l to below 3.9 mmol/l. Each insulin bolus size had to achieve similar target insulin levels in all patients. When PG reached 3.9 mmol/l (t=0), 1 of 17 subcutaneous glucagon boluses was administered. Treatment success of each glucagon dose was assessed on whether following peak PG was within 5 mmol/l (**Green line**: treatment limit) and 10 mmol/l (**Blue line**: Hyperglycaemia limit), and whether PG 120 min after the glucagon bolus was above 3.9 mmol/l (**Red lines**: Hypoglycaemia limit).

FIG. 2: Percentages of patients achieving treatment criteria as a function of glucagon dose and stratified by serum insulin concentrations. Treatment criteria were achieved if glucagon could increase PG to a peak between 5 mmol/l (**Green line**) and 10 mmol/l (**Blue line**), and keep PG above 3.9 mmol/l for 120 min after glucagon bolus (**Red lines**). The lowest optimal glucagon dose for each serum insulin concentration (**Black vertical line**) was chosen based on the highest weighted success rate of the three treatments criteria.
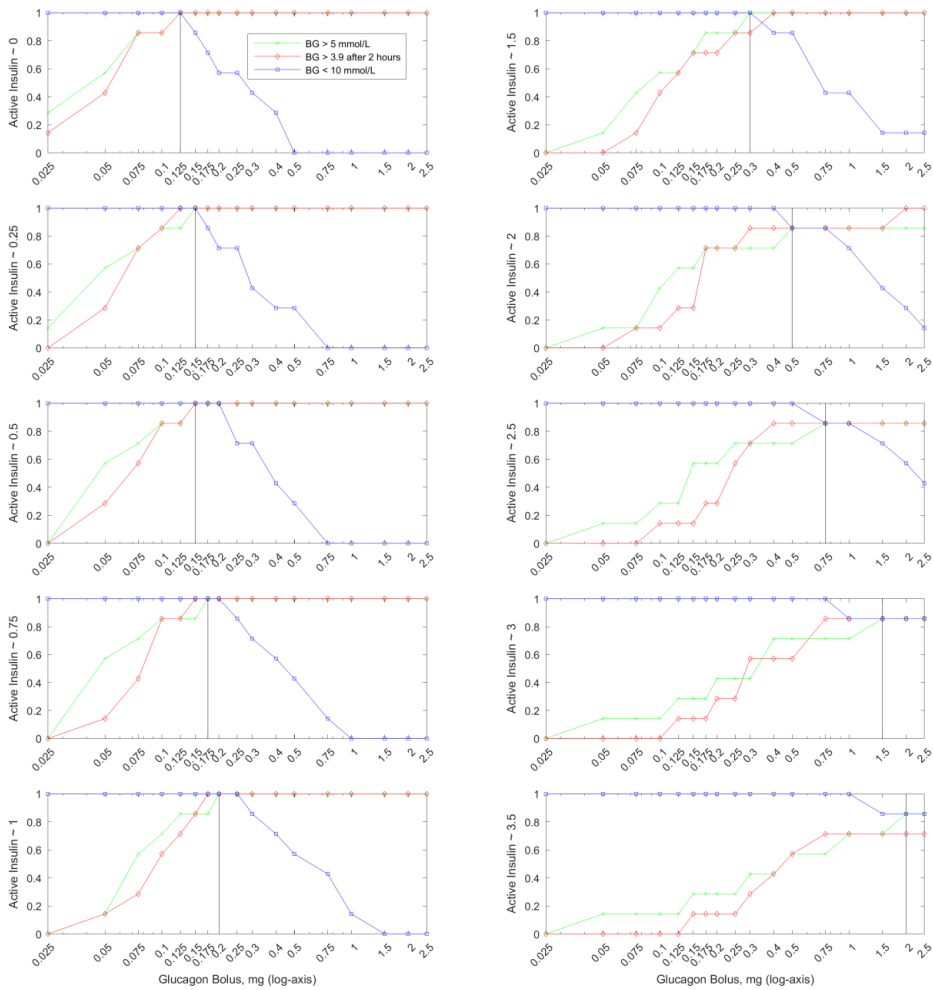
FIG. 3: Percentages of patients achieving treatment criteria as a function of glucagon dose and stratified by insulin on board. Treatment criteria were achieved if glucagon could increase PG to a peak between 5 mmol/l (**Green line**) and 10 mmol/l (**Blue line**), and keep PG above 3.9 mmol/l for 120 min after glucagon bolus (**Red lines**). The lowest optimal glucagon dose for each serum insulin concentration (**Black vertical line**) was chosen based on the highest weighted success rate of the three treatments criteria.
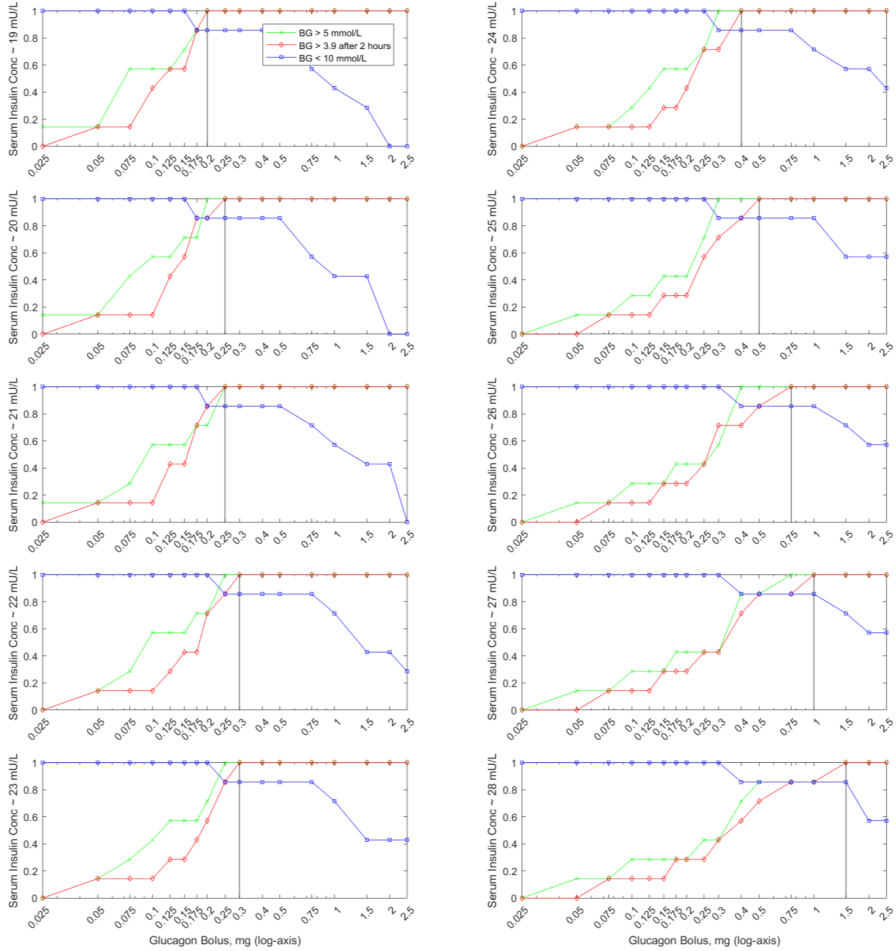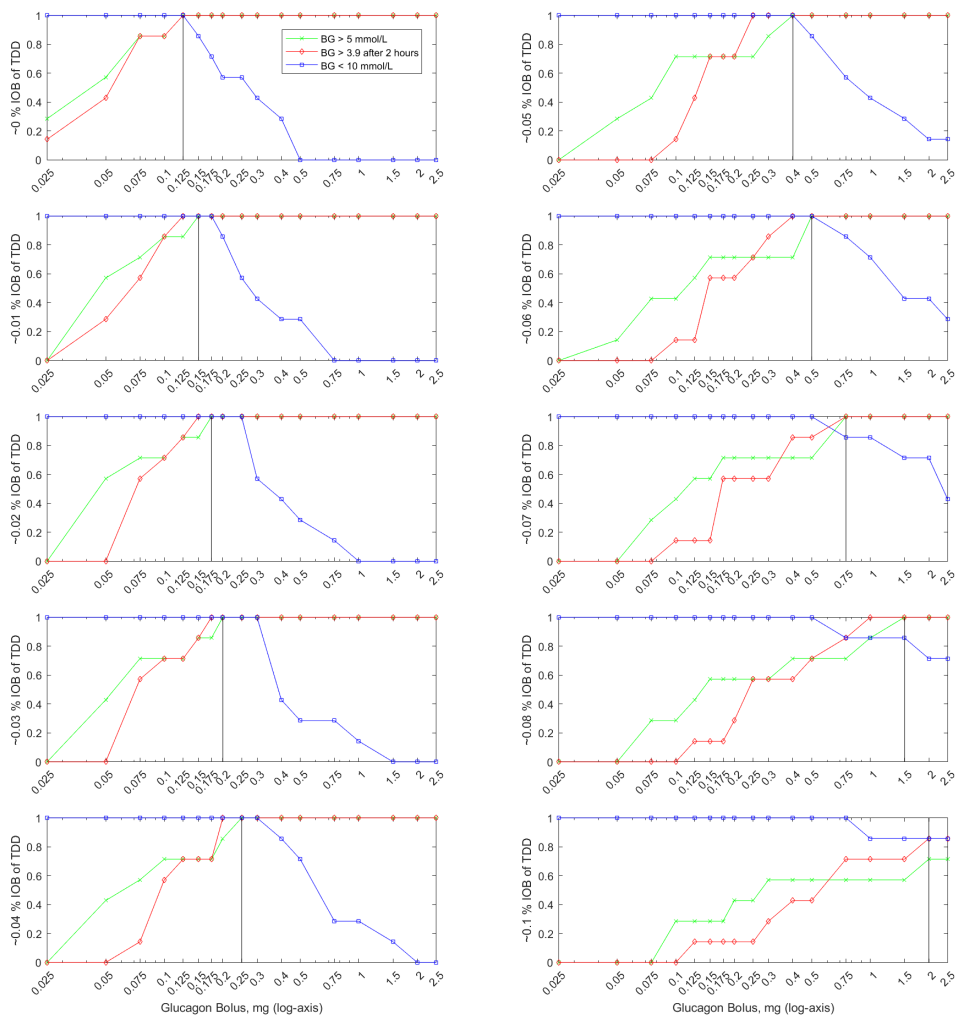
FIG. 4: Percentages of patients achieving treatment criteria as a function of glucagon dose and stratified by insulin on board normalised to total daily insulin dose. Treatment criteria were achieved if glucagon could increase PG to a peak between 5 mmol/l (**Green line**) and 10 mmol/l (**Blue line**), and keep PG above 3.9 mmol/l for 120 min after glucagon bolus (**Red lines**). The lowest optimal glucagon dose for each serum insulin concentration (**Black vertical line**) was chosen based on the highest weighted success rate of the three treatments criteria.
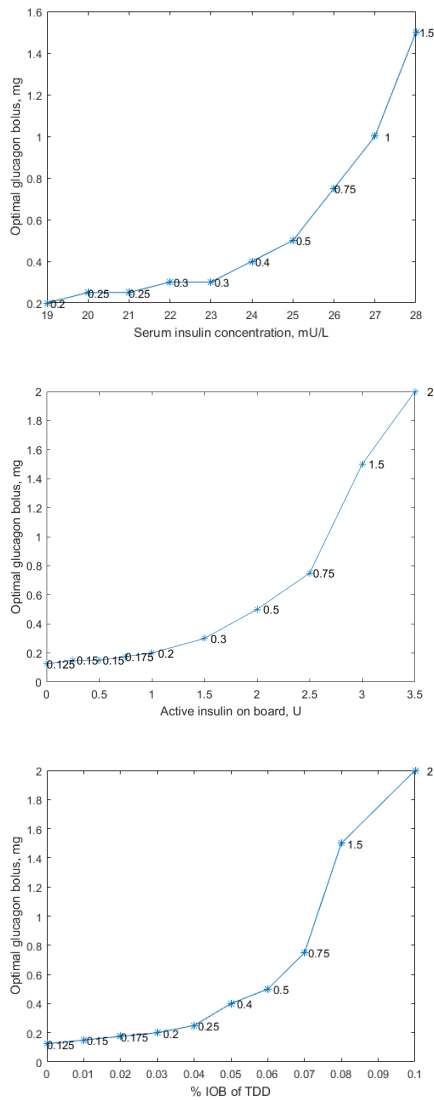
FIG. 5: Optimal glucagon dose as a function of ambient insulin levels stratified by serum insulin concentration (upper panel), insulin on board (middle panel), and insulin on board normalised to total daily insulin dose (lower panel). Virtual patients performed 170 experiments per panel to obtain predefined ratios of insulin and glucagon (each dot in the graphs) at PG level of 3.9 mmol/l. The optimal glucagon dose was chosen if able to increase PG from 3.9 mmol/l to peak between 5 mmol/l and 10 mmol/l, and keep PG above 3.9 mmol/l for 120 min after glucagon bolus.

PTID	TDD, U	IAT, hrs	Glucagon, µg	Insulin, Unit	Time to PG=3.9, min	IOB,U	IOB/TDD	PG >5	PG <10	PG$_{120}$ >3.9	All criteria
1	20.3	5	0	1.60	180	0.64	3.2%	N	Y	N	N
			100	1.55	150	0.78	3.8%	Y	Y	N	N
			200	2.40	150	1.20	5.9%	Y	Y	Y	Y
			300	1.40	210	0.42	2.1%	Y	Y	Y	Y
2	16.6	5	0	0.30	60	0.24	1.4%	N	Y	N	N
			100	1.20	210	0.36	2.2%	Y	Y	N	N
			200	0.45	90	0.32	1.9%	Y	Y	Y	Y
			300	0.50	180	0.20	1.2%	Y	Y	N	N
3	34.5	5	0	3.00	90	2.10	6.1%	N	Y	N	N
			100	2.70	120	1.62	4.7%	N	Y	N	N
			200	2.40	90	1.68	4.9%	Y	Y	N	N
			300	3.20	210	0.96	2.8%	Y	Y	Y	Y
4	37.0	4	0	3.10	180	0.78	2.1%	N	Y	N	N
			100	3.55	210	0.44	1.2%	Y	Y	Y	Y
			200	1.30	180	0.33	0.9%	Y	Y	N	N
			300	3.45	150	1.29	3.5%	Y	Y	Y	Y
5	54.7	4	0	1.80	90	1.13	2.1%	N	Y	N	N
			100	5.00	210	0.63	1.1%	Y	Y	N	N
			200	2.75	150	1.03	1.9%	Y	Y	Y	Y
			300	3.45	120	1.73	3.2%	Y	Y	N	N
6	29.5	4	0	4.50	210	0.56	1.9%	N	Y	N	N
			100	3.40	150	1.28	4.3%	Y	Y	N	N
			200	3.00	210	0.38	1.3%	Y	Y	N	N
			300	3.00	150	1.13	3.8%	Y	Y	N	N
7	58.3	4	0	4.60	120	2.30	3.9%	N	Y	N	N
			100	1.05	60	0.79	1.4%	Y	Y	Y	Y
			200	4.60	180	1.15	2.0%	Y	Y	N	N
			300	1.60	120	0.80	1.4%	Y	N	Y	N
8	27.0	4	0	2.60	180	0.65	2.4%	N	Y	N	N
			100	1.50	210	0.19	0.7%	Y	Y	N	N
			200	2.40	210	0.30	1.1%	Y	Y	Y	Y
			300	1.40	120	0.70	2.6%	Y	Y	Y	Y
											H-index
Mean	34.7	4.4	0	2.69	138.7	1.05	2.9%	0	8	0	0%
			100	2.49	165.0	0.76	2.4%	7	8	2	60%
			200	2.41	157.5	0.80	2.5%	8	8	4	83%
			300	2.25	157.5	0.90	2.6%	8	7	5	85%

Supplemental table 1: Table overview of treatment assessment in an *in vivo* dose finding study (Ranjan *et al.* DOM 2016). For each patient insulin action time (IAT) and total daily insulin dose (TDD) was known and four study visits were performed. An insulin dose was given to induce a mild hypoglycaemia of PG(PG) below 3.9 mmol/l. When the PG was 3.9 mmol/l, either a saline or glucagon bolus (100, 200, 300 µg) was

given. The table shows the insulin on board (IOB) and the normalized IOB (IOB/TDD) at the moment when glucagon was administered. Further, the right side of the table shows how many patients with the given glucagon dose could increase PG from 3.9 mmol/l to peak between 5 mmol/l (PG>5) and 10 mmol/l (PG<10), and keep PG above 3.9 mmol/l for 120 min after glucagon bolus (PG$_{120}$>3.9). The H-index for the weighted success rate is also shown as the far right panel.

Bibliography

[1] World Health Organisation. (2017) Diabetes. [Online]. Available: http://www.who.int/diabetes/en/

[2] Juvenile Diabetes Research Foundation Continuous Glucose Monitoring Study Group, "Continuous glucose monitoring and intensive treatment of type 1 diabetes," *New England Journal of Medicine*, vol. 2008, no. 359, pp. 1464–1476, 2008.

[3] DCCT Research Group, "Epidemiology of severe hypoglycemia in the diabetes control and complications trial," *The American Journal of Medicine*, vol. 90, no. 4, pp. 450–459, 1991.

[4] D. Elleri, C. L. Acerini, J. M. Allen, J. Hayes, C. Pesterfield, M. E. Wilinska, D. B. Dunger, and R. Hovorka, "Parental attitudes towards overnight closed-loop glucose control in children with type 1 diabetes." *Diabetes Technology & Therapeutics*, vol. 12, no. 1, pp. 35–39, 2010.

[5] E. Davis, B. Keating, G. Byrne, M. Russell, and T. Jones, "Hypoglycemia: incidence and clinical predictors in a large population-based sample of children and adolescents with IDDM," *Diabetes Care*, vol. 20, no. 1, pp. 22–25, 1997.

[6] O. Sovik and H. Thordarson, "Dead-in-bed syndrome in young diabetic patients," *Diabetes Care*, vol. 22, pp. B40–B42, 1999.

[7] P. A. Bakhtiani, L. M. Zhao, J. El Youssef, J. R. Castle, and W. K. Ward, "A review of artificial pancreas technologies with an emphasis on bi-hormonal therapy." *Diabetes, Obesity and Metabolism*, vol. 15, no. 12, pp. 1065–1070, 2013.

[8] R. Hovorka, "Closed–loop insulin delivery: from bench to clinical practice." *Nature Reviews Endocrinology*, vol. 7, no. 7, pp. 385–395, 2011.

[9] F. H. El-Khatib, J. Jiang, and E. R. Damiano, "Adaptive closed-loop control provides blood-glucose regulation using dual subcutaneous insulin and glucagon infusion in diabetic swine." *Journal of Diabetes Science and Technology*, vol. 1, no. 2, pp. 181–192, 2007.

[10] A. Haidar, M. R. Smaoui, L. Legault, and R. Rabasa-Lhoret, "The role of glucagon in the artificial pancreas." *The Lancet Diabetes & Endocrinology*, vol. 4, no. 6, pp. 476–479, 2016.

[11] M. A. Jackson, N. Caputo, J. R. Castle, L. L. David, C. T. Roberts Jr, and W. K. Ward, "Stable liquid glucagon formulations for rescue treatment and bi–hormonal closed–loop pancreas." *Current Diabetes Reports*, vol. 12, no. 6, pp. 705–710, 2012.

[12] W. K. Ward, J. Engle, H. M. Duman, C. P. Bergstrom, S. F. Kim, and I. F. Federiuk, "The benefit of subcutaneous glucagon during closed-loop glycemic control in rats with type 1 diabetes," *IEEE Sensors Journal*, vol. 8, no. 1, pp. 89–96, 2008.

[13] S. Kumar, S. K. Singh, X. Wang, B. Rup, and D. Gill, "Coupling of aggregation and immunogenicity in biotherapeutics: T-and b-cell immune epitopes may contain aggregation-prone regions," *Pharmaceutical Research*, vol. 28, no. 5, p. 949, 2011.

[14] Zealand Pharma A/S. (2016) Dasiglucagon (ZP4207) single-dose rescue treatment for acute, severe hypoglycemia events. [Online]. Available: http://www.zealandpharma.com/portfolio/glucagon-rescue-peng

[15] D. Boiroux, "Model predictive control algorithms for pen and pump insulin administration," Ph.D. dissertation, Technical University of Denmark, 2012.

[16] A. Duun-Henriksen, "Stochastic differential equations in artificial pancreas modelling," Ph.D. dissertation, Technical University of Denmark, 2013.

[17] S. Schmidt, "New technologies in the treatment of type 1 diabetes," Ph.D. dissertation, University of Copenhagen, 2013.

[18] S. L. Wendt, J. K. Møller, C. B. Knudsen, H. Madsen, A. Haidar, and J. B. Jørgensen, "PK/PD modelling of glucose–insulin–glucagon dynamics in healthy dogs after a subcutaneous bolus administration of native glucagon or a novel glucagon analogue." Technical University of Denmark, Tech. Rep. 2, April 2016.

[19] S. L. Wendt, J. K. Møller, A. Haidar, C. B. Knudsen, H. Madsen, and J. B. Jørgensen, "Modelling of glucose–insulin–glucagon pharmacodynamics in man." in *Proceedings of the 38th Annual International Conference of the IEEE Engineering in Medicine and Biology Society.* IEEE EMBS, 2016.

[20] S. L. Wendt, A. Ranjan, J. K. Møller, S. Schmidt, C. B. Knudsen, J. J. Holst, S. Madsbad, H. Madsen, K. Nørgaard, and J. B. Jørgensen, "Cross–validation of a glucose–insulin–glucagon pharmacodynamics model for simulation using data from patients with type 1 diabetes." *Journal of Diabetes Science and Technology*, 2017.

[21] S. L. Wendt, A. Ranjan, J. K. Møller, C. B. Knudsen, J. J. Holst, S. Madsbad, H. Madsen, K. Nørgaard, and J. B. Jørgensen, "Simulating clinical studies of the glucoregulatory system: *in vivo* meets *in silico*." Technical University of Denmark, Tech. Rep. 1, February 2017.

[22] A. Ranjan, S. L. Wendt, S. Shcmidt, S. Madsbad, J. J. Holst, H. Madsen, J. B. Jørgensen, and K. Nørgaard, "Insulin dependent regimen of mini-dose glucagon treatment of mild hypoglycaemia in patients with type 1 diabetes - a simulation study," *Diabetes Technology & Therapeutics*, 2017, draft.

[23] R. R. Seeley, T. D. Stephens, and T. Philip, *Anatomy & Physiology*, 7th ed. McGraw-Hill, 2006.

[24] C. J. Graf, J. R. Woodworth, M. E. Seger, J. H. Holcombe, R. R. Bowsher, and R. Lynch, "Pharmacokinetic and glucodynamic comparisons of recombinant and animal–source glucagon after IV, IM, and SC injection in healthy volunteers." *Journal of Pharmaceutical Sciences*, vol. 88, no. 10, pp. 991–995, 1999.

[25] H. Blauw, I. Wendl, J. H. DeVries, T. Heise, and T. Jax, "Pharmacokinetics and pharmacodynamics of various glucagon dosages at different blood glucose levels." *Diabetes, Obesity and Metabolism*, vol. 18, no. 1, pp. 34–39, 2016.

[26] I. Mühlhauser, J. Koch, and M. Berger, "Pharmacokinetics and bioavailability of injected glucagon: differences between intramuscular, subcutaneous, and intravenous administration." *Diabetes Care*, vol. 8, no. 1, pp. 39–42, 1985.

[27] S. Rosenbaum, *Basic pharmacokinetics and pharmacodynamics: An integrated textbook and computer simulations.*, 1st ed. John Wiley & Sons, Inc., 2011.

[28] A. Haidar, C. Duval, L. Legault, and R. Rabasa-Lhoret, "Pharmacokinetics of insulin aspart and glucagon in type 1 diabetes during closed–loop

operation." *Journal of Diabetes Science and Technology*, vol. 7, no. 6, pp. 1507–1512, 2013.

[29] D. Lv, M. D. Breton, and L. S. Farhy, "Pharmacokinetics modeling of exogenous glucagon in type 1 diabetes mellitus patients." *Diabetes Technology & Therapeutics*, vol. 15, no. 11, pp. 935–941, 2013.

[30] J. Gabrielsson and D. Weiner, *Pharmacokinetic and pharmacodynamic data analysis: concepts and applications.* CRC Press, 2001, vol. 1.

[31] J. A. Yáñez, C. M. Remsberg, C. L. Sayre, M. L. Forrest, and N. M. Davies, "Flip-flop pharmacokinetics-delivering a reversal of disposition: challenges and opportunities during drug development," *Therapeutic Delivery*, vol. 2, no. 5, pp. 643–672, 2011.

[32] N. J. W. Albrechtsen, B. Hartmann, S. Veedfald, J. A. Windeløv, A. Plamboeck, K. N. Bojsen-Møller, T. Idorn, B. Feldt-Rasmussen, F. K. Knop, T. Vilsbøll, S. Madsbad, C. F. Deacon, and J. J. Holst, "Hyperglucagonaemia analysed by glucagon sandwich elisa: nonspecific interference or truly elevated levels?" *Diabetologia*, vol. 57, no. 9, pp. 1919–1926, 2014.

[33] L. K. Roskos, A. Schneider, I. Vainshtein, M. Schwickart, R. Lee, H. Lu, R. Faggioni, and M. Liang, "PK–PD modeling of protein drugs: implications in assay development." *Bioanalysis*, vol. 3, no. 6, pp. 659–675, 2011.

[34] M. A. Felmlee, M. E. Morris, and D. E. Mager, "Mechanism–based pharmacodynamic modeling." *Methods in Molecular Biology*, vol. 929, pp. 583–600, 2012.

[35] L. Hinshaw, A. Mallad, C. Dalla Man, R. Basu, C. Cobelli, R. E. Carter, Y. C. Kudva, and A. Basu, "Glucagon sensitivity and clearance in type 1 diabetes: insights from in vivo and in silico experiments." *American Journal of Physiology, Endocrinology and Metabolism*, vol. 309, no. 5, pp. E474–E486, 2015.

[36] A. D. Cherrington, "Control of glucose production in vivo by insulin and glucagon." in *Comprehensive Physiology 2011, Supplement 21: Handbook of Physiology, The Endocrine System, The Endocrine Pancreas and Regulation of Metabolism*, First published in print 2001, pp. 759–785.

[37] F. Q. Nuttall, A. Ngo, and M. C. Gannon, "Regulation of hepatic glucose production and the role of gluconeogenesis in humans: is the rate of gluconeogenesis constant?" *Diabetes/Metabolism Research and Reviews*, vol. 24, no. 6, pp. 438–458, 2008.

[38] R. L. Dobbins, C. C. Connolly, D. W. Neal, L. J. Palladino, A. F. Parlow, and A. D. Cherrington, "Role of glucagon in countering hypoglycemia

induced by insulin infusion in dogs." *American Journal of Physiology-Endocrinology and Metabolism*, vol. 261, no. 24, pp. E773–E781, 1991.

[39] A. Cherrington, P. Williams, G. Shulman, and W. Lacy, "Differential time course of glucagon's effect on glycogenolysis and gluconeogenesis in the conscious dog." *Diabetes*, vol. 30, no. 3, pp. 180–187, 1981.

[40] M. Wada, C. C. Connolly, C. Tarumi, D. W. Neal, and A. D. Cherrington, "Hepatic denervation does not significantly change the response of the liver to glucagon in conscious dogs." *American Journal of Physiology - Endocrinology and Metabolism*, vol. 268, no. 2, pp. E194–E203, 1995.

[41] M. Matsuda, R. A. DeFronzo, L. Glass, A. Consoli, M. Giordano, P. Bressler, and S. DelPrato, "Glucagon dose-response curve for hepatic glucose production and glucose disposal in type 2 diabetic patients and normal individuals." *Metabolism*, vol. 51, no. 9, pp. 1111–1119, 2002.

[42] F. R. DeRubertis and P. Craven, "Reduced sensitivity of the hepatic adenylate cyclase–cyclic AMP system to glucagon during sustained hormonal stimulation." *Journal of Clinical Investigation*, vol. 57, no. 2, pp. 435–443, 1976.

[43] T. Reilly, S. Beckner, and M. Blecher, "Uncoupling of the glucagon receptor-adenylate cyclase system by glucagon in cloned differentiated rat hepatocytes." *Journal of Receptor Research*, vol. 1, no. 2, pp. 277–311, 1980.

[44] A. Adkins, R. Basu, M. Persson, B. Dicke, P. Shah, A. Vella, W. F. Schwenk, and R. Rizza, "Higher insulin concentrations are required to suppress gluconeogenesis than glycogenolysis in nondiabetic humans." *Diabetes*, vol. 52, no. 9, pp. 2213–2220, 2003.

[45] G. Boden, P. Cheung, and C. Homko, "Effects of acute insulin excess and deficiency on gluconeogenesis and glycogenolysis in type 1 diabetes." *Diabetes*, vol. 52, no. 1, pp. 133–137, 2003.

[46] R. A. Rizza, L. J. Mandarino, and J. E. Gerich, "Dose-response characteristics for effects of insulin on production and utilization of glucose in man." *American Journal of Physiology-Endocrinology And Metabolism*, vol. 240, no. 3, pp. E630–E639, 1981.

[47] K. E. Steiner, P. E. Williams, W. W. Lacy, and A. D. Cherrington, "Effects of insulin on glucagon–stimulated glucose production in the conscious dog." *Metabolism*, vol. 39, no. 12, pp. 1325–1333, 1990.

[48] J. El Youssef, J. R. Castle, P. A. Bakhtiani, A. Haidar, D. L. Branigan, M. Breen, and W. K. Ward, "Quantification of the glycemic response to

microdoses of subcutaneous glucagon at varying insulin levels." *Diabetes Care*, vol. 37, no. 11, pp. 3054–3060, 2014.

[49] S. J. Russell, F. H. El-Khatib, D. M. Nathan, and E. R. Damiano, "Efficacy determinants of subcutaneous microdose glucagon during closed-loop control." *Journal of Diabetes Science and Technology*, vol. 4, no. 6, pp. 1288–1304, 2010.

[50] A. M. Arbelaez, D. Xing, P. E. Cryer, C. Kollman, R. W. Beck, J. Sherr, K. J. Ruedy, W. V. Tamborlane, N. Mauras, E. Tsalikian, D. M. Wilsom, and N. H. White, "Blunted glucagon but not epinephrine responses to hypoglycemia occurs in youth with less than 1 yr duration of type 1 diabetes mellitus." *Pediatric Diabetes*, vol. 15, no. 2, pp. 127–134, 2014.

[51] G. Harris, A. Diment, M. Sulway, and M. Wilkinson, "Glucagon administration − underevaluated and undertaught." *Practical Diabetes International*, vol. 18, no. 1, pp. 22–25, 2001.

[52] Novo Nordisk A/S. (2016) Glucagen hypokit (glucagon [rDNA origin] for injection). [Online]. Available: http://www.glucagenhypokit.com/

[53] Eli Lilly and Company. (2016) Glucagon for injection (rDNA origin). [Online]. Available: http://www.lillyglucagon.com/

[54] S. T. Chung and M. W. Haymond, "Minimizing morbidity of hypoglycemia in diabetes: A review of mini-dose glucagon." *Journal of Diabetes Science and Technology*, vol. 9, no. 1, pp. 44–51, 2015.

[55] N. Taleb, A. Haidar, V. Messier, V. Gingras, L. Legault, and R. Rabasa-Lhoret, "Glucagon in the artificial pancreas systems; potential benefits and safety profile of future chronic use." *Diabetes, Obesity and Metabolism*, 2016.

[56] A. Ranjan, S. Schmidt, S. Madsbad, J. J. Holst, and K. Nørgaard, "Effects of subcutaneous, low−dose glucagon on insulin-induced mild hypoglycaemia in patients with insulin pump treated type 1 diabetes." *Diabetes, Obesity and Metabolism*, vol. 18, no. 4, pp. 410–418, 2016.

[57] M. Reiter, F. Reiterer, and L. del Re, "Bihormonal glucose control using a continuous insulin pump and a glucagon-pen." in *Control Conference (ECC), 2016 European.* IEEE, 2016, pp. 2435–2440.

[58] A. Ranjan, S. Schmidt, C. Damm-Frydenberg, I. Steineck, T. R. Clausen, J. J. Holst, S. Madsbad, and K. Nørgaard, "Low carbohydrate diet impairs the effect of glucagon in the treatment of insulin−induced mild hypoglycemia: A randomized cross−over study." *Diabetes Care*, vol. 40, no. 1, pp. 132–135, 2017.

[59] J. R. Castle, J. El Youssef, P. A. Bakhtiani, Y. Cai, J. M. Stobbe, D. Branigan, K. Ramsey, P. Jacobs, R. Reddy, M. Woods, and W. K. Ward, "Effect of repeated glucagon doses on hepatic glycogen in type 1 diabetes: Implications for a bihormonal closed–loop system." *Diabetes care*, vol. 38, no. 11, pp. 2115–2119, 2015.

[60] F. H. El-Khatib, J. Jiang, and E. R. Damiano, "A feasibility study of bihormonal closed-loop blood glucose control using dual subcutaneous infusion of insulin and glucagon in ambulatory diabetic swine." *Journal of Diabetes Science and Technology*, vol. 3, no. 4, pp. 789–803, 2009.

[61] S. Trevitt, S. Simpson, and A. Wood, "Artificial pancreas device systems for the closed-loop control of type 1 diabetes: what systems are in development?" *Journal of Diabetes Science and Technology*, vol. 10, no. 3, pp. 714–723, 2016.

[62] A. Pinkos, G. Arreaza-Rubin, W. J. Heetderks, I. Irony, H. V. Joffe, B. Schneider, and C. L. Zimliki, "FDA's proactive role in the development of an artificial pancreas for the treatment of diabetes mellitus." *Drug Discovery Today: Technologies*, vol. 4, no. 1, pp. 25–28, 2007.

[63] FDA. (2016) The 670g system. [Online]. Available: http://www.fda.gov/MedicalDevices/ProductsandMedicalProcedures/ DeviceApprovalsandClearances/Recently-ApprovedDevices/ucm522764. htm

[64] D. Lewis, S. Leibrand, and the #OpenAPS Community, "Real-world use of open source artificial pancreas systems." *Journal of Diabetes Science and Technology*, vol. 10, no. 6, p. 1411, 2016.

[65] A. Haidar, L. Legault, M. Dallaire, A. Alkhateeb, A. Coriati, V. Messier, P. Cheng, M. Millette, B. Boulet, and R. Rabasa-Lhoret, "Glucose–responsive insulin and glucagon delivery (dual–hormone artificial pancreas) in adults with type 1 diabetes: a randomized crossover controlled trial." *Canadian Medical Association Journal*, vol. 185, no. 4, pp. 297–305, 2013.

[66] H. Blauw, A. C. van Bon, R. Koops, and J. H. DeVries, "Performance and safety of an integrated bihormonal artificial pancreas for fully automated glucose control at home." *Diabetes, Obesity and Metabolism*, vol. 18, no. 7, pp. 671–677, 2016.

[67] F. H. El-Khatib, S. J. Russell, D. M. Nathan, R. G. Sutherlin, and E. R. Damiano, "A bihormonal closed-loop artificial pancreas for type 1 diabetes," *Science Translational Medicine*, vol. 2, no. 27, p. 27ra27, 2010.

[68] F. H. El-Khatib, C. Balliro, M. A. Hillard, K. L. Magyar, L. Ekhlaspour, M. Sinha, D. Mondesir, A. Esmaeili, C. Hartigan, M. J. Thompson, S. Malkani, J. P. Lock, D. M. Harlan, P. Clinton, E. Frank, D. M. Wilson, D. DeSalvo, L. Norlander, T. Ly, B. A. Buckingham, J. Diner, M. Dezube, L. A. Young, A. Goley, M. S. Kirkman, J. B. Buse, H. Zheng, R. R. Selagamsetty, E. R. Damiano, and S. J. Russell, "Home use of a bihormonal bionic pancreas versus insulin pump therapy in adults with type 1 diabetes: a multicentre randomised crossover trial," *The Lancet*, vol. 389, no. 10067, pp. 369–380, 2017.

[69] S. J. Russell, F. H. El-Khatib, M. Sinha, K. L. Magyar, K. McKeon, L. G. Goergen, C. Balliro, M. A. Hillard, D. M. Nathan, and E. R. Damiano, "Outpatient glycemic control with a bionic pancreas in type 1 diabetes." *The New England Journal of Medicine*, vol. 371, no. 4, pp. 313–325, 2014.

[70] S. J. Russell, M. A. Hillard, C. Balliro, K. L. Magyar, R. Selagamsetty, M. Sinha, K. Grennan, D. Mondesir, L. Ehklaspour, H. Zheng, E. R. Damiano, and F. H. El-Khatib, "Day and night glycaemic control with a bionic pancreas versus conventional insulin pump therapy in preadolescent children with type 1 diabetes: a randomised crossover trial." *The Lancet Diabetes & Endocrinology*, vol. 4, pp. 233–243, 2016.

[71] A. Kowalski, "Pathway to artificial pancreas systems revisited: moving downstream." *Diabetes Care*, vol. 38, no. 6, pp. 1036–1043, 2015.

[72] S. J. Russell, "Progress of artificial pancreas devices toward clinical use: the first outpatient studies." *Current Opinion in Endocrinology, Diabetes, and Obesity*, vol. 22, no. 2, pp. 106–111, 2015.

[73] J. Kropff and J. H. DeVries, "Continuous glucose monitoring, future products, and update on worldwide artificial pancreas projects." *Diabetes Technology & Therapeutics*, vol. 18, no. S2, pp. 53–63, 2016.

[74] H. Thabit and R. Hovorka, "Coming of age: the artificial pancreas for type 1 diabetes." *Diabetologia*, vol. 59, no. 9, pp. 1795–1805, 2016.

[75] J. R. Castle, J. M. Engle, J. El Youssef, R. G. Massoud, K. C. J. Yuen, R. Kagan, and W. K. Ward, "Novel use of glucagon in a closed-loop system for prevention of hypoglycemia in type 1 diabetes." *Diabetes Care*, vol. 33, no. 6, pp. 1282–1287, 2010.

[76] A. Haidar, L. Legault, V. Messier, T. M. Mitre, C. Leroux, and R. Rabasa-Lhoret, "Comparison of dual–hormone artificial pancreas, single-hormone artificial pancreas, and conventional insulin pump therapy for glycaemic control in patients with type 1 diabetes: an open–label randomised controlled crossover trial." *The Lancet Diabetes & Endocrinology*, vol. 3, no. 1, pp. 17–26, 2015.

[77] A. Haidar, L. Legault, L. Matteau-Pelletier, V. Messier, M. Dallaire, M. Ladouceur, and R. Rabasa-Lhoret, "Outpatient overnight glucose control with dual–hormone artificial pancreas, single–hormone artificial pancreas, or conventional insulin pump therapy in children and adolescents with type 1 diabetes: an open–label, randomised controlled trial." *The Lancet Diabetes & Endocrinology*, vol. 3, no. 8, pp. 595–604, 2015.

[78] A. Haidar, R. Rabasa-Lhoret, L. Legault, L. E. Lovblom, R. Rakheja, V. Messier, É. D'aoust, C. M. Falappa, T. Justice, A. Orszag, H. Tschirhart, M. Dallaire, M. Ladouceur, and B. A. Perkins, "Single- and dual-hormone artificial pancreas for overnight glucose control in type 1 diabetes," *The Journal of Clinical Endocrinology & Metabolism*, vol. 101, no. 1, pp. 214–223, 2016.

[79] A. Haidar, V. Messier, L. Legault, M. Ladouceur, and R. Rabasa-Lhoret, "Outpatient 60-hour day-and-night glucose control with dual-hormone artificial pancreas, single-hormone artificial pancreas, or sensor-augmented pump therapy in adults with type 1 diabetes: an open-label, randomised, crossover, controlled trial." *Diabetes, Obesity and Metabolism*, 2017.

[80] N. Taleb, A. Emami, C. Suppere, V. Messier, L. Legault, M. Ladouceur, J.-L. Chiasson, A. Haidar, and R. Rabasa-Lhoret, "Efficacy of single-hormone and dual-hormone artificial pancreas during continuous and interval exercise in adult patients with type 1 diabetes: randomised controlled crossover trial." *Diabetologia*, vol. 59, no. 12, pp. 2561–2571, 2016.

[81] P. G. Jacobs, J. El Youssef, R. Reddy, N. Resalat, D. Branigan, J. Condon, N. Preiser, K. Ramsey, M. Jones, C. Edwards, K. Kuehl, J. Leitschuh, U. Rajhbeharrysingh, and J. R. Castle, "Randomized trial of a dual-hormone artificial pancreas with dosing adjustment during exercise compared with no adjustment and sensor-augmented pump therapy." *Diabetes, Obesity and Metabolism*, vol. 18, no. 11, pp. 1110–1119, 2016.

[82] M. C. Riddell, I. W. Gallen, C. E. Smart, C. E. Taplin, P. Adolfsson, A. N. Lumb, A. Kowalski, R. Rabasa-Lhoret, R. J. McCrimmon, C. Hume, F. Annan, P. A. Fournier, C. Graham, B. Bode, P. Galassetti, T. W. Jones, I. San Millán, T. Heise, A. L. Peters, A. Petz, and L. M. Laffel, "Exercise management in type 1 diabetes: a consensus statement," *The Lancet Diabetes & Endocrinology*, 2017.

[83] V. Gingras, R. Rabasa-Lhoret, V. Messier, M. Ladouceur, L. Legault, and A. Haidar, "Efficacy of dual–hormone artificial pancreas to alleviate the carbohydrate–counting burden of type 1 diabetes: A randomized crossover trial." *Diabetes & Metabolism*, vol. 42, pp. 47–54, 2016.

[84] H. Thabit, S. Hartnell, J. M. Allen, A. Lake, M. E. Wilinska, Y. Ruan, M. L. Evans, A. P. Coll, and R. Hovorka, "Closed-loop insulin delivery in

inpatients with type 2 diabetes: a randomised, parallel-group trial." *The Lancet Diabetes & Endocrinology*, 2016.

[85] B. G. Fahy, A. M. Sheehy, and D. B. Coursin, "Glucose control in the intensive care unit." *Critical Care Medicine*, vol. 37, no. 5, pp. 1769–1776, 2009.

[86] M. Güemes and K. Hussain, "Hyperinsulinemic hypoglycemia." *Pediatric Clinics of North America*, vol. 62, no. 4, pp. 1017–1036, 2015.

[87] J. S. Owen and J. Fiedler-Kelly, *Introduction to population pharmacokinetic/pharmacodynamic analysis with nonlinear mixed effects models.* John Wiley & Sons, 2014.

[88] D. Rylander Jr, "Glucagon in the artificial pancreas supply and marketing challenges." *Journal of Diabetes Science and Technology*, vol. 9, no. 1, pp. 52–55, 2015.

[89] S. S. Steiner, M. Li, R. Hauser, and R. Pohl, "Stabilized glucagon formulation for bihormonal pump use." *Journal of Diabetes Science and Technology*, vol. 4, no. 6, pp. 1332–1337, 2010.

[90] R. Pohl, M. Li, A. Krasner, and E. De Souza, "Development of stable liquid glucagon formulations for use in artificial pancreas," *Journal of Diabetes Science and Technology*, vol. 9, no. 1, pp. 8–16, 2015.

[91] W. K. Ward, R. G. Massoud, C. J. Szybala, J. M. Engle, J. El Youssef, J. M. Carroll, C. T. Roberts, and R. D. DiMarchi, "*In vitro* and *in vivo* evaluation of native glucagon and glucagon analog (MAR-D28) during aging: lack of cytotoxicity and preservation of hyperglycemic effect." *Journal of Diabetes Science and Technology*, vol. 4, no. 6, pp. 1311–1321, 2010.

[92] J. R. Chabenne, M. A. DiMarchi, V. M. Gelfanov, and R. D. DiMarchi, "Optimization of the native glucagon sequence for medicinal purposes." *Journal of Diabetes Science and Technology*, vol. 4, no. 6, pp. 1322–1331, 2010.

[93] Eli Lilly and Company. (2016) Clinical development pipeline. [Online]. Available: https://www.lilly.com/pipeline/index.html

[94] Xeris Pharmaceuticals. (2015) Pipeline. [Online]. Available: http://www.xerispharma.com/pipeline

[95] Adocia. (2014) Biochaperone human glucagon. [Online]. Available: http://www.adocia.fr/WP/products/biochaperone-human-glucagon/

[96] J. L. Sherr, K. J. Ruedy, N. C. Foster, C. A. Piché, H. Dulude, M. R. Rickels, W. V. Tamborlane, K. E. Bethin, L. A. DiMeglio, L. A. Fox, R. P. Wadwa, D. A. Schatz, B. M. Nathan, S. M. Marcovina, E. Rampakakis, L. Meng, and R. W. Beck, "Glucagon nasal powder: A promising alternative to intramuscular glucagon in youth with type 1 diabetes." *Diabetes Care*, vol. 39, no. 4, pp. 555–562, 2016.

[97] M. R. Rickels, K. J. Ruedy, N. C. Foster, C. A. Piché, H. Dulude, J. L. Sherr, W. V. Tamborlane, K. E. Bethin, L. A. DiMeglio, R. P. Wadwa, A. J. Ahmann, M. J. Haller, B. M. Nathan, S. M. Marcovina, E. Rampakakis, L. Meng, and R. W. Beck, "Intranasal glucagon for treatment of insulin-induced hypoglycemia in adults with type 1 diabetes: a randomized crossover noninferiority study." *Diabetes Care*, vol. 39, no. 2, pp. 264–270, 2016.

[98] B. Newswanger, S. Ammons, N. Phadnis, W. K. Ward, J. Castle, R. W. Campbell, and S. J. Prestrelski, "Development of a highly stable, nonaqueous glucagon formulation for delivery via infusion pump systems." *Journal of Diabetes Science and Technology*, vol. 9, no. 1, pp. 24–33, 2015.

[99] Novo Nordisk A/S. (2015) GlucaGen (glucagon [rDNA origin] for injection) patient information. [Online]. Available: http://www.novo-pi.com/glucagenhypokit.pdf

[100] J. R. Castle, J. El Youssef, D. Branigan, B. Newswanger, P. Strange, M. Cummins, L. Shi, and S. Prestrelski, "Comparative pharmacokinetic/pharmacodynamic study of liquid stable glucagon versus lyophilized glucagon in type 1 diabetes subjects." *Journal of Diabetes Science and Technology*, vol. 10, no. 5, pp. 1101–1107, 2016.

[101] M. W. Haymond, M. J. Redondo, S. McKay, M. J. Cummins, B. Newswanger, J. Kinzell, and S. Prestrelski, "Nonaqueous, mini-dose glucagon for treatment of mild hypoglycemia in adults with type 1 diabetes: A dose-seeking study." *Diabetes Care*, vol. 39, no. 3, pp. 465–468, 2016.

[102] Zealand Pharma A/S. (2016) Dasiglucagon (ZP4207) for multi-dose with potential as an important component in an artificial pancreas. [Online]. Available: http://www.zealandpharma.com/portfolio/glucagon-multiple-dose-version-zp4207

[103] CTSM–R development team. (2015, April) Continuous time stochastic modeling in R: User's guide and reference manual. [Online]. Available: http://ctsm.info/pdfs/ctsmr-reference.pdf

[104] R. Juhl, J. K. Møller, J. B. Jørgensen, and H. Madsen, *Prediction Methods for Blood Glucose Concentration.* Springer, 2016, ch. Modeling and prediction using stochastic differential equations.

[105] J. Møller and H. Madsen, "From state dependent diffusion to constant diffusion in stochastic differential equations by the lamperti transform." Technical University of Denmark, Tech. Rep. 16, December 2010.

[106] J. K. Møller, J. Carstensen, and H. Madsen, "Structural identification and validation in stochastic differential equation based models – with application to a marine ecosystem NP–model." *Journal of the Royal Statistical Society, Series C*, 2011.

[107] B. Øksendal, *Stochastic differential equations: An Introduction with Applications*, 6th ed., ser. Universitext.   Springer, 2003.

[108] A. Jazwinski, *Stochastic processes and filtering theory*, 1st ed.   Academic Press, 1970, vol. 64.

[109] C. Kreutz, A. Raue, D. Kaschek, and J. Timmer, "Profile likelihood in systems biology." *The FEBS Journal*, vol. 208, pp. 2564–2571, 2013.

[110] H. Madsen and P. Thyregod, *Introduction to general and generalized linear models.*   CRC Press, 2011.

[111] N. R. Kristensen, H. Madsen, and S. B. Jørgensen, "Parameter estimation in stochastic grey-box models." *Automatica*, vol. 40, no. 2, pp. 225–237, 2004.

[112] D. Boiroux, R. Juhl, H. Madsen, and J. B. Jörgensen, "An efficient UD-based algorithm for the computation of maximum likelihood sensitivity of continuous-discrete systems," in *2016 IEEE 55th Conference on Decision and Control (CDC).*   IEEE, 2016, pp. 3048–3053.

[113] A. Haidar, M. E. Wilinska, J. A. Graveston, and R. Hovorka, "Stochastic virtual population of subjects with type 1 diabetes for the assessment of closed–loop glucose controllers." *IEEE Transactions on Biomedical Engineering*, vol. 60, no. 12, pp. 3524–3533, 2013.

[114] A. Emami, J. El Youssef, R. Rabasa-Lhoret, J. Pineau, J. R. Castle, and A. Haidar, "Modelling glucagon action in patients with type 1 diabetes." *IEEE Journal of Biomedical Health Informatics*, 2016.

[115] J. Nocedal and S. J. Wright, *Numerical Optimization*, 2nd ed., T. V. Mikosch, S. I. Resnick, and S. M. Robinson, Eds.   Springer, 2006.

[116] M. Gen and R. Cheng, *Genetic algorithms and engineering optimization.* John Wiley & Sons, 2000, vol. 7.

[117] R. Hovorka, F. Shojaee-Moradie, P. V. Carroll, L. J. Chassin, I. J. Gowrie, N. C. Jackson, R. S. Tudor, A. M. Umpleby, and R. H. Jones, "Partitioning glucose distribution/transport, disposal, and endogenous production during IVGTT." *American Journal of Physiology-Endocrinology and Metabolism*, vol. 282, no. 5, pp. E992–E1007, 2002.

[118] B. P. Kovatchev, M. Breton, C. Dalla Man, and C. Cobelli, "In silico pre-clinical trials: a proof of concept in closed–loop control of type 1 diabetes." *Journal of Diabetes Science and Technology*, vol. 3, no. 1, pp. 44–55, 2009.

[119] O. Vahidi, K. E. Kwok, R. B. Gopaluni, and F. K. Knop, "A comprehensive compartmental model of blood glucose regulation for healthy and type 2 diabetic subjects." *Medical & Biological Engineering & Computing*, vol. 54, no. 9, pp. 1383–1398, 2016.

[120] P. Palumbo, S. Ditlevsen, A. Bertuzzi, and A. De Gaetano, "Mathematical modeling of the glucose–insulin system: A review." *Mathematical Biosciences*, vol. 244, no. 2, pp. 69–81, 2013.

[121] R. N. Bergman, Y. Z. Ider, C. R. Bowden, and C. Cobelli, "Quantitative estimation of insulin sensitivity." *American Journal of Physiology-Endocrinology And Metabolism*, vol. 236, no. 6, pp. E667–E677, 1979.

[122] P. Herrero, P. Georgiou, N. Oliver, M. Reddy, D. Johnston, and C. Toumazou, "A composite model of glucagon-glucose dynamics for *in silico* testing of bihormonal glucose controllers." *Journal of Diabetes Science and Technology*, vol. 7, no. 4, pp. 941–951, 2013.

[123] C. Dalla Man, F. Micheletto, D. Lv, M. Breton, B. Kovatchev, and C. Cobelli, "The UVA/PADOVA type 1 diabetes simulator: New features." *Journal of Diabetes Science and Technology*, vol. 8, no. 1, pp. 26–34, 2014.

[124] K. B. Schneck, X. Zhang, R. Bauer, M. O. Karlsson, and V. P. Sinha, "Assessment of glycemic response to an oral glucokinase activator in a proof of concept study: application of a semi–mechanistic, integrated glucose–insulin–glucagon model." *Journal of Pharmacokinetics and Pharmacodynamics*, vol. 40, no. 1, pp. 67–80, 2013.

[125] J. Z. Peng, W. S. Denney, B. J. Musser, R. Liu, K. Tsai, L. Fang, M. L. Reitman, M. D. Troyer, S. S. Engel, L. Xu, A. Stoch, J. A. Stone, and K. G. Kowalski, "A semi–mechanistic model for the effects of a novel glucagon receptor antagonist on glucagon and the interaction between glucose, glucagon, and insulin applied to adaptive phase II design." *The AAPS Journal*, vol. 16, no. 6, pp. 1259–1270, 2014.

[126] R. Hovorka, H. Jayatillake, E. Rogatsky, V. Tomuta, T. Hovorka, and D. T. Stein, "Calculating glucose fluxes during meal tolerance test: a new computational approach," *American Journal of Physiology-Endocrinology and Metabolism*, vol. 293, no. 2, pp. E610–E619, 2007.

[127] G. Toffolo, R. Basu, C. Dalla Man, R. Rizza, and C. Cobelli, "Assessment of postprandial glucose metabolism: conventional dual- vs. triple-tracer method," *American Journal of Physiology-Endocrinology And Metabolism*, vol. 291, no. 4, pp. E800–E806, 2006.

[128] R. Hovorka, V. Canonico, L. J. Chassin, U. Haueter, M. Massi-Benedetti, M. O. Federici, T. R. Pieber, H. C. Schaller, L. Schaupp, T. Vering, and M. E. Wilinska, "Nonlinear model predictive control of glucose concentration in subjects with type 1 diabetes." *Physiological Measurement*, vol. 25, no. 4, pp. 905–920, 2004.

[129] N. Cohen, P. Sabhachandani, S. Sarkar, L. Kahanovitz, N. Lautsch, S. J. Russell, and T. Konry, "Microsphere based continuous-flow immunoassay in a microfluidic device for determination of clinically relevant insulin levels," *Microchimica Acta*, pp. 1–7, 2017.